From the Institute of Phytopathology at Kiel University

The impact of abiotic and biotic factor on the soil microbial processes regulating organic matter decomposition

Dissertation

in fulfilment of the requirements for the doctoral degree

of the Faculty of Agricultural and Nutritional Sciences

at Christian-Albrechts-Universität zu Kiel

submitted by

M.Sc Shang Wang

Born on June 1996 in Laiyang, China

Kiel, March 2024

Dean: Prof. Dr. Georg Thaller

First examiner: Jun-Prof. Bahar S. Razavi

Second examiner: Prof. Sandra Spielvogel

Date of the oral examination: July 3rd, 2024

Summary

Soil enzyme activity indicates the soil community's metabolic requirements and nutrients demand. It drives the decomposition of soil organic matter (SOM), a fundamental process in carbon cycling within ecosystems. Biotic and abiotic factors significantly influence enzymatic reactions, regulating SOM decomposition rates. This interplay between enzymes and biotic and abiotic conditions affects carbon cycling dynamics. Carbon use efficiency (CUE) measures the fraction of assimilated carbon retained by organisms for growth and metabolic processes. These processes underscore the pivotal role of enzymes in mediating carbon fluxes and highlight the sensitivity of ecosystem dynamics to environmental changes.

This thesis aims to investigate the effect of biotic and abiotic factors on soil microbial process, enzymatic mobilization and organic matter decomposition. Soil samples were collected from variety of land uses globally: farmlands in the North China Plain, the Vietnam Red River Delta, the Dikopshof Germany, and grasslands in the German Elbe estuary. The soil was then incubated under different biotic and abiotic conditions in the lab to test abiotic factors include AMF inoculation and plant species, while the biotic factors include straw returning, soil moisture, salinity levels, warming, carbon substrate availability, and quality. During incubation, soil samples were taken to measure enzyme kinetics, microbial biomass, respiration, and heat release. Subsequently, CUE was estimated based on respired carbon and microbial biomass carbon. Additionally, a 2-D imaging method was conducted to visualize in situ enzyme activity and glucose concentration in soil hotspots such as the rhizosphere, detritusphere, and mycorrhizosphere.

The biotic factor (AMF, plant species) regulates microbial activity in soil hotspots. In particular, the distinct nutrient demands of plant species (wheat vs. soybean) appear to regulate the impact of AMF on the characteristics of microbial activities in the rhizosphere. Meanwhile, the cooperation between soybean and AMF induced the formation of favorable microsites around the root, specifically in overlapping localities between the rhizosphere and mycorrhizosphere, characterized by enhanced glucose release, increased rhizosphere expansion, high enzyme activities, and shortened substrate turnover time.

Abiotic factors (straw returning, soil moisture, warming, salinity, substrate quality) directly and indirectly affect soil microbial activity and SOM decomposition. Specifically, straw incorporation forms another soil enzyme activity hotspot (detritusphere) and promotes enzyme activities in the rhizosphere and soil profile. Moreover, soil with a history of dry-rewetting (D/W) cycles triggers the recovery of microbial activities after D/W cycles, and rewetting has a significant impact on enzyme systems, while flooding induces more effects on enzyme synthesis. On the other hand, soil salinity

negatively impacts soil respiration and microbial growth, especially in soils subjected to warming or organic matter input, with the negative effect being promoted with the input of labile substrate. Even a 2°C increase in temperature can increase SOM decomposition and microbial growth. Meanwhile, labile carbon substrates can activate microbes and subsequently accelerate the decomposition of recalcitrant carbon substrates when combined in soil. Furthermore, the dynamic patterns of enzyme activity and microbial CUE are closely associated with SOM decomposition and microbial growth and retardation stages.

This thesis demonstrates the variable effects of multiple abiotic and biotic factors on soil enzyme activity and organic matter decomposition through soil incubation, 2D imaging, and soil sample measurements. The straw incorporation and AMF symbiosis could extend the soil enzymatic hotspot area and increase enzyme activity. Soil subjected to dry-rewetting cycles triggers microbial activity recovery, while flooding primarily affects enzyme synthesis. In addition, salinity negatively affects soil respiration and microbial growth, especially under warming or organic matter input, with labile substrates exacerbating the negative effects. Enzyme activity dynamics and microbial carbon use efficiency correlate with microbial growth stages. Meanwhile, labile carbon substrates are more readily utilized by soil microbes compared to recalcitrant carbon substrate, and their presence can accelerate the decomposition of recalcitrant carbon substrates in soil. Collectively, these results emphasize the importance of multi-factor interactive effects on soil microbial processes, enzymatic mobilization, and organic matter decomposition. Further studies are suggested to focus on modeling the effects of abiotic and biotic factors on soil processes and predicting potential outcomes under climatic change conditions.

Zusammenfassung

Die Aktivität von Bodenenzymen zeigt die metabolischen Anforderungen und den Nährstoffbedarf der Bodengemeinschaft an. Sie treibt den Abbau von organischer Bodensubstanz (SOM) voran, einen grundlegenden Prozess im Kohlenstoffkreislauf innerhalb von Ökosystemen. Biotische und abiotische Faktoren beeinflussen enzymatische Reaktionen signifikant und regulieren die Abbauraten von SOM. Diese Wechselwirkung zwischen Enzymen und biotischen sowie abiotischen Bedingungen beeinflusst die Dynamik des Kohlenstoffkreislaufs. Die Kohlenstoffnutzungseffizienz (CUE) misst den Anteil des assimilierten Kohlenstoffs, der von Organismen für Wachstum und Stoffwechselprozesse zurückgehalten wird. Diese Prozesse unterstreichen die entscheidende Rolle von Enzymen bei der Vermittlung von Kohlenstoffflüssen und verdeutlichen die Empfindlichkeit der Ökosystemdynamik gegenüber Umweltveränderungen.

Diese Arbeit zielt darauf ab, den Einfluss biotischer und abiotischer Faktoren auf bodenmikrobielle Prozesse, enzymatische Mobilisierung und den Abbau von organischen Stoffen zu untersuchen. Bodenproben wurden weltweit von verschiedenen Landnutzungsformen gesammelt: Ackerflächen in der Nordchinesischen Ebene, dem Vietnam Roten Fluss Delta, dem Dikopshof Deutschland und Grünlandgebieten in der deutschen Elbmündung. Der Boden wurde dann unter verschiedenen biotischen und abiotischen Bedingungen im Labor inkubiert, um abiotische Faktoren wie AMF-Inokulation und Pflanzenarten zu testen, während die biotischen Faktoren Stroh-Rückführung, Bodenfeuchtigkeit, Salzgehalt, Erwärmung, Verfügbarkeit und Qualität von Kohlenstoffsubstraten umfassen. Während der Inkubation wurden Bodenproben entnommen, um Enzymkinetik, mikrobielle Biomasse, Atmung und Wärmeabgabe zu messen. Anschließend wurde die CUE basierend auf abgeatmetem Kohlenstoff und mikrobieller Biomasse geschätzt. Darüber hinaus wurde eine 2-D-Bildgebungsmethode durchgeführt, um die in situ Enzymaktivität und Glukosekonzentration in Boden-Hotspots wie der Rhizosphäre, Detritusphäre und Mykorrhizosphäre zu visualisieren.

Der biotische Faktor (AMF, Pflanzenart) reguliert die mikrobielle Aktivität in Boden-Hotspots. Insbesondere scheinen die unterschiedlichen Nährstoffanforderungen von Pflanzenarten (Weizen vs. Sojabohne) den Einfluss von AMF auf die Merkmale mikrobieller Aktivitäten in der Rhizosphäre zu regulieren. In der Zwischenzeit führte die Zusammenarbeit zwischen Sojabohne und AMF zur Bildung günstiger Mikrostandorte um die Wurzel herum, speziell an überlappenden Orten zwischen Rhizosphäre und Mykorrhizosphäre, gekennzeichnet durch erhöhte Glukosefreisetzung, vergrößerte Rhizosphärenausbreitung, hohe Enzymaktivitäten und verkürzte Substratumsetzungsdauer.

Abiotische Faktoren (Stroh-Rückführung, Bodenfeuchtigkeit, Erwärmung, Salzgehalt, Substratqualität) beeinflussen direkt und indirekt die mikrobielle Aktivität im Boden und den Abbau von SOM. Insbesondere fördert die Stroheinarbeitung die Bildung eines weiteren Boden-Enzymaktivität-Hotspots (Detritusphäre) und steigert die Enzymaktivitäten in der Rhizosphäre und im Bodenprofil. Darüber hinaus löst Boden mit einer Geschichte von Trocken-Nass-Zyklen die Wiederherstellung mikrobieller Aktivitäten nach den Zyklen aus, wobei die Benetzung einen signifikanten Einfluss auf Enzymsysteme hat, während Überschwemmungen mehr Effekte auf die Enzymsynthese hervorrufen. Andererseits beeinträchtigt Bodensalzgehalt negativ die Bodenatmung und das mikrobielle Wachstum, insbesondere in Böden, die Erwärmung oder organische Stoffe ausgesetzt sind, wobei der negative Effekt durch die Zugabe von labilem Substrat verstärkt wird. Selbst eine Temperaturerhöhung um 2°C kann den Abbau von SOM und das mikrobielle Wachstum erhöhen. In der Zwischenzeit können labile Kohlenstoffsubstrate Mikroben aktivieren und anschließend den Abbau von recalcitranten Kohlenstoffsubstraten beschleunigen, wenn sie im Boden kombiniert werden. Darüber hinaus sind die dynamischen Muster der Enzymaktivität und der mikrobiellen CUE eng mit SOM-Abbau- und mikrobiellen Wachstums- und Verzögerungsphasen verbunden.

Diese Arbeit zeigt die variablen Effekte mehrerer abiotischer und biotischer Faktoren auf die Aktivität von Bodenenzymen und den Abbau von organischem Material durch Bodeninkubation, 2D-Bildgebung und Bodenprobenmessungen auf. Die Stroheinarbeitung und die AMF-Symbiose könnten den Bereich des enzymatischen Boden-Hotspots erweitern und die Enzymaktivität erhöhen. Boden, der Trocken-Nass-Zyklen ausgesetzt ist, löst die Wiederherstellung der mikrobiellen Aktivität aus, während Überschwemmungen hauptsächlich die Enzymsynthese beeinflussen. Darüber hinaus beeinträchtigt Salzgehalt negativ die Bodenatmung und das mikrobielle Wachstum, insbesondere unter Erwärmung oder organischer Stoffzufuhr, wobei labile Substrate die negativen Effekte verstärken. Die Dynamik der Enzymaktivität und die mikrobielle Kohlenstoffnutzungseffizienz korrelieren mit den Wachstumsphasen der Mikroben. Im Vergleich zu recalcitranten Kohlenstoffsubstraten werden labile Kohlenstoffsubstrate von Bodenmikroben leichter genutzt, und ihre Anwesenheit kann den Abbau von recalcitranten Kohlenstoffsubstraten im Boden beschleunigen. Zusammenfassend betonen diese Ergebnisse die Bedeutung der multiplen interaktiven Effekte auf bodenmikrobielle Prozesse, enzymatische Mobilisierung und Abbau von organischem Material. Weitere Studien sollten sich darauf konzentrieren, die Auswirkungen abiotischer und biotischer Faktoren auf Bodenprozesse zu modellieren und potenzielle Ergebnisse unter klimatischen Veränderungsbedingungen vorherzusagen.

Acknowledgement

I express my deepest gratitude to all those who have contributed to my Ph.D. study.

First and foremost, I extend immense thanks to Jun-Prof. Bahar S. Razavi for accepting me as her Ph.D. student and for her unwavering support, guidance, and expertise throughout the entire research journey. Her insightful feedback and constructive criticism have been instrumental in shaping the direction and quality of my Ph.D. study. Additionally, her patient encouragement has been a source of solace and confidence during moments of confusion, challenges, and discontent in both my academic and personal life.

I also want to extend my appreciation to Dr. Evgenia Blagodataskaya for her significant support during my joint study at UFZ Halle. Her critical and helpful suggestions for my experiments and manuscripts, along with opportunities to attend conferences and present my work, have been invaluable.

Special thanks go to Dr. Duyen Hoang for her collaboration on the initial stages of my study. Without her support, I might not have smoothly completed and published the manuscript. I would also like to appreciate Prof. Sandra Spielvogel, Dr. Thomas Reitz, Prof. Mika Tarkka, Dr. Huadong Zang, Prof. Zhaohai Zeng, Dr. Yadong Yang and Dr. Xiquan Wang for their insightful suggestions regarding both my study and life.

Gratitude is extended to Yijie Shi, Kaikai Min, Mehdi Rashtabri, Fatemeh Dehghani, Shiyue Yang, Dr. Guodong Shao, and other colleagues and group members for their assistance. I also thank the secretaries and technicians for their support in my work and study. Special appreciation goes to Cheng Peng, Biao Wang, Hanyou Xie, Dr. Yuecheng Wu, and Dr. Peixin Wang, as well as all my international and Chinese friends, for their assistance and support during my Ph.D.

I would like to acknowledge the resources and facilities provided by Kiel University. The conducive academic environment and access to libraries, laboratories, and other facilities have been crucial to the success of this research.

My sincere thanks go to the China Scholarship Council for the financial support of my study and life in Germany. Additionally, I am grateful to DFG for providing financial support for my Ph.D. research.

Thank you all.

Shang Wang

Table of Contents

List of Figures

Extended summary

Study 1

Study 2

Study 3

Study 4

Study 5

Study 6

List of Tables

Study 1

Study 2

Study 5

Study 6

Abbreviation

C	Carbon
N	Nitrogen
P	Phosphorus
SOM	Soil organic matter
SOC	Soil organic matter
TN	Total nitrogen
DOC	Dissolved organic carbon
DON	Dissolved organic nitrogen
RLD	Root length density
RSD	Root surface density
AEM	Anion exchange membrane
AMF	Arbuscular mycorrhizal fungi
V_{max}	Enzyme activity
K_m	Substrate affinity
K_a	Catalytic efficiency
T_t	Turnover time
[S]	Substrate concentration
RS	Resistance index
WHC	Water holding capacity
D/W	Dry-rewetting
BR	Basal respiration
SIR	Substrate induced respiration
SIGR	Substrate induced growth respiration
CUE	Carbon use efficiency
TMB	Total microbial biomass
GMB	Growing microbial biomass
μ	Specific growth rate
CR	Calorespirometric ratios
EC	Electrical conductivity
G	Glucose addition
S	Starch addition
G+S	Glucose + Starch addition

1 Extended summary

1.1 Introduction

Soil organic matter (SOM) is particularly vital for sustaining the productivity of terrestrial ecosystems, with its decomposition regarded as a critical process in regulating global carbon cycling (Schmidt et al., 2011). As a primarily microbial process, SOM decomposition is influenced by external factors that control microbial activity and function (Blagodatsky et al., 2010; Dungait et al., 2012). These factors include abiotic elements such as temperature, moisture, salinity, nutrient availability, substrate quality and accessibility, as well as biotic interactions like competition and predation among plants and soil microorganisms (Allison et al., 2014; Qiu et al., 2018). Enzymes play a central role in depolymerizing macromolecular organic compounds and generating soluble oligomers and monomers that can be transported into cells (Nannipieri et al., 1996). Enzyme activity impacts SOM decomposition and nutrient cycling by regulating soil biochemical processes, including the formation and decomposition of labile organic substrates and nutrients (Luo et al., 2017). Therefore, it is crucial to determine the direct and indirect contributions of individual factors and identify the key drivers of SOM mineralization.

1.1.1 Biotic factors

Soil biotic factors encompass a diverse array of living organisms inhabiting the soil ecosystem, including plant roots, bacteria, fungi, protozoa, nematodes, earthworms, and other macrofauna. These organisms directly participate in SOM decomposition through their metabolic activities, breaking down complex organic compounds into simpler forms that can be utilized by plants and other soil biota (Qiu et al., 2018). Bacteria and fungi are primary decomposers in soil ecosystems, secreting enzymes that catalyze the breakdown of organic matter into soluble compounds. These enzymes, such as cellulases, ligninases, proteases, and lipases, target specific components of organic matter, facilitating its degradation into smaller molecules (Nannipieri et al., 1996). The diversity and activity of microbial communities in soil play a critical role in determining the rates and pathways of organic matter decomposition. Moreover, interactions among different microbial species and between microbes and soil fauna further modulate SOM decomposition dynamics (Condron et al., 2010). For instance, certain microorganisms produce enzymes essential for breaking down recalcitrant organic compounds, which can subsequently be utilized by other organisms. In this study, we selected plant root and arbuscular mycorrhizal fungi (AMF) inoculation as key biotic factors.

AMF represent the dominant mycorrhizal type, forming symbiotic associations with approximately 71% of all flowering plants, including many important crops such as wheat, barley, corn, and soybean (Brundrett and Tedersoo, 2019). AMF symbiosis contributes to soil carbon (C) flux by incorporating carbon into intra- and extraradical mycelium, transporting and exuding carbon through the extraradical mycelium, stabilizing soil structure, and providing carbon to the microbial community (Rillig, 2004; Jones et al., 2009; Hoang et al., 2022). Furthermore, AMF can promote free-living microbial communities by releasing labile substrates via exudation and hyphal turnover, stimulating microbial growth, and providing energy for enzyme production and soil organic matter decomposition (Schmidt et al., 2011; Feizi et al., 2024). Compared to root-free soil, soil organic matter decomposition with living roots can be altered by as much as -70% to 380% (Cheng et al., 2014). Although there is a

general consensus that roots stimulate microbial activity (Kuzyakov and Blagodatskaya, 2015), it remains unclear how interactions between roots, AMF, and saprotrophic microorganisms alter belowground carbon inputs and, consequently, SOM decomposition and carbon storage. Several studies have reported that AMF symbiosis can enhance litter decomposition and support plant nitrogen capture, assuming enhanced carbon flow to microbial communities (Hodge, 2001; Cheng et al., 2012). Conversely, some studies found that AMF symbiosis did not significantly affect litter decomposition (Nottingham et al., 2013; Leifheit et al., 2014). Thus, the mechanisms underlying the effects of AMF symbiosis on soil organic matter decomposition remain unresolved.

Plant roots significantly influence the rhizosphere, a dynamic biological interface recognized as one of the most active zones in the soil system (Kuzyakov and Blagodatskaya, 2015). This influence is most pronounced at the root surface, extending several millimeters into the soil. The spatial distribution of the rhizosphere is shaped by factors such as root morphology, microbial colonization, nutrient uptake, root exudation, and rhizodeposition (Zhang et al., 2019; Wang et al., 2023a; Kaloterakis et al., 2024). Microbial activity in the rhizosphere is strongly driven by root exudates and other rhizodeposits (Bilyera et al., 2020), which constitute about one-third of plants' photosynthetic products released into the soil, fostering plant-microbial interactions (Bais et al., 2006). Rhizodeposits encompass various forms of organic matter released by roots, stimulating microbial activity, extracellular enzyme production, and soil organic matter decomposition (Pausch and Kuzyakov, 2018; Zhu et al., 2018). Plant root physiology and exudate composition play pivotal roles in shaping microbial community composition and their ability to utilize carbon and nutrient sources (Iannucci et al., 2021). Microbial diversity within rhizospheres varies among plant species, cultivars, root segments, and developmental stages (Prashar et al., 2013). However, further study is needed to explore the interaction between plant roots and other factors.

Understanding the complex interplay between biotic factors, including AMF and plant roots, and soil microbial and enzyme activity is essential for elucidating the mechanisms driving SOM decomposition in terrestrial ecosystems. In this thesis, we investigate the effect of plant root species (Studies 1 and 4) and AMF inoculation (Studies 3 and 4) on SOM decomposition and enzyme kinetics.

1.1.2 Abiotic factors

Soil abiotic factors such as climate, soil texture, moisture content, pH, and temperature play fundamental roles in shaping the dynamics of soil organic matter (SOM) decomposition and enzyme activity (Razavi et al., 2017; Zhang et al., 2021). Climate, through temperature and precipitation patterns, dictates microbial activity rates (Cui et al., 2019), while soil texture affects water retention and nutrient availability, influencing microbial communities and enzyme production (Zheng et al., 2019). Soil pH profoundly influences decomposition and enzyme activity, with acidic soils generally supporting slower rates (Neina, 2019). Oxygen availability and soil structure further regulate these processes, favoring aerobic conditions for decomposition (Walz et al., 2017). Understanding the complex interactions among these abiotic factors is essential for predicting ecosystem responses to environmental changes and implementing sustainable soil management practices amidst anticipated alterations in climate and land use patterns, which could significantly impact nutrient cycling dynamics and ecosystem functioning. In particular, we selected soil warming, drought, rewetting, salinity, and substrate quality as abiotic factors in this thesis.

Warming alters soil processes and functions. Generally, warming promotes soil microbial activity and growth, accelerating SOM decomposition and nutrient cycling if water is not limiting (Singh et al., 2010). Predicted global temperature rise by approximately 1.5℃ by mid-century (IPCC, 2018) introduces further uncertainty regarding soil responses to other factors. Soil respiration may increase by a factor of 3-4 with a 10℃ warming (Q_{10}), indicating a stronger loss of SOM and carbon emissions in the soil ecosystem (Meyer et al., 2018). In the short term, warming has a positive effect on enzyme catalytic power, while in the long term or with strong warming amplitude, enzyme activity may decrease (Fanin et al., 2022). However, the effects of moderate warming on soil microbial activity and SOM remain poorly investigated.

Moisture is crucial for influencing soil biogeochemical processes (Butcher et al., 2020), mediated by microbial communities and activities. Environmental history can serve as a distal control on microbe-derived processes in response to dry-rewetting cycles (Evans and Wallenstein, 2012). These cycles result in sequential changes in soil biophysical and chemical properties, including: i) Cracked aggregates releasing more accessible organic matter to microorganisms (Mikha et al., 2005; Sun et al., 2017), ii) Desorption of substrate from mineral surfaces (Kalbitz et al., 2000), iii) Mobilization of C, N, and P from preceding microbial residues triggered by the drought legacy effect (Schimel et al., 2011; Leitner et al., 2017; Brödlin et al., 2019). These changes contribute to shifts in microbial community composition and decoupling of microbial respiration and growth (de Nijs et al., 2019; Brangarí et al., 2020), thereby affecting carbon use efficiency in response to dry-rewetting (Navarro-García et al., 2012). This alteration of liquid pathways decreases solute diffusion rates while increasing soil aeration (Ebrahimi and Or, 2016), and may change the chemical form of elements (Makino et al., 2000; Sardans and Peñuelas, 2005). Some of these elements serve as cofactors required for cellular and enzyme functions (Tebo et al., 2005), thus enhancing microbial growth, activity, and SOM decomposition (Ross et al., 2001). Moreover, when nutrient and exoenzyme diffusion are restricted under drought, it affects nutrient availability to microorganisms, leading to nutrient starvation (Bär et al., 2002; Zarebanadkouki et al., 2019). However, the effects of abrupt waterlogging of dry soil on microbial activities are still poorly understood.

Salinity directly impacts soil quality and function, significantly influencing soil microbial activity and organic matter decomposition (Wong et al., 2010). High salinity hinders the growth of plant roots and soil fauna, resulting in reduced bioturbation and aeration, ultimately leading to poor soil physical structure (Otlewska et al., 2020). Salinity alters the osmotic and matric potential of the soil solution, greatly affecting soil microbial activity and diversity (Song et al., 2022; Zhang et al., 2019). These salinity-induced changes have substantial implications for soil enzyme production and structure (Singh, 2016). High salinity has been found to decrease soil enzyme activity in grasslands (Pan et al., 2013), while having no impact on enzyme activity in paddy fields or wetlands (Sritongon et al., 2022). The impact of salinity on enzyme activity is related to specific enzyme types and other soil factors (Singh, 2016). Further research is needed to investigate the impact of soil salinization on enzyme activity and organic matter turnover.

Substrate quality significantly impacts the dynamics of SOM decomposition and enzyme activity. Soil substrates exhibit wide variations in chemical composition, physical structure, and biochemical properties, influencing the metabolic activities of microbial communities and enzymatic functions (Allison et al., 2014). Organic substrates range from labile compounds like sugars and amino acids to

recalcitrant materials such as lignin and cellulose. Generally, the decomposition rates of organic substrates are inversely related to the presence of recalcitrant compounds such as lignin, phenols, and tannins (Castellano et al., 2015).

Crop straw (e.g., leaves and stems) is considered high quality compared to belowground residues like roots, which are relatively recalcitrant to decomposition (Shahbaz et al., 2017). The role of residue quality in SOM formation is debated. The traditional perspective that recalcitrant root residues decompose slowly and contribute significantly to SOM conflicts with the notion that easily decomposable residues substantially contribute to SOM formation.

Glucose and starch are crucial organic compounds in terrestrial ecosystems, serving as primary energy and substrate sources for various organisms (Martínez-Trinidad et al., 2010; Strickland et al., 2012). Both are primarily derived in soil ecosystems from organic matter originating from plants, microorganisms, decomposition of dead organisms, and organic amendments, albeit with differing qualities (Gunina and Kuzyakov, 2015). Glucose, a simple sugar, serves as a fundamental energy and carbon source for plants and various soil microorganisms. Starch, similar to glucose, is a common component of plant litter and an important energy and carbon source for soil microorganisms (Guggenberger et al., 1999; Mooney, 1972). However, starch is a polysaccharide composed of glucose units linked in long chains, rendering it more recalcitrant for microbial degradation than labile substrates like glucose (French, 1973). Soil microbial activity is significantly influenced by the carbon substrates present in the soil. Upon entering the soil ecosystem, carbon substrates undergo decomposition mediated by soil microbial communities (Olagoke et al., 2022). The decomposition of these substrates accelerates microbial metabolism and contributes to the turnover of soil organic matter (Loeppmann et al., 2016; Wen et al., 2019). Understanding the dynamics of mixed substrate decomposition involving glucose and starch in soil ecosystems is crucial for elucidating the mechanisms governing nutrient cycling and ecosystem functioning in terrestrial environments.

In this thesis, we investigate the effect of crop straw incorporation (Study 1), soil warming (Study 5), drought (Studies 3 and 4), dry-rewetting (Study 2), salinization (Study 5), and substrate quality (Study 6) on SOM decomposition and enzyme kinetics.

1.2 Objective

The primary objective of this thesis is to explore the effects of abiotic and biotic factors on soil organic matter decomposition and enzyme activity.

1) Assess the effect of biotic factors on enzyme activity and microbial processes in soil hotspots.
    a. To demonstrate the impact of AMF symbiosis on soil enzymatic hotspots, enzyme activity, and substrate availability (Study 3 and 4)
    b. To evaluate the response of soil enzyme activity and microbial biomass to various types of plant roots (Study 4)
2) Assess the effect of abiotic factors on soil enzyme activity and substrate decomposition.
    a. To illustrate the influence of crop straw incorporation patterns on soil enzymatic hotspots and enzyme activity (Study 1)
    b. To examine the impact of drought and dry-rewetting patterns on soil enzymatic hotspots and enzyme kinetics (Study 2 and 3)

c. To evaluate the response of soil enzyme activity and substrate decomposition to soil salinization, warming, and their interaction (Study 5)
d. To assess the response of soil enzyme activity and substrate decomposition to substrate quality (Study 6)

3) Assess the effect of abiotic factors on soil carbon use efficiency and microbial energy response to substrate.
   a. To estimate the carbon use efficiency and calorespirometric ratio response to soil warming, salinization, and substrate quality (Study 5 and 6)

1.3 Material and Method

1.3.1 Soil sampling

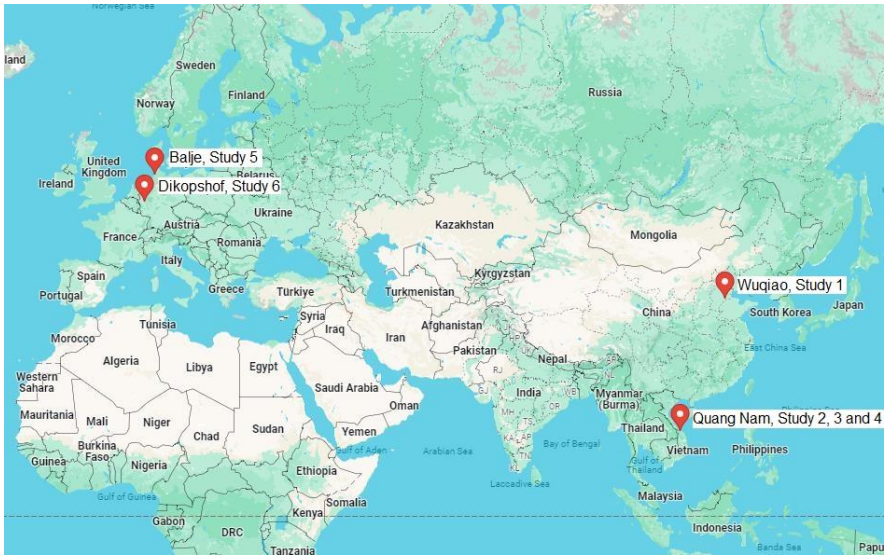

Figure ES1 *World map from Google Map [https://www.google.com/maps] including soil sampling locations*

The soil for study 1 was sampled from a depth of 0-20 cm at the Wuqiao experimental station of China Agricultural University, located in Cangzhou city, Hebei province, China (37°41′N, 116°35′E). The soil is classified as a Calcaric Fluvisol developed on an alluvial plain with a sandy loamy texture.

The soil for study 2, 3 and 4 was sampled from a depth of 0-20 cm at a rice and soybean rotation field in the Red River Delta, located in Quang Nam province, Vietnam (20° 25′ N, 106° 16′ E). The soil is classified as a Fluvisols with a sandy clay loam texture.

The soil for study 5 was sampled from a depth of 0-20 cm at a grassland site of the Elbe Estuary, located in Balje, Lower Saxony, Germany (53°8′N, 9°05′E). The soil is classified as a Tidalic Gleysol with clear stratification due to storm tides.

The soil for study 6 was sampled from a depth of 0-20 cm at a long-term manure application experiment at Dikopshof, University of Bonn, Germany (53°50′N, 6°58′E). The soil is classified as Haplic Luvisol and has a silty loam texture.

1.3.2 Experiment set up

The soil samples were kept cool (~4°C) during transportation and later were sieved through 2 mm mesh to exclude any stone and plant residue, homogenized. To minimize the sequent effects of

sampling, sieving and moisture adjustment on microbial activities, soil was preconditioned at room temperature in the dark for two weeks prior to the main experiment (Blagodatskaya and Kuzyakov, 2013).

In Study 1, 3, and 4, soil was initially placed in the rhizoboxes. Plant seeds were pre-germinated on wet filter paper, and then one germinated seed was placed in the middle of each rhizobox. Subsequently, the rhizoboxes were transferred to greenhouse conditions with various experimental treatments. In Study 2, 5, and 6, after soil pre-incubation, the soil was placed in plastic cups and incubated in laboratory conditions with various experimental treatments.

1.3.3 Soil zymography

In Study 1, and 3, soil zymography was employed to visualize spatial distributions and localize hotspots of maximal enzyme activities (Razavi et al., 2019). Polyamide membrane filters (Tao Yuan, China) with a pore size of 0.45 µm were saturated with fluorogenic substrates based on 4-methylumbelliferone (MUF) and 7-amino-4-methylcoumarin (AMC). These saturated membranes were then placed on the soil surface. Following a 1-hour incubation period, the membranes were carefully lifted off the soil surfaces, and any attached soil particles were gently removed using a small brush. Subsequently, the membranes were photographed under ultraviolet (UV) light in a dark room using a camera. A calibration line featuring a series of increasing concentrations of MUF or AMC was used to transform gray values into enzyme activities.

1.3.4 Optimized glucose imaging

In Study 4, optimized glucose imaging was used to demonstrate the dependence of the spatial and temporal patterns of glucose distribution (Hoang et al., 2022). Phosphate powder was dissolved in distilled water to create a buffer solution of 0.05 M. Subsequently, 100 mL of the buffer solution was added to 0.00107 g of glucose oxidase from Aspergillus niger, 0.003 g of peroxidase from horseradish, and 0.005144 g of Ampliflu red dissolved in 60 µL of dimethyl sulfoxide (McLaughlin and Boyer, 2004, Voothuluru et al., 2018). Concurrently, polyamide membrane filters (Tao Yuan, China) were tailored to fit the size of the rhizobox. These membranes were saturated with the prepared solution before being affixed to the rooted sides of the rhizoboxes. In this study, glucose imaging was enhanced by incorporating the solution described above, which turns red when glucose oxidase and horseradish peroxidase catalyze the glucose-based conversion of colorless Ampliflu Red into magenta-colored resorufin, using membranes instead of gel. This modification enables glucose imaging at the soil surface and significantly reduces the diffusion artifacts that occur in gel. After a 20-minute incubation period, the membranes were promptly removed and placed in a dark room under UV light with a wavelength of 355 nm. The magenta-colored area on the membrane indicated glucose exudation, as hydrogen peroxide generated from the reaction between glucose and the enzyme glucose oxidase, catalyzed by horseradish peroxidase, converted colorless Ampliflu red into magenta color.

1.3.5 Enzyme kinetics

In Study 2, 3, 4, 5, and 6, the activity of exoenzymes were determined. Briefly, 0.5 g of soil was mixed with 50 ml of sterile water. Following a 2-minute low energy sonication or shaking, 50 µl of soil suspension, 100 µl of substrate with varying concentrations, and 50 µl of buffer (MES, TRIZMA, or Na-acetate) were added into a 96-well black microplate (German et al., 2011). Fluorescence

measurements were taken using a microplate read (Victor or TECAN) at 0, 30 minutes, 1 hour, and 2 hours. The Michaelis-Menten equation was utilized to determine V_{max} and K_m by equation (1)

$$v = \frac{V_{max} \times [S]}{K_m + [S]} \quad (1)$$

where v is the reaction rate, [S] is the substrate concentration, V_{max} is the maximum reaction rate, and K_m is the substrate concentration at the half-maximum reaction rate. The substrate turnover time (Tt) was calculated according to equation (2) (Panikov et al., 1992), where [S] is the substrate concentration regarding to the V_{max}. The catalytic efficiency (K_a) of enzymes was determined by equation (3) (Zhang et al., 2019):

$$T_t = \frac{K_m + [S]}{V_{max}} \quad (2)$$

$$K_a = \frac{V_{max}}{K_m} \quad (3)$$

1.3.6 Microbial biomass

In Study 1, 5 and 6, MBC and MBN content were determined using fumigation method (Vance et al., 1987) in study 1, 5 and 6. To extract the samples, 5 g of soil was mixed with 20 mL of 0.05M K_2SO_4. Another 5 g of soil was fumigated with chloroform in a desiccator for 72 h and then extracted. The TOC/N analyzer was used to analyze the extracts for dissolved organic carbon (DOC) and nitrogen (DON) content. MBC and MBN calculations were based on the difference between K_2SO_4-extractable C and N in fumigated and non-fumigated soils, using the conversion factors of 0.45 for MBC and 0.54 for MBN. While in Study 2, MBC was determined based on initial rate of substrate induced respiration after 6 h of glucose addition and calculated as C_{mic} = SIR × 40.04. Where C_{mic} is MBC value (µg g^{-1} soil), SIR is the initial respiration rate (µl CO_2 g^{-1} soil h^{-1}) after soil amendment with glucose, 40.04 is the correction factor (Anderson and Domsch, 1978).

In Study 2 and 3, MBP was measured using fumigation extraction of soils with anion exchange membranes (Yevdokimov et al., 2016). 3 g soil, 30 ml sterilized water and one strip of AEM (1.5 cm × 6.25 cm) with or without 300 µl chloroform were placed in 50 ml plastic tubes. All tubes were tightly closed and shaken for 24 h to induce the recovery of inorganic P from the soil extract. After shaking, each AEM strip was cleaned in sterilized water and shaken with 45 ml H_2SO_4 (0.25 M) in other 50 ml plastic tubes for 3 h to release membrane-fixed P back to the solution. Thereafter, 150 µl extractant was mixed with ammonium molybdate tetrahydrate and Malachite Green in a 96-well transparent microplate and read by CLARIO Star Plus at 630 nm.

1.3.7 Soil microbial respiration and kinetics of the substrate-induced growth response

In Study 2, microbial respiration was measured using the MicroResp™ system, as described by Campbell et al. (2003). 0.3 g of soil was placed in each well of a 96-deep well plate using the standard filling device. The plates were sealed and pre-incubated at room temperature for 3 days to re-establish microbial activity. Each substrate solution (25 µl) and sterilized water as a control were dispensed into deep-well plates containing soil. The following substrates were used: The 96 deep well plates were then assembled to a colorimetric indicator plate with a rubber seal and incubated in the dark for 6 hours at 25 °C (Campbell et al., 2003). To measure basal respiration, 96 deep well plates were filled with sterilized water instead of substrate. The absorbance of the indicator plate was measured at 570 nm

before and after the incubation period using CLARIO Star Plus. The absorbance was then normalized and converted to CO_2 concentration according to Brolsma et al. (2015), as shown in equation (4):

$$\%CO_2 = 0.002 \times {A_{570}}^{-3.11} \quad (4)$$

where $\%CO_2$ (vol/vol) is the concentration in the headspace after incubation and A_{570} is the normalized absorbance of the indicator plate. Each substrate induced CO_2 rate (μg CO_2-C g^{-1} dry soil h^{-1}) was calculated according to Cameron (2007) as in equation (5):

$$CO_2 rate = \frac{\left({\%CO_2}/{100}\right) \times V \times ({12}/{44}) \times {273}/{273+T}}{DW \times IT} \quad (5)$$

where V is the headspace volume (945 μl) of deep well plates, 44/22.4 is the gas constant to convert the CO_2 concentration to weight, 12/44 is the molecular mass ratio to convert the CO_2 to CO_2-C, T is the incubation temperature (25°C), DW is soil dry weight (g), and IT is incubation time (hour).

In study 5 and 6, fresh soil in a tube was amended with a mixture containing glucose and mineral salts (Blagodatskaya et al., 2009). The soil samples were then incubated in the modified Respicond system, and the CO_2 production rate was monitored every 20 minutes. The theory of microbial growth kinetics has been extensively described earlier (Panikov, 1995). Microbial respiration in glucose amended soil was used to calculate the following kinetic parameters: the microbial maximal specific growth rate (μ), the growing microbial biomass (GMB) that capable for immediate growth on glucose, the total microbial biomass (TMB) responding by respiration to glucose addition, and the lag time (Blagodatskaya et al., 2010).

1.3.8 Soil heat release and calorespirometric ratio

In Study 5 and 6, heat production in the course of microbial metabolism on glucose was determined using microcalorimetry. The soil was amended with the same nutrient and glucose solution as described above for the SIGR method. Then, all the samples were sealed in airtight glass ampoules and then placed in to a TAM Air. Heat production was continuously measured. The calorespirometric ratio was calculated by equation (6):

$$\gamma = \mathrm{Q} \div CO_2 \quad (6)$$

where γ is the calorespirometric ratio (kJ mol^{-1} CO_2), Q is the heat production rate (W g^{-1} soil) and CO_2 is the respiration rate (mol CO_2 h^{-1} g^{-1} soil).

1.3.9 Soil residual glucose measurement

In Study 5, the residual glucose content in the soil was assessed using the Glucose Assay Kit (MAK263, Sigma-Aldrich), which oxidizes glucose to produce a fluorometric product proportional to the amount of glucose present. To perform the assay, 0.4 g of soil was mixed and extracted with 40 mL of sterilized water (pH = 7.0) in a centrifuge tube, which was then shaken at 180 rpm for 30 minutes. The tubes were then centrifuged at 4000 rpm for 10 minutes to obtain the supernatant, which was then diluted tenfold to ensure that the final fluorescence was within the range of the standard curve. For the determination of glucose content, 35 μL of diluted supernatant, 15 μL of glucose assay buffer and 50 μL of master reaction mix were added to each well of a 96-well black microplate. The microplate was then incubated at 37°C and shaken vigorously for 30 minutes to enhance the reaction. Fluorescence was measured using a TECAN microplate reader at γ_{ex} = 535/γ_{em} = 590 nm. In addition, a glucose standard solution was used to generate a glucose standard curve to establish the relationship between fluorescence and glucose content. Further details can be found in the manufacturer's technical bulletin.

1.3.10 Microbial carbon use efficiency calculation

In Study 5 and 6, microbial substrate carbon use efficiency for added carbon substrates was calculated based on the cumulative amount of respired CO_2 and glucose-C consumption during incubation period using equation (7) and (8) (Sinsabaugh et al., 2013). Furthermore, the CUE was also determined by considering the increment of microbial biomass C in course of substrate utilization (equation 9 and 10):

$$\mathrm{CUE}_1 = 1 - \frac{C_{SIR} - C_{BR}}{C_{metabolized}} \quad (7)$$

$$\mathrm{CUE}_2 = 1 - \frac{C_{SIR} - C_{BR}}{C_{added}} \quad (8)$$

$$\mathrm{CUE}_3 = \frac{MBC_i - MBC_0}{(MBC_i - MBC_0) + (C_{SIR} - C_{BR})} \quad (9)$$

$$\mathrm{CUE}_4 = \frac{MBC_i - MBC_0}{C_{metabolized}} \quad (10)$$

where C_{SIR} represents the cumulative amount of C respired from glucose-amended soil, and C_{BR} is the cumulative amount of C respired from unamended soil. The cumulative amount of respired carbon is determined over time and respiration rate, measured by the Respicond V respirometer. *MBCi* and MBC_0 represent the microbial biomass C measured by fumigation method at 0 and i hours after glucose addition. $C_{metabolized}$ is the glucose-C consumed, measured using the Glucose Assay Kit method. C_{added} is the amount of glucose-C added. As glucose was unlabeled, we were not able to correctly estimate soil priming effect. We assumed, therefore, that considering a short-term experiment, the priming effect (if any) was mainly apparent due to pool substitution mechanism (Blagodatskaya and Kuzyakov, 2008), and the metabolized C was either incorporated into MBC or respired.

1.4 Main results and discussion

1.4.1 Synthesis of highlights and main results of the studies

Abiotic and biotic factors affect plant growth, soil enzymatic hotspot, enzyme activity, enzyme system, glucose exudation, substrate decomposition, carbon use efficiency and calorespirometric ratio.

Study 1: The hotspot area of enzyme activity which induced by straw incorporation and plant root was consistent in both the rhizosphere and detritusphere, with enzyme activities decreasing over time in both areas, while straw incorporation enhanced enzyme activity in the rhizosphere and soil surface; however, homogenized straw inhibited plant growth due to nutrient competition between roots and microbes.

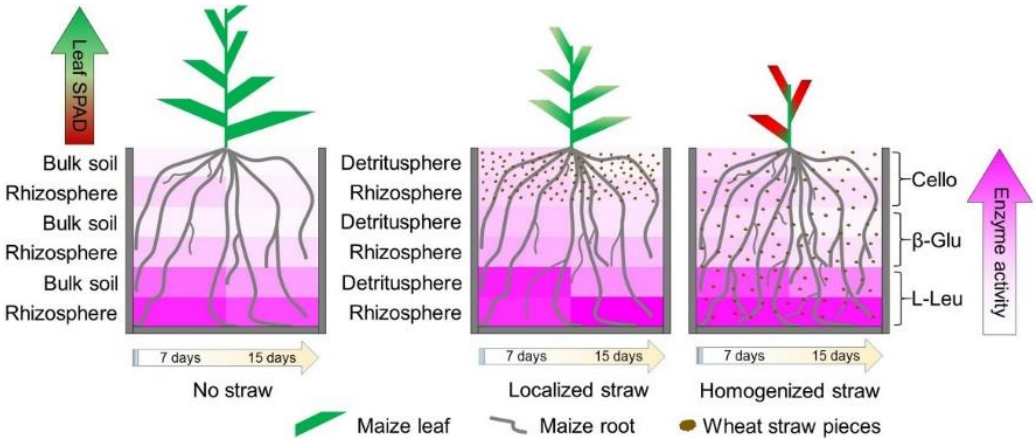

Figure ES2 *Main results summary of Study 1. The effect of straw incorporation on plant growth and the spatial and temporal distribution of soil enzyme activity.*

Study 2: The soil enzyme activities declined during extended drought but showed partial or full recovery after rewetting, indicating microbial resource reallocation in response to dry-rewetting, with MBC positively associated with chitinase and β-glucosidase activities at the drought onset, whereas rewetting at 60% WHC affected enzyme systems, while flooding at 100% WHC prompted enzyme synthesis.

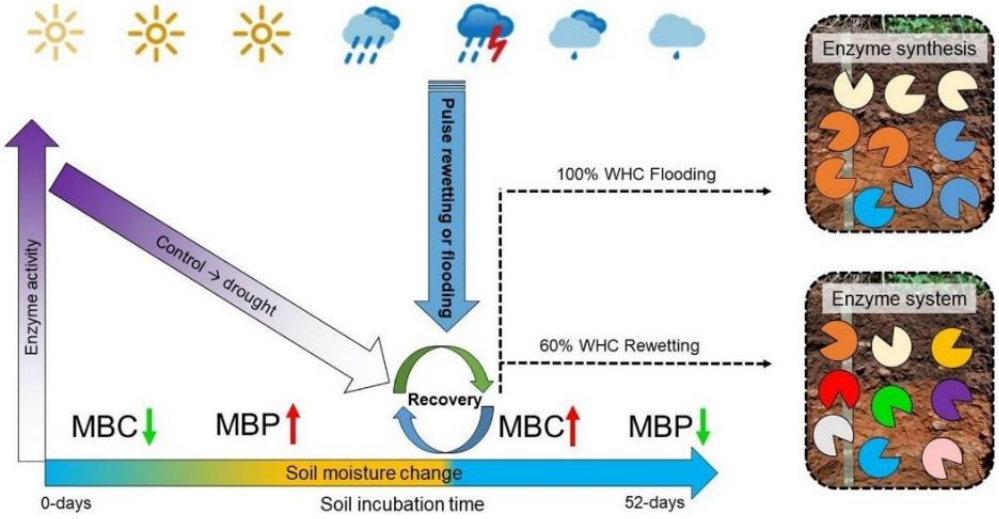

Figure ES3 *Main results summary of Study 2. The effect of dry-rewetting pattern on soil enzyme kinetics and microbial biomass.*

Study 3: Under drought conditions, mycorrhizal plant roots exhibit higher glucose exudation compared to control plants, with AMF inoculation expanding enzymatic hotspot areas, thereby enhancing the drought resistance of enzymes in mycorrhizal plants.

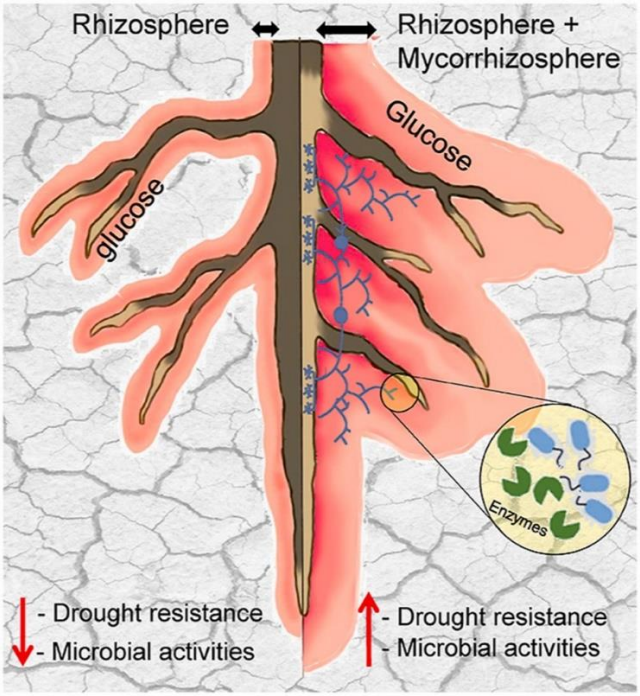

Figure ES4 *Main results summary of Study 3. The response of soil hotspot and glucose exudation to AMF symbiosis and drought conditions.*

Study 4: Under the influence of AMF inoculation, β-glucosidase activity rises in the rooted areas of maize and soybean, while chitinase activity increases in rooted areas of maize but decreases in soybean, suggesting that nutrient demands play a role in regulating AMF's impacts on rhizosphere microbial activities of both maize and soybean.

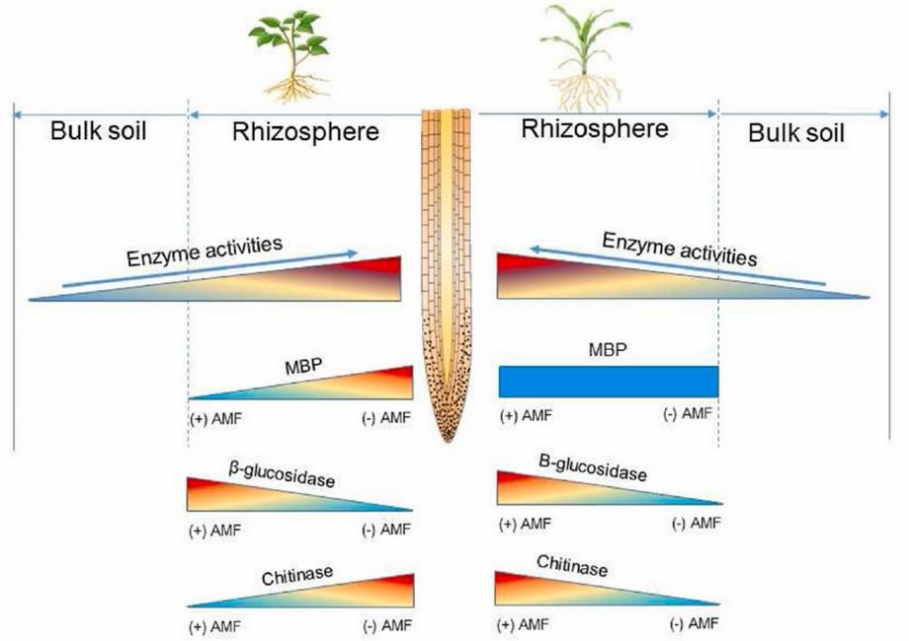

Figure ES5 *Main results summary of Study 4. The effect of plant species and AMF symbiosis on soil enzyme activity and MBP amount in bulk soil and rhizosphere soil.*

Study 5: The response of CO_2 and heat release to warming differed between unamended and glucose-amended soil, with 2℃ warming exerting a stronger promotion on soil microbial activity compared to 3.5-fold salinization; however, increasing salinity inhibited microbial growth, highlighting that the CUE is overestimated if the growth retardation stage is neglected, while the stable calorespirometric ratios ratio of 469 kJ mol^{-1} CO_2 was exclusively observed during the exponential growth stage.

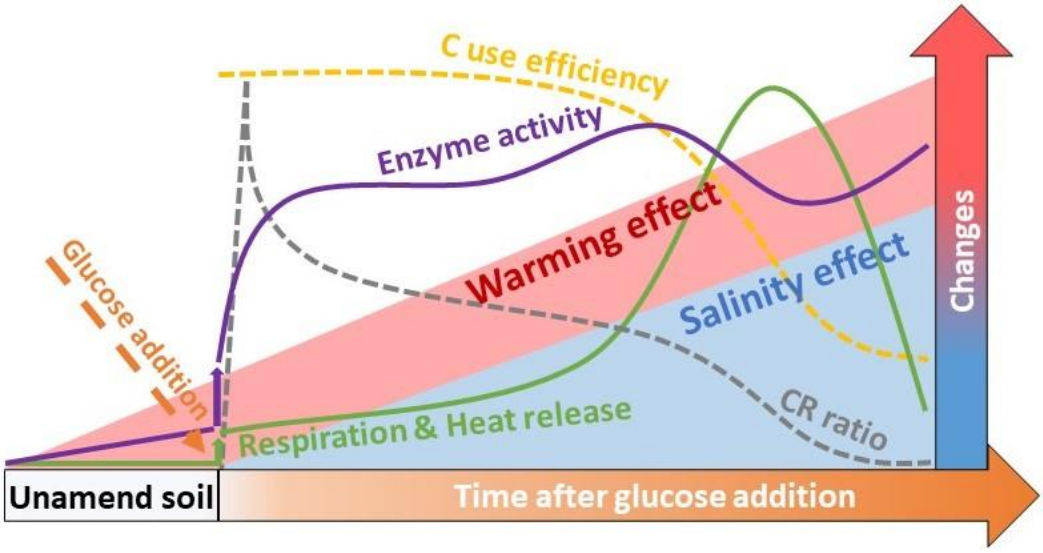

Figure ES6 *Main results summary of Study 5. The effect of soil warming and salinity on respiration, enzyme activity, and carbon use efficiency during organic matter decomposition.*

Study 6: Combining labile C with recalcitrant C in soil can expedite the decomposition of recalcitrant C, where labile C substrate predominantly influences the calorespirometric ratio dynamics regardless of the recalcitrant C substrate, while the CUE peaks at the initial substrate addition but diminishes towards the end of decomposition, indicating that the response of hydrolase to substrate quality and decomposition outweighs that of oxidase.

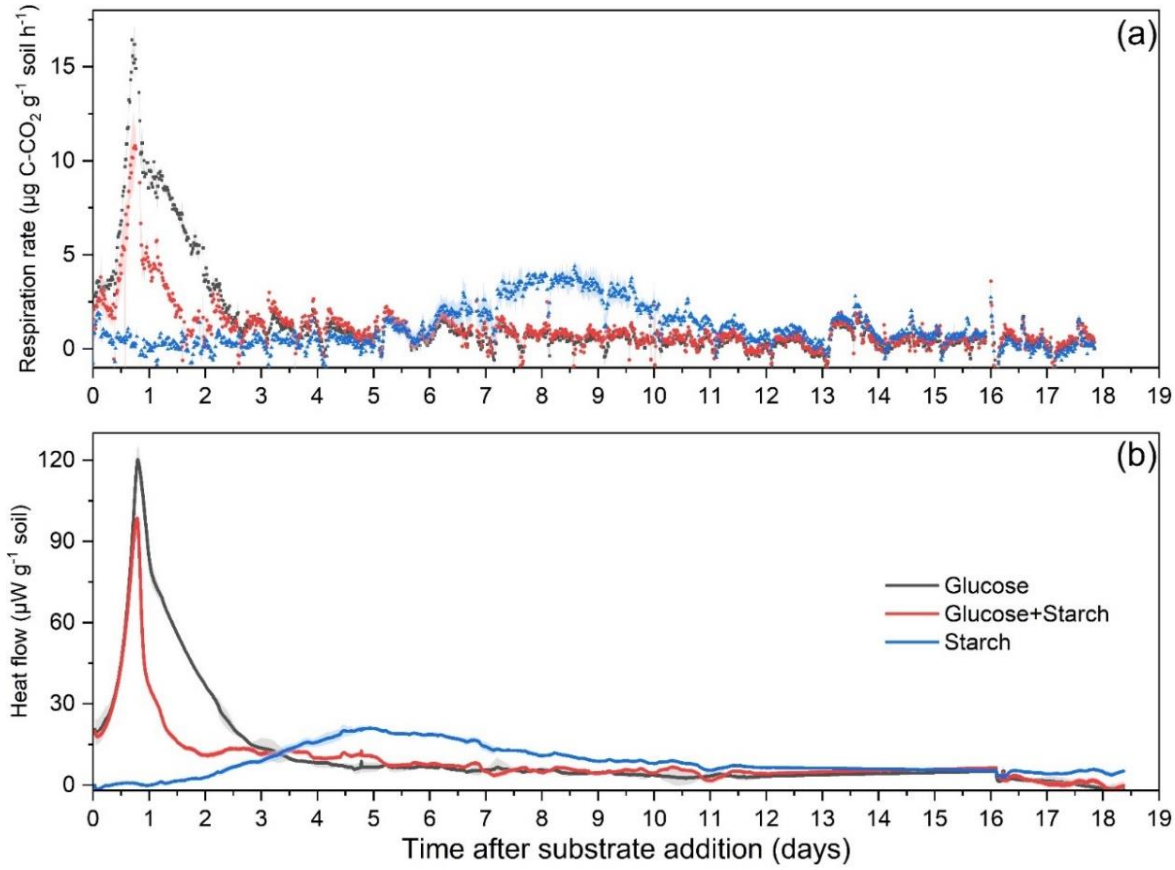

Figure ES7 *Main results summary of Study 6. The dynamics of respiration and heat release rates during the decomposition of glucose and starch.*

1.4.2 Effect of biotic and abiotic factors on soil enzyme activity

1.4.2.1 Straw incorporation and localization

The distribution of β-glucosidase, cellobiohydrolase, and leucine-aminopeptidase activities was strongly linked to the location of straw within the soil profile, indicating the primary pathways for carbon and nitrogen movement between straw and soil. This indicates that the detritusphere plays a crucial role in soil carbon and nitrogen cycling. The activity of the C-acquiring enzyme in the detritusphere was higher on day 7 than on day 15 (Figure ES8). This increase could be attributed to the availability of cellulose-rich substrates from added straw (Cenini et al., 2016). However, the activity of the C-acquiring enzyme decreased on day 15, mainly due to the reduction in easily available substrates and the presence of recalcitrant lignin-dominated straw fractions (Zhao and Zhang, 2018). It is important to note that our case study was based on lab incubation, which only focused on short-term effects after straw incorporation. To evaluate the long-term effects, especially considering the

complex soil temperature and moisture variation, future in situ field studies are needed. Additionally, leucine-aminopeptidase activity in the detritusphere decreased from day 7 to day 15. Ma et al. (2018) found a correlation between the composition of the microbial proteolytic community, their proteolytic gene expression, protease activity, and plant nitrogen uptake. Consequently, the decrease in leucine-aminopeptidase activity may be attributed to a shift in enzyme production from degrading relatively labile polypeptides, such as leucine-aminopeptidase, to relatively complex compounds, such as chitinase, for N. The straw-induced detritusphere is generally the main pathway for translocating C and N between straw and soil (Vidal et al., 2021). Straw decomposition limits the hot moment of enzyme activities in the detritusphere (Kuzyakov and Blagodatskaya, 2015).

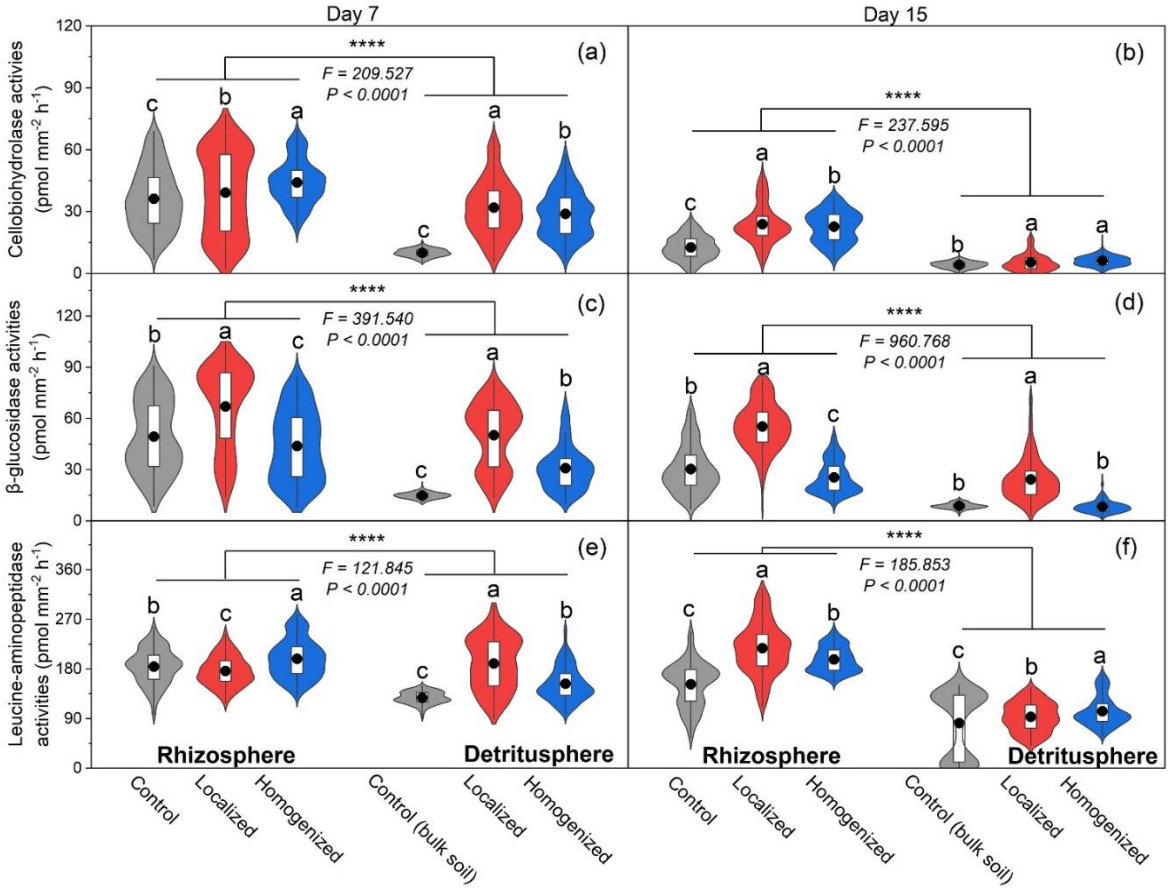

Figure ES8 *Rhizosphere and detritusphere enzyme activity in soil without straw (Control), with localized and homogenized straw incorporation on day 7 and 15.*

The activity of the C-acquiring enzyme in the rhizosphere was larger on day 7 than on day 15 in both straw localizations, with a notably higher effect size on day 15. This is likely due to strong nutrient competition between roots and microorganisms during the initial stage of straw decomposition, which stimulated enzyme activity in the rhizosphere (Peng et al., 2016). However, the enzyme activities responsible for C and N acquisition in the detritusphere were higher compared to those in the bulk soil. This indicates that the addition of exogenous organic matter (i.e. straw) has a significant stimulating effect on enzyme activity. Moreover, the amount of straw per unit volume in the localized soil is six times greater than that in the homogenized soil layer. As a result, the activity of C- and N-acquiring enzymes in the detritusphere of the localized straw treatment was significantly higher than that in the homogenized straw treatment.

1.4.2.2 AMF symbiosis, moisture and plant species

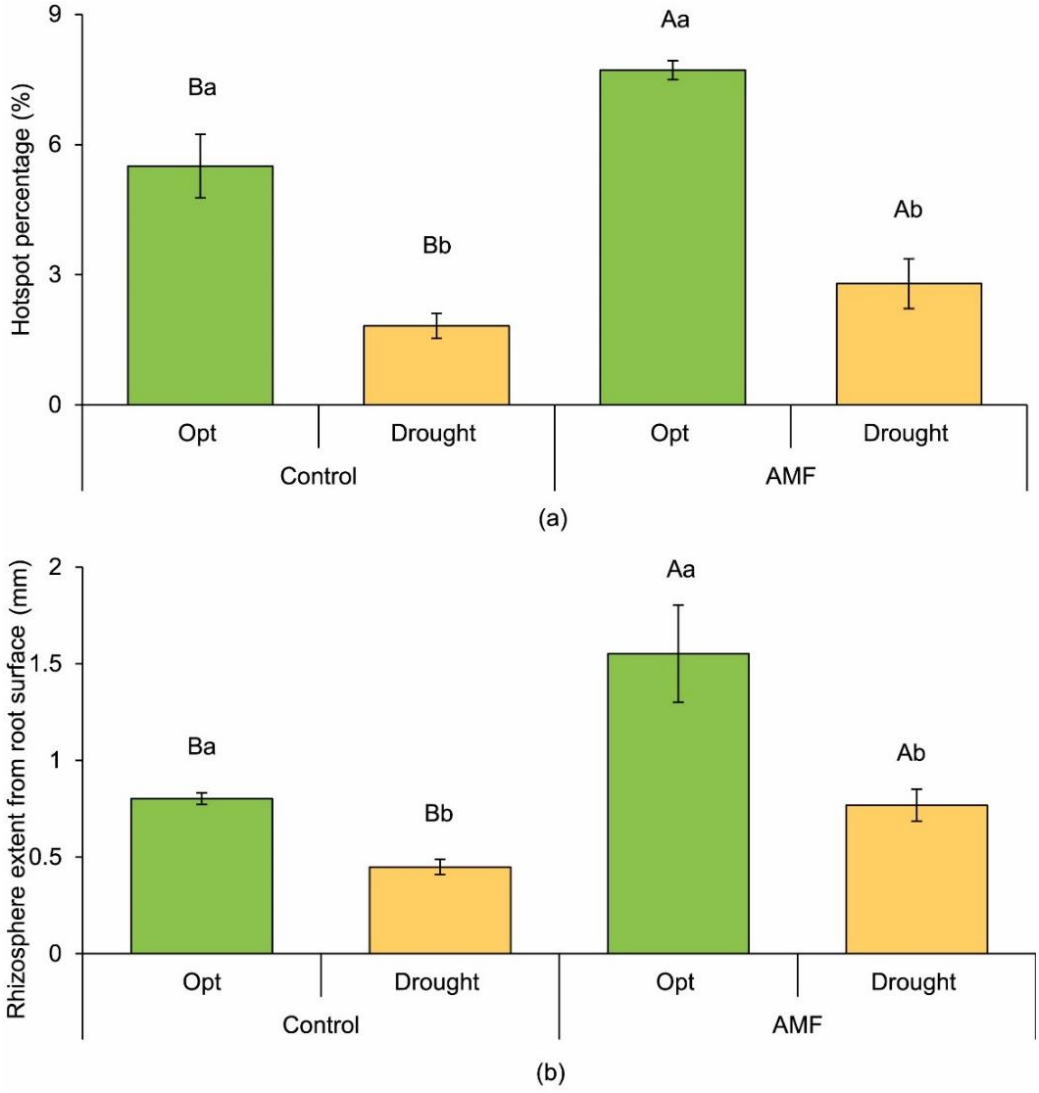

Figure ES9 *Hotspot percentage and rhizosphere extent under AMF and drought condition.*

Under drought conditions, the absence of AMF resulted in a threefold reduction of the acid phosphomonoesterase hotspot percentage compared to the optimum condition (Figure ES9). However, with AMF inoculation, the reduction was only twofold which indicating AMF boosts the P availability for plants in the enzymatic pathway by enlarging acid phosphomonoesterase hotspots and rhizosphere expansion. The presence of AMF increased the hotspot area by 40% and 53% in optimum and drought conditions, respectively, compared to conditions without AMF. This can be explained by the fact that AMF can play the role of root hairs and enlarge the overall extent of the absorbing surface of the host roots by 40 times (Pepe et al., 2016). Enzymatic hotspot area increased by 9% under drought conditions compared to optimum conditions with AMF symbiosis. Under water stress conditions, the rhizosphere size was reduced by 78% compared to the optimum condition. However, in plants inoculated with AMF, the rhizosphere extent was almost the same as that under the optimum condition (without AMF), and 71% higher than the non-mycorrhizal rhizosphere under the same stress. Thus, AMF stimulated microbial-mediated processes and extended hotspots around the roots under water stress by forming favorable microsites for microorganisms (Hoang et al., 2022).

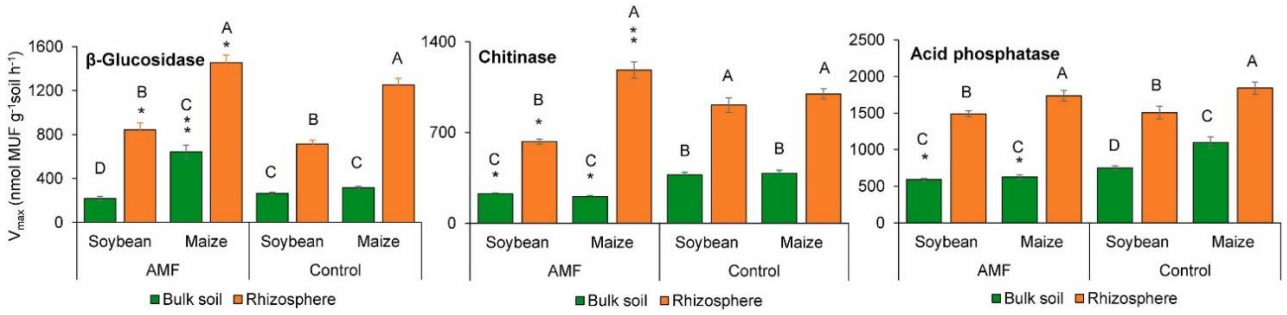

Figure ES10 *Activities of β-Glucosidase, chitinase and acid phosphatase in rooted soil and bulk soil of maize and soybean.*

The symbiotic relationship with AMF resulted in an increase in β-glucosidase activity in both maize and soybean (Figure ES10). However, it decreased chitinase activity in soybean, while there was no effect on acid phosphatase activities. The competition for carbon demand between free-living microorganisms and symbiotic AMF promoted the generation of β-glucosidase in the rhizosphere compared to the bulk soil. The opposite patterns of chitinase activity between maize and soybean can be explained by two mechanisms. Soybean roots synthesize isoflavonoids to attract N-fixing bacteria and form nodules, enabling the fixation of N2 from the atmosphere (Weston and Mathesius, 2013). These organic N compounds are released into the soybean rhizosphere as a source of inorganic N after microbial decomposition (Jalonen et al., 2009). Additionally, AMF hyphae transfer N from the surrounding area to the rooted zone (Sierra and Daudin, 2010). The rooted-zone microbial community prioritizes the uptake of available N source, which reduces the activation of chitinase synthesis in the soybean rhizosphere. Consequently, chitinase activities in soybean treated with AMF were lower than in the control. On the other hand, maize exhibited higher chitinase activity in the rhizosphere than in the bulk soil, indicating that the chitinase activity of microorganisms under AMF effects depends on the level of symbiosis between plants and fungi. In both (+AMF) and (-AMF) treatments, maize exhibited higher acid phosphatase activity than soybean. This finding may be attributed to the higher demand for phosphorus in maize during harvesting, which stimulated the production of acid phosphatase enzymes in both maize and microbes.

1.4.2.3 Dry-rewetting pattern

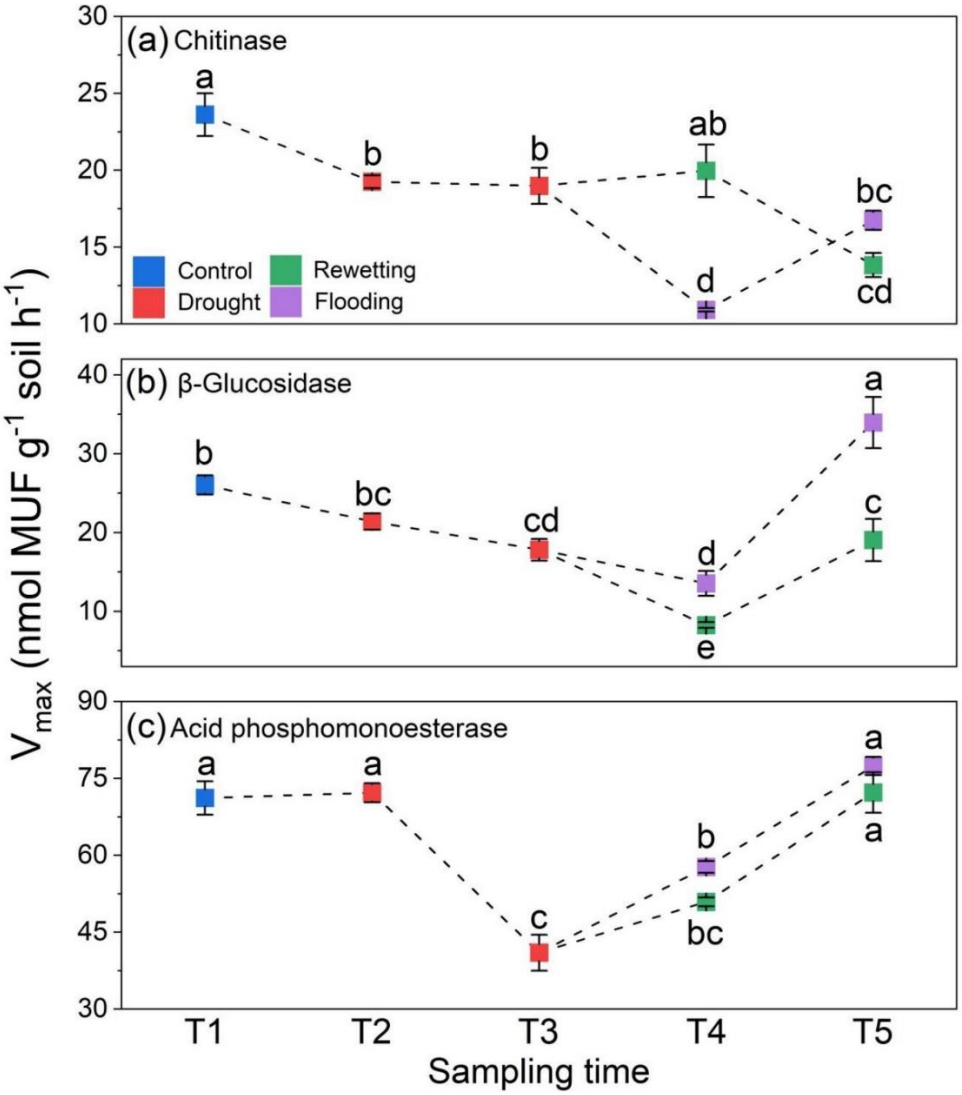

Figure ES11 *Soil enzyme activities of chitinase, β-D-glucosidase and acid phosphomonoesterase of 5 sampling times under rewetting and flooding patterns, respectively.*

Drought led to a decrease in enzyme activities (Figure ES11), indicating adverse effects on microbial functions, attributable to a significant decline in environmental water potential caused by drought, leading to an imbalance between the water potential inside and outside microbial cells (Schimel, 2018). Acid phosphomonoesterase exhibited a delayed response to drought, whereas prolonged water stress reduced all three enzyme activities. The initial decline in chitinase and β-glucosidase activities during drought suggests the decomposition of chitin and cellobiose, which are more vulnerable to water stress than phosphate ester hydrolysis. The soil in our study was sampled during the dry season and preconditioned to 60% of its water holding capacity before drought exposure. Thus, the reduction in enzyme activities during experimental drought may indicate a return to the initial natural state or reflect the historical memory of the original condition. The varied responses of enzyme activity reduction to drought underscore the significant influence of environmental and climate history on moisture response through microbial community selection (Evans et al., 2022).

All enzyme activities exhibited diverse responses to rewetting (Figure ES11). Abrupt rewetting and flooding possibly caused an osmotic shock for microbial communities, resulting in a further

decline in chitinase and β-glucosidase activities. Under flooding conditions (100% WHC), these activities reached even lower values compared to drought. However, acid phosphomonoesterase activities immediately increased after rewetting and flooding due to available labile organic P compounds (Nguyen and Marschner, 2005), serving as substrates for microorganisms. Compared to abrupt rewetting and flooding at T4, prolonged rewetting and flooding led to increased activities of β-glucosidase and acid phosphomonoesterase, irrespective of moisture levels. However, the response of chitinase activity to prolonged rewetting and flooding produced contrasting results. Prolonged flooding may boost chitinase activity due to soil denitrification, reducing nitrogen availability for microbial demand and stimulating chitinase production (Tomasek et al., 2019; Luo et al., 2019). Conversely, rewetting might trigger the release of osmolytes rich in nitrogen compounds, resulting in reduced chitinase activity (Csonka, 1989). Collectively, enzyme activity recovery after prolonged rewetting while flooding induced a greater recovery of enzyme activities compared to rewetting (Wang et al., 2023b).

1.4.2.4 Soil warming, increasing salinity and microbial growth stage

The enzyme activities increased up to 2.9 times after 48 hours of incubation of the unamended soil, compared to the initial state of the soil. This increase can be attributed to the addition of a nitrogen and phosphorus nutrient solution prior to soil incubation, resulting in a higher increase in C-acquiring enzyme activities compared to N- and P-acquiring enzyme activities. Furthermore, salinity alone did not significantly affect the activities of β-Glu, Leu, and Phos after 48 hours of basal respiration in non-amended soil. This suggests that the metabolic processes associated with these enzymes are not altered by salinity. However, upon the addition of glucose, all measured enzyme activities increased by 68-336% within the first 12 hours, indicating preparation for microbial growth (Mason-Jones et al., 2022). Notably, the activities of enzymes that acquire C (β-Glu, Cello) increased more strongly than those that acquire N (Leu) and P (Phos), despite the input of external labile carbon (glucose). Subsequently, all measured enzyme activities remained stable or slightly decreased until the end of the experiment (Figure ES12), indicating that substrate demand remained constant during the microbial growth and retardation stage. The dynamics of enzyme activity during microbial growth and retardation did not change with warming and increased salinity, suggesting that the microbial community is relatively resistant to moderate environmental changes (Wang et al., 2023b).

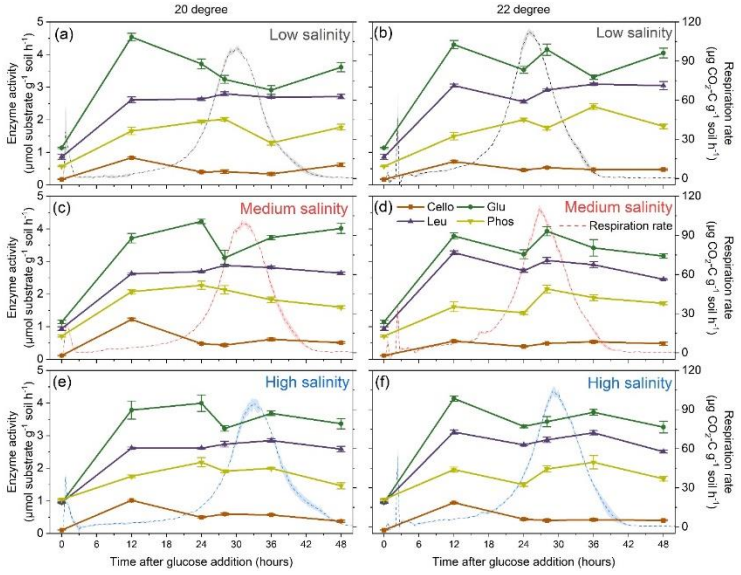

Figure ES12 *Glucose induced soil respiration rate and soil enzyme activity (V_{max}) of cellobiohydrolase (Cello), β-D-glucosidase (Glu), leucine aminopeptidase (Leu) and acid phosphomonesterase (Phos) at 20 and 22 ℃*

1.4.2.5 Substrate quality and decomposition stage

The activity of α-GLU increased after substrate addition, especially with G+S, indicating a quick microbial response to easily available substrates (Figure ES13). The higher α-Glu activity on day 1 suggests early starch decomposition compared to the S treatment, as α-Glu is a specific enzyme for starch decomposition (German et al., 2011). This implies that glucose addition could prime the soil organisms (Kuzyakov, 2010), thus accelerating starch decomposition. In contrast, β-Glu activity showed a significant increase on day 6, indicating a change in microbial community dynamics or substrate utilization patterns. This is because the glucose substrate was depleted initially, resulting in the release of more β-Glu to obtain more labile substrate for microbial growth at a later stage. Chit activity initially declined, possibly due to the complexity of chitin as a substrate. However, it stabilized thereafter, with higher activity observed with the S treatment, indicative of distinct microbial preferences. The activity of Phos increased significantly after the addition of substrate, indicating a microbial response to phosphorus-containing compounds. The G+S treatment showed sustained higher activity, suggesting synergistic substrate effects.

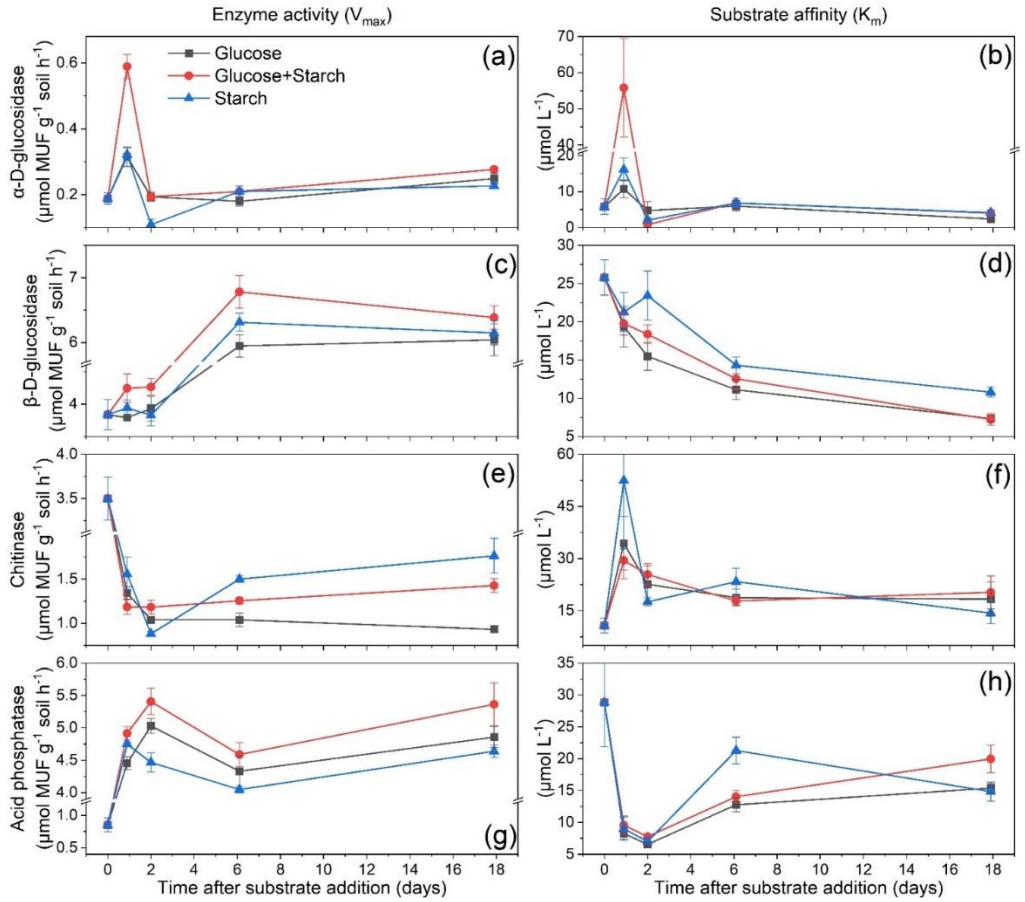

Figure ES13 *Soil enzyme activity (V_{max}) and substrate affinity (K_m) of α-D-glucosidase, β-D-glucosidase, chitinase and acid phosphatase.*

Regardless of substrate quality, oxidase activity exhibited a similar trend during substrate decomposition (Figure ES14). This suggests that oxidative enzymes are less substrate-specific than

hydrolytic enzymes. Peroxidases produce oxygen radicals that can attack a diverse array of substrates (Schnecker et al., 2019; Sinsabaugh, 2010). The correlation between peroxidase and total oxidative activity demonstrates the interdependence of enzymatic pathways in response to substrate availability. Additionally, oxidase activities were higher in the G treatment compared to the G+S and G treatments from day 6 to 18, suggesting that substrate limitation may stimulate oxidase activity. Microorganisms frequently transition to oxidative enzymes to break down complex organic material after labile substrates are exhausted (McDaniel et al., 2014). The enzyme activity dynamics results show that substrate addition can increase enzyme activity. However, hydrolase activity responds more specifically and strongly to substrate decomposition with different qualities compared to oxidase activity.

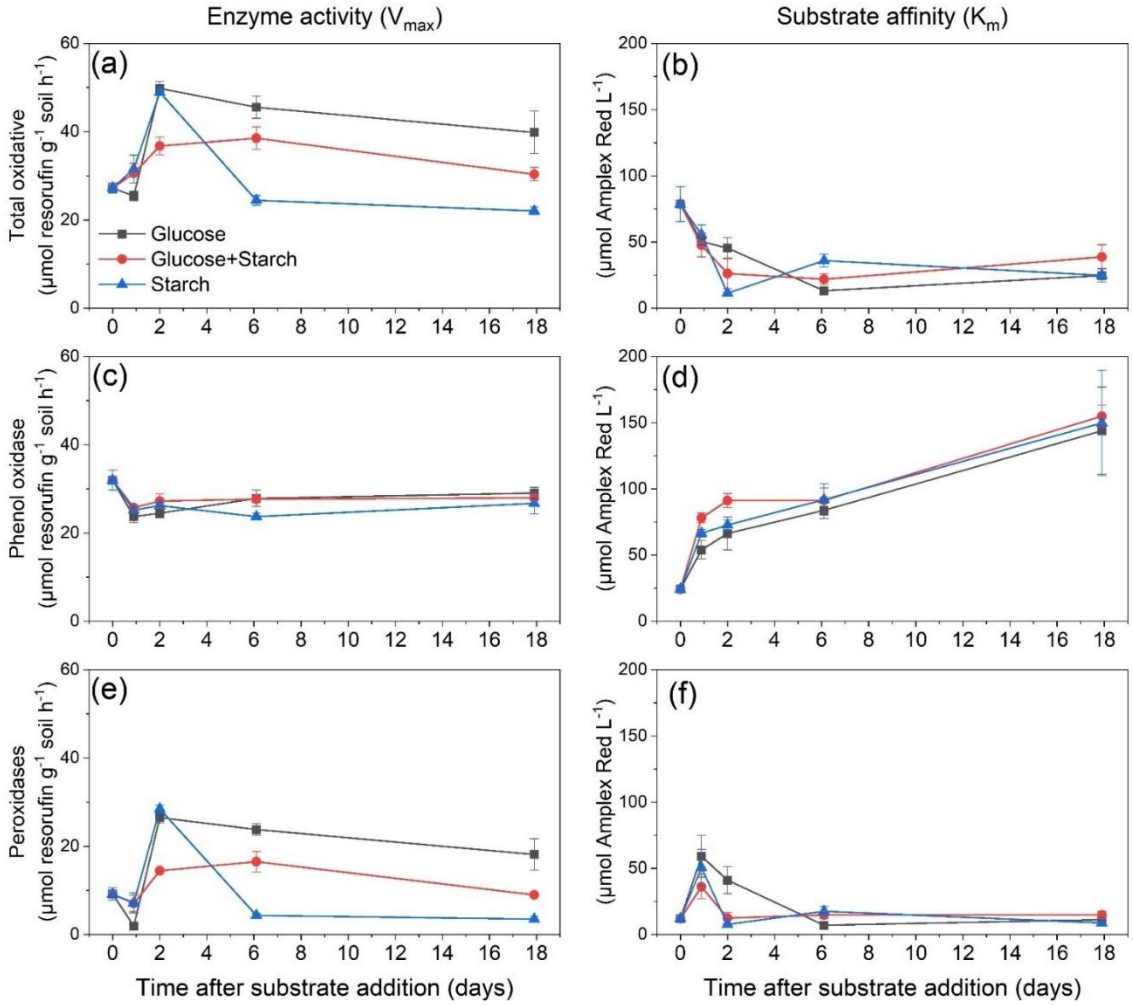

Figure ES14*. Soil gross oxidative enzyme activities and substrate affinity of total oxidative, phenol oxidase, and peroxidase.*

1.4.3 Effect of biotic and abiotic factors on soil organic matter decomposition

1.4.3.1 Glucose exudation response to AMF symbiosis and moisture

Under optimal conditions, glucose was evenly exuded along the root and root tips (Figure ES15). However, drought significantly reduced glucose exudation, resulting in an overall decrease in exudation (Liese et al., 2018), particularly from the mature part of the root. Interestingly, AMF greatly enhanced glucose hotspots compared to non-mycorrhizal plants. Glucose exuded from roots is

characterized by its lability and ready utilization, and can be directly absorbed by AMF as a source of carbon (Bücking et al., 2008), stimulating AMF hyphae branching and lengthening. Conversely, AMF may contribute to glucose release through the expression of β-glucosidase, mobilizing oligo- and polysaccharides, or glycosylated compounds. Therefore, the enhanced detected glucose signal could be attributed to the concomitant direct secretion from plant roots or produced as a final product of β-glucosidase activity within the rhizosphere.

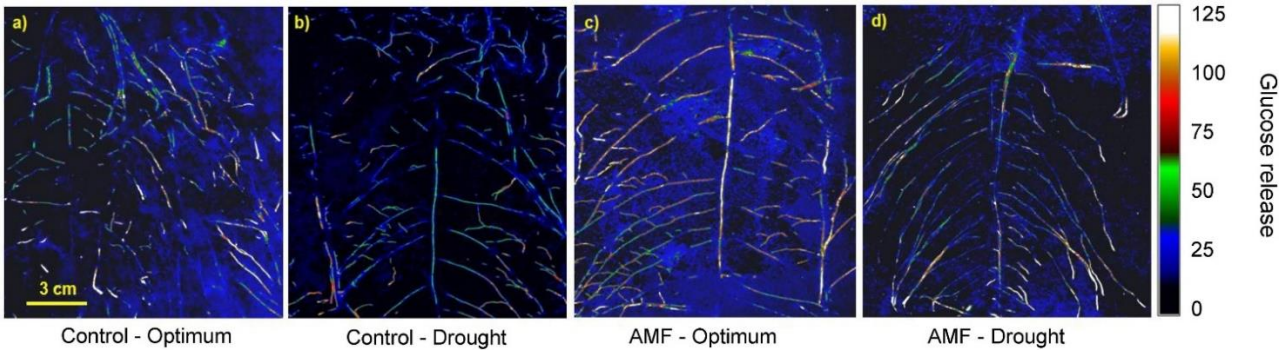

Figure ES15 *The exudation of glucose (nmol cm^{-2}) along root and root tips shown in white color.*

1.4.3.2 Substrate affinity response to soil rewetting level

The substrate affinity (K_m) remained stable after an abrupt change in soil moisture, both during prolonged drought and after rewetting (Figure ES16). This observation suggests that the soil microbial community adopts a survival strategy following drought, allocating greater energy and nutrients towards maintaining the efficiency of enzyme-substrate interactions to support biomass accumulation. The stronger response of SIR to rewetting compared to drought could be attributed to the C use efficiency of the dominated microbial communities (Figure 2-6). The study found a positive correlation between the SIR pattern and the qCO_2 (Figure 2-7), suggesting that microbial communities prioritize maintaining respiration processes over cell growth and reproduction (Sun et al., 2017). Additionally, there may be a shift towards less C-efficient groups in the microbial community. This resulted in longer substrate turnover times for chitinase and β-glucosidase after rewetting compared to drought (Figure 2-5). However, according to Nguyen and Marschner (2005), the release of labile organic P immediately after abrupt rewetting accelerated the activities and catalytic efficiency of acid phosphomonoesterase. This led to a shorter substrate turnover time compared to prolonged drought. Microbial responses to dry-rewetting are specific to enzymes and dependent on the level of rewetting. Enzyme systems are more impacted by rewetting at 60% WHC, while enzyme synthesis is more affected by flooding at 100% WHC (Wang et al., 2023b).

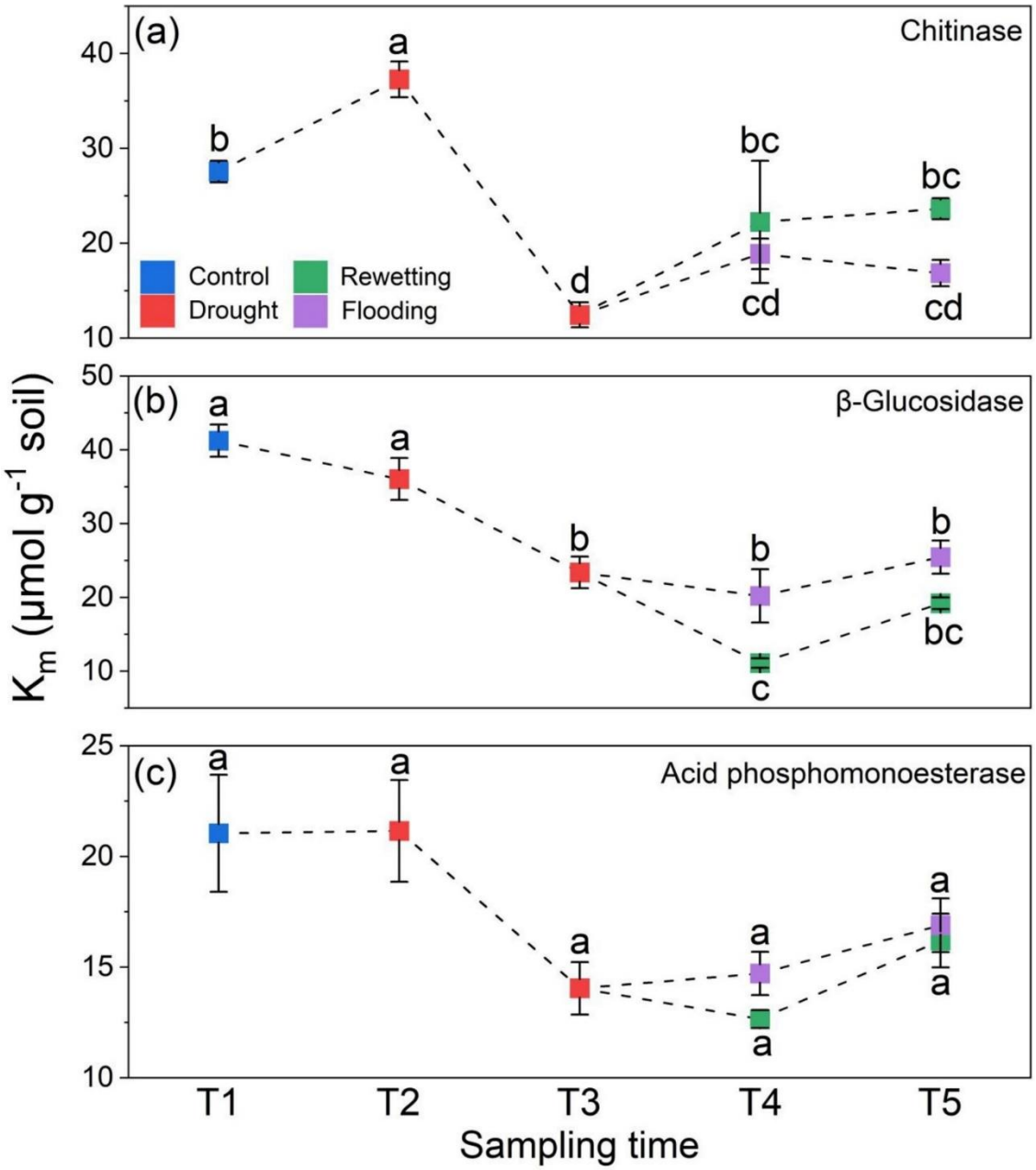

Figure ES16 *Soil enzyme substrate affinities (K_m) of chitinase, β-D-glucosidase and acid phosphomonoesterase of 5 sampling times under rewetting and flooding patterns, respectively.*

1.4.3.3 Interactive effect of increasing salinity and warming on respiration and heat release

The impact of salinity on soil respiration and heat release is highly dependent on the availability of organic substrate and the state of microbial activity (Figure ES17). In non-amended soil, increasing salinity did not have a significant effect on either respiration or heat release (Figure 5-1), indicating a certain level of resilience in the microbial community to stress induced by salinity. According to Blagodatskaya et al. (2007), the limited activity and sensitivity of microbial processes to changes in salinity levels may be attributed to the absence of labile organic matter, such as glucose. Increasing salinity significantly delayed all phases of microbial growth on glucose, including lag-time, exponential growth, time of the peak, and growth retardation, as monitored by respiration and heat release (Figure 5-4). This delay can be attributed to osmotic stress imposed on microbial cells and

substrate availability (Rath and Rousk, 2015). Although the soil pH decreased by only 1.8%, it had a significant impact on the microbial growth. High levels of salinity can disrupt the osmotic balance within cells, which in turn affects their physiological functions. This osmotic stress can lead to a decrease in microbial metabolic activity, including glucose decomposition.

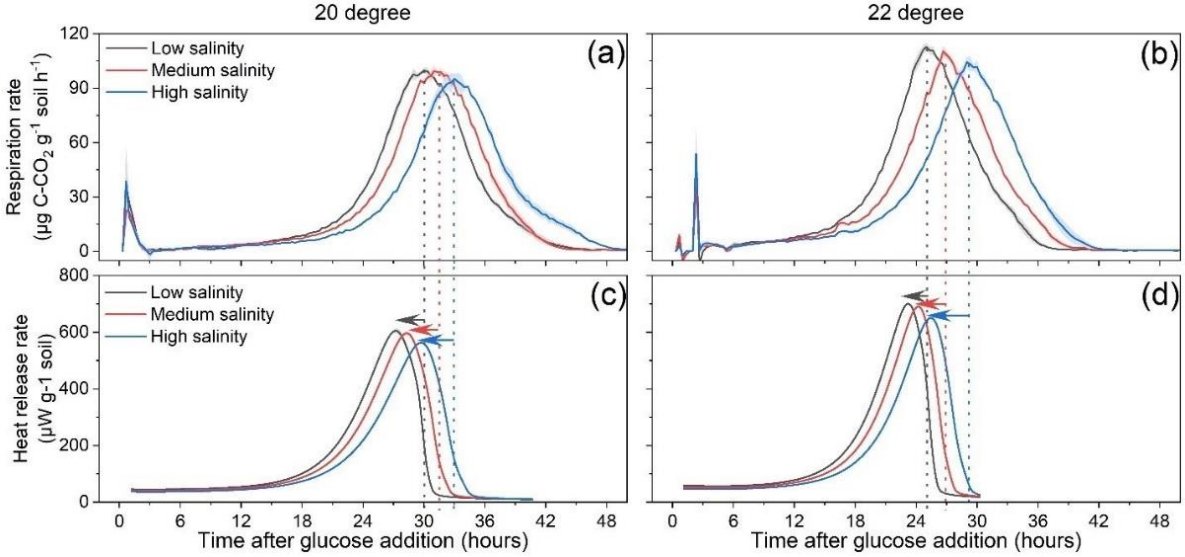

Figure ES17 *Glucose induced soil respiration rate and heat release rate under 3 salinity levels at 20 and 22 ℃.*

1.4.3.4 Decomposition dynamic response to substrate quality

The respiration rate and heat flow associated with starch exhibited a delay compared to glucose at equivalent concentrations of carbon substrate addition (Figure ES17), implying a greater difficulty in starch decomposition relative to glucose, suggesting the involvement of distinct metabolic pathways and enzymatic processes in their breakdown (Gunina and Kuzyakov, 2015). The decomposition of starch and glucose in soil is characterized by unique dynamics in the patterns of heat release rate and respiration rate. The degradation of starch begins with an early surge in heat release rate, which is caused by the enzymatic breakdown of its complex polysaccharide structure into labile carbon substrates such as glucose. This breakdown results in heat production as a byproduct (Baker and Allison, 2017). However, the respiration rate showed a delay, indicating a microbial adaptation delay in utilizing the labile carbon substrate for energy production. In contrast, glucose decomposition showed a simultaneous increase in heat release and respiration rates, indicating its direct metabolism by soil microbes without the need for extensive enzymatic breakdown.

When glucose and starch were added together, the respiration and heat release rates remained constant for three days after the glucose decomposition slowed down, indicating that starch decomposition began earlier compared to when only starch was added. This observation suggests that glucose decomposition acted as a catalyst for starch decomposition in soil ecosystems. This phenomenon may be attributed to various mechanisms, such as enzyme production, increased microbial activity, and enhanced nutrient availability resulting from glucose decomposition (Blagodatskaya et al., 2009; Dungait et al., 2012). The presence of glucose stimulates microorganisms to produce more enzymes for starch breakdown, thereby accelerating decomposition rates. The decomposition of glucose releases nutrients and energy that can support microbial growth and activity,

which may accelerate the decomposition of starch and other recalcitrant substrates in the soil. This finding highlights the impact of labile carbon substrates, such as glucose, on the decomposition of recalcitrant carbon substrates, such as starch, in soil ecosystems.

1.4.4 Effect of biotic and abiotic factors on carbon use efficiency and calorespirometric ratio

1.4.4.1 CUE and CR ratio response to microbial growth stage, increasing salinity and warming

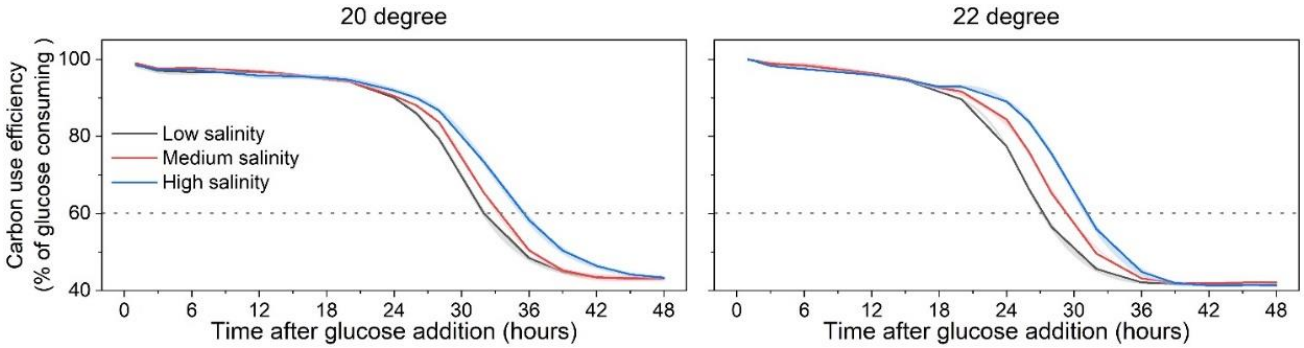

Figure ES18 *Carbon use efficiency during the glucose decomposition dynamic under salinity and warming condition.*

The decrease in CUE during the exponential growth and retardation phase was postponed by increasing salinity (Figure ES 18). This delay can be attributed to the slowdown of glucose consumption and microbial growth caused by the higher salinity. However, the CUE estimated during exponential growth before substrate exhaustion essentially exceeded the maximal values of growth on glucose in pure microbial cultures (Sinsabaugh et al., 2013). The estimated CUE at the peak of CO_2 release varied between 65-70%, indicating a slight overestimation but aligning well with the actual CUE. The contribution of priming, i.e. SOM-C co-decomposed with glucose-C, was not considered as the added glucose was unlabeled. However, any positive priming effect would have decreased the CUE values, which was not observed in our study. The CUE values only declined below the 60% threshold after glucose uptake reached 95-98%, which corresponds to the actual CUE. Therefore, it is suggested that CUE estimation should be performed when the values stabilize, which occurs after 36-42 hours (at 22 ℃). Additionally, at the end of the retardation stage, the CUE remained stable at approximately 0.42 under limited substrate availability. This value is slightly higher than the theoretical value of approximately 0.30 observed in multi-resource-limited natural systems (Sinsabaugh et al., 2013), which suggests a potential overestimation of CUE even during the retardation stage until the whole amount of substrate is metabolized. During the growth preparation and exponential growth stages, CUE was overestimated, which aligns with the apparent CUE. However, during the retardation stage, CUE decreased to around 60%, indicating a closer correspondence to the actual CUE.

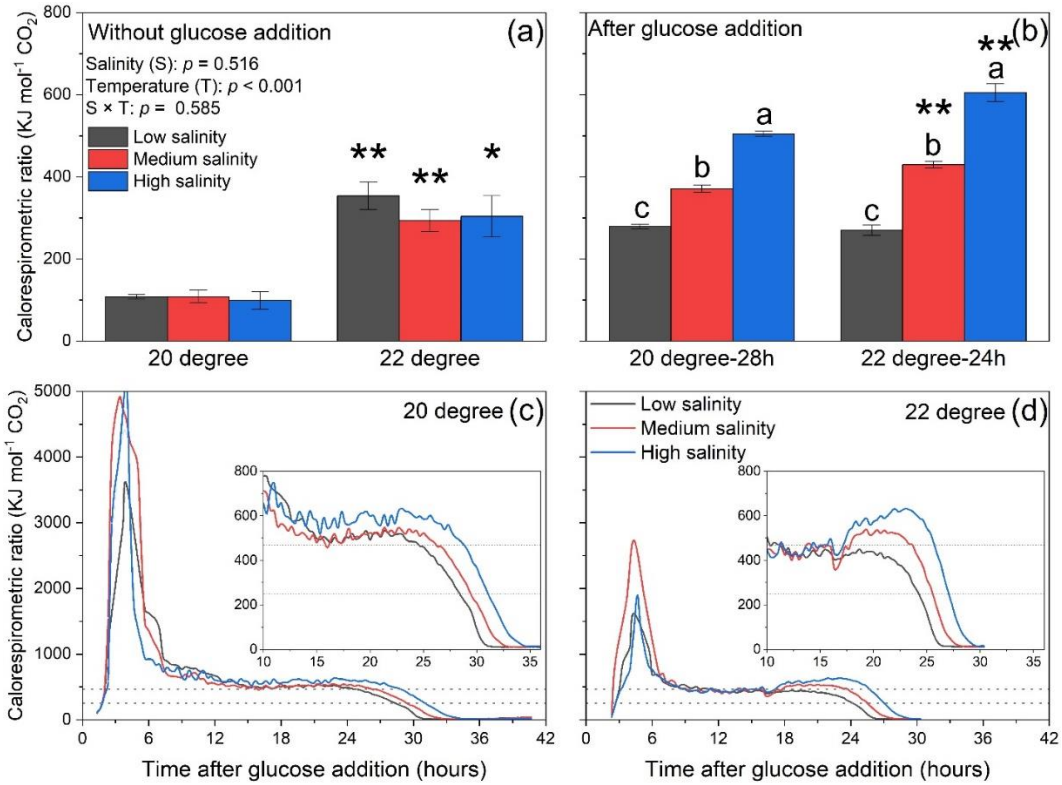

Figure ES19 *Calorespirometric ratio obtained before glucose addition, 28 hours after glucose addition at 20 ℃ and 24 hours after glucose addition at 22 ℃, and calorespirometric ratio dynamic after glucose addition at 20 and 22℃.*

At the onset of glucose addition, the CR ratio exhibited a sharp increase (Figure ES19), suggesting the allocation of substrate and energy towards processes beyond respiration (Hansen et al., 2004). Within the initial 6 hours following glucose addition, the CR ratio significantly surpassed the oxycaloric equivalent (469 kJ mol^{-1} CO_2) for aqueous glucose combustion, indicating either additional heat release from accompanying processes or a lower respiration rate compared to the complete oxidation of glucose. This surplus heat might result from priming due to the metabolism of highly reduced substrates other than carbohydrates or the incomplete oxidation of the substrate to CO_2 (Chakrawal et al., 2020). Moreover, this excess heat could also be directed towards the synthesis of storage compounds or the enhancement of enzyme activity. Throughout the exponential growth phase, the CR ratio remained stable and generally corresponded to 469 kJ mol-1 CO_2 (Geyer et al., 2019). Notably, increasing salinity subsequently augmented the CR ratio by 81-126% during both the exponential growth and retardation phases. After reaching the peak of respiration and entering the retardation stage, the CR ratio gradually declined to below 250 kJ mol^{-1} CO_2, indicative of a stronger reduction in heat production compared to complete glucose oxidation. Thus, during the retardation stage, the added glucose was not entirely oxidized to CO_2 under the conditions of fermentation or combined fermentation and aerobic decomposition (Chakrawal et al., 2021).

1.4.4.2 The CUE and calorespirometric ratio response to different substrate quality

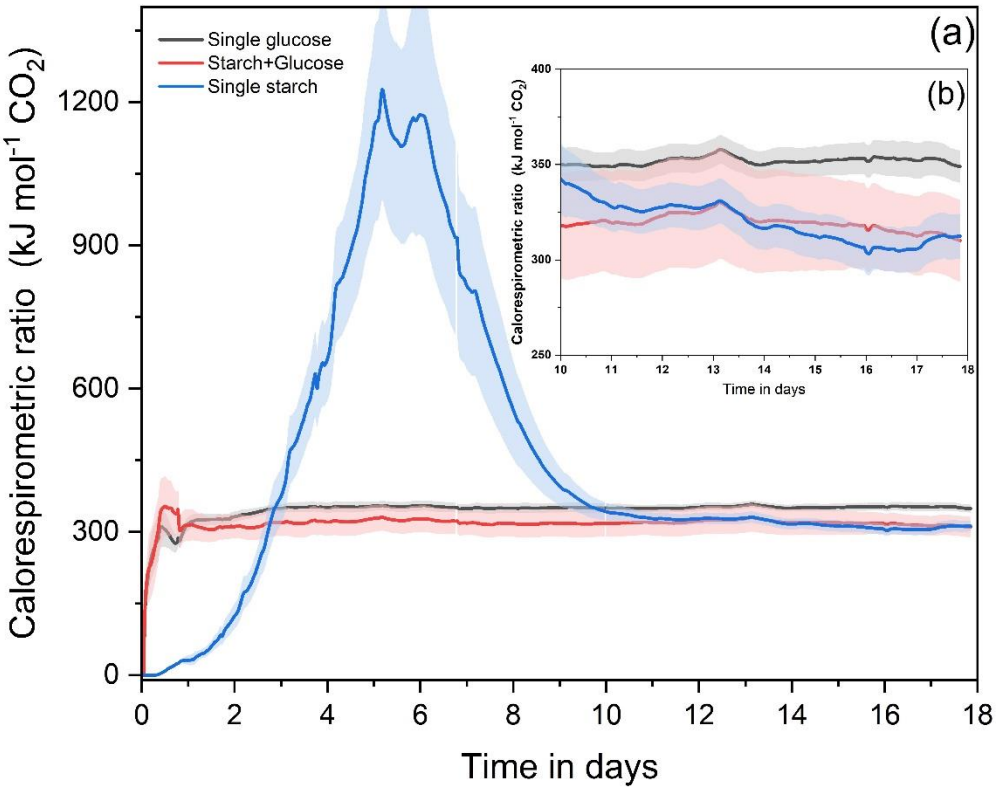

Figure ES20 *Calorespirometric ratio dynamic after substrate addition. Line and shadow represent mean ± standard error (n =3).*

The Carbon Use Efficiency of substrate addition with different qualities exhibited varying patterns concerning substrate decomposition dynamics. The CUE of the G and G+S treatments exceeded 79% on day 1, whereas the CUE of the S treatment remained higher than 92% until day 6. The higher CUE values observed before the added substrate began decomposing indicate a microbial shift to the growth preparation stage, where a substantial portion of substrate and energy is directed towards the synthesis of storage compounds or specific enzymes not directly associated with CO2 production (Mason-Jones et al., 2022). The notable increase in MBC on day 1 supports this observation. The CUE of S surpassed 100%, possibly due to lower substrate-induced respiration at the initial stage following starch addition (Figure ES7). This led to SIR rates lower than basal respiration, resulting in negative respired carbon. The estimation prior to the peak of SIR indicated overestimated values (above 60%), corresponding to apparent rather than real CUE (Sinsabaugh et al., 2013). The CUE declined after the peak of respiration rate until the end of the experiment, suggesting that soil microorganisms allocated more substrate and energy towards respiration rather than the synthesis of storage compounds (Dijkstra et al., 2015). Furthermore, MBC also decreased during the later stage of incubation, potentially induced by limited substrate and nutrient resources, implying microbial death, which can further decrease the CUE.

On the other hand, at the beginning of substrate addition in the G and G+S treatments, the CR ratio showed a rapid increase (Figure ES20), indicating a stronger allocation of substrate and energy to processes other than respiration. Following this, the CR ratio remained stable and lower than the oxycaloric equivalent (469 kJ mol^{-1} CO_2) for aqueous glucose combustion until the end of the incubation. This suggests a balance between the allocation of substrate and energy to processes and respiration, and a higher respiration rate compared to the complete oxidation of the substrate. However,

the CR ratio of the S treatment gradually increased to 1200 kJ mol^{-1} CO_2 by day 5 and remained around 1100 kJ mol^{-1} CO_2 from day 5 to day 7, exceeding the oxycaloric equivalent (469 kJ mol^{-1} CO_2) for aqueous glucose combustion. This indicates either additional heat release from accompanying processes or a lower respiration rate compared to the complete oxidation of the substrate. The additional heat could result from priming due to the metabolism of substrates with lower availability other than carbohydrates, or the incomplete oxidation of the substrate to CO_2 (Chakrawal et al., 2020). Additionally, the excess heat generated can be used for synthesizing storage compounds or enhancing enzyme activity. The simultaneous occurrence of CR ratio peaks of S treatment suggests that the decomposition of recalcitrant carbon substrates requires more enzymes and energy. Finally, the CR ratio of all treatments remained below the oxycaloric equivalent (469 kJ mol^{-1} CO_2) from day 10 to day 18, indicating a significant reduction in heat production compared to complete glucose oxidation. This suggests that the added substrate was not entirely oxidized to CO_2 under fermentation or combined fermentation and aerobic decomposition conditions (Chakrawal et al., 2021). Thus, our third hypothesis was confirmed: the CUE and CR ratio change with the microbial growth stage.

1.5 Conclusions

This thesis investigates the impact of abiotic and biotic factors on soil enzyme activity, organic matter decomposition, and carbon use efficiency. Specifically, the incorporation of straw into soil creates a hotspot for soil enzyme activity, known as the detritusphere, which enhances enzyme activities in both the rhizosphere and soil profile. However, homogenized straw incorporation intensifies nutrient competition between microorganisms and roots, thereby limiting plant performance. Additionally, soils subjected to dry-rewetting cycles trigger microbial activity recovery, while flooding primarily affects enzyme synthesis. Moreover, the symbiosis between plants and arbuscular mycorrhizal fungi (AMF) creates favorable microsites, enhancing glucose release and enzyme activities in the rhizosphere and mycorrhizosphere, which aids resistance to drought stress. The nutrient demands of different plant species influence the impact of AMF on enzyme activity characteristics in the rhizosphere. Furthermore, salinity negatively affects soil respiration and microbial growth, particularly under conditions of warming or organic matter input, with labile substrates exacerbating these negative effects. The dynamics of enzyme activity and microbial carbon use efficiency correlate with microbial growth stages. Labile carbon substrates are more readily utilized by soil microbes compared to recalcitrant ones, and their presence can accelerate the decomposition of recalcitrant carbon substrates in soil.

Overall, this thesis demonstrates the variable effects of multiple abiotic and biotic factors on soil enzyme activity and organic matter decomposition through soil incubation experiments, 2D imaging, and soil sample measurements. The importance of multi-factor interactions on soil microbial processes, enzymatic mobilization, and organic matter decomposition is emphasized. Further studies are suggested to focus on modeling the effects of abiotic and biotic factors on soil processes and predicting potential outcomes under changing climatic conditions.

1.6 Reference

Allison, S. D., Chacon, S. S., & German, D. P. (2014). Substrate concentration constraints on microbial decomposition. Soil Biology and Biochemistry, 79, 43-49.
Anderson, J. P., & Domsch, K. H. (1978). A physiological method for the quantitative measurement of microbial biomass in soils. Soil biology and biochemistry, 10(3), 215-221.
Bais, H. P., Weir, T. L., Perry, L. G., Gilroy, S., & Vivanco, J. M. (2006). The role of root exudates in rhizosphere interactions with plants and other organisms. Annu. Rev. Plant Biol., 57, 233-266.
Bilyera, N., Kuzyakova, I., Guber, A., Razavi, B. S., & Kuzyakov, Y. (2020). How "hot" are hotspots: Statistically localizing the high-activity areas on soil and rhizosphere images. Rhizosphere, 16, 100259.
Blagodatskaya, E., & Kuzyakov, Y. (2013). Active microorganisms in soil: critical review of estimation criteria and approaches. Soil Biology and Biochemistry, 67, 192-211.
Blagodatskaya, E. V., Blagodatsky, S. A., Anderson, T. H., & Kuzyakov, Y. (2009). Contrasting effects of glucose, living roots and maize straw on microbial growth kinetics and substrate availability in soil. European Journal of Soil Science, 60(2), 186-197.
Blagodatskaya, E. V., Blagodatsky, S. A., Anderson, T. H., & Kuzyakov, Y. (2007). Priming effects in Chernozem induced by glucose and N in relation to microbial growth strategies. applied soil ecology, 37(1-2), 95-105.
Blagodatskaya, E., Blagodatsky, S., Dorodnikov, M., & Kuzyakov, Y. (2010). Elevated atmospheric CO_2 increases microbial growth rates in soil: results of three CO2 enrichment experiments. Global Change Biology, 16(2), 836-848.
Blagodatsky, S., Blagodatskaya, E., Yuyukina, T., & Kuzyakov, Y. (2010). Model of apparent and real priming effects: linking microbial activity with soil organic matter decomposition. Soil biology and biochemistry, 42(8), 1275-1283.
Brangarí, A. C., Manzoni, S., & Rousk, J. (2020). A soil microbial model to analyze decoupled microbial growth and respiration during soil drying and rewetting. Soil Biology and Biochemistry, 148, 107871.
Brolsma, K. M., Vonk, J. A., Hoffland, E., Mulder, C., & de Goede, R. G. (2015). Effects of GM potato Modena on soil microbial activity and litter decomposition fall within the range of effects found for two conventional cultivars. Biology and Fertility of Soils, 51, 913-922.
Brundrett, M., & Tedersoo, L. (2019). Misdiagnosis of mycorrhizas and inappropriate recycling of data can lead to false conclusions. New Phytologist, 221(1), 18-24.
Butcher, K. R., Nasto, M. K., Norton, J. M., & Stark, J. M. (2020). Physical mechanisms for soil moisture effects on microbial carbon-use efficiency in a sandy loam soil in the western United States. Soil Biology and Biochemistry, 150, 107969.
Bär, M., Hardenberg, J., Meron, E., & Provenzale, A. (2002). Modelling the survival of bacteria in drylands: the advantage of being dormant. Proceedings of the Royal Society of London. Series B: Biological Sciences, 269(1494), 937-942.
Bücking, H., Abubaker, J., Govindarajulu, M., Tala, M., Pfeffer, P. E., Nagahashi, G., ... & Shachar-Hill, Y. (2008). Root exudates stimulate the uptake and metabolism of organic carbon in germinating spores of Glomus intraradices. New Phytologist, 180(3), 684-695.
Cameron, C. (2007). MicroResp™ Technical Manual—A Versatile Soil Respiration System. Macaulay Institute, Craigiebuckler, Aberdeen, Scotland, UK.
Campbell, C. D., Chapman, S. J., Cameron, C. M., Davidson, M. S., & Potts, J. M. (2003). A rapid microtiter plate method to measure carbon dioxide evolved from carbon substrate amendments so as to determine the physiological profiles of soil microbial communities by using whole soil. Applied and environmental microbiology, 69(6), 3593-3599.
Castellano, M. J., Mueller, K. E., Olk, D. C., Sawyer, J. E., & Six, J. (2015). Integrating plant litter quality, soil organic matter stabilization, and the carbon saturation concept. Global change biology, 21(9), 3200-3209.

Cenini, V. L., Fornara, D. A., McMullan, G., Ternan, N., Carolan, R., Crawley, M. J., ... & Lavorel, S. (2016). Linkages between extracellular enzyme activities and the carbon and nitrogen content of grassland soils. Soil Biology and Biochemistry, 96, 198-206.

Chakrawal, A., Herrmann, A. M., & Manzoni, S. (2021). Leveraging energy flows to quantify microbial traits in soils. Soil Biology and Biochemistry, 155, 108169.

Chakrawal, A., Herrmann, A. M., Šantrůčková, H., & Manzoni, S. (2020). Quantifying microbial metabolism in soils using calorespirometry—a bioenergetics perspective. Soil Biology and Biochemistry, 148, 107945.

Cheng, L., Booker, F. L., Tu, C., Burkey, K. O., Zhou, L., Shew, H. D., ... & Hu, S. (2012). Arbuscular mycorrhizal fungi increase organic carbon decomposition under elevated CO2. Science, 337(6098), 1084-1087.

Cheng, W., Parton, W. J., Gonzalez-Meler, M. A., Phillips, R., Asao, S., McNickle, G. G., ... & Jastrow, J. D. (2014). Synthesis and modeling perspectives of rhizosphere priming. New Phytologist, 201(1), 31-44.

Condron, L., Stark, C., O'Callaghan, M., Clinton, P., & Huang, Z. (2010). The role of microbial communities in the formation and decomposition of soil organic matter. Soil microbiology and sustainable crop production, 81-118.

Csonka, L. N. (1989). Physiological and genetic responses of bacteria to osmotic stress. Microbiological reviews, 53(1), 121-147.

Cui, Y., Fang, L., Deng, L., Guo, X., Han, F., Ju, W., ... & Zhang, X. (2019). Patterns of soil microbial nutrient limitations and their roles in the variation of soil organic carbon across a precipitation gradient in an arid and semi-arid region. Science of the Total Environment, 658, 1440-1451.

de Nijs, E. A., Hicks, L. C., Leizeaga, A., Tietema, A., & Rousk, J. (2019). Soil microbial moisture dependences and responses to drying–rewetting: The legacy of 18 years drought. Global Change Biology, 25(3), 1005-1015.

Dungait, J. A., Hopkins, D. W., Gregory, A. S., & Whitmore, A. P. (2012). Soil organic matter turnover is governed by accessibility not recalcitrance. Global Change Biology, 18(6), 1781-1796.

Evans, S., Allison, S., & Hawkes, C. (2022). Microbes, memory and moisture: Predicting microbial moisture responses and their impact on carbon cycling. Functional Ecology, 36(6), 1430-1441.

Evans, S. E., & Wallenstein, M. D. (2012). Soil microbial community response to drying and rewetting stress: does historical precipitation regime matter? Biogeochemistry, 109, 101-116.

Fanin, N., Mooshammer, M., Sauvadet, M., Meng, C., Alvarez, G., Bernard, L., ... & Nottingham, A. T. (2022). Soil enzymes in response to climate warming: Mechanisms and feedbacks. Functional ecology, 36(6), 1378-1395.

French, D. (1973). Chemical and physical properties of starch. Journal of animal science, 37(4), 1048-1061.

German, D. P., Weintraub, M. N., Grandy, A. S., Lauber, C. L., Rinkes, Z. L., & Allison, S. D. (2011). Optimization of hydrolytic and oxidative enzyme methods for ecosystem studies. Soil Biology and Biochemistry, 43(7), 1387-1397.

Geyer, K. M., Dijkstra, P., Sinsabaugh, R., & Frey, S. D. (2019). Clarifying the interpretation of carbon use efficiency in soil through methods comparison. Soil Biology and Biochemistry, 128, 79-88.

Guggenberger, G., Elliott, E. T., Frey, S. D., Six, J., & Paustian, K. (1999). Microbial contributions to the aggregation of a cultivated grassland soil amended with starch. Soil Biology and Biochemistry, 31(3), 407-419.

Gunina, A., & Kuzyakov, Y. (2015). Sugars in soil and sweets for microorganisms: review of origin, content, composition and fate. Soil Biology and Biochemistry, 90, 87-100.

Hoang, D. T. T., Rashtbari, M., Anh, L. T., Wang, S., Tu, D. T., Hiep, N. V., & Razavi, B. S. (2022). Mutualistic interaction between arbuscular mycorrhiza fungi and soybean roots enhances

drought resistant through regulating glucose exudation and rhizosphere expansion. Soil Biology and Biochemistry, 171, 108728.
Hodge, A. (2001). Arbuscular mycorrhizal fungi influence decomposition of, but not plant nutrient capture from, glycine patches in soil. New Phytologist, 725-734.
Iannucci, A., Canfora, L., Nigro, F., De Vita, P., & Beleggia, R. (2021). Relationships between root morphology, root exudate compounds and rhizosphere microbial community in durum wheat. Applied Soil Ecology, 158, 103781.
IPCC, 2018. Global Warming of 1.5°C: An IPCC Special Report on the impacts of global warming of 1.5°c above pre-industrial levels and related global greenhouse gas emission pathways, in the context of strengthening the global response to the threat of climate change, sustainable development, and efforts to eradicate poverty.
Jalonen, R., Nygren, P., & Sierra, J. (2009). Transfer of nitrogen from a tropical legume tree to an associated fodder grass via root exudation and common mycelial networks. Plant, cell & environment, 32(10), 1366-1376.
Jones, D. L., Nguyen, C., & Finlay, R. D. (2009). Carbon flow in the rhizosphere: carbon trading at the soil–root interface.
Kalbitz, K., Solinger, S., Park, J. H., Michalzik, B., & Matzner, E. (2000). Controls on the dynamics of dissolved organic matter in soils: a review. Soil science, 165(4), 277-304.
Kaloterakis, N., Rashtbari, M., Razavi, B. S., Braun-Kiewnick, A., Giongo, A., Smalla, K., ... & Brüggemann, N. (2024). Preceding crop legacy modulates the early growth of winter wheat by influencing root growth dynamics, rhizosphere processes, and microbial interactions. Soil Biology and Biochemistry, 109343.
Kuzyakov, Y. (2010). Priming effects: interactions between living and dead organic matter. Soil Biology and Biochemistry, 42(9), 1363-1371.
Kuzyakov, Y., & Blagodatskaya, E. (2015). Microbial hotspots and hot moments in soil: concept & review. Soil Biology and Biochemistry, 83, 184-199.
Liese, R., Lübbe, T., Albers, N. W., & Meier, I. C. (2018). The mycorrhizal type governs root exudation and nitrogen uptake of temperate tree species. Tree physiology, 38(1), 83-95.
Loeppmann, S., Blagodatskaya, E., Pausch, J., & Kuzyakov, Y. (2016). Substrate quality affects kinetics and catalytic efficiency of exo-enzymes in rhizosphere and detritusphere. Soil Biology and Biochemistry, 92, 111-118.
Luo, G., Wang, T., Li, K., Li, L., Zhang, J., Guo, S., ... & Shen, Q. (2019). Historical nitrogen deposition and straw addition facilitate the resistance of soil multifunctionality to drying-wetting cycles. Applied and Environmental Microbiology, 85(8), e02251-18.
Luo, L., Meng, H., & Gu, J. D. (2017). Microbial extracellular enzymes in biogeochemical cycling of ecosystems. Journal of Environmental Management, 197, 539-549.
Ma, X., Liu, Y., Zarebanadkouki, M., Razavi, B. S., Blagodatskaya, E., & Kuzyakov, Y. (2018). Spatiotemporal patterns of enzyme activities in the rhizosphere: effects of plant growth and root morphology. Biology and Fertility of Soils, 54, 819-828.
MacNeill, G. J., Mehrpouyan, S., Minow, M. A., Patterson, J. A., Tetlow, I. J., & Emes, M. J. (2017). Starch as a source, starch as a sink: the bifunctional role of starch in carbon allocation. Journal of experimental botany, 68(16), 4433-4453.
Makino, T., Hasegawa, S., Sakurai, Y., Ohno, S., Utagawa, H., Maejima, Y., & Momohara, K. (2000). Influence of soil-drying under field conditions on exchangeable manganese, cobalt, and copper contents. Soil science and plant nutrition, 46(3), 581-590.
Martínez-Trinidad, T., Todd Watson, W., Arnold, M. A., & Lombardini, L. (2010). Microbial activity of a clay soil amended with glucose and starch under live oaks. Journal of Arboriculture, 36(2), 66.
Mason-Jones, K., Robinson, S. L., Veen, G. F., Manzoni, S., & van der Putten, W. H. (2022). Microbial storage and its implications for soil ecology. The ISME journal, 16(3), 617-629.

McLaughlin, J. E., & Boyer, J. S. (2004). Glucose localization in maize ovaries when kernel number decreases at low water potential and sucrose is fed to the stems. Annals of Botany, 94(1), 75-86.
Meyer, N., Welp, G., Rodionov, A., Borchard, N., Martius, C., & Amelung, W. (2018). Nitrogen and phosphorus supply controls soil organic carbon mineralization in tropical topsoil and subsoil. Soil Biology and Biochemistry, 119, 152-161.
Mikha, M. M., Rice, C. W., & Milliken, G. A. (2005). Carbon and nitrogen mineralization as affected by drying and wetting cycles. Soil Biology and Biochemistry, 37(2), 339-347.
Mooney, H. (1972). The carbon balance of plants. Annual review of ecology and systematics, 3(1), 315-346.
Nannipieri, P., Sequi, P., & Fusi, P. (1996). Humus and enzyme activity. In Humic substances in terrestrial ecosystems (pp. 293-328). Elsevier Science BV.
Navarro-García, F., Casermeiro, M. Á., & Schimel, J. P. (2012). When structure means conservation: effect of aggregate structure in controlling microbial responses to rewetting events. Soil Biology and Biochemistry, 44(1), 1-8.
Neina, D. (2019). The role of soil pH in plant nutrition and soil remediation. Applied and environmental soil science, 2019, 1-9.
Nguyen, B. T., & Marschner, P. (2005). Effect of drying and rewetting on phosphorus transformations in red brown soils with different soil organic matter content. Soil Biology and Biochemistry, 37(8), 1573-1576.
Nottingham, A. T., Turner, B. L., Winter, K., Chamberlain, P. M., Stott, A., & Tanner, E. V. (2013). Root and arbuscular mycorrhizal mycelial interactions with soil microorganisms in lowland tropical forest. FEMS Microbiology Ecology, 85(1), 37-50.
Otlewska, A., Migliore, M., Dybka-Stępień, K., Manfredini, A., Struszczyk-Świta, K., Napoli, R., ... & Pinzari, F. (2020). When salt meddles between plant, soil, and microorganisms. Frontiers in plant science, 1429.
Olagoke, F. K., Bettermann, A., Nguyen, P. T. B., Redmile-Gordon, M., Babin, D., Smalla, K., ... & Vogel, C. (2022). Importance of substrate quality and clay content on microbial extracellular polymeric substances production and aggregate stability in soils. Biology and Fertility of Soils, 58(4), 435-457.
Pausch, J., & Kuzyakov, Y. (2018). Carbon input by roots into the soil: quantification of rhizodeposition from root to ecosystem scale. Global change biology, 24(1), 1-12.
Panikov, N. S. (1995). Microbial growth kinetics.
Peng, C., Lai, S., Luo, X., Lu, J., Huang, Q., & Chen, W. (2016). Effects of long term rice straw application on the microbial communities of rapeseed rhizosphere in a paddy-upland rotation system. Science of the Total Environment, 557, 231-239.
Pepe, A., Giovannetti, M., & Sbrana, C. (2016). Different levels of hyphal self-incompatibility modulate interconnectedness of mycorrhizal networks in three arbuscular mycorrhizal fungi within the Glomeraceae. Mycorrhiza, 26(4), 325-332.
Prashar, P., Kapoor, N., & Sachdeva, S. (2014). Rhizosphere: its structure, bacterial diversity and significance. Reviews in Environmental Science and Bio/Technology, 13, 63-77.
Qiu, H., Ge, T., Liu, J., Chen, X., Hu, Y., Wu, J., ... & Kuzyakov, Y. (2018). Effects of biotic and abiotic factors on soil organic matter mineralization: Experiments and structural modeling analysis. European Journal of Soil Biology, 84, 27-34.
Rath, K. M., & Rousk, J. (2015). Salt effects on the soil microbial decomposer community and their role in organic carbon cycling: a review. Soil Biology and Biochemistry, 81, 108-123.
Razavi, B. S., Liu, S., & Kuzyakov, Y. (2017). Hot experience for cold-adapted microorganisms: Temperature sensitivity of soil enzymes. Soil Biology and Biochemistry, 105, 236-243.

Razavi, B. S., Zhang, X., Bilyera, N., Guber, A., & Zarebanadkouki, M. (2019). Soil zymography: simple and reliable? Review of current knowledge and optimization of the method. Rhizosphere, 11, 100161.

Rillig, M. C. (2004). Arbuscular mycorrhizae and terrestrial ecosystem processes. Ecology letters, 7(8), 740-754.

Ross, D. J., Scott, N. A., Tate, K. R., Rodda, N. J., & Townsend, J. A. (2001). Root effects on soil carbon and nitrogen cycling in a Pinus radiata D. Don plantation on a coastal sand. Soil Research, 39(5), 1027-1039.

Sardans, J., & Peñuelas, J. (2005). Drought decreases soil enzyme activity in a Mediterranean Quercus ilex L. forest. Soil Biology and Biochemistry, 37(3), 455-461.

Schimel, J. P. (2018). Life in dry soils: effects of drought on soil microbial communities and processes. Annual review of ecology, evolution, and systematics, 49, 409-432.

Schmidt, M. W., Torn, M. S., Abiven, S., Dittmar, T., Guggenberger, G., Janssens, I. A., ... & Trumbore, S. E. (2011). Persistence of soil organic matter as an ecosystem property. Nature, 478(7367), 49-56.

Schnecker, J., Bowles, T., Hobbie, E. A., Smith, R. G., & Grandy, A. S. (2019). Substrate quality and concentration control decomposition and microbial strategies in a model soil system. Biogeochemistry, 144, 47-59.

Shahbaz, M., Kuzyakov, Y., Sanaullah, M., Heitkamp, F., Zelenev, V., Kumar, A., & Blagodatskaya, E. (2017). Microbial decomposition of soil organic matter is mediated by quality and quantity of crop residues: mechanisms and thresholds. Biology and Fertility of Soils, 53, 287-301.

Shahzad, T., Chenu, C., Genet, P., Barot, S., Perveen, N., Mougin, C., & Fontaine, S. (2015). Contribution of exudates, arbuscular mycorrhizal fungi and litter depositions to the rhizosphere priming effect induced by grassland species. Soil Biology and Biochemistry, 80, 146-155.

Sierra, J., & Daudin, D. (2010). Limited 15N transfer from stem-labeled leguminous trees to associated grass in an agroforestry system. European Journal of Agronomy, 32(3), 240-242.

Singh, B. K., Bardgett, R. D., Smith, P., & Reay, D. S. (2010). Microorganisms and climate change: terrestrial feedbacks and mitigation options. Nature Reviews Microbiology, 8(11), 779-790.

Singh, K. (2016). Microbial and enzyme activities of saline and sodic soils. Land Degradation & Development, 27(3), 706-718.

Sinsabaugh, R. L. (2010). Phenol oxidase, peroxidase and organic matter dynamics of soil. Soil Biology and Biochemistry, 42(3), 391-404.

Sinsabaugh, R. L., Manzoni, S., Moorhead, D. L., & Richter, A. (2013). Carbon use efficiency of microbial communities: stoichiometry, methodology and modelling. Ecology letters, 16(7), 930-939.

Song, X., Razavi, B. S., Ludwig, B., Zamanian, K., Zang, H., Kuzyakov, Y., ... & Gunina, A. (2020). Combined biochar and nitrogen application stimulates enzyme activity and root plasticity. Science of the Total Environment, 735, 139393.

Sritongon, N., Sarin, P., Theerakulpisut, P., & Riddech, N. (2022). The effect of salinity on soil chemical characteristics, enzyme activity and bacterial community composition in rice rhizospheres in Northeastern Thailand. Scientific Reports, 12(1), 20360.

Strickland, M. S., Wickings, K., & Bradford, M. A. (2012). The fate of glucose, a low molecular weight compound of root exudates, in the belowground foodweb of forests and pastures. Soil Biology and Biochemistry, 49, 23-29.

Sun, D., Li, K., Bi, Q., Zhu, J., Zhang, Q., Jin, C., ... & Lin, X. (2017). Effects of organic amendment on soil aggregation and microbial community composition during drying-rewetting alternation. Science of the Total Environment, 574, 735-743.

Tebo, B. M., Johnson, H. A., McCarthy, J. K., & Templeton, A. S. (2005). Geomicrobiology of manganese (II) oxidation. Trends in Microbiology, 13(9), 421-428.

Tomasek, A. A., Hondzo, M., Kozarek, J. L., Staley, C., Wang, P., Lurndahl, N., & Sadowsky, M. J. (2019). Intermittent flooding of organic-rich soil promotes the formation of denitrification hot moments and hot spots. Ecosphere, 10(1), e02549.

Vance, E. D., Brookes, P. C., & Jenkinson, D. S. (1987). Microbial biomass measurements in forest soils: the use of the chloroform fumigation-incubation method in strongly acid soils. Soil Biology and Biochemistry, 19(6), 697-702.

Vidal, A., Klöffel, T., Guigue, J., Angst, G., Steffens, M., Hoeschen, C., & Mueller, C. W. (2021). Visualizing the transfer of organic matter from decaying plant residues to soil mineral surfaces controlled by microorganisms. Soil Biology and Biochemistry, 160, 108347.

Voothuluru, P., Braun, D. M., & Boyer, J. S. (2018). An in vivo imaging assay detects spatial variability in glucose release from plant roots. Plant Physiology, 178(3), 1002-1010.

Walz, J., Knoblauch, C., Böhme, L., & Pfeiffer, E. M. (2017). Regulation of soil organic matter decomposition in permafrost-affected Siberian tundra soils-Impact of oxygen availability, freezing and thawing, temperature, and labile organic matter. Soil Biology and Biochemistry, 110, 34-43.

Wang, S., Hoang, D. T. T., Luu, A. T., Mostafa, T., & Razavi, B. S. (2023b). Environmental memory of microbes regulates the response of soil enzyme kinetics to extreme water events: Drought-rewetting-flooding. Geoderma, 437, 116593.

Wang, S., Zhang, X., Zhou, J., Xu, Z., Ma, Q., Chu, J., ... & Razavi, B. S. (2023a). Transition of spatio-temporal distribution of soil enzyme activity after straw incorporation: From rhizosphere to detritusphere. Applied Soil Ecology, 186, 104814.

Wen, Y., Zang, H., Freeman, B., Musarika, S., Evans, C. D., Chadwick, D. R., & Jones, D. L. (2019). Microbial utilization of low molecular weight organic carbon substrates in cultivated peats in response to warming and soil degradation. Soil Biology and Biochemistry, 139, 107629.

Weston, L. A., & Mathesius, U. (2013). Flavonoids: their structure, biosynthesis and role in the rhizosphere, including allelopathy. Journal of chemical ecology, 39, 283-297.

Wong, V. N., Greene, R. S. B., Dalal, R. C., & Murphy, B. W. (2010). Soil carbon dynamics in saline and sodic soils: a review. Soil use and management, 26(1), 2-11.

Yevdokimov, I., Larionova, A., & Blagodatskaya, E. (2016). Microbial immobilisation of phosphorus in soils exposed to drying-rewetting and freeze-thawing cycles. Biology and Fertility of Soils, 52, 685-696.

Zarebanadkouki, M., Fink, T., Benard, P., & Banfield, C. C. (2019). Mucilage facilitates nutrient diffusion in the drying rhizosphere. Vadose Zone Journal, 18(1), 1-13.

Zhang, X., Dippold, M. A., Kuzyakov, Y., & Razavi, B. S. (2019). Spatial pattern of enzyme activities depends on root exudate composition. Soil Biology and Biochemistry, 133, 83-93.

Zhang, X., Myrold, D. D., Shi, L., Kuzyakov, Y., Dai, H., Hoang, D. T. T., ... & Razavi, B. S. (2021). Resistance of microbial community and its functional sensitivity in the rhizosphere hotspots to drought. Soil Biology and Biochemistry, 161, 108360.

Zhao, S., & Zhang, S. (2018). Linkages between straw decomposition rate and the change in microbial fractions and extracellular enzyme activities in soils under different long-term fertilization treatments. PLoS One, 13(9), e0202660.

Zheng, Q., Hu, Y., Zhang, S., Noll, L., Böckle, T., Dietrich, M., ... & Wanek, W. (2019). Soil multifunctionality is affected by the soil environment and by microbial community composition and diversity. Soil Biology and Biochemistry, 136, 107521.

Zhu, Z., Ge, T., Liu, S., Hu, Y., Ye, R., Xiao, M., ... & Wu, J. (2018). Rice rhizodeposits affect organic matter priming in paddy soil: the role of N fertilization and plant growth for enzyme activities, CO_2 and CH_4 emissions. Soil Biology and Biochemistry, 116, 369-377.

1.7 Contribution to the included manuscripts

The Ph.D. thesis is a cumulative study, which comprises five published, one submitted and one in preparation manuscripts elaborated in cooperation with various co-authors. The extent of the doctoral candidate's contribution to the manuscripts is assessed on the following scale:

A. Has contributed to the work (0-33%)

B. Has made a substantial contribution (34-66%)

C. Did the majority of the work independently (67-100%)

Study 1. **Wang, S.,** Zhang, X., Zhou, J., Xu, Z., Ma, Q., Chu, J., Zang, H., Yang, Y., Peixoto, L., Zeng, Z., Razavi, B. S. (2023). Transition of spatio-temporal distribution of soil enzyme activity after straw incorporation: From rhizosphere to detritusphere. *Applied Soil Ecology*, 186, 104814.

Conceptual design: B

Planning: C

Implementation: C

Preparation of the manuscript: C

Study 2. **Wang, S.,** Hoang, D. T. T., Luu, A. T., Mostafa, T., Razavi, B. S. (2023). Environmental memory of microbes regulates the response of soil enzyme kinetics to extreme water events: Drought-rewetting-flooding. *Geoderma*, 437, 116593.

Conceptual design: B

Planning: C

Implementation: C

Preparation of the manuscript: C

Study 3. Hoang, D. T. T., Rashtbari, M., Anh, L. T., **Wang, S.,** Tu, D. T., Hiep, N. V., Razavi, B. S. (2022). Mutualistic interaction between arbuscular mycorrhiza fungi and soybean roots enhances drought resistant through regulating glucose exudation and rhizosphere expansion. *Soil Biology and Biochemistry*, 171, 108728.

Conceptual design: A

Planning: A

Implementation: B

Preparation of the manuscript: A

Study 4. Feizi, A., Luu, A. T., Mai, V. D., Tuyet, T. T. T., **Wang, S.,** Hoang, D. T. T., (2024). Divergent response of maize and soybean rhizosphere to arbuscular mycorrhiza. *Rhizosphere*, 29, 100834.

Conceptual design: A

Planning: A

Implementation: C

Preparation of the manuscript: B

Study 5. **Wang, S.,** Razavi, B. S., Spielvogel, S., Blagodatskaya, E. Energy and matter dynamics in response to soil salinization and climate warming: A case study on labile carbon decomposition. (under review)

Conceptual design: A

Planning: B

Implementation: C

Preparation of the manuscript: C

Study 6. **Wang, S.,** Blagodatskaya, E., Razavi, B. S. Contrasting soil substrate quality effects on organic matter turnover and microbial activity. (in preparation)

Conceptual design: A

Planning: B

Implementation: C

Preparation of the manuscript: C

2. Manuscript

2.1 Study 1. Transition of spatio-temporal distribution of soil enzyme activity after straw incorporation: From rhizosphere to detritusphere

Shang Wang [a,c], Xuechen Zhang [b], Jie Zhou [a], Zhuo Xu [a], Qianhan Ma [a], Juncong Chu [a], Huadong Zang [a], Yadong Yang [a], Leanne Peixoto [d], Zhaohai Zeng [a], Bahar S. Razavi [c]

Status: Published in *Applied Soil Ecology*

[a] *College of Agronomy and Biotechnology, China Agricultural University, Beijing 100193, China*

[b] *College of Natural Resources and Environment, Northwest A&F University, Yangling 712100, China*

[c] *Department of Soil and Plant Microbiome, Institute of Phytopathology, Christian-Albrechts-University of Kiel, Kiel 24118, Germany*

[d] *Department of Agroecology, Aarhus University, Blichers Allé 20, Tjele 8830, Denmark*

Wang, S., Zhang, X., Zhou, J., Xu, Z., Ma, Q., Chu, J., ... & Razavi, B. S. (2023). Transition of spatio-temporal distribution of soil enzyme activity after straw incorporation: From rhizosphere to detritusphere. Applied Soil Ecology, 186, 104814. https://doi.org/10.1016/j.apsoil.2023.104814

Abstract

The rhizosphere and detritusphere are hotspots of soil enzyme-mediated microbial processes, but little is known about their spatio-temporal distribution and interactions *in situ*, especially after straw incorporation. To answer this question, we planted maize in rhizosboxes with three wheat straw localizations: a) straw incorporated in the upper 2cm of soil (straw localized); b) straw mixed with all the soil (straw homogenized); and 3) without straw (control). Zymography was used to investigate the spatio-temporal distribution of soil C- and N- acquiring enzyme activities in the rhizosphere (living roots) and detritusphere (straw induced), which depends on straw localization (localized vs. homogenized) and time (7 vs. 15 days after planting). The hotspot area of enzyme activities was similar in the detritusphere compared to the rhizosphere at the early stage (day 7), suggesting the importance of detritusphere in driving C and N cycling. Compared with homogenized straw, higher C- and N-acquiring enzyme activities in detritusphere were observed in the treatment with localized straw, which indicates that straw localization had a marked impact on the enzyme activity in the detritusphere. Although enzyme activities in rhizosphere and detritusphere decreased with time from straw application, straw incorporation increased the enzyme activities in the rhizosphere (especially with localized straw) compared to control at the late stage (day 15). Furthermore, homogenized straw greatly reduced plant height (-36%), leaf area (-49%), SPAD (-49%), and shoot weight (-53%) than control at the late stage, but localized straw had little impact on plant performance. In conclusion, straw incorporation forms another soil enzyme activity hotspot (detritusphere) and promotes enzyme activities in the rhizosphere and soil profile. Collectively, homogenized straw incorporation intensified nutrient competition between microorganisms and roots and restricted plant performance.

Keywords: Localized straw; Homogenized straw; Zymography; Microbial hotspot; Nutrient competition; Plant growth

1. Introduction

Straw incorporation is conventional management for carbon (C) sequestration and nutrient input, and has great potential in enhancing soil fertility and crop yield in agricultural ecosystems (Liu et al., 2014). It is well known that the impact of straw incorporation on crop yield and biomass depends on its localization (i.e., straw mulching and incorporation) (Xu et al., 2019; Wang et al., 2021a). Where the core effect of straw incorporation on plant growth is linked to the belowground processes effecting C and nutrient turnover in microbial hotspots (rhizosphere and detritusphere), these microbial hotspots become the key areas of belowground processes (Zhang et al., 2021). The input of large quantities of straw-derived C into the soil may form the detritusphere (i.e. at the soil-straw interface) causing the formation of microbial hotspots through the stimulation of microbial activity, as well as biogeochemical processes (Li et al., 2019; Liu et al., 2021a; Zhou et al., 2021b). However, it remains unknown how straw localization affects the biogeochemical processes and enzyme activities in these detritusphere hotspots.

The spatial localization of microorganisms within the detritusphere plays a vital role in C and nutrient cycling by influencing microbial nutrient utilization and subsequent turnover (Bastian et al., 2009; Li et al., 2021). Specifically, microorganisms can decrease the N availability for plants via N immobilization (Kuzyakov and Xu, 2013). Thus, more N will be incorporated into the microbial biomass and consequently decreasing the N availability for plant growth (Dunn et al., 2006). Furthermore, straw incorporation processes are not exclusive drivers in the formation of the detritusphere, but also influence rhizosphere processes (Sun et al., 2020). The rhizosphere acts as the interaction area between roots and surrounding soil contains high concentrations of labile C in the form of root exudates, creating a microbial hotspot of nutrient cycling (Zhang et al., 2020). Thereby, the identification of both rhizosphere and detritusphere induced hotspots allows a precise assessment of their influence on biogeochemical processes along with the soil profile and at the ecosystem scale. However, we lack *in situ* knowledge for the comparison of spatial distribution of straw-induced detritusphere and rhizosphere microbial hotspots.

Soil enzymes are key factors in the mediation of soil organic matter decomposition and nutrient cycling (i.e., soil biogeochemical processes) (Sinsabaugh et al., 2008). Whereby, the determination of soil enzyme activity has been widely used to explore the effect of straw incorporation on the interaction between plants and microbes (Wu et al., 2020). Specifically, straw localization may influence the spatial position of soil-microbe interactions by affecting nutrient availability and soil properties, and thereby have a diverse effect on enzymatic activity (Nevins et al., 2020; Tian et al., 2020; Xiao et al., 2021). Direct soil zymography, is a non-destructive *in situ* technique based on two-dimensional imaging that enables visualization of the spatial extent of enzyme activity (Razavi et al., 2019). To obtain a mechanistic understanding of the impact of straw localization on plant-microbe-soil interactions, zymography is essential to evaluate the spatial distribution of enzymes in the microbial hotspots (i.e., rhizosphere and detritusphere).

Here, we identified the impact of straw incorporate localization (localized and homogenized) on

maize growth and soil biochemical properties. Specifically, direct soil zymography was used to identify the spatial and temporal distribution of enzyme activities involved in the acquisition of C and N in the rhizosphere, detritusphere, and bulk soil. Overall, we hypothesized that: 1) the response of enzyme activities related to C- and N-acquisition to straw localization is greater in detritusphere than rhizosphere due to the released available substrates from straw degradation; 2) homogenized straw intensified the nutrient competition between microorganisms and plants more than localized straw, since straw is decomposed homogeneously through the soil profile.

2. Materials and Methods

2.1 Soil and straw preparation

The soil was sampled from a depth of 0-20 cm at the Wuqiao experimental station of China Agricultural University, located in Cangzhou city, Hebei province, China (37°41′N, 116°35′E). The soil is classified as a calcaric fluvisol (WRB, 2015) developed on an alluvial plain with a sandy loamy texture (Liu et al., 2022). Soil samples were homogenized, sieved (< 2 mm), and visible plant residues and stones were manually removed for rhizobox experiments. The main soil properties were pH (1:2.5 H_2O) 7.7, soil organic carbon (SOC) 9.0 g kg^{-1}, total nitrogen (TN) 1.3 g kg^{-1}, total phosphorous (TP) 1.7 mg kg^{-1}, available phosphorous (Olsen-P) 89.9 mg kg^{-1} and available potassium (K) 87.5 mg kg^{-1}. For detailed information regarding the measured soil properties refer to Wang et al., (2020). The wheat (*Triticum aestivum* L., cv. Jimai 22) material was harvested at maturity and prepared by drying and crushing straw into 2 mm pieces. The C, N, and P of the straw were 417.1 g C kg^{-1}, 6.2 g N kg^{-1}, and 3.1 g P kg^{-1}, respectively.

2.2 Experimental setup

The experiment was designed to simulate the winter wheat-summer maize rotation system. Three straw localizations were characterized as follows: a) straw localized incorporation: straw was mixed with the top 2 cm of soil; b) straw homogenized incorporation: straw was mixed into the whole soil profile; c) control: soil without straw incorporation (Figure 1). The dry weight of added straw was 1 g per rhizosbox, which was equivalent to the normal field incorporation rates (7 Mg ha^{-1}) in this region (Liu et al., 2021b), and the soil water content of added fresh soil was equivalent to 60% of water holding capacity. For the straw localized incorporation, 320 g of fresh soil was initially placed in the rhizoboxes (12 × 12 × 2 cm), and then 1 g dry straw was mixed with 40 g fresh soil in a 2 cm topsoil layer. For the straw homogenized incorporation, 1 g dry straw was mixed with 360 g fresh soil and then placed in the rhizoboxes. The control only contained 360 g fresh soil without any straw incorporation. Each treatment consisted of six replicates corresponding to a total of 18 rhizoboxes. Before plantation, the soil and straw were pre-incubated in the rhizoboxes for 28 days under darkness at room temperature (~25 ºC). Maize (*Zea mays* L., cv. *Zaohuangnuo*) seeds were pre-germinated on wet filter paper (72 h in the dark), and then one germinated seed was placed in the middle of the rhizoboxes. After maize plantation, the rhizoboxes were kept an angle of 45°, thus the maize roots could grow near the lower wall of the rhizosbox due to gravity. Furthermore, the rhizoboxes were incubated at room temperature (~25 °C) and constant humidity (~65%) with a photoperiod of 12 h light and 12 h night. Every two days water was added to the rhizoboxes to maintain soil moisture at 60% water holding capacity. Every two days water was added to the rhizoboxes to maintain soil moisture at 60% water holding capacity throughout the experiment by weighting.

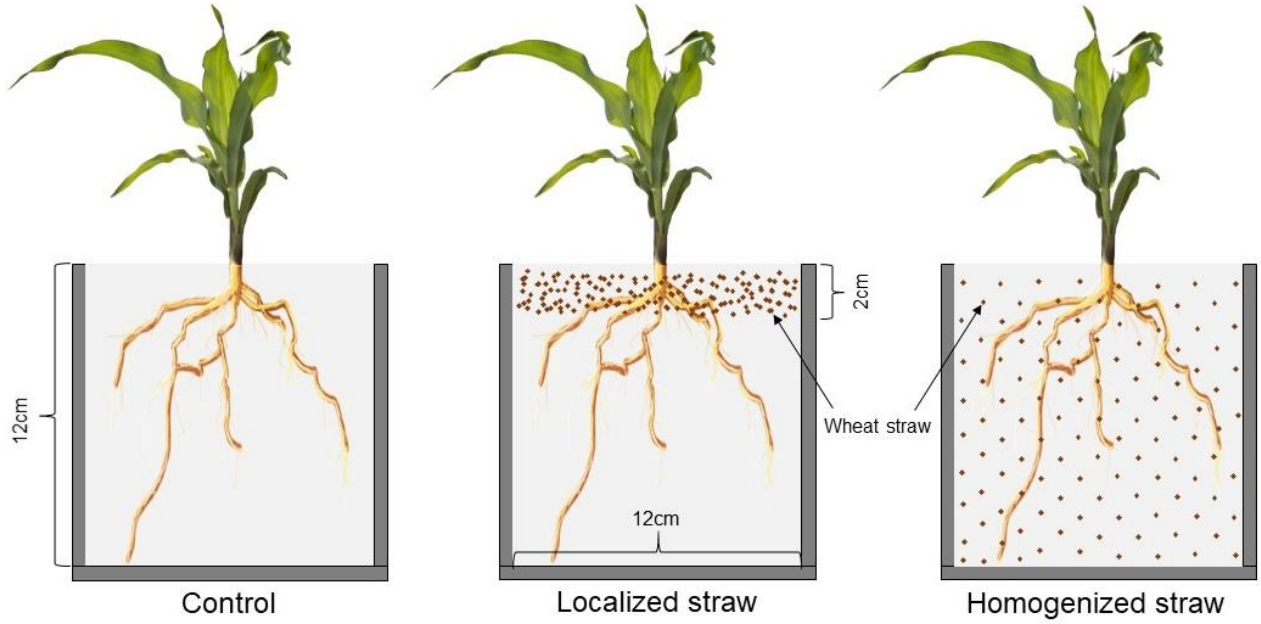

Figure 1-1 *Schematic representation of the experimental design with the localized and homogenized straw treatments, as well as the control. Brown dots in the rhizobox represent wheat straw pieces.*

2.3 Soil zymography

At 7 and 15 days after plantation, soil zymography was used to visualize the distribution of enzymes on the soil surface (Razavi et al., 2016). β-glucosidase (EC 3.2.1.21), cellobiohydrolase (EC 3.2.1.91), and leucine-aminopeptidase (EC 3.4.11.1) enzyme activities were detected by 4-methylumbelliferone (MUF)-β-D-glucoside, 4-MUF-β-D-cellobioside, and l-leucine-7-amido-4-methylcoumarin (AMC), respectively. The function of these enzymes can be found in Table S1. Each of these substrates were dissolved separately in a 0.1 M 4-morpholineethane sulphonic acid hemisodium salt (MES) buffer (for MUF substrate) and 0.05 M 2-amino-2-(hydroxymethyl)-1,3-propanediol (TRIZMA) buffer (for AMC substrate).

The rhizoboxes were carefully opened from root side on day 7 and 15, respectively. Then, the polyamide membrane filters (size: 12 × 12 cm; pore size: 0.45 μm; Taoyuan, China) were directly placed on the soil-root surfaces and saturated with the corresponding enzyme substrates. Soil zymography was performed first for cellobiohydrolase, then for β-glucosidase, last for leucine-aminopeptidase, in all cases with freshly prepared membranes. Cover membrane with a glass plate during incubation to keep the membrane closely contact with the soil-root surface and prevent evaporation (Figure S1). After 1h incubation, the membranes were carefully lifted off the soil-root surfaces and any attached soil particles were gently removed with a soft brush. The membranes were placed under UV light with 356 nm wavelengths and zymograms were taken with a camera (Canon EOS 750D). The distance between zymograms and equipment (i.e., UV light and camera) was fixed at 30 cm during zymography.

The gray-values (representing the fluorescence signal) of the zymograms were converted to enzyme activities according to standard calibration. This was prepared from the polyamide membranes (2 cm × 2 cm) soaked in a solution of MUF (0, 0.02, 0.05, 0.1, 0.2, 0.4, 0.6, 0.8 and 1.0 mM) and AMC concentrations (0, 0.1, 0.25, 0.5, 1.0, 2.5 and 5.0 mM). The membranes were imaged under the same conditions as the samples.

2.4 Measurement of soil biochemical properties

After zymography at 15 days after plantation, maize plant was destructively sampled from each rhizobox and soil was carefully collected for further analysis. The soil from the straw localized rhizoboxes was divided into upper soil (from top 2 cm of rhizobox) and lower soil (from 2cm to bottom of rhizobox). The soil of straw homogenized and the control was sampled uniformly and randomly from each rhizoboxes. Nitrate (NO_3^-N), ammonium nitrogen (NH_4^+-N), microbial biomass carbon (MBC), and nitrogen (MBN) were measured immediately after sampling. Subsamples were stored at 4 ºC for total nitrogen (TN) and soil organic carbon (SOC) analyses. All soil samples were sieved (< 2mm) before these determinations and the final results were related to dry soil.

SOC was analyzed using the $K_2Cr_2O_7$-H_2SO_4 oxidation method (Wyland et al., 1994), and TN was measured using the Kjeldahl method (Mebius 1960). NH_4^+-N and NO_3^-N were extracted at a ratio of 5 g fresh soil to 40 mL KCl (2.0 mol L^{-1}) and determined with a continuous flow analytical system (San++ system, Skalar, Holland). Microbial biomass C and N were determined by chloroform fumigation extraction (Vance et al., 1987), and detail operation can be found in "Materials and Methods" section of supplementary.

2.5 Plant trait analysis

The maize leaf chlorophyll content (SPAD value) was determined using a portable chlorophyll meter (SPAD-502 Plus, Konica Minolta, Tokyo, Japan) and was measured from 10:00 am to 12:00 am at 15 days after plantation. In terms of leaf size, three-six representative points on each leaf were randomly selected for SPAD measurement and all the leaves of all plants were measured, then the plant SPAD was defined as the average SPAD value of all its leaves.

Leaf area per plant was calculated as the sum of expanded and rolled leaf area (Wang et al., 2021b) as follows:

$$\text{Expanded leaf area} = \text{leaf length} \times \text{maximum width} \times 7.5 \quad (1)$$

$$\text{Rolled leaf area} = \text{leaf length} \times \text{maximum width} \times 0.5 \quad (2)$$

For root morphological analysis, all roots were carefully picked with tweezers to avoid destroying the fine roots and then immersed in water to clean them. The cleaned roots were put in a clear perspex tray with a film of 0.9% NaCl saline and scanned with a modified flatbed scanner (EPSON Perfection V800, Seiko Epson, Nagano, Japan). The WinRHIZO software (Regent Instruments, Quebec City, Canada) was used to measure root diameter, root length, and surface area. Root length density (RLD) was determined as the total length divided by the soil volume (240 cm^3), and root surface density (RSD) was calculated as the total surface area divided by soil volume. Root and shoot biomass were weighed after oven-drying at 75 ℃ for 48 h.

2.6 Calculations

All the calculations regarding zymograms were based on gray-values extracted from the images (see supplementary materials). We define the 2mm range outward from the root center as rhizosphere, and the 2mm range outward from the straw center as detritusphere. The criterium for hotspot identification is the gray-values higher than mean + 2 standard deviations of whole soil surface (Zhang et al., 2020). Specifically, soil with high color intensities (dark red) represents rhizosphere and detritusphere hotspots, while low intensities (blue) indicate bulk soil on the zymograms (Zhou et al., 2021a).

Effects of straw incorporation on enzyme activities were determined as effect sizes:

$$\text{Effect size} = \frac{E_S - E_{CON}}{E_{CON}} \quad (3)$$

when calculating the effect size of rhizosphere enzyme activity, E_S is the rhizosphere enzyme activity with the straw incorporation (localized or homogenized), and E_{CON} is the rhizosphere enzyme activity of control; when calculating the effect size of soil profile enzyme activity, E_S is the soil profile enzyme activity with the straw incorporation (localized or homogenized), and E_{CON} is the soil profile enzyme activity of control, and soil profile enzyme activity means the enzyme activity of the whole zymogram, including enzyme activity of bulk soil, rhizosphere and detritusphere. An effect size > 0 indicates that the straw localization has a positive effect on enzyme activity.

To study the gradient of enzyme activity along the rhizosphere or detritusphere, we randomly drew 12 vertical lines from the center of the root or litter in each zymography image then converted the gray-values of the root by the calibrated standard curve for enzyme activity, then the enzyme activities in rhizosphere and detritusphere of each zymography image were defined as the average value of 12 vertical lines, respectively.

2.7 Statistical analysis

All data are presented as the means of six replicates ± standard error (n = 6). The Shapiro-Wilk test was used to check normality, and Levene tests were performed to check the homogeneity of variances prior to the analysis. All the results passed the normality and homogeneity test. One-way ANOVA followed by a post hoc least significant difference (LSD) test was applied to compare differences between straw localizations on the root, shoot and soil properties. The effects of straw localization and sampling location (rhizosphere and detritusphere) on enzyme activity and effect size were analyzed by a two-way ANOVA (n = 6). The significant difference of rhizosphere or detritusphere (bulk soil) enzyme activity between straw localizations was analyzed by one-way ANOVA followed by a post hoc LSD test. The significant difference of effect size between rhizosphere and soil profile was analyzed by T.Test. The Pearson correlation analysis was carried out to identify the pairwise relationship between soil enzyme activity, soil properties, and plant growth. Statistical analyses were considered using SPSS (version 20.0, IBM SPSS Inc., USA) for Windows. All bar, curve, and violin graphs were drawn using Origin 2019b (Origin Lab, MA USA). Significant differences were conducted at $p < 0.05$.

3. Results

3.1 Spatio-temporal pattern of enzyme activities

The hotspots of enzyme activity were location-specific and concentrated around the root and added straw, regardless of straw localizations. The interaction effects of straw localization and measuring location (rhizosphere, detritusphere) strongly influenced enzyme activity (Table S2). The hotspot area of enzyme activity in the detritusphere was similar to that in the rhizosphere on day 7 (Figure 2, S1, and S2).

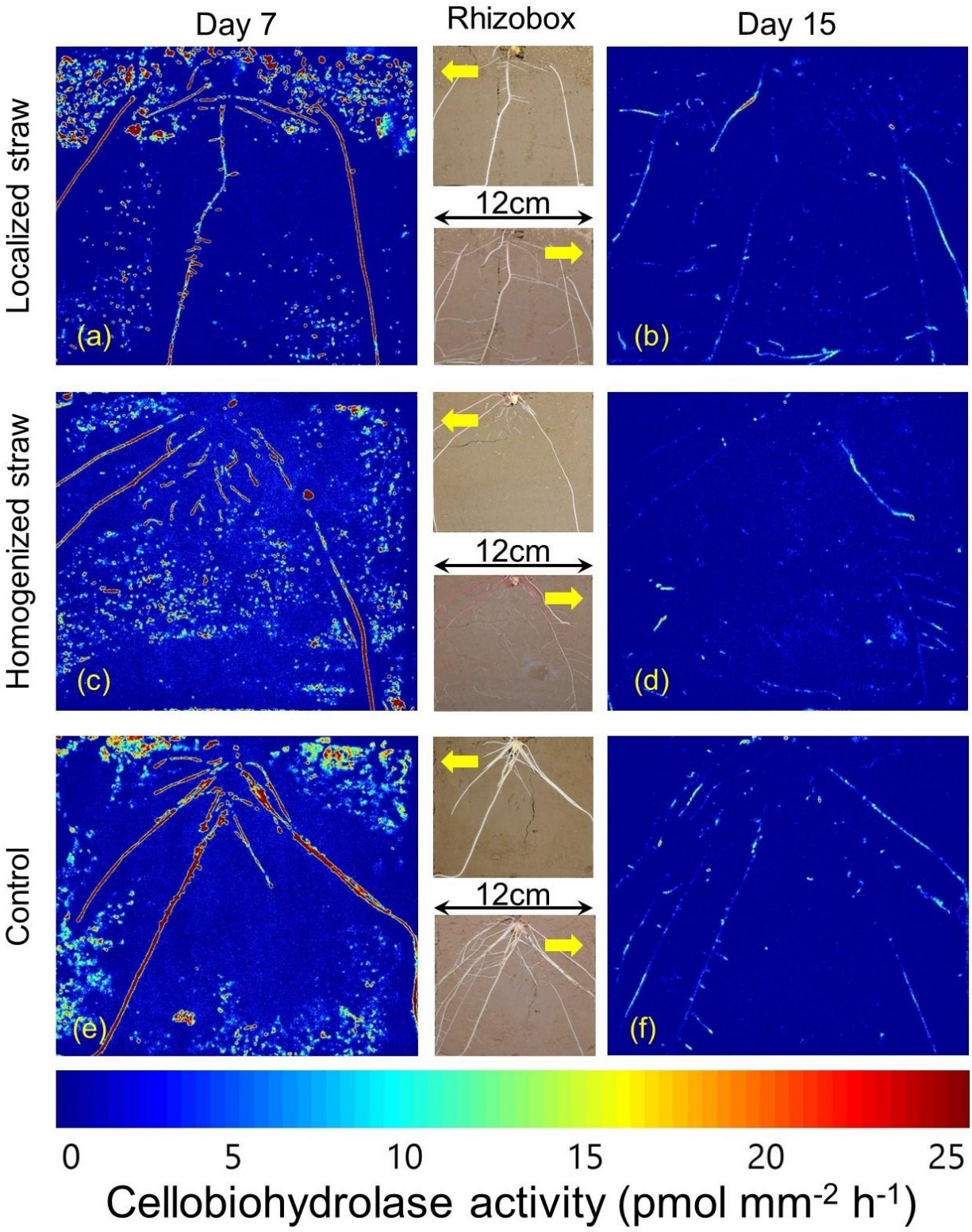

Figure 1-2 *Example of maize roots grown in rhizoboxes (center) and cellobiohydrolase zymography showing the spatial distribution of enzyme activities with straw localization (localized straw, homogenized straw and control) and plant growth (day 7 and 15).*

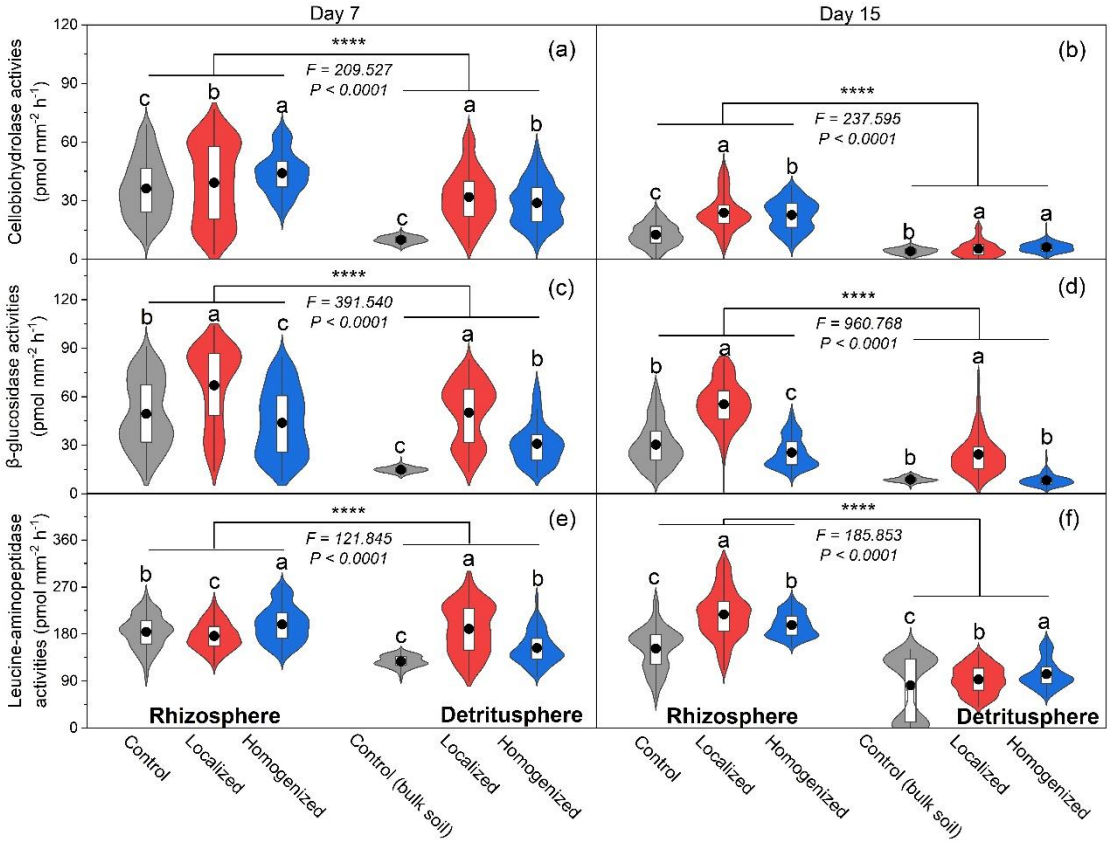

Figure 1-3 *Rhizosphere and detritusphere enzyme activity in soil without straw (Control), with localized and homogenized straw incorporation on day 7 and 15. Letters indicate significant differences among straw localizations ($p < 0.05$). The black circle in the violin plot indicates the mean value. Asterisks indicate significant differences among rhizosphere and detritusphere, **** indicates significance at the 0.0001 level.*

All measured enzyme activities decreased over time and the enzyme activities were lower in the detritusphere compared to the rhizosphere ($p < 0.0001$; Figure 3). Furthermore, all measured detritusphere enzyme activities of localized straw were higher than those of homogenized straw on day 7 ($p < 0.05$, Figure 3). However, the opposite trend was observed for leucine-aminopeptidase activity on day 15. In contrast, all measured rhizosphere enzyme activities of localized straw were notably higher than that of homogenized straw and control on day 15 ($p < 0.05$, Figure 3). Specifically, cellobiohydrolase activity in the rhizosphere of localized and homogenized straw was 8-22% and 80-89% larger in comparison to control, respectively. The β-glucosidase activity in the rhizosphere increased with localized straw, but decreased with homogenized straw ($p < 0.05$). Leucine-aminopeptidase activity in the rhizosphere of homogenized straw was 5-13% higher than that of localized straw ($p < 0.05$) whereas in the rhizosphere of control was 9-30% lower than localized straw ($p < 0.05$). Moreover, all measured detritusphere enzyme activity of both localized and homogenized straw were higher than bulk soil from control ($p < 0.05$; Figure 3), except β-glucosidase activity on day 15. Overall, straw localization has a much stronger effect on enzyme activities in the detritusphere than in the rhizosphere on day 7, and all measured rhizosphere enzyme activity of localized straw were higher than those of homogenized straw on day 15.

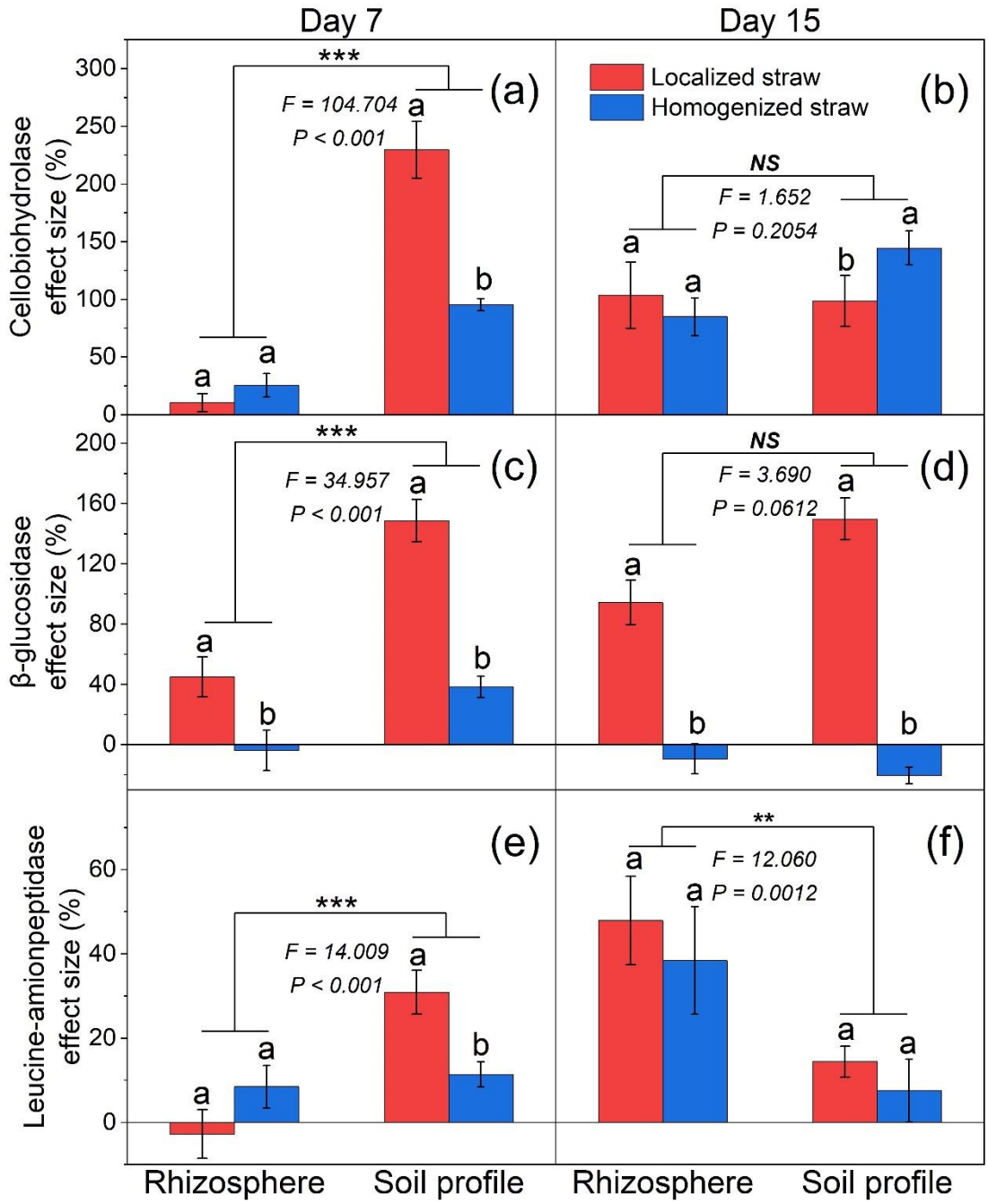

Figure 1-4 *Effects of straw localization on cellobiohydrolase (a, b), β-glucosidase (c, d), and leucine-aminopeptidase (e, f) activities in the whole soil profile or rhizosphere on day 7 and 15. The soil profile includes bulk soil, rhizosphere, and detritusphere. Letters indicate significant differences among straw localization ($p < 0.05$). Error bars represent standard errors ($n = 12$). Asterisks indicate significant differences among rhizosphere and soil surface, *** indicates significance at the 0.001 level, ** indicates significance at the 0.01, NS indicates no significant difference ($p > 0.05$).*

Furthermore, localized straw generally promoted enzyme activities in the rhizosphere, except leucine-aminopeptidase on day 7, and the positive effect was more pronounced on day 15 (Figure 4). On the soil profile, all measured enzyme activities notably increased by localized and homogenized straw according to the positive effect size on both day 7 and 15, except β-glucosidase of homogenized straw on day 15. Furthermore, the effect size on soil profile was significantly higher than that on rhizosphere, and the effect size on soil profile of straw localized was significantly higher than that of

straw homogenized on day 7 ($p < 0.05$; Figure 4). However, although straw incorporation affected the enzyme activities in the rhizosphere and detritusphere, it had slight impact on enzyme activities spatial range (Figure S4).

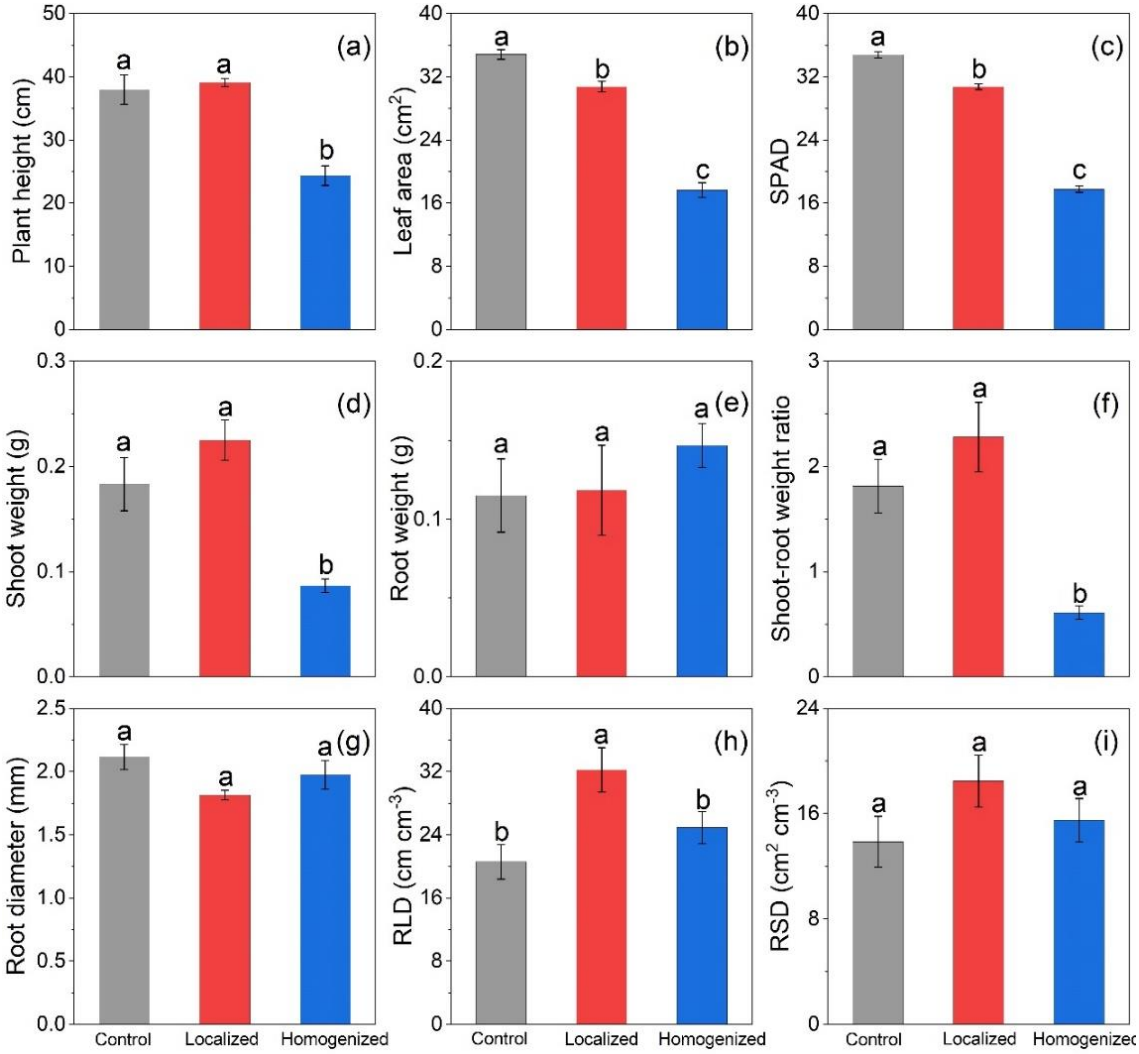

Figure 1-5 *Plant height (a), leaf area (b), SPAD-leaf chlorophyll content (c), shoot weight (d), root weight (e), shoot-root weight ratio (f), root diameter (g), RLD-root length density (h), RSD-root surface density (i) of maize grown in soil without straw (Control), with localized and homogenized straw incorporation. Letters indicate significant differences among straw localizations ($p < 0.05$). Error bars represent standard errors ($n = 6$).*

3.2 Plant growth and soil biochemical properties

In general, the majority of all measured parameters of aboveground plantlets properties were considerably lower under homogenized straw as compared to the control and localized straw treatments with minimal variation between these two treatments (Figure 5). Specifically, homogenized straw greatly reduced plant height (36%), leaf area (49%), SPAD (49%), and shoot weight (53%) as compared with the control treatment ($p < 0.05$; Figure 5a-d). Particularly, aside from the RLD, both straw localized and homogenized incorporation did not affect root parameters (i.e., root weight, root diameter, and RSD) ($p > 0.05$; Figure 5e, 5g and 5i). Moreover, as compared with localized straw and control, the shoot:root ratio of homogenized straw decreased by 73% and 67%, respectively ($p < 0.05$) (Figure 5f). Additionally, the RLD of homogenized straw was 23% lower than that observed under

localized straw ($p < 0.05$), but did not differ from the control (Figure 5h).

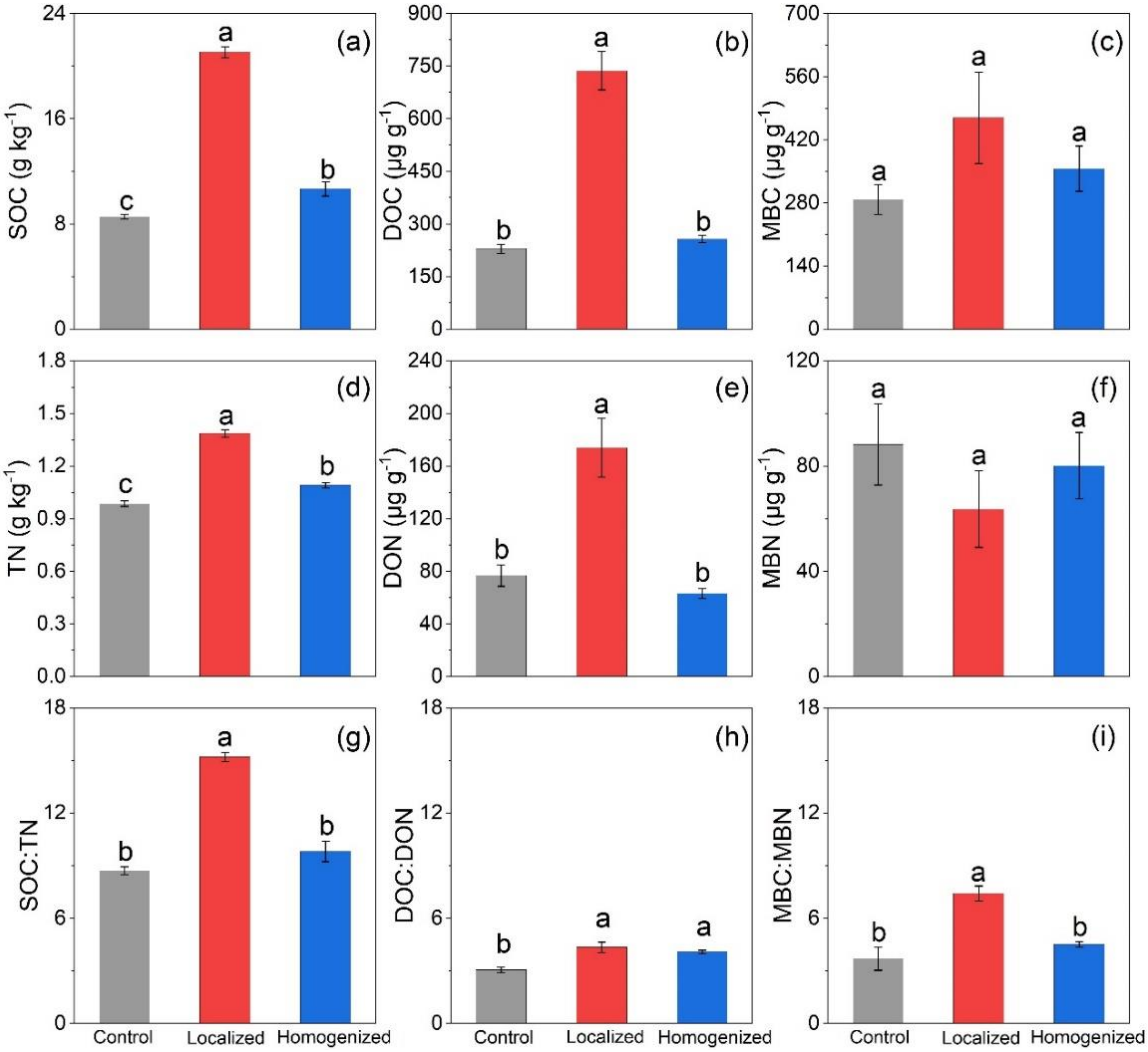

Figure 1-6 *Soil organic carbon (SOC) (a), dissolved organic carbon (DOC) (b), microbial biomass carbon (MBC) (c), total nitrogen (TN) (d), dissolved organic nitrogen (DON) (e), microbial biomass nitrogen (MBN) (f), SOC:TN (g), DOC:DON (h) and MBC:MBN (i) in dry soil without straw (Control), with localized and homogenized straw incorporation. Letters indicate significant differences among straw localization ($p < 0.05$). Error bars represent standard errors ($n = 6$). For localized straw, the soil properties represent the upper soil with straw incorporation.*

Given that the soil properties from the lower soil of localized straw treatment were similar to those in the control treatment, we only show data from the upper soil (top 2 cm of the rhizoboxes) in the results. The MBC and MBN did not differ with straw localization (Figure 6). Moreover, as compared with control, localized straw increased the SOC/TN by 75%, while both localized and homogenized straw increased DOC/DON and MBC/MBN ($p < 0.05$; Figure 6g-i). Overall, localized straw increased the incorporation of C and N in the soil and increased the C/N, while homogenized straw displayed minimal effects on these soil properties.

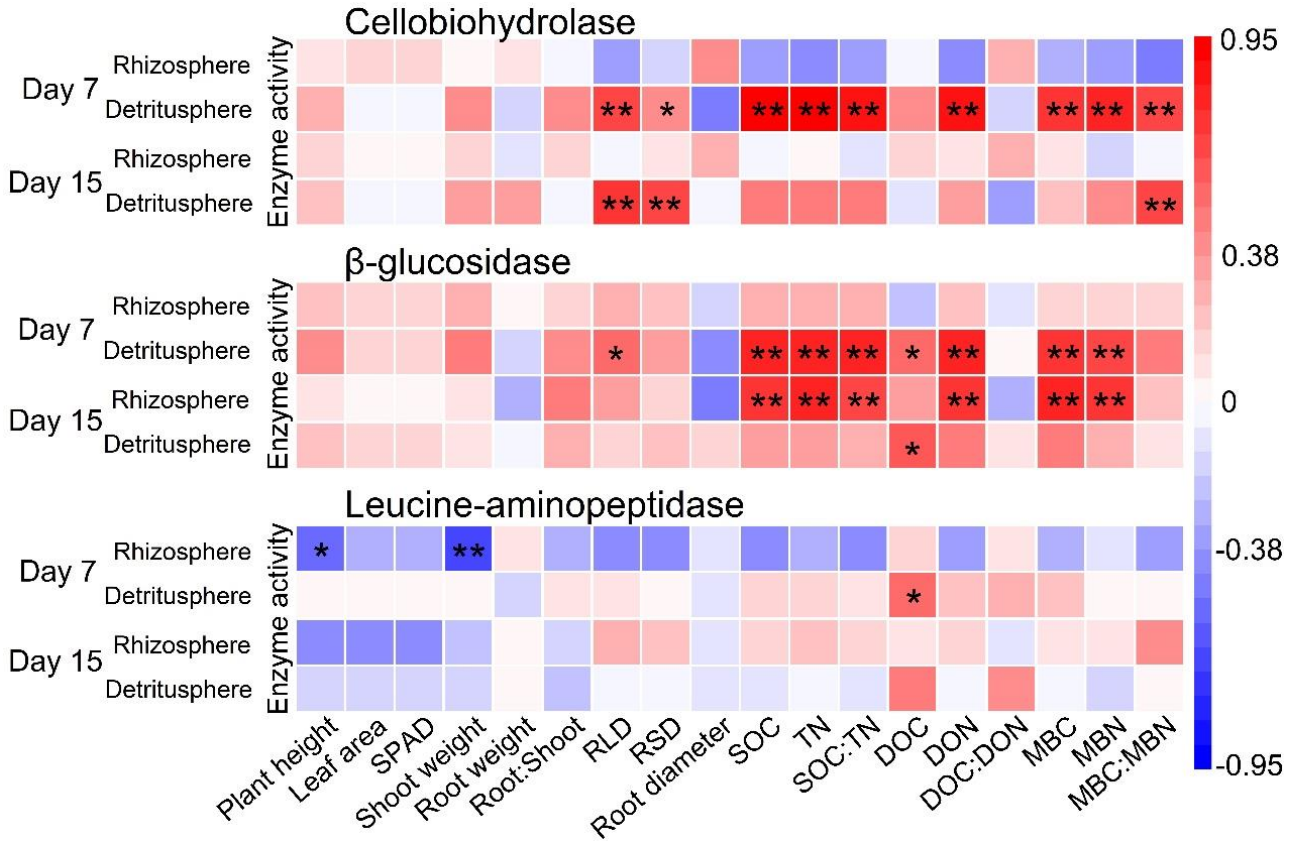

Figure 1-7 *Heat map of correlations between plant growth, soil properties (X-axis), and soil enzyme activities (Y-axis) based on Pearson correlation coefficients. * indicates correlation is significant at the 0.05 level, **indicates correlation is significant at the 0.01 level.*

The activities of cellobiohydrolase in the detritusphere after both straw localized and homogenized incorporation on day 7 and 15 were positively correlated with plant RLD and RSD (Figure 7). In contrast, leucine-aminopeptidase activity in the hotspots after both straw localized and homogenized incorporation on day 7 and 15 was negatively correlated with plant aboveground factors, except detritusphere on day 7 (Figure 7). On the other hand, the activities of cellobiohydrolase and β-glucosidase in the detritusphere were predominately positively correlated with SOC, TN, SOC:TN, DOC, MBC and MBN on day 7, same as β-glucosidase activity in the detritusphere on day 15 ($p < 0.05$; Figure 7). However, leucine-aminopeptidase activity in the hotspots had no significant correlation with soil properties (Figure 7).

4. Discussion

4.1 Enzyme activities in the rhizosphere and detritusphere

The spatial distribution of β-glucosidase, cellobiohydrolase, and leucine-aminopeptidase activities was highly associated with straw locations within the soil profile highlighting the main pathways for C and N translocation between straw and soil. This is consistent with our first hypothesis, suggesting that detritusphere is an important hotspot for soil C and N cycling. The C-acquiring enzyme activity in the detritusphere was higher on early stage (day 7) than that on late stage (day 15), which could be stimulated by the availability of cellulose-rich substrates from added straw (Cenini et al., 2016). Then, the C-acquiring enzyme activity in the detritusphere decreased on day 15, mainly due to the reduction in easily available substrates and remaining recalcitrant lignin-dominated straw fractions

(Zhao and Zhang, 2018). It should be noted that our case study was estimated based on lab incubation, which only focused on short-term effects after straw incorporation. Future in situ field study is needed to evaluate the long-term effects, especially considering the complex soil temperature and moisture variation. Furthermore, leucine-aminopeptidase activity in the detritusphere also decreased from day 7 to day 15. The microbial proteolytic community composition and their proteolytic gene expression and protease activity are correlated with plant N uptake (Ma et al., 2018). Consequently, the decrease of leucine-aminopeptidase activity may be attributed to a shift in enzymes production from degrading relatively labile polypeptides (e.g., leucine-aminopeptidase) to relatively complex compounds (e.g., chitinase) for N, and the labile polypeptides could be exhausted by the plant without regular nutrient supply (Schimel and Schaeffer, 2012; Hoang et al., 2022). Generally, the straw-induced detritusphere is the main pathway for C and N translocation between straw and soil (Védère et al., 2020; Vidal et al., 2021), and the hot moment of enzyme activities in detritusphere is limited by straw decomposition (Kuzyakov and Blagodatskaya, 2015).

Across both straw localizations, the C-acquiring enzyme activity in the rhizosphere on day 7 was larger than day 15 and the effect size was notably higher on day 15. This is likely a response to the strong nutrient competition between roots and microorganisms during the initial stage (day 7) of straw decomposition, which stimulated the enzyme activities in the rhizosphere (Peng et al., 2016). On the other hand, the C- and N-acquiring enzyme activities in the detritusphere were higher than in bulk soil, which that demonstrates the exogenous organic matter addition (i.e., straw) has an intense stimulation effect on enzyme activity. Furthermore, as the straw amount per unit volume of localized straw in the upper soil is 6 times that of homogenized straw in the whole soil layer, the C- and N-acquiring enzyme activity in the detritusphere of localized straw was markedly larger compared with that in the homogenized straw treatment.

Enzyme activity as a function of the distance from the root suggests that the rhizosphere extent was stable within straw localized and homogenized incorporation. Over time, however, the rhizosphere extent did not change (Figure S4), which may reflect the balanced root input and output, and relatively stable nutrient gradient from rhizosphere to bulk soil (Sun et al., 2021). These complex environmental relationships may explain why we did not find changes in rhizosphere enzyme activities with straw localizations in the short term. Such a stable rhizosphere extent was also observed in lentil and rice incubation experiments (Ge et al., 2017; Ma et al., 2018). This stable structure is competitive for plants to obtain nutrients efficiently in a such narrow root zone that is independent of straw incorporation (Grossmann et al., 2011).

4.2 Plant growth and soil biochemical properties

The plant growth was regulated by straw localization, and a poor shoot growth was found in the homogenized straw as compared to localized straw and control, which is consistent with our second hypothesis. This is likely due to the notion that straw incorporation stimulates soil microbial growth (Kuzyakov, 2010) resulting in enhanced nutrient competition between plants and microorganisms in the rhizosphere (Xu et al., 2008; Kuzyakov and Xu, 2013), thus temporarily decreasing plant nutrient availability and depressing plant seedling growth (Jannoura et al., 2012; Maarastawi et al., 2019). Moreover, there is a greater soil water demand during the initial stages of straw decomposition on homogenized straw leading to greater water retention, thus restricting plant growth due to reduced water availability (Yang et al., 2016). Moreover, shoot growth was not affected by localized straw

based on comparable shoot growth dynamics as that of the control treatment. This may be caused by the pre-existing and newly mineralized nutrients in localized straw were easily leached downward and may benefit to root nutrient uptake. Moreover, since there is no straw exist in lower 10 cm soil, the competition between microbes and plant roots in lower 10cm soil was weaker than for the homogenized straw (Liu et al., 2017). As such, the spatial niche separation for the straw-induced microbial community and roots could have reduced their nutrient competition but enhanced nutrient uptake (Bastian et al., 2009). In contrast, there was no significant difference of shoot weight among two straw localization and control, maybe due to the seedling plants preferentially allocate the nutrients to their root rather than shoot to ensure its ability to absorb nutrients when the soil nutrient is limited (Yu et al., 2014).

The SOC and TN considerably increased with localized and homogenized straw， which is in line with the notion that straw incorporation can change the soil nutrient stock and availability (Akhtar et al., 2019). The straw amount in the upper 2cm soil of localized straw was 6 times higher than that of homogenized straw, which explains the higher C and N nutrients in the upper soil of localized straw. This is further associated with the downward leaching of nutrients from the upper soil which could benefit to plant growth of localized straw. Conversely, the poor maize growth and associated lower soil C and N nutrients under homogenized than localized straw suggest that nutrient limitation induced by microbial competition restricts maize growth (Tian et al., 2020; Yang et al., 2021). In summary, the homogenous mixture of straw and soil could stimulate nutrient competition between microbes and plant roots, resulting in poor growth of maize shoot at the seedling stage.

Conclusion

In this study, we visualized and clarified the influences of straw localization on *in situ* soil enzyme activities spatially and temporally. The straw-induced detritusphere increased enzyme activities in soil, but remained lower than the rhizosphere (as affected by maize roots) in both localized and homogenized straw incorporation. Compared with the homogenized straw, localized straw improved the detritusphere enzyme activity, especially at the early stage. Enzyme activities in rhizosphere hotspots increased with straw incorporation (especially for localized straw), which indicated the strong interactions among roots, microbes, and added straw. Furthermore, localized straw had a limited impact on plant growth, but homogenized straw suppressed shoot performance compared with control. Collectively, we conclude that homogenized straw incorporation intensified nutrient competition between microorganisms and roots and simultaneously restricted plant performance under short-term lab incubation. Further *in situ* field studies are needed to clarify the long-term straw incorporation on soil enzyme dynamic.

Acknowledgements

This study was financially supported by the National Key Research & Development Program of China (2022YFD1901100), the National Natural Science Foundation of China (32101850), and the Young Elite Scientists Sponsorship Program by CAST (2020QNRC001).

Statements and Declarations

The authors declare no competing interests.

Reference

Akhtar, K., Wang, W., Khan, A., Ren, G., Zaheer, S., Sial, T.A., Feng, Y., Yang, G., 2019. Straw mulching with fertilizer nitrogen: An approach for improving crop yield, soil nutrients and enzyme activities. Soil Use and Management 35, 526-535.

Bastian, F., Bouziri, L., Nicolardot, B., Ranjard, L., 2009. Impact of wheat straw decomposition on successional patterns of soil microbial community structure. Soil Biology and Biochemistry 41(2), 262-275.

Cenini, V.L., Fornara, D.A., McMullan, G., Ternan, N., Carolan, R., Crawley, M.J., Clement, J.C., Lavorel, S., 2016. Linkages between extracellular enzyme activities and the C and N content of grassland soils. Soil Biology and Biochemistry 96, 198206.

Dunn, R.M., Mikola, J., Bol, R., Bardgett, R.D., 2006. Influence of microbial activity on plant–microbial competition for organic and inorganic nitrogen. Plant and Soil 289, 321-334.

Ge, T., Wei, X., Razavi, B.S., Zhu, Z., Hu, Y., Kuzyakov, Y., Jones, D.L., Wu, J., 2017. Stability and dynamics of enzyme activity patterns in the rice rhizosphere: Effects of plant growth and temperature. Soil Biology and Biochemistry 113, 108-115.

Grossmann, G., Guo, W.J., Ehrhardt, D.W., Frommer, W.B., Sit, R.V., Quake, S.R., Meier, M., 2011. The RootChip: An Integrated Microfluidic Chip for Plant Science. The Plant Cell 23(12), 4234-4240.

Hoang, D.T.T., Rashtbari, M., Anh, L.T., Wang, S., Tu, D.T., Hiep, N.V., Razavi, B.S., 2022. Mutualistic interaction between arbuscular mycorrhiza fungi and soybean roots enhances drought resistant through regulating glucose exudation and rhizosphere expansion. Soil Biology and Biochemistry 171, 108728.

Hoang, D.T.T., Razavi, B.S., Kuzyakov, Y., 2016. Earthworm burrows: kinetics and spatial distribution of enzymes of C-, N- and P- cycles. Soil Biology and Biochemistry 99, 94-103.

Jannoura, R., Kleikamp, B., Dyckmans, J., Joergensen, R.G., 2012. Impact of pea growth and arbuscular mycorrhizal fungi on the decomposition of 15N-labeled maize residues. Biology and Fertility of Soils 48, 547-560.

Kuzyakov, Y., 2010. Priming effects: interactions between living and dead organic matter. Soil Biology and Biochemistry 42, 1363-1371.

Kuzyakov, Y., Blagodatskaya, E., 2015. Microbial hotspots and hot moments in soil: Concept & review. Soil Biology and Biochemistry 83, 184-199.

Kuzyakov, Y., Xu, X., 2013. Competition between roots and microorganisms for nitrogen: mechanisms and ecological relevance. New Phytologist 198, 656–669.

Li, Y., Duan, Y., Wang, G., Wang, A., Shao, G., Meng, X., Hu, H., Zhang, D., 2021. Straw alters the soil organic carbon composition and microbial community under different tillage practices in a meadow soil in Northeast China. Soil and Tillage Research 208, 104879.

Li, Z., Rui, Z., Zhang, D., Feng, X., Lu, X., Shen, S., Zheng, J., Li, L., Song, Z., Pan, G., 2019. Macroaggregates as biochemically functional hotspots in soil matrix: Evidence from a rice paddy under long-term fertilization treatments in the Taihu Lake Plain, eastern China. Applied Soil Ecology 138, 262-273.

Liu, C., Lu, M., Cui, J., Li, B., Fang, C., 2014. Effects of straw carbon input on carbon dynamics in agricultural soils: a meta-analysis. Global Change Biology 20(5), 1366-1381.

Liu, C., Zhang, Y., Liu, H., Liu, X., Ren, D., Wang, L., Guan, D., Li, Z., Zhang, M., 2022. Fertilizer stabilizers reduce nitrous oxide emissions from agricultural soil by targeting microbial nitrogen transformations. Science of The Total Environment 806(3), 151225.

Liu, J., Liang, B., Shen, J., Zhu, X., Yi, W., Wu, J., 2021a. Contrasting effects of straw and straw-derived biochar applications on soil carbon accumulation and nitrogen use efficiency in double-rice cropping systems. Agriculture Ecosystems and Environment 311, 1047286.

Liu, S., Razavi, B.S., Su, X., Maharjan, M., Zarebanadkouki, M., Blagodatskaya, E., Kuzyakov, Y., 2017. Spatio-temporal patterns of enzyme activities after manure application reflect mechanisms

of niche differentiation between plants and microorganisms. Soil Biology and Biochemistry 112, 100-109.
Liu, T., Wang, X., Du, Z., Wu, L., 2021b. Impacts of continuous biochar application on major carbon fractions in soil profile of North China Plain's cropland: In comparison with straw incorporation. Agriculture, Ecosystems & Environment 315, 107445.
Ma, X., Liu, Y., Zarebanadkouki, M., Razavi, B.S., Blagodatskaya, E., Kuzyakov, Y., 2018. Spatiotemporal patterns of enzyme activities in the rhizosphere: effects of plant growth and root morphology. Biology and Fertility of Soils 54, 819-828.
Maarastawi, S.A., Frindte, K., Bodelier, P.L.E., Knief, C., 2019. Rice straw serves as additional carbon source for rhizosphere microorganisms and reduces root exudate consumption. Soil Biology and Biochemistry 135, 235-238.
Mebius, L.J., 1960. A rapid method for the determination of organic carbon in soil. Analytica Chimica Acta 22, 120-124.
Nevins, C.J., Lacey, C., Armstrong, S., 2020. The synchrony of cover crop decomposition, enzyme activity, and nitrogen availability in a corn agroecosystem in the Midwest United States. Soil and Tillage Research 197, 104518.
Peixoto, L., Elsgaard, L., Rasmussen, J., Kuzyakov, Y., Banfield, C.C., Dippold, M.A., Olesen, J.E., 2020. Decreased rhizodeposition, but increased microbial carbon stabilization with soil depth down to 3.6 m. Soil Biology and Biochemistry 150, 108008.
Peng, C., Lai, S., Luo, X., Lu, J., Huang, Q., Chen, W., 2016. Effects of long term rice straw application on the microbial communities of rapeseed rhizosphere in a paddy-upland rotation system. Science of The Total Environment 557-558, 231-239.
Razavi, B.S., Zarebanadkouki, M., Blagodatskaya, E., Kuzyakov, Y., 2016. Rhizosphere shape of lentil and maize: Spatial distribution of enzyme activities. Soil Biology and Biochemistry 96, 229-237.
Razavi, B.S., Zhang, X., Bilyera, N., Guber, A., Zarebanadkouki, M., 2019. Soil zymography: Simple and reliable? Review of current knowledge and optimization of the method. Rizosphere 11, 100161.
Schimel, J.P., Schaeffer, S. M., 2012. Microbial control over carbon cycling in soil. Frontiers in Microbiology 3, 348.
Sinsabaugh, R.L., Lauber, C.L., Weintraub, M.N., Ahmed, B., Allison, S.D., Crenshaw, C., Contosta, A.R., Cusack, D., Frey, S., Gallo, M.E., Gartner, T.B., Hobbie, S.E., Holland, K., Keeler, B, L., Powers, J.S., Stursova, M., Takacs-Vesbach, C., Waldrop, M, P., Wallenstein, M, D., Zak, D.R., Zeglin, L.H., 2008. Stoichiometry of soil enzyme activity at global scale. Ecology Letters 11, 1252-1264.
Sun, C., Wang, D., Shen, X., Li, C., Liu, J., Lan, T., Wang, W., Xie, H., Zhang, Y., 2020. Effects of biochar, compost and straw input on root exudation of maize (Zea mays L.): From function to morphology. Agriculture Ecosystems and Environment 297, 106952.
Sun, X., Ye, Y., Ma, Q., Guan, Q., Jones, D.L., 2021. Variation in enzyme activities involved in carbon and nitrogen cycling in rhizosphere and bulk soil after organic mulching. Rhizosphere 19, 100376.
Tian, P., Lian, H., Wang, Z., Jiang, Y., Li, Y., Sui, P., Qi, H., 2020. Effects of deep and shallow tillage with straw incorporation on soil organic carbon, total nitrogen and enzyme activities in northeast China. Sustainability 12(20), 8679.
Vance, E.D., Brookes, P.C., Jenkinson, D.S., 1987. Microbial biomass measurements in forest soils: The use of the chloroform fumigation-incubation method in strongly acid soils. Soil Biology and Biochemistry 19(6), 697-702.
Védère, C., Gonod, L.V., Pouteau, V., Girardin, C., Chenu, C., 2020. Spatial and temporal evolution of detritusphere hotspots at different soil moistures. Soil Biology and Biochemistry 150, 107975.
Vidal, A., Klöffel, T., Guigue, G., Angst, G., Steffens, M., Hoeschen, C., Mueller, C.W., 2021. Visualizing the transfer of organic matter from decaying plant residues to soil mineral surfaces controlled by microorganisms. Soil Biology and Biochemistry 160, 108347.

Wang, X., Nie, J., Wang, P., Zhao, J., Yang, Y., Wang, S., Zeng, Z., Zang, H., 2020. Does the replacement of chemical fertilizer nitrogen by manure benefit water use efficiency of winter wheat-summer maize systems? Agricultural Water Management 243, 106428.

Wang, X., He, C., Cheng, H., Liu, B., Li, S., Wang, Q., Liu, Y., Zhao, X., Zhang, H., 2021a. Responses of greenhouse gas emissions to residue returning in China's croplands and influential factors: A meta-analysis. Journal of Environmental Management 289, 112486.

Wang, Y., Sheng, D., Zhang, P., Dong, X., Yan, Y., Hou, X., Wang, P., Huang, B., 2021b. High temperature sensitivity of kernel formation in different short periods around silking in maize. Environmental and Experimental Botany 183, 104343.

WRB, 2015. World Reference Base for Soil Resources 2014, Update 2015. International Soil Classification System for Naming Soils and Creating Legends for Soil Maps. World Soil Resources Reports. Fao, Rome.

Wu, L., Ma, H., Zhao, Q., Zhang, S., Wei, W., Ding, X., 2020. Changes in soil bacterial community and enzyme activity under five years straw returning in paddy soil. European Journal of Soil Biology 100, 103215.

Wyland, L.J., Jackson, L.E., Brooks, P.D., 1994. Eliminating nitrate interference during Kjeldahl digestion of soil extracts for microbial biomass determination. Soil Science Society of America Journal 58(2), 357-360.

Xiao, Y., Zhao, Z., Chen, L., Li, Y., 2021. Arbuscular mycorrhizal fungi mitigate the negative effects of straw incorporation on Trifolium repens in highly Cd-polluted soils. Applied Soil Ecology 157, 103736.

Xu, X., Stange, C.F., Richter, A., Wanek, W., Kuzyakov, Y., 2008. Light affects competition for inorganic and organic nitrogen between maize and rhizosphere microorganisms. Plant and Soil 304, 59-72.

Xu, J., Han, H., Ning, T., Li, Z., Lal, R., 2019. Long-term effects of tillage and straw management on soil organic carbon, crop yield, and yield stability in a wheat-maize system. Field Crops Research 231, 33-40.

Yang, H., Feng, J., Zhai, S., Dai, Y., Xu, M., Wu, J., Shen, M., Bian, X., Koide, R.T., Liu, J., 2016. Long-term ditch-buried straw return alters soil water potential, temperature, and microbial communities in a rice-wheat rotation system. Soil and Tillage Research 163, 21-31.

Yang, Y., Ji, R., Zhang, H., Christie, P., Feng, G., Li, X., Gai, J., 2021. Stoichiometric analysis of an arable crop-soil-microbe system after repeated fertilizer and compost application for 10 years. Journal of Soils and Sediments 21, 1466-1475.

Yu, P., White, P. J., Hochholdinger, F., Li, C, 2014. Phenotypic plasticity of the maize root system in response to heterogeneous nitrogen availability. Planta 240(4), 667-678.

Zhang, X., Kuzyakov, Y., Zang, H., Dippold, M., Shi, L., Spielvogel, S., Razavi, B.S., 2020. Rhizosphere hotspots: Root hairs and warming control microbial efficiency, carbon utilization and energy production. Soil Biology and Biochemistry 148, 107872.

Zhang, X., Myrold, D.D., Shi, L., Kuzyakov, Y., Dai, H., Hoang, D.T.T., Dippold, M., Meng, X., Song, X., Li, Z., Zhou, J., Razavi, B.S., 2021. Resistance of microbial community and its functional sensitivity in the rhizosphere hotspots to drought. Soil Biology and Biochemistry 161, 108360.

Zhao, S., Zhang, S., 2018. Linkages between straw decomposition rate and the change in microbial fractions and extracellular enzyme activities in soils under different long-term fertilization treatments. PLoS One 13 (9), e0202660.

Zhou, J., Wen, Y., Marshall, M.R., Zhao, J., Gui, H., Yang, Y., Zeng, Z., Jones, D.L., Zang, H., 2021a. Microplastics as an emerging threat to plant and soil health in agroecosystems. Science of the Total Environment 787, 147444.

Zhou, J., Wen, Y., Shi, L., Marshall, M.R., Kuzyakov, Y., Blagodatskaya, E., Zang, H., 2021b. Strong priming of soil organic matter induced by frequent input of labile carbon. Soil Biology and Biochemistry 152, 108069.

Supplementary materials

Material and Method

Brief introduction of MBC and MBN measurement

Briefly, 5 g of soil was extracted with 40 mL of K_2SO_4 (0.5 mol L^{-1}). Another 5 g of soil was fumigated with chloroform in a desiccator for 24 h and extracted thereafter. The extracts were analyzed for dissolved organic carbon (DOC) and dissolved nitrogen (DN) content by a TOC/TIC analyzer (TOC-L, Shimadzu, Japan). The difference between K_2SO_4-extractable C and N in fumigated and non-fumigated soils was used for MBC and MBN calculations with the underlying conversion factors of 0.45 for MBC and 0.54 for MBN (Wei et al., 2019; Song et al., 2020).

Zymography calculation

Image processing consisted of three steps: 1) transformation of projected signal (fluorescence) on the images to gray-values, 2) background adjustment, and 3) conversion of gray-values to enzyme activities. Visible fluorescence on the zymograms under UV light shows the areas where the substrate has been enzymatically hydrolyzed, and the intensity of fluorescence is proportional to the enzyme activity. The images were processed using MATLAB (2016b) and ImageJ. Briefly, the zymograms were first transformed into a 16-bit gray image matrix, and environmental and camera noise was then corrected (Razavi et al., 2016). The background gray-values were then subtracted from all the zymograms. The gray value for each zymography pixel on all images was converted to enzyme activity using the standard calibration curve.

The processed 16-bit grayscale images were used for further analysis where 12 straight lines were randomly arranged on the rhizosphere, detritusphere, and bulk soil. Then the gray-values of each line were converted to enzyme activity in rhizosphere (E_R), detritusphere (E_D), and bulk soil (E_B) by the standard calibration curve.

Supplementary data

Table S1-1 *Enzyme measured in this experiment, and their functions*

Enzyme	Enzyme function
Cellobiohydrolase	Catalyzes the hydrolysis of 1,4-β-D-glucosidic linkages in cellulose and cellotetraose, releasing cellobiose. Enzyme is related to C-acquisition.
β-glucosidase	Catalyzes the hydrolysis of terminal 1,4-linked β-d-glucose residues from β-d-glucosides, including short chain cellulose oligomers. Enzyme is related to C-acquisition.
Leucine-aminopeptidase	Catalyzes the hydrolysis of leucine and other amino acid residues from the N-terminus of peptides. Enzyme is related to N-acquisition.

Modified from German et al., (2011).

Table S1-2 *F values of two-way ANOVA showing the effects of straw localization and measuring location (rhizosphere, detritusphere) on the enzyme activity of Cellobiohydrolase, β-glucosidase and Leucine-aminopeptidase across sampling times. Significant differences at: **, p < 0.01. D7, 7 days after plantation; D15, 15 days after plantation.*

	Enzyme category	Straw localization	Measuring location	Straw localization × Measuring location
D7	Cellobiohydrolase	1.385	200.109**	25.201**
	β-glucosidase	386.698**	190.756**	2.998
	Leucine-aminopeptidase	13.294**	62.403**	219.692**
D15	Cellobiohydrolase	0.195	2373.433**	8.058**
	β-glucosidase	1509.351**	1663.266**	137.187**
	Leucine-aminopeptidase	8.536**	3779.915**	74.623**

Figure S1

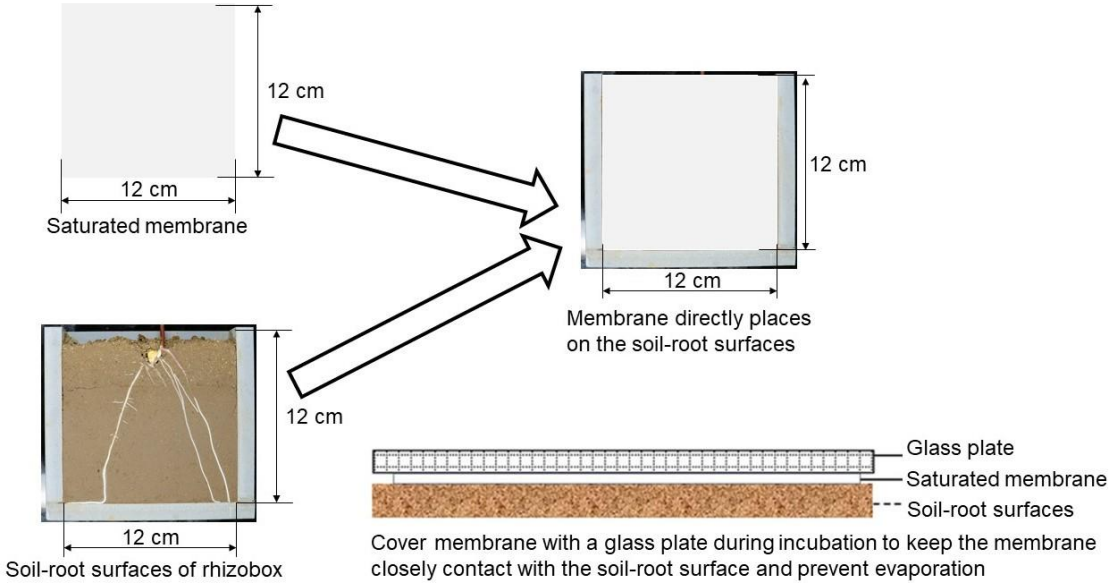

Figure S1-1 *Illustration of rhizobox and membrane size, and contact between membrane and soil-root surfaces. Modified from Razavi et al. (2017).*

Figure S2

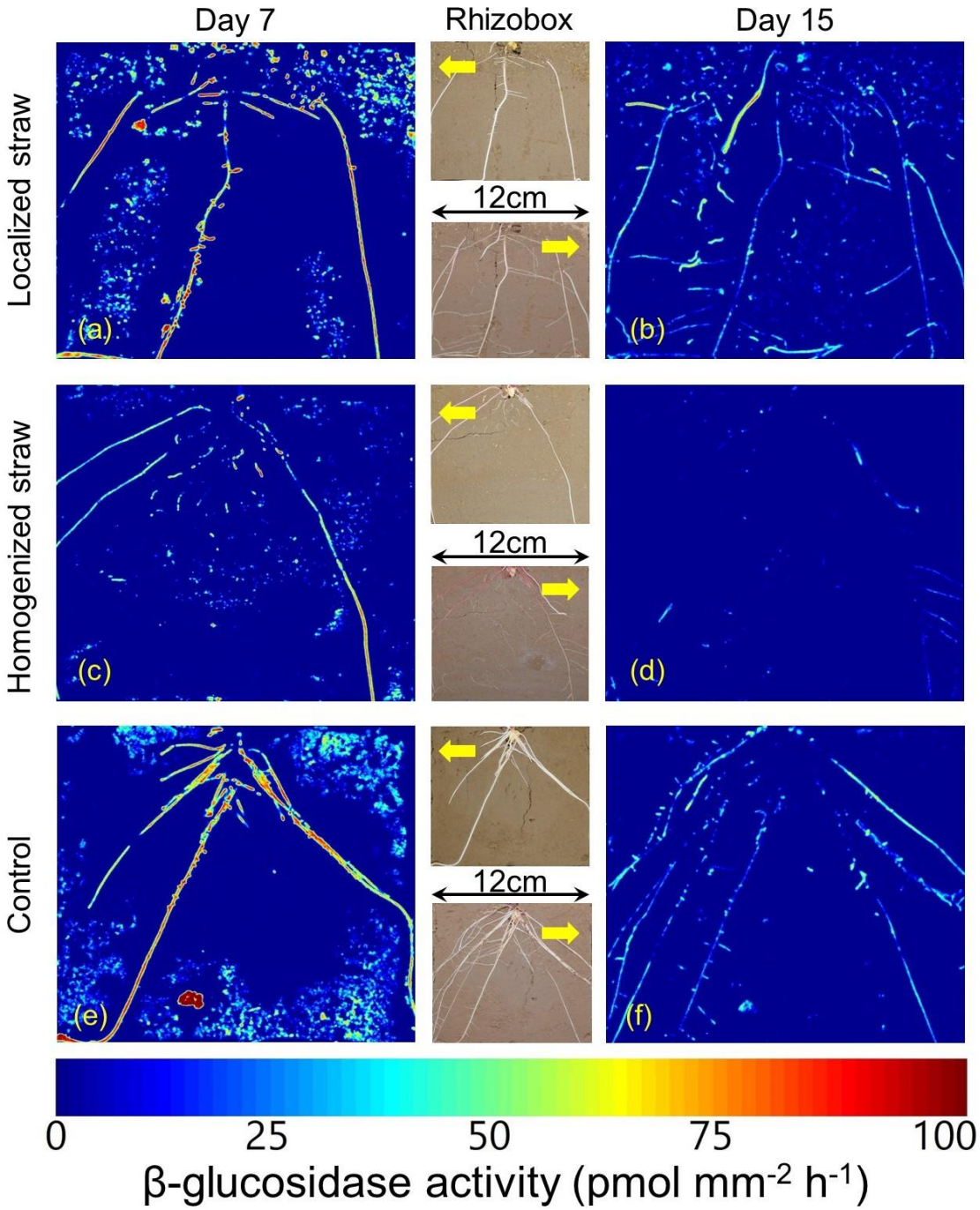

Figure S1-2 *Example of maize roots grown in rhizoboxes (center) and β-glucosidase zymography; showing spatial distribution of enzyme activities under different straw localizations (localized straw, homogenized straw and control) and sampling date.*

Figure S3

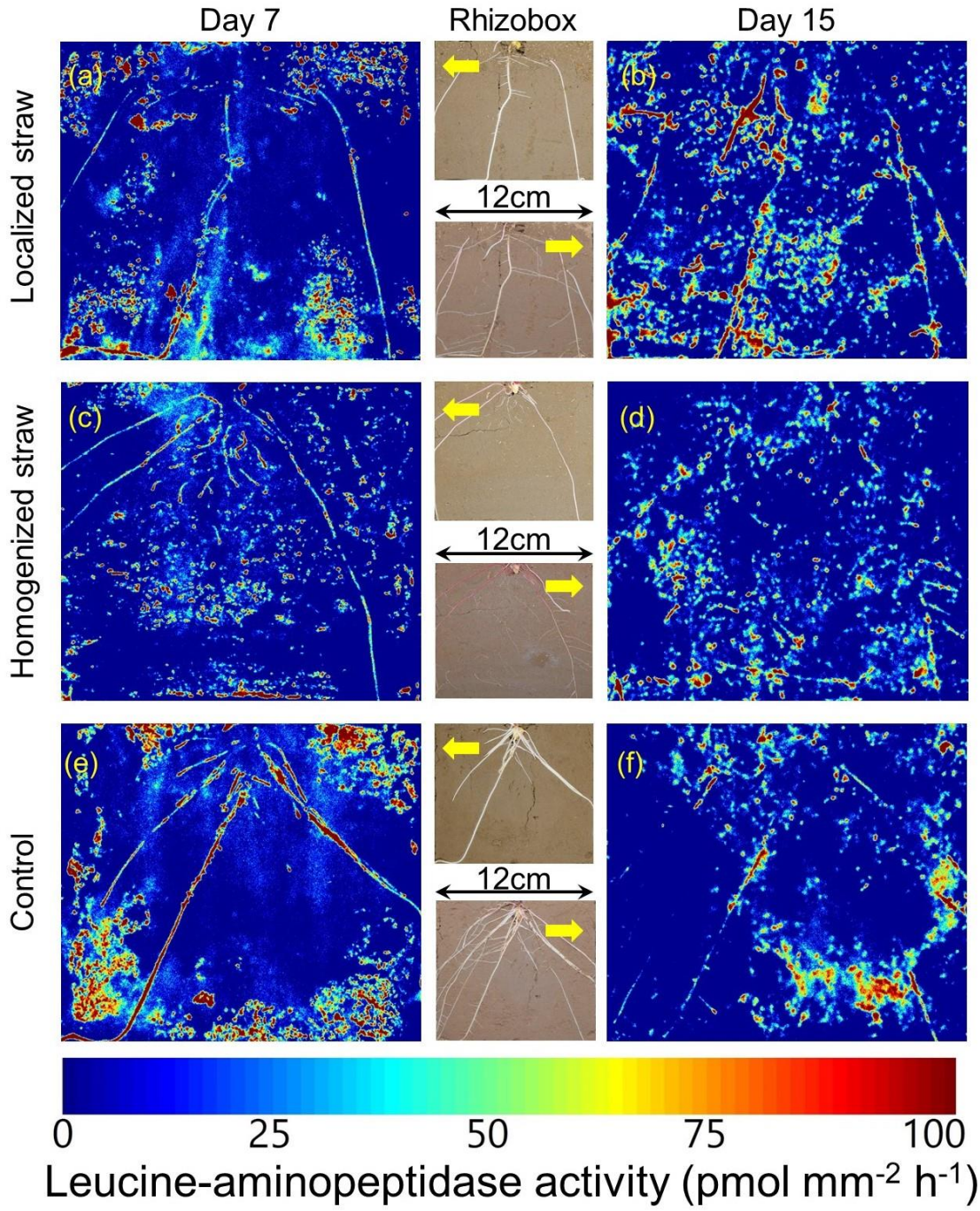

Figure S1-3 *Example of maize roots grown in rhizoboxes (center) and Leucine-aminopeptidase zymography; showing spatial distribution of enzyme activities under different straw localizations (localized straw, homogenized straw and control) and sampling date.*

Figure S4

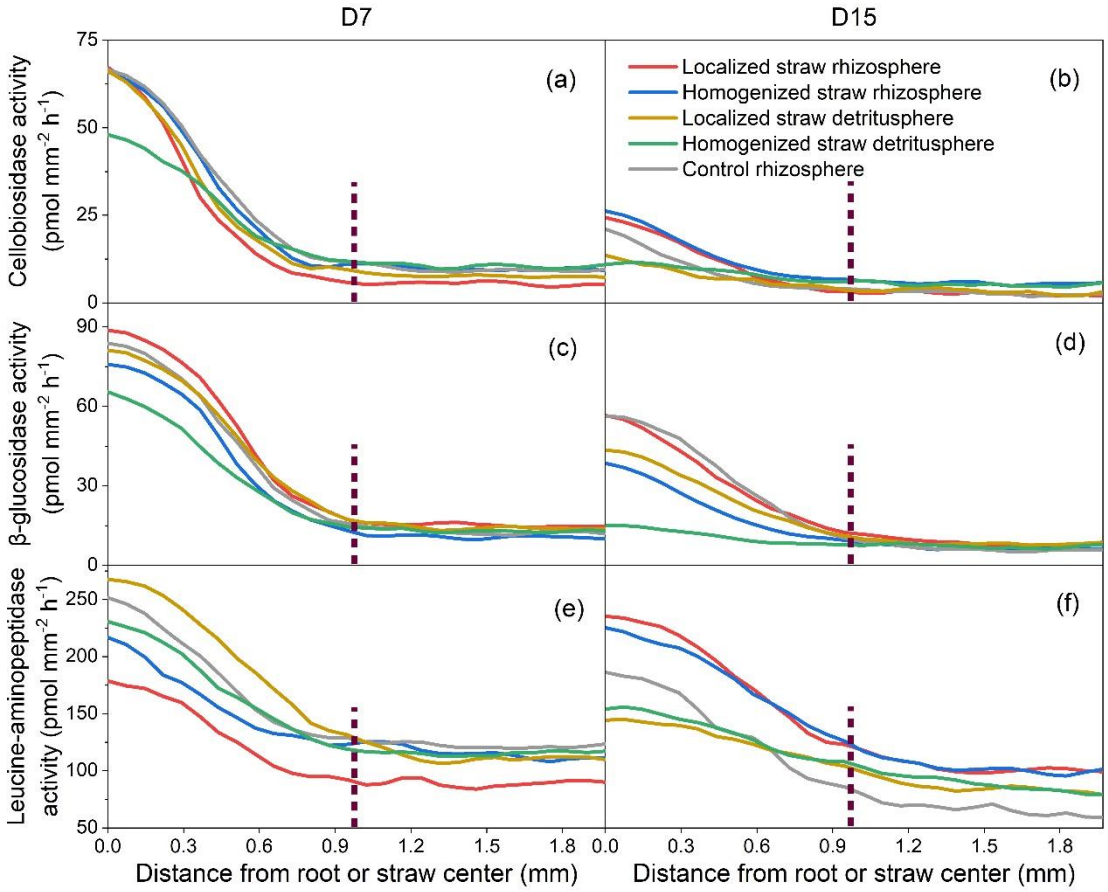

Figure S1-4 *Enzyme activity as a function of distance from maize root or wheat straw center on day 7 and 15. Each line refers to the mean enzyme activity around roots. Vertical lines indicate the average root radius.*

Reference

German, D.P., Weintraub, M.N., Grandy, A.S., Lauber, C.L., Rinkes, Z.L., Allison, S.D., 2011. Optimization of hydrolytic and oxidative enzyme methods for ecosystem studies. Soil Biology and Biochemistry 43, 1387-1397

Razavi, B. S., Hoang, D., Kuzyakov, Y., 2017. Visualization of enzyme activities in earthworm biopores by in situ soil zymography. In Zymography, Humana Press, New York, NY, 229-238.

Razavi, B.S., Zarebanadkouki, M., Blagodatskaya, E., Kuzyakov, Y., 2016. Rhizosphere shape of lentil and maize: Spatial distribution of enzyme activities. Soil Biology and Biochemistry 96, 229-237.

Song, X., Razavi, B.S., Ludwig, B., Zamanian, K., Zang, H., Kuzyakov, Y., Dippold, M.A., Gunina, A., 2020. Combined biochar and nitrogen application stimulates enzyme activity and root plasticity. Science of The Total Environment 735, 139393.

Wei, L., Razavi, B.S., Wang, W., Zhu, Z., Liu, S., Wu, J., Kuzyakov, Y., Ge, T., 2019. Labile carbon matters more than temperature for enzyme activity in paddy soil. Soil Biology and Biochemistry 135, 134-143

2.2 Study 2. Environmental memory of microbes regulates the response of soil enzyme kinetics to extreme water events: Drought-rewetting-flooding

Shang Wang [a,c], Duyen Thi Thu Hoang [a,b*], Anh The Luu [c], Tasfia Mostafa [a], Bahar S. Razavi [a]

Status: Published in *Geoderma*

[a] *Department of Soil and Plant Microbiome, Institute of Phytopathology, Christian-Albrechts-University of Kiel, Kiel 24118, Germany*

[b] *Smart Agriculture and Sustainability Program, VNU Vietnam-Japan University, Vietnam National University, Hanoi, Vietnam*

[c] *VNU-Central Institute of Natural Resources and Environmental Studies, Vietnam National University, Hanoi, Vietnam*

Wang, S., Hoang, D. T. T., Luu, A. T., Mostafa, T., & Razavi, B. S. (2023). Environmental memory of microbes regulates the response of soil enzyme kinetics to extreme water events: Drought-rewetting-flooding. Geoderma, 437, 116593. https://doi.org/10.1016/j.geoderma.2023.116593

Abstract

How environmental history mediates the response of microbial activities to dry-wet cycle (D/W) in monsoon regions is poorly investigated. In this study, soil from Red River Delta of Vietnam was incubated for 52 days, which included 14 days at 20% water holding capacity (WHC), followed by 14 days rewetted to 60% WHC (rewetting) or 100% WHC (flooding). The kinetics of β-glucosidase, chitinase and acid phosphomonoesterase enzymes, microbial respiration, microbial biomass C and P were measured.

The activities of all soil enzymes (V_{max}) decreased by 20-42% due to drought but partially or totally recovered after two weeks of rewetting or flooding. The substrate affinity (K_m) of all measured enzymes were fluctuating at initial drought and then dropped down by 33-55% after 14 days prolonged drought. Chitinase was the only enzyme showing the decoupling of V_{max} and K_m at the onset of drought, indicating different factors regulating enzyme synthesis and substrate affinity for the N demands of microorganisms. Pulse rewetting significantly reduced catalytic efficiency (K_a) but boosted turnover time (T_t) of chitinase and β-glucosidase. Rewetting prolonged T_t as compared to flooding by the end of the experiment. Moreover, both soil basal respiration and substrate induced respiration were significantly inhibited by drought and recovered to the control level after rewetting. In conclusion, soil with history of D/W triggers the recovery of microbial activities after D/W cycles and rewetting has a great impact on enzyme systems, while flooding induces more effects on enzyme synthesis.

Keywords: Localized straw; Homogenized straw; Zymography; Microbial hotspot; Nutrient competition; Plant growth

1. Introduction

Extreme drought and heavy precipitation have been enhanced by climate change in recent years (IPCC, 2021), leading to frequent and intensive dry-flooding events in soil (Lesk et al., 2016). Soil moisture is a crucial factor that influences the biogeochemical processes (Butcher et al., 2020) mediated by microbial communities and activities. However, the environmental history can serve as a distal control on microbe-derived processes in response to dry-rewetting (D/W) (Evans and

Wallenstein, 2012). The significant changes in soil moisture from a prolonged drought period to the rewetting phase trigger osmotic shocks on microbes (Fierer and Schimel, 2003), which contemporarily impact the ecosystem carbon (C) balance (Austin et al., 2004; Xiang et al., 2008) and soil nutrient cycles (Qi et al., 2018). The acceleration of C, N and P mineralization is primarily attributed to Birch effect, which is caused by drought-induced lysis and rewetting-fostered cell rupture of microbes (Gao et al., 2020). However, the acceleration of biogeochemical processes (e.g. mineralization) in soil C, N and P pools due to D/W cycles is inconsistent, while other research showed a significant decrease of N mineralization (Harrison-Kirk et al., 2014) or even no impact (Fuchslueger et al., 2014). Consequently, the perturbation of soil C and nutrient pools leads to changes in more susceptible microbial groups (Huygens et al., 2011) and alterations in the community structure (Hicks et al., 2022). Meanwhile, microbes' "memory" of variable moisture induces better resistant capacity to D/W (de Nijs et al., 2018) by regulating microbial respiration, enzyme activity, and microbial community functions (Allison and Treseder, 2008; Zhu and Cheng, 2013).

The alternative dry and rewetting results in sequent changes in soil biophysical and chemical properties such as i) cracked aggregates releasing more accessible organic matter to microorganisms (Mikha et al. 2005; Sun et al., 2017), ii) the desorption of substrate from mineral surfaces (Kalbitz et al., 2000), iii) the mobilization of C (Schimel et al., 2011), N (Leitner et al., 2017) and P (Brödlin et al., 2019) from preceding microbial residues triggered by the drought legacy effect, and iv) pH modification associated with ammonification and nitrification (Haynes and Swift, 1989; Walworth, 1992). These changes contribute to shifts in microbial community composition (de Nijs et al., 2019) and decoupling of microbial respiration and growth (Brangarí et al., 2020), thereby affecting carbon use efficiency (Navarro-García et al., 2012) in response to D/W. This alteration of liquid pathways decreases solute diffusion rates while increasing soil aeration (Ebrahimi and Or, 2016), (e.g. pattern valid for micropores, which are normally in anoxic conditions), and may change the chemical form of the elements (Makino et al. 2000; Sardans and Peñuelas 2005). Some of these elements serve as co-factors required for cellular and enzyme functions (Tebo et al. 2005), thus their bioavailability can enhance microbial growth, activity, and soil organic matter (SOM) decomposition (Ross et al. 2001). Moreover, when nutrient and exoenzyme diffusion is restricted under drought, it affects nutrient availability to microorganisms (Zarebanadkouki et al. 2019), leading to nutrient starvation (Bär et al. 2002). However, the effects of abrupt waterlogging dry soil on microbial activities are still poorly known, although Yang et al. (2016) evidently supposed a negative impact of flooding on functional microbial communities or Hamonts et al. (2013) demonstrated a significant N loss in the waterlogged soil.

Enzymes are synthesized selectively by microbes as an efficient use of energy and nutrients (Allison et al., 2010). However, their synthesis is sensitive in response to various abiotic factors such as soil moisture, temperature, and nutrient availability (Razavi et al., 2017; Zhang et al., 2021). Soil moisture plays a crucial role in mediating enzyme activity by affecting soil water films, substrate concentration, and microbial activity (Butcher et al., 2020). Moreover, catalytic efficiency, denoted as K_a and calculated based on both V_{max} and K_m parameters, has been found to persist under water scarcity condition (Ahmed et al., 2018). The response of enzyme activity to soil moisture is complex and enzyme specific (Stock et al., 2019). For instance, the activities of β-glucosidase, which hydrolyzes C compounds generally decrease with reduced soil moisture. However, the activities of enzymes

involved in P and N acquisition decrease more significantly than those related to C (Ahmed et al., 2018). In contrast to the declining pattern observed during drought, enzyme activities end to recover after rewetting (Pohlon et al., 2013; Sun et al., 2017), but the extent of recovery varies with moisture levels (Borowik and Wyszkowska, 2016). Nevertheless, recent studies on D/W effects have focused on moisture of 35-55% water holding capacity (WHC; Fierer et al., 2003; Gordon et al., 2008; Ouyang and Li, 2020), which is more representative of soil moisture condition in arid and semi-arid regions. However, in monsoon regions, flooding caused by heavy rainfall after a prolonged drought period can completely saturate soil pores. Yet, there is limited research on the effects of flooding on soil enzymes and microorganisms in this region.

Direct and indirect impacts of extreme events, such as drought and flooding, on microbial responses can vary depending on different scenarios, including the duration, frequency, intensity, and periodicity (Brödlin et al., 2019; Fierer et al., 2003; Leitner et al., 2017). In general, these extreme events can be categorized as pulses or presses, with pulses referring to shorter periods of higher stress followed by phases of lower stress, allowing organisms to recover (de Nijs et al., 2018). On the other hand, long-term exposure to extreme event (press) can lead to irreversible species loss or foundation of habitats (Hueso et al., 2011). In this study, we aimed to investigate the microbial activities and their functional resistance to pulse rewetting of dry soil until reaching a saturated condition. Specifically, we focused on the expression of β-glucosidase, chitinase, and acid phosphomonoesterase as important microbial functionalities involved nutrient and energy acquisition (Wang et al., 2023; Wei et al., 2019). These enzymes are shared by both plants and microorganisms, and directly influence soil C, N and P dynamics. In addition, they are sensitive to biotic and abiotic factors, making them reliable indicators of soil quality and fertility (Nannipieri and Eldor, 2009).

With regards to this, we incubated the soil from a monsoon region of northern Vietnam for total 52 days, which included 14 days of dry condition (20% WHC), followed by rewetted for 14 days to reach moisture levels of 60% WHC (rewetting) and 100% WHC (flooding). Soil samples were collected at five different harvest times throughout the experiment. Microbial respiration, substrate-induced respiration, microbial biomass P and C, and metabolic quotient were determined to clarify two hypotheses: i) the history pattern of intensified rainfall during summer and dry conditions during the winter in the monsoon region may trigger the recovery of microbial activities after D/W cycles; ii) the recovery of microbial activities is higher at rewetting compared to flooding.

2. Materials and methods

2.1 Soil sampling

The Red River delta of Vietnam is located in a sub-tropical monsoon region characterized with two different seasons: rainy (May – October) and dry season (November – April) (Nguyen et al., 2015). Soil for the experiment was collected from a rice and soybean rotation field in the Red River Delta (20° 25' 34.4" N; 106° 16' 33.4" E) in December 2020 when the precipitation was lowest of the year (Figure S1). The soil is classified as Fluvisols and shows a sandy clay loam soil texture (as referred to USDA soil taxonomy) consisting of 79.5% sand, 10.8% clay, and 9.7% loam. The soil contains 0.12% total N, 0.18% total P, 0.37% organic C, and a pH of 7.07. The soil samples were kept cool (~4°C) during transportation and later were sieved through 2 mm mesh to exclude any stone and plant residue, homogenized. To minimize the sequent effects of sampling, sieving and moisture adjustment on

microbial activities, soil was preconditioned at room temperature in the dark for two weeks prior to the main experiment (Blagodatskaya and Kuzyakov, 2013).

2.2 Experiment setup

Two-hundred grams of soil (dry weight equivalent) was weighed in each 500 ml-plastic jar which was assorted into 3 sets in correspondence to 3 treatments as rewetting (60% WHC), flooding (100% WHC), and control (60% WHC). Each set of treatment was arranged into 5 other subsets (with similar jar volume) to be collected at 5 different times during D/W cycle. Each subset composed of 4 replicates. Two sets for D/W treatments were initially incubated at 60% WHC during 14 days prior to a drought exposure (20% WHC) for consecutive 14 days (excluding 10 days of transition stage from optimum to drought). The two followed rewetting patterns were conducted by adding sterilized water to dry soil to bring up the moisture to 60% WHC in the moderate treatment (rewetting) and 100% WHC in the flooding. The moderate rewetting and flooding periods were sustained for 14 days until the final sampling. Briefly, each soil subset was sampled at different time points as (T1) - after the first 14-day incubation at optimum moisture, (T2) – beginning of drought stage, (T3) – ending of drought stage, (T4) – immediately after rewetting, and (T5) – after 14-day soil moisture sustained at two distinct rewetting levels (Figure 1).

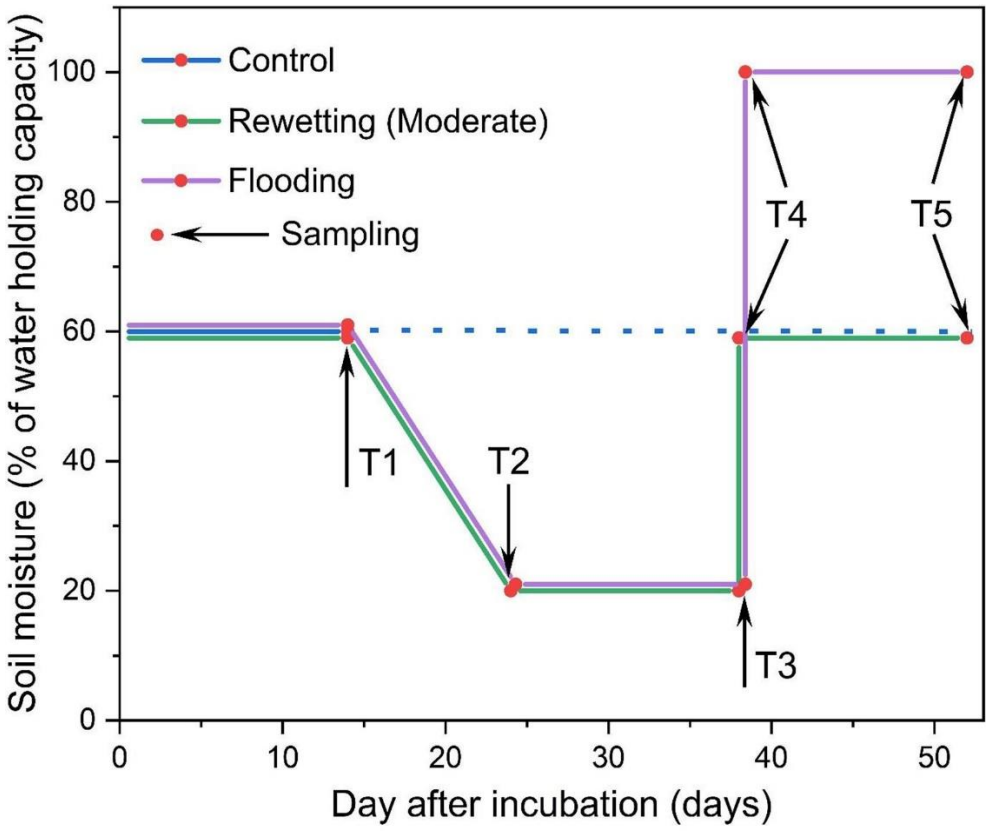

Figure 2-1 *Experiment design of alternative dry-rewetting periods. Soil moisture was expressed in percentage of water hold capacity.*

The set for control treatment was incubated at 60% WHC and harvested at T1-T5, respectively. All of the jars were placed in the dark and kept at a constant temperature (~ 20 °C) till the end of the experiment. In order to make figures more viewable, we averaged the control results of T1-T5, since

the enzyme activities of control were less variable. Similarly, the results of rewetting and flooding at T2 were combined and averaged, the same for T3.

2.3 Enzyme kinetics

Soil sample from each subset was used to measure the kinetics of chitinase, β-glucosidase and acid phosphomonoesterase utilizing fluorogenic substrates of 4-MUF-N-acetyl-β-D-glucosaminide (MUF-N), 4-MUF-β-D-glucopyranoside (MUF-G), 4-MUF-phosphate (MUF-P) (Sigma Aldrich, Germany), respectively. These substrates were separately dissolved in dimethylsulfoxide (C_2H_6SO) and sterilized water to make a stock solution of 10 mM, followed by a dilution of the stock solution using MES ($C_6H_{13}NO_4SNa_{0.5}$) buffer (pH 6.5) to make a working solution of 1 mM. Activities of the three enzymes were determined in a range of substrate concentrations of 0, 5, 10, 15, 20, 25, 50, 100, 200 µmol L^{-1} to ensure saturated point. Three grams of soil (dry weight equivalence) was prepared in 50 mL sterilized water to make a soil suspension. Thereafter, 50 µL soil suspension, 100 µL substrate solution and 50 µL MES buffer were added to a 96-well microplate (Koch et al., 2007; German et al., 2011). The fluorescence was measured using CLARIO Star Plus (Germany) at an excitation wavelength of 355 nm and an emission wavelength of 460 nm. Enzyme activities (V_{max}) were recorded at 4 timings (0, 30 min, 1 h and 2 h) and expressed as nmol MUF g^{-1} soil h^{-1} (Razavi et al., 2016), while the substrate affinity (K_m) was denoted as µmol g^{-1} soil. Two h time point was used for V_{max} and K_m calculation and further analysis. The measurement was calibrated using spectrum of MUF concentration of 0, 10, 20, 30, 40, 50, 100 µM. V_{max} and K_m were calculated with the Michaelis-Menten equation (1):

$$v = \frac{V_{max} \times [S]}{K_m + [S]} \quad (1)$$

where v is the reaction rate, [S] is the substrate concentration, K_m is the substrate concentration at the half-maximum reaction rate, and V_{max} is the maximum reaction velocity.

The substrate turnover time (T_t) was calculated according to equation (2) (Panikov et al., 1992), where [S] is the substrate concentration regarding to the V_{max}. In the current study, [S] = 100 µmol L^{-1} for chitinase, β-glucosidase and acid phosphomonoesterase. The catalytic efficiency (K_a) of enzymes was determined by equation (3) (Zhang et al., 2019):

$$T_t = \frac{K_m + [S]}{V_{max}} \quad (2)$$

$$K_a = \frac{V_{max}}{K_m} \quad (3)$$

2.4 Soil microbial respiration

Microbial respiration was measured by MicroResp™ system as described by Campbell et al. (2003). We placed 0.3 g soil in to each well of 96-deep well plate using the standard filling device. The plates were sealed and pre-incubated at room temperature for 3 days to re-establish the microbial activity. Seven carbon substrates (30 mg g^{-1} soil water) existing in root exudate, microbial residues, and plant residues (Bérard et al., 2014) were selected for the measurement: D-(+)-Glucose, D-(+)-Trehalose dehydrate, L-(+)-Arabinose, L-(-)-Malic acid, Oxalic acid, D-(-)-Fructose, D-(+)-Galactose. Accordingly, 25 µl of each substrate solutions, and sterilized water as a control, were dispensed into deep-well plates containing soil. Thereafter, 96 deep well plates were assembled to a colorimetric indicator plate with a rubber seal and incubated in the dark for 6 h at 25 °C (Campbell et al., 2003). Sterilized water was added to 96 deep well plates instead of substrate so as to measure basal respiration

(BR). The absorbance of the indicator plate was measured at 570 nm before and after the incubation period by CLARIO Star Plus. The absorbance was normalized and converted to CO_2 concentration according to Brolsma et al. (2015) as in equation (4):

$$\%CO_2 = 0.002 \times {A_{570}}^{-3.11} \ (R^2 = 0.93) \quad (4)$$

where $\%CO_2$ (vol/vol) is the concentration in the headspace after incubation and A_{570} is the normalized absorbance of the indicator plate. Each substrate induced CO_2 rate (μg CO_2-C g^{-1} dry soil h^{-1}) was calculated according to Cameron (2007) as in equation (5):

$$CO_2 \text{ rate} = \frac{(\%CO_2/100)\times V\times(44/22.4)\times(12/44)\times(273/(273+T))}{DW\times IT} \quad (5)$$

where V is the headspace volume (945μl) of deep well plates, 44/22.4 is the gas constant to convert the CO_2 concentration to weight, 12/44 is the molecular mass ratio to convert the CO_2 to CO_2-C, T is the incubation temperature (25℃), DW is soil dry weight (g), and IT is incubation time (hour). While the respiration induced by added sterilized water was considered as a basal respiration (Anderson and Domsch, 1990). Furthermore, the MicroResp can only accurately measure the substrate induced respiration of soil with 20-60% WHC according to the instruction, so the respiration and MBC (calculated based on glucose induced respiration) data of flooding (100%WHC) at T4 and T5 are missing.

2.5 Microbial biomass carbon and phosphorus

Soil microbial biomass C (MBC) was determined based on initial rate of substrate induced respiration after 6 hours of glucose addition and calculated as the equation (6):

$$C_{mic} = \text{SIR} \times 40.04 \quad (6)$$

Where C_{mic} is MBC value (μg g^{-1} soil), SIR is the initial respiration rate (μl CO_2 g^{-1} soil h^{-1}) after soil amendment with glucose, 40.04 is the correction factor (Anderson and Domsch, 1978). Although the correction factor may vary depending on soil type and condition, which primarily affects the absolute values for MBC (Beck et al., 1997; Kaiser et al., 1992). The SIR method can still be reliably used to determine relative differences in MBC between samples (Creamer et al., 2014). The metabolic quotient (qCO_2) was determined by the ratio of basal respiration to MBC (Anderson and Domsch, 1990) and denoted as μg CO_2-C mg^{-1} C_{mic} h^{-1}.

Soil microbial biomass phosphorus (MBP) was measured using fumigation extraction of soils with anion exchange membranes (AEM) (Yevdokimov et al., 2016; Maranguit et al., 2017). Three g soil, 30 ml sterilized water and one strip of AEM (1.5 cm × 6.25 cm) with or without 300 μl chloroform were placed in 50 ml plastic tubes. All tubes were tightly closed and shaken for 24h to induce the recovery of inorganic P from the soil extract. After shaking, each AEM strip was cleaned in sterilized water and shaken with 45 ml H_2SO_4 (0.25 mol L^{-1}) in other 50 ml plastic tubes for 3h to release membrane-fixed P back to the solution. Thereafter, 150 μl extractant was mixed with ammonium molybdate tetrahydrate and Malachite Green in a 96-well transparent microplate (D'Angelo et al., 2001) and read by CLARIO Star Plus at 630 nm.

2.6 Statistical analysis

The enzyme kinetic parameters (V_{max} and K_m) were fitted via the non-linear regression routine of SigmaPlot (version 12.5). All data were presented as mean ± standard error (mean ± SE). In order to make figures more viewable, we averaged the control results of T1-T5 (n = 16), since the enzyme activities of control were less variable (Table S1). Similarly, the results of rewetting and flooding at

T2 were combined and averaged the same for T3 (n = 8) (Table S2). The result replicates of rewetting and flooding at T4 and T5 are 4 (n = 4). The results of microbial biomass and substrate induced respiration also presented follow above pattern.

ANOVA assumptions of normality and variance homogeneity were checked using Shapiro-Wilk test and Levene test prior to the analysis of variance. One-way ANOVA followed by a Tukey-Kramer post-hoc test was applied to unequal sample size, for analyzing the differences in soil biochemical properties between rewetting and flooding patterns and their changes with soil moisture. The Pearson correlation analysis was carried out to identify the pairwise relationship between soil enzyme kinetic and microbial biomass in T1-T3. All analyses were performed using IBM SPSS Statistics (Version 20.0) at a significant level of $p < 0.05$.

3. Results

3.1 Enzyme activity responses to drought and rewetting

When soil attained dry condition (T2), activities of chitinase and β-glucosidase decreased by 18.5% and 17.8% relative to optimum moisture, respectively (Figure 2). Prolonged drought to the 14-days (T3) reduced the activities of all enzymes by 19.6-42.4% as compared to the control (T1) ($p < 0.05$), including acid phosphomonoesterase whose activities seemed unaffected during the initial drought period (T2). The onset of soil rewetting and flooding on T4 continued accelerating the reduction of β-glucosidase activities while the reduction of chitinase activities was only seen in flooding condition. In contrast, acid phosphomonoesterase partially recovered after the abrupt rewetting and flooding but was still 18.9-28.5% lower than the control ($p < 0.05$). After two weeks of rewetting and flooding incubation (T5), activities of all three enzymes recovered but the recovery level was enzyme specific and dependent on rewetting scenario. For examples, while the acid phosphomonoesterase and β-glucosidase activities returned to similar or higher than the control after prolong rewetting, chitinase activities were still 29.1-26.8% lower than the control ($p < 0.05$). The recovery of enzyme activities was higher in flooding than rewetting, especially in chitinase and β-glucosidase. In short, the V_{max} of all measured soil enzymes decreased due to drought and partially or totally recovered after two weeks of rewetting and flooding incubation, except chitinase of rewetting pattern.

Beginning of the dry period significantly increased K_m of chitinase (Figure 3). However, a reduction in K_m was detected in all three enzymes as the drought prolonged. The pulse rewetting (T4) only induced the decrease of K_m of β-glucosidase while triggered a decrease of chitinase substrate affinity (increased K_m) but the effect of flooding on K_m value is absent. After prolonged rewetting and flooding, K_m values of all three enzymes had no significant change in comparison with T4, but altered compared to the control with the alteration depending of enzyme specific.

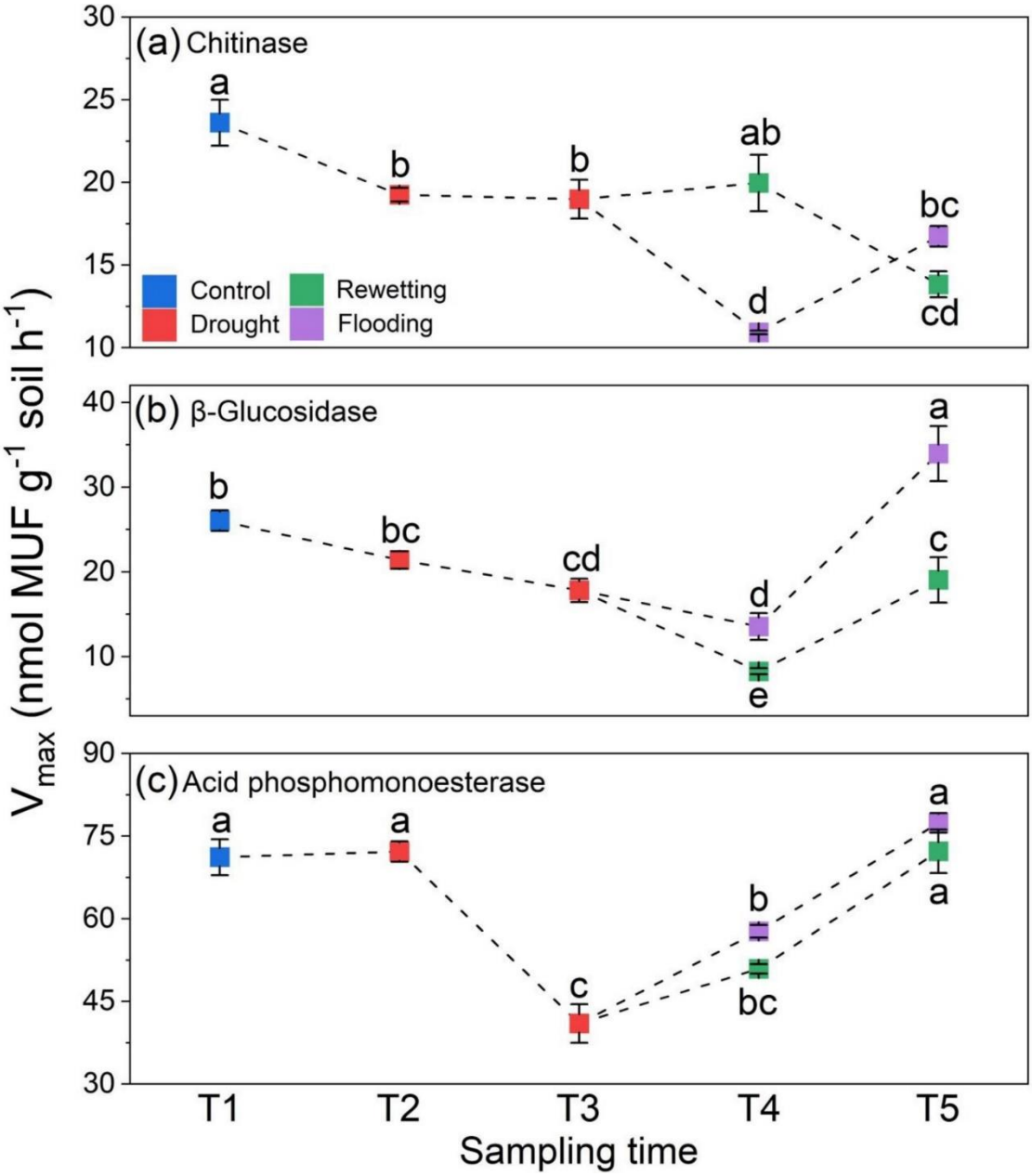

Figure 2-2 *Soil enzyme activities (V_{max}) of chitinase (a), β-D-glucosidase (b) and acid phosphomonoesterase (c) of 5 sampling times under rewetting and flooding patterns, respectively. Values are means ± standard error (n = 24 for T1, n = 8 for T2-T3 and n = 4 for T4-T5). Different lowercase letters above or below the error bar in each sub-figure indicated significant difference in V_{max} under different sampling times or rewetting patterns at* $p < 0.05$*, based on one-way ANOVA followed by a Tukey-Kramer post-hoc test.*

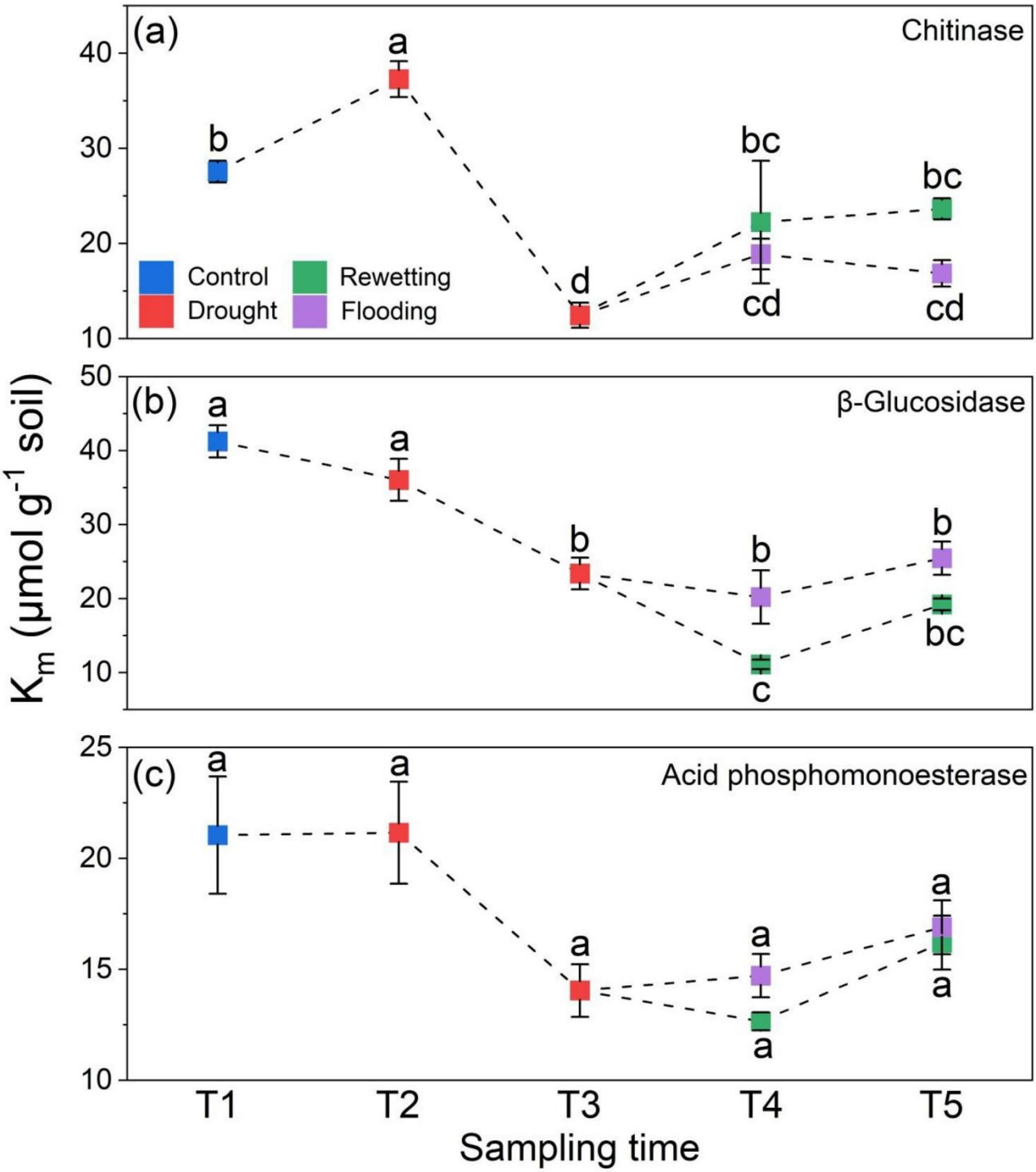

Figure 2-3 *Soil enzyme substrate affinities (K_m) of chitinase (a), β-D-glucosidase (b) and acid phosphomonoesterase (c) of 5 sampling times under rewetting and flooding patterns, respectively. Values are means ± standard error (n = 24 for T1, n = 8 for T2-T3 and n = 4 for T4-T5). Different lowercase letters above or below the error bar in each sub-figure indicated significant difference in K_m under different sampling times or rewetting patterns at* $p < 0.05$*, based on one-way ANOVA followed by a Tukey-Kramer post-hoc test.*

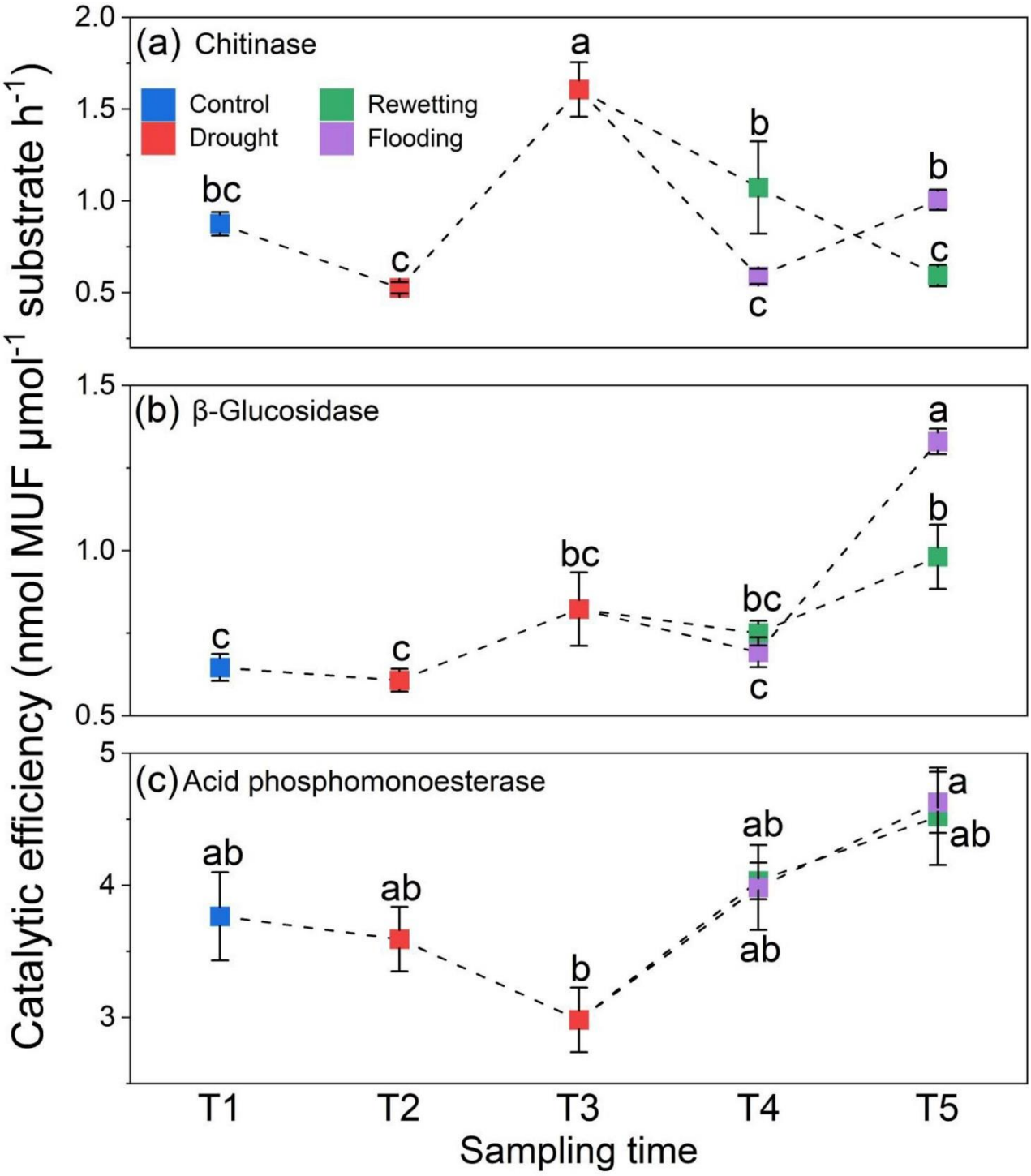

Figure 2-4 *Catalytic efficiency of chitinase (a), β-D-glucosidase (b) and acid phosphomonoesterase (c) in soil from the 5 sampling times under rewetting and flooding patterns, respectively. [S] = 100 µmol L^{-1}. Values are means ± standard error (n = 24 for T1, n = 8 for T2-T3 and n = 4 for T4-T5). Different lowercase letters above or below the error bar in each sub-figure indicated significant difference in catalytic efficiency under different sampling times or rewetting patterns at* $p < 0.05$*, based on one-way ANOVA followed by a Tukey-Kramer post-hoc test.*

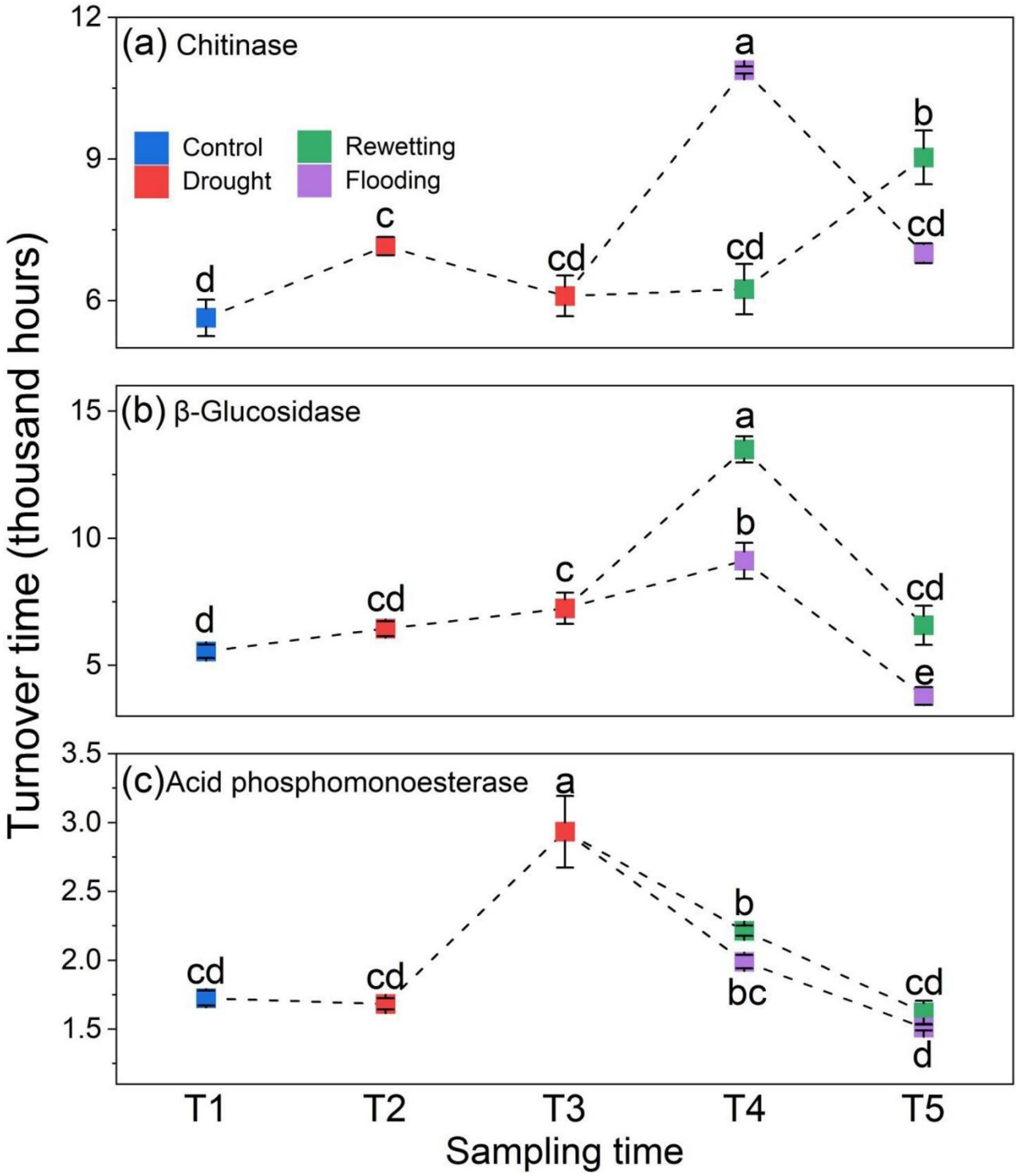

Figure 2-5 *Turnover time (Tt) of chitinase (a), β-D-glucosidase (b) and acid phosphomonoesterase (c) in soil from the 5 sampling times under rewetting and flooding patterns, respectively. Values are means ± standard error (n = 24 for T1, n = 8 for T2-T3 and n = 4 for T4-T5). Different lowercase letters above or below the error bar in each sub-figure indicated significant difference in* T_t *under different sampling times or rewetting patterns at* $p < 0.05$*, based on one-way ANOVA followed by a Tukey-Kramer post-hoc test.*

3.2 Catalytic efficiency and turnover time of the substrate

The catalytic efficiency (K_a) of chitinase decreased by 31.3% when WHC dropped to 20% in T2 ($p < 0.01$), however, it unexpectedly increased by 83.6% compared with control after two weeks of drought incubation in T3 ($p < 0.01$) (Figure 4). Meanwhile, K_a of acid phosphomonoesterase dropped in T3 by 20.8%. The pulse rewetting and flooding significantly reduced K_a of chitinase while the prolonged rewetting and flooding induced an increase of K_a of three enzymes (an exception for chitinase at rewetting).

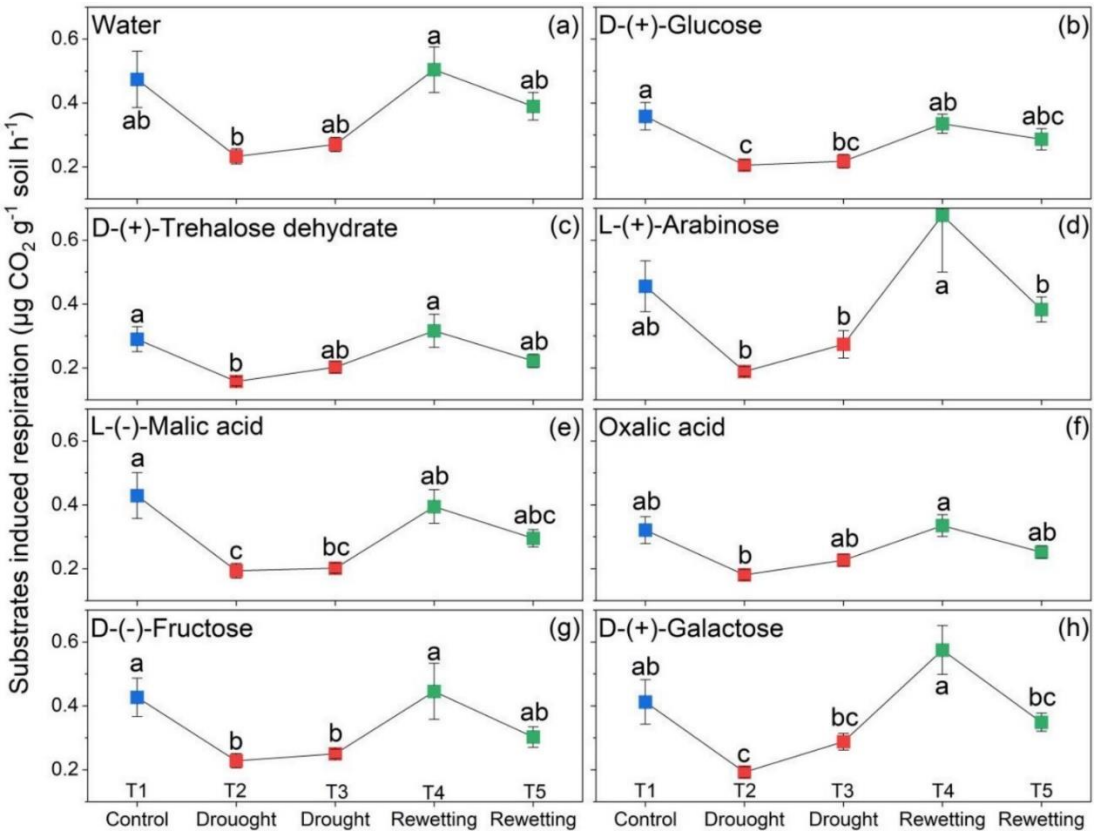

Figure 2-6 *Soil microbial respiration induced by water and 7 substrates from the 5 sampling times under rewetting patterns, respectively. Values are means ± standard error (n = 24 for T1, n = 8 for T2-T3 and n = 4 for T4-T5). Different lowercase letters above or below the error bar in each sub-figure indicated significant difference in soil microbial respiration under different sampling times at* p < *0.05, based on one-way ANOVA followed by a Tukey-Kramer post-hoc test.*

The turnover time (T_t) of enzymes were strongly influenced by drought and rewetting as well as flooding (Figure 5). The T_t of chitinase and β-glucosidase extended by 26.9 and 16.0%, respectively, when WHC dropped to 20% in T2. At the beginning of drought (T2), T_t of acid phosphomonoesterase and β-glucosidase was more or less similar to the initial period (T1) but the T_t of these two enzymes increased in association with prolonged drought. The pulse rewetting and flooding boosted T_t of chitinase and β-glucosidase which then reduced with the time of rewetting incubation in compare to the control. However, T_t of acid phosphomonoesterase significantly decreased after rewetting and flooding. Rewetting seemed to prolong the T_t as compared to flooding by the end of the experiment.

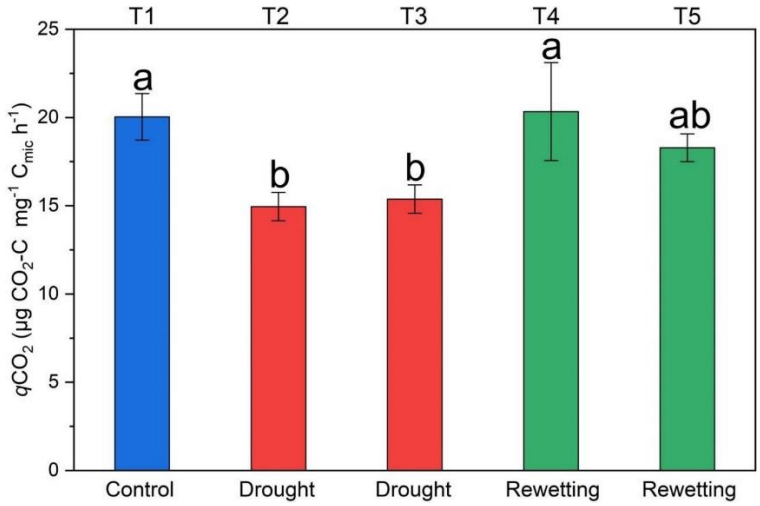

Figure 2-7 *qCO_2 from the 5 sampling times under rewetting pattern. Values are means ± standard error (n = 24 for T1, n = 8 for T2-T3 and n = 4 for T4-T5). Different lowercase letters above the error bar indicated significant difference in qCO_2 under different sampling times at $p < 0.05$, based on one-way ANOVA followed by a Tukey-Kramer post-hoc test.*

3.3 Drought and rewetting effects on microbial respiration and microbial biomass

Both soil basal respiration and substrate-induced respirations (SIRs) were strongly altered by drought and rewetting (Figure 6). The soil basal respiration was 50.9% inhibited by drought ($p < 0.05$), and recovered to the control level after rewetting. The same pattern was seen in the SIRs for all tested substrates. The metabolic quotient (qCO_2) decreased by 25.4% and 23.3% during two weeks of drought incubation on T2 and T3 ($p < 0.01$), respectively and recovered to be comparative with control after rewetting (Figure 7).

When WHC dropped to 20% in T2, MBC dramatically decreased by 42.7% relative to the control, while MBP surged over the control treatment (Figure 8). However, a recovery of MBC was found after rewetting soil, which was not obviously demonstrated in MBP.

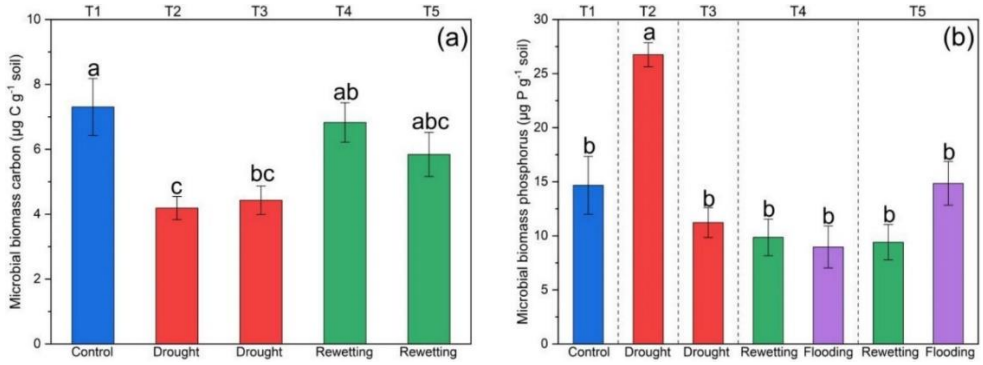

Figure 2-8 *Soil microbial biomass carbon (a) and phosphorus (b) content from the 5 sampling times under rewetting and flooding patterns, respectively. Values are means ± standard error (n = 24 for T1, n = 8 for T2-T3 and n = 4 for T4-T5). Different lowercase letters above the error bar in each sub-figure indicated significant difference in microbial biomass under different sampling times or rewetting patterns at* $p < 0.05$*, based on one-way ANOVA followed by a Tukey-Kramer post-hoc test.*

4. Discussion

4.1 Environmental history relevant to responses of microbial activities to dry period followed by different rewetting levels

Drought resulted in decreased enzyme activities, indicating its negative impacts on microbial activities. This can be attributed to the significant reduction in environmental water potential caused by drought, creating an imbalance between the water potential inside and outside microbial cells (Schimel, 2018). There was a time lag in the response of acid phosphomonoesterase to drought, whereas prolonged water stress decreased all three enzyme activities. Therefore, the reductions of chitinase and β-glucosidase activities that occurred at the beginning of drought (T2) reflected the decompositions of chitin and cellobiose are more susceptible to water stress than the hydrolysis of phosphate esters. Similar findings been observed in studies conducted in arid and semiarid regions (Sardans and Peñuelas, 2005; Sanaullah et al., 2011; Hueso et al., 2011). Our study, conducted on soil samples taken from a monsoon region, confirmed the negative effects of drought regardless of climatic regions. Notably, soil in our study was sampled during the dry season and then brought up to 60% WHC as a pre-condition step before exposing to drought. Therefore, the reduction of all enzyme activities during the experimental drought is possibly a return to the initial natural state or reflect historical memory of the original condition. Various indirect factors contribute to the decline in enzyme activities during drought, including microbial biomass decline (Baldrian et al., 2010), enzyme adsorption onto soil particle surface as it gets drier (Steinweg et al., 2012), and limited organic substrate availability (Acosta-Martínez et al., 2014). Moreover, diverse responses of enzyme activity reduction to drought highlighted the significant influence of environmental and climate history on moisture response through microbial community selection (Evans et al., 2022).

Our findings demonstrated a strong and positive correlation between chitinase and β-glucosidase activities with MBC during the transition from optimal to drought conditions, as well as prolonged drought period. This supports the speculation that the decline in MBC was the main factor contributing to the reduction in enzyme excretion (Figure S2). In contrast, the lack of correlation between acid phosphomonoesterase activities and MBP suggested that factor other than microbial biomass regulate acid phosphomonoesterase activities during the drought period (Figure S2). Furthermore, Zornoza et al. (2006) found no significant effects of soil air drying on phosphomonoesterase and β-glucosidase activities and proposed that the resistance of these enzymes to drought is the primary reason. Therefore, our findings indicated that in monsoon regions, microbial communities reallocate resources, resulting in a preference for less biomass C but more biomass P accumulation as an adaptive strategy to drought.

Rewetting reversed the negative effects of drought by releasing microbes from the stress of water potential and flushing available substrates through the soil (Tan et al., 2023). But, the three measured enzyme activities exhibited different responses to rewetting (Figure 2). Abrupt rewetting and flooding likely induced an osmotic shock for microbial communities, resulting in a further decline in chitinase and β-glucosidase activities. These activities reached even lower values compared to drought, especially under flooding condition (100%WHC). In contrast, acid phosphomonoesterase activities immediately increased after rewetting and flooding due to the presence of available labile organic P compounds (Nguyen and Marschner, 2005), which served as available substrates for microorganisms. In comparison with the effects of abrupt rewetting and flooding at T4, the prolonged rewetting and flooding resulted in elevated activities of β-glucosidase and acid phosphomonoesterase regardless of moisture levels. However, the response of chitinase activity to prolonged rewetting and flooding yielded opposite results. Prolonged flooding may increase chitinase activity as a consequence of soil denitrification process, which triggers the shortage of N availability for microbial demand and

subsequently stimulates chitinase production (Tomasek et al., 2019; Guo et al., 2019). Conversely, rewetting may trigger the release of osmolytes rich in N compounds, resulting in a reduction of chitinase activities (Csonka, 1989). Based on these findings, our study confirmed the first hypothesis regarding the recovery of enzyme activities after prolonged rewetting. However, the second hypothesis was rejected, as flooding at the 100% WHC level induced a greater recovery of enzyme activities compared to rewetting at the 60% WHC level.

4.2 Microbial responses to dry-rewetting are dependent of enzyme specific and rewetting level

Under prolonged drought conditions, lower enzyme activities were observed alongside higher substrate affinity (lower K_m), indicating the presence of the isoenzymes in the ecosystem (Stone et al., 2014). These isoenzymes, with similar functions but different conformation and structure, arose from changes in microbial species or alternations in microbial community structures as an adaptation strategy to environmental stress (Razavi et al., 2017; Zhang et al., 2018; Wang et al., 2020). The responses of these enzymes suggested a shift in the microbial community towards expressing enzyme systems with higher substrate efficiency in response to unfavorable soil moisture conditions. However, the effects of the beginning period of drought on enzyme system remain unclear. In contrast, SIR was significantly lower under drought compared to optimal condition, with the most notable differences observed at the onset of drought. Additionally, chitinase was the only enzyme that exhibited a decoupling of V_{max} and K_m at the onset of drought, implying different factors regulating enzyme synthesis and substrate affinity to chitin decomposition (Razavi et al., 2015). Consequently, the enzyme catalytic processes involved in the decomposition of chitin were unpredictable, particularly during the early stages of the drought period.

The substrate affinity (K_m) remained relatively unchanged after an abrupt change of soil moisture, both during prolonged drought and after rewetting. This observation suggested that the soil microbial community adopts a survival strategy following drought, allocating greater energy and nutrients towards maintaining the efficiency of enzyme-substrate interactions to support biomass accumulation. As a result, there was a reduction in the community's specific investment in enzyme production relative to biomass (Evans et al., 2022). The stronger response of SIR to rewetting compared to drought could be attributed to C use efficiency of the dominated microbial communities. Meanwhile, the positive correlation between the SIR pattern and the metabolic quotient (qCO_2) implied that microbial communities prioritize allocating their energy to maintain respiration processes rather than focusing on cell growth and reproduction (Sun et al., 2017). Alternatively, there may be a shift in the microbial community towards less C-efficient groups. As a result, the substrate turnover time for chitinase and β-glucosidase was longer after rewetting compared to drought. However, the release of labile organic P immediately after abrupt rewetting (Nguyen and Marschner, 2005) accelerated the activities and catalytic efficiency of acid phosphomonoesterase, leading to a shorter substrate turnover time in comparison with prolonged drought. Therefore, microbial responses to dry-rewetting are enzyme specific and dependent on the rewetting level: rewetting at 60% WHC has a greater impact on enzyme systems, while flooding at 100% WHC has a greater effect on enzyme synthesis.

The prolonged rewetting resulted in increased enzyme activities of β-glucosidase and acid phosphomonoesterase regardless of moisture levels. Meanwhile, the substrate affinities remained similar to those observed at the abrupt rewetting points. These findings demonstrated that

microorganisms seemed to adapt to moisture conditions by conserving their energy and P resources rather than expending them on adjusting enzyme system.

Similar responses to the addition of substrates were observed between initial drought and prolonged drought, as well as and between initial rewetting and prolonged rewetting. This suggested that moisture fluctuation played a crucial role in regulating microbial activities during the dry-rewetting cycle. These findings are consistent with the study by Conant et al. (2004), which demonstrated a strong relationship between microbial respiration and potential soil moisture. Furthermore, the fluctuation of soil moisture can influence the dynamic of SIR by inducing changes in microbial community structure and abundance (Bell et al., 2009), as well as altering the availability of substrates (Gao et al., 2022) during alternative dry-rewetting events.

5. Conclusion

Overall, we found that the experience of microbes to dry-rewetting in monsoon region can trigger the recovery of microbial activities after dry-rewetting cycles. These findings indicated the reallocation of C and nutrient resources by soil microbes to adapt to dry-rewetting cycle. This acclimation effect has implications for the efficiency of C, N, and P mobilizations, thereby affects biological and chemical properties of the soil. However, microbial responses to dry-rewetting are enzyme specific and depending on rewetting level: rewetting at 60% WHC has a greater impact on enzyme systems, while flooding at 100% WHC induces more effects on enzyme synthesis. In summary, our study highlights the importance of considering microbial stress sensitivity and long-term stress memory in understanding the impacts of dry-rewetting on soil microbial activities. Therefore, these findings contribute to our understanding of soil ecosystem functioning and nutrient cycling processes.

Acknowledgment

This study was funded by National Foundation for Science and Technology Development, Vietnam (Project code: Nafosted, 105.99-2020.23). We gratefully acknowledge the China Scholarship Council for financial support to Shang Wang in Germany.

References

Acosta-Martínez, V., Cotton, J., Gardner, T., Moore-Kucera, J., Zak, J., Wester, D., Cox, S., 2014. Predominant bacterial and fungal assemblages in agricultural soils during a record drought/heat wave and linkages to enzyme activities of biogeochemical cycling. Applied Soil Ecology, 84, 69-82.

Ahmed, M.A., Sanaullah, M., Blagodatskaya, E., Mason-Jones, K., Jawad, H., Kuzyakov, Y., Dippold, M.A., 2018. Soil microorganisms exhibit enzymatic and priming response to root mucilage under drought. Soil Biology and Biochemistry, 116, 410-418.

Allison, S.D., Treseder, K.K., 2008. Warming and drying suppress microbial activity and carbon cycling in boreal forest soils. Global Change Biology, 14, 2898-2909.

Allison, S.D., Weintraub, M.N., Gartner, T.B., Waldrop, M.P., 2010. Evolutionary-economic principles as regulators of soil enzyme production and ecosystem function. In: Shukla, G., Varma, A. (eds) Soil Enzymology. Soil Biology, vol 22. Springer, Berlin, Heidelberg.

Anderson, J.P.E., Domsch, K.H., 1978. A physiological method for the quantitative measurement of microbial biomass in soils. Soil Biology and Biochemistry, 10(3) 215-221.

Anderson, T-H, Domsch, K.H., 1990. Application of eco-physiological quotients (qCO2 and qD) on microbial biomasses from soils of different cropping histories. Soil Biology and Biochemistry, 22, 2, 251-255.

Austin, A.T., Yahdjian, L., Stark, J.M., Belnap, J., Porporato, A., Norton, U., Racetta, D.A., Schseffer,

S.M., 2004. Water pulses and biogeochemical cycles in arid and semiarid ecosystems. Oecologia, 141, 221-235.
Baldrian, P., Merhautová, V., Petránková, M., Cajthaml, T., Šnajdr, J., 2010. Distribution of microbial biomass and activity of extracellular enzymes in a hardwood forest soil reflect soil moisture content. Applied Soil Ecology, 46, 2, 177-182.
Beck, T., Joergensen, R.G., Kandeler, E., Makeschin, F., Nuss, E., Oberholzer, H.R., Scheu, S. 1997. An inter-laboratory comparison of ten different ways of measuring soil microbial biomass C. Soil Biology and Biochemistry, 29(7), 1023-1032.
Bell, C.W., Acosta-Martínez, V., McIntyre, N.E., Cox, S., Tissue, D.T., Zak, J.C., 2009. Linking microbial community structure and function to seasonal differences in soil moisture and temperature in a chihuahuan desert grassland. Microbial Ecology, 58, 827-842.
Bérard, A., Mazzia, C., Sappin-Didier, V., Capowiez, L., Capowiez, Y., 2014. Use of the MicroResp™ method to assess Pollution-Induced Community Tolerance in the context of metal soil contamination. Ecological Indicators 40, 27-33.
Blagodatskaya, E., Kuzyakov, Y., 2013. Active microorganisms in soil: critical review of estimation criteria and approaches. Soil Biology and Biochemistry, 67, 192-211.
Borowik, A., Wyszkowska, J., 2016. Soil moisture as a factor affecting the microbiological and biochemical activity of soil. Plant, soil and Environment, 62(6), 250-255.
Brangarí, A.C., Manzoni, S., Rousk, J., 2020. A soil microbial model to analyze decoupled microbial growth and respiration during soil drying and rewetting. Soil Biology and Biochemistry, 148, 107871.
Brolsma, K.M., Vonk, J.A., Hoffland, E., Mulder, C., Goede, R.G.M., 2015. Effects of GM potato Modena on soil microbial activity and litter decomposition fall within the range of effects found for two conventional cultivars. Biology and Fertility of Soils, 51, 913-922.
Brödlin, D., Kaiser, K., Kessler, A., Hagedom, F., 2019. Drying and rewetting foster phosphorus depletion of forest soils. Soil Biology and Biochemistry, 128, 22-34.
Butcher, K.R., Nasto, M.K., Norton, J.M., Stark, J.M., 2020. Physical mechanisms for soil moisture effects on microbial carbon-use efficiency in a sandy loam soil in the western United States. Soil Biology and Biochemistry, 150, 107969.
Bär, M., Hardenberg, J., Meron, E., Provenzale, A., 2002. Modelling the survival of bacteria in drylands: the advantage of being dormant. Proceedings of the Royal Society of London. Series B: Biological Sciences, 269(1494), 937-942.
Campbell, C.D., Chapman, S.J., Cameron, C.M., Davidson, M.S., Potts, J.M., 2003. A rapid microtiter plate method to measure carbon dioxide evolved from carbon substrate amendments so as to determine the physiological profiles of soil microbial communities by using whole soil. Applied and Environmental Microbiology, 69, 3593-3599.
Cameron, C., 2007. MicroResp™ Technical Manual—A Versatile Soil Respiration System. Macaulay Institute, Craigiebuckler, Aberdeen, Scotland, UK.
Conant, R.T., Dalla-Betta, P., Klopatek, C.C., Klopatek, J.M., 2004. Controls on soil respiration in semiarid soils. Soil Biology and Biochemistry, 36(6), 945-951.
Csonka, L.N., 1989. Physiological and genetic responses of bacteria to osmotic stress. Microbiological Reviews, 53(1), 121-147.
D'Angelo, E., Crutchfield, J., Vandiviere, M., 2001. Rapid, sensitive, microscale determination of phosphate in water and soil. Journal of Environmental Quality, 30, 2206-2209.
de Nijs, E.A., Hicks, L.C., Leizeaga, A., Tietema, A., Rousk, J., 2019. Soil microbial moisture dependences and responses to drying-rewetting: The legacy of 18 years drought. Global Change Biology, 25, 1005-1015.
Ebrahimi, A., Or, D., 2016. Microbial community dynamics in soil aggregates shape biogeochemical gas fluxes from soil profiles–upscaling an aggregate biophysical model. Global Change Biology, 22, 9, 3141-3156.

Evans, S.E., Allison, S.D., Hawkes, C.V., 2022. Microbes, memory and moisture: Predicting microbial moisture responses and their impact on carbon cycling. Functional Ecology, 36, 1430-1441.
Evans, S.E., Wallenstein, M.D., 2012. Soil microbial community response to drying and rewetting stress: does historical precipitation regime matter? Biogeochemistry, 109, 101-116.
Fierer, N., Schimel, J.P., 2003. A proposed mechanism for the pulse in carbon dioxide production commonly observed following the rapid rewetting of a dry soil. Soil Science Society of America Journal, 67, 798-805.
Fuchslueger, L., Bahn, M., Fritz, K., Hasibeder, R., Richter, A., 2014. Experimental drought reduces the transfer of recently fixed plant carbon to soil microbes and alters the bacterial community composition in a mountain meadow. New Phytologist, 201, 916-927.
Gao, D., Bai, E., Li, M., Zhao, C., Yu, K., Hagedorn, F., 2020. Responses of soil nitrogen and phosphorus cycling to drying and rewetting cycles: A meta-analysis. Soil Biology and Biochemistry, 148, 107896.
Gao, F., Fan, H., Chapman, S.J., Yao, H., 2022. Changes in soil microbial community activity and composition following substrate amendment within the MicroResp™ system. Journal of Soils and Sediments, 22, 1242-1251.
German, D.P., Weintraub, M.N., Grandy, A.S., Lauber, C.L., Rinkes, Z.L., Allison, S.D., 2011. Optimization of hydrolytic and oxidative enzyme methods for ecosystem studies. Soil Biology and Biochemistry, 43(7), 1387-1397.
Gordon, H., Haygarth, P.M., Bardgett, R.D., 2008. Drying and rewetting effects on soil microbial community composition and nutrient leaching. Soil Biology and Biochemistry, 40(2), 302-311.
Guo, G., Wang, T., Li, K., Li, L., Zhang, J., Guo, S., Ling, N., Shen, Q., 2019. Historical nitrogen deposition and straw addition facilitate the resistance of soil multifunctionality to drying-wetting cycles. Applied and Environmental Microbiology, 85(8), e02251-18.
Hamonts, K., Clough, T.J., Stewart, A., Clinton, P.W., Richardson, A.E., Wakelin, S.A., O'Callaghan, M., Condron, L.M., 2013. Effect of nitrogen and waterlogging on denitrifier gene abundance, community structure and activity in the rhizosphere of wheat. FEMS microbiology ecology, 83, 3, 568-584.
Harrison-Kirk, T., Beare, M.H., Meenken, E.D., Condron, L.M., 2014. Soil organic matter and texture affect responses to dry/wet cycles: Changes in soil organic matter fractions and relationships with C and N mineralization. Soil Biology and Biochemistry, 74, 50-60.
Haynes, R.J., Swift, R.S., 1989. Effect of rewetting air-dried soils on pH and accumulation of mineral nitrogen. European Journal of Soil Science, 40, 341-347.
Hicks, L.C., Lin, S., Rousk, J., 2022. Microbial resilience to drying-rewetting is partly driven by selection for quick colonizers. Soil Biology and Biochemistry, 167, 108581.
Hueso, S., Hernández, T., García, C., 2011. Resistance and resilience of the soil microbial biomass to severe drought in semiarid soils: The importance of organic amendments. Applied Soil Ecology, 50, 27-36.
Huygens, D., Schouppe, J., Roobroeck, D., Alvarez, M., Oscar, B., Valenzuela, E., Pinochet, D., Boeckx, P., 2011. Drying–rewetting effects on N cycling in grassland soils of varying microbial community composition and management intensity in south central Chile. Applied Soil Ecology, 48(3), 270-279.
IPCC, 2021: Summary for Policymakers. In: Climate Change 2021: The Physical Science Basis. Contribution of Working Group I to the Sixth Assessment Report of the Intergovernmental Panel on Climate Change [Masson-Delmotte, V., P. Zhai, A. Pirani, S.L. Connors, C. Péan, S. Berger, N. Caud, Y. Chen, L. Goldfarb, M.I. Gomis, M. Huang, K. Leitzell, E. Lonnoy, J.B.R. Matthews, T.K. Maycock, T. Waterfield, O. Yelekçi, R. Yu, and B. Zhou (eds.)]. In Press.
Kaiser, E.A., Mueller, T., Joergensen, R.G., Insam, H., Heinemeyer, O., 1992. Evaluation of methods to estimate the soil microbial biomass and the relationship with soil texture and organic matter. Soil biology and biochemistry, 24(7), 675-683.

Kalbitz, K., Solinger, S., Park, J.H., Michalzik, B., Matzner, E., 2000. Controls on the dynamics of dissolved organic matter in soils: a review. Soil Science, 165, 4, 277-304.
Koch, O., Tscherko, D., Kandeler, E., 2007. Temperature sensitivity of microbial respiration, nitrogen mineralization, and potential soil enzyme activities in organic alpine soils. Global Biogeochemical Cycles, 21, GB4017.
Leitner, S., Minixhofer, P., Inselsbacher, E., Keiblinger, K.M., Zimmermann, M., Zechmeister-Boltenstern, S., 2017. Short-term soil mineral and organic nitrogen fluxes during moderate and severe drying-rewetting events. Applied Soil Ecology, 114, 28-33.
Lesk, C., Rowhani, P., Ramankutty, N., 2016. Influence of extreme weather disasters on global crop production. Nature, 529, 84-87.
Makino, T., Hasegawa, S., Sakurai, Y., Ohno, S., Utagawa, H., Maejima, Y., Momohara, K., 2000. Influence of soil-drying under field conditions on exchangeable manganese, cobalt, and copper contents. Soil Science and Plant Nutrition, 46(3), 581-590.
Maranguit, D., Guillaume, T., Kuzyakov, Y., 2017. Land-use change affects phosphorus fractions in highly weathered tropical soils. Catena 149, 385–393.
Mikha, M.M., Rice, C.W., Miliken, G.A., 2005. Carbon and nitrogen mineralization as affected by drying and wetting cycles. Soil Biology and Biochemistry, 37(2), 339-347.
Navarro-Garcia, F., Casermeiro, M.A., Schimel, J.P., 2012. When structure means conservation: Effect of aggregate structure in controlling microbial responses to rewetting events. Soil Biology and Biochemistry, 44(1), 1-8.
Nannipieri, P., Eldor, P., 2009. The chemical and functional characterization of soil N and its biotic components. Soil biology and biochemistry, 41(12), 2357-2369.
Nguyen, B.T., Marschner, P., 2005. Effect of drying and rewetting on phosphorus transformations in red brown soils with different soil organic matter content. Soil Biology and Biochemistry, 37(8), 1573-1576.
Nguyen, O.V., Kawamura, K., Trong, D.P., Gong, Z., Suwandana, E., 2015. Temporal change and its spatial variety on land surface temperature and land use changes in the Red River Delta, Vietnam, using MODIS time-series imagery. Environmental Monitoring and Assessment, 187, 464.
Ouyang, Y., Li., X., 2020. Effect of repeated drying-rewetting cycles on soil extracellular enzyme activities and microbial community composition in arid and semi-arid ecosystems. European Journal of Soil Biology, 98, 103187.
Panikov, N.S., Blagodatsky, S.A., Blagodatskaya, J.V., Glagolev, M.V., 1992. Determination of microbial mineralization activity in soil by modified Wright and Hobbie method. Biology and Fertility of Soils, 14, 280-287.
Pohlon, E., Fandino, A.O., Marxsen, J., 2013. Bacterial community composition and extracellular enzyme activity in temperate streambed sediment during drying and rewetting. Plos One, 8(12), e83365.
Qi, J., Markewitz, D., Foroughi, M., Jokela, E., Strahm, B., Vogel, J., 2018. Drying-wetting cycles: effect on deep soil carbon. Soil Systems, 2(1), 3.
Razavi, B.S., Blagodatskaya, E., Kuzyakov, Y., 2016. Temperature selects for static soil enzyme systems to maintain high catalytic efficiency. Soil Biology and Biochemistry, 97, 15-22.
Razavi, B.S., Liu, S.B., Kuzyakov, Y., 2017. Hot experience for cold-adapted microorganisms: Temperature sensitivity of soil enzymes. Soil Biology and Biochemistry, 105, 236-243.
Ross, D.J., Scott, N.A., Tate, K.R., Rodda, N.J., Townsend, J.A., 2001. Root effects on soil carbon and nitrogen cycling in a Pinus radiata D. Don plantation on a coastal sand. Soil Research, 39(5), 1027-1039.
Sanaullah, M., Blagodatskaya, E., Chabbi, A., Rupel, C., Kuzyakov, Y., 2011. Drought effects on microbial biomass and enzyme activities in the rhizosphere of grasses depend on plant community composition. Applied Soil Ecology, 48(1), 38-44.
Sardans, J., Peñuelas, J., 2005. Drought decreases soil enzyme activity in a Mediterranean Quercus

ilex L. forest. Soil Biology and Biochemistry, 37(3), 455-461.
Schimel, J.P., 2018. Life in dry soils: effects of drought on soil microbial communities and processes. Annual Review of Ecology, Evolution and Systematics, 49, 409-432.
Schimel, J.P., Wetterstedt, J.Å.M., Holden, P.A., Trumbore, S.E., 2011. Drying/rewetting cycles mobilize old C from deep soils from a California annual grassland. Soil Biology and Biochemistry, 43(5), 1101-1103.
Steinweg, J.M., Dukes, J.S., Wallenstein, M.D., 2012. Modeling the effects of temperature and moisture on soil enzyme activity: Linking laboratory assays to continuous field data. Soil Biology and Biochemistry, 55, 85-92.
Stock, S.C., Köster, M., Dippold, M.A., Nájera, F., Matus, F., Merino, C., Boy, J., Spielvogel, S., Gorbushina, A., Kuzyakov, Y., 2019. Environmental drivers and stoichiometric constraints on enzyme activities in soils from rhizosphere to continental scale. Geoderma, 337, 973-982.
Stone, M.M., DeForest, J.L., Plante, A.F., 2014. Changes in extracellular enzyme activity and microbial community structure with soil depth at the Luquillo Critical Zone Observatory. Soil Biology and Biochemistry, 75, 237-247.
Sun, D., Li, K., Bi, Q., Zhu, J., Zhang, Q., Jin, C., Lu, L., Lin, X., 2017. Effects of organic amendment on soil aggregation and microbial community composition during drying-rewetting alternation. Science of The Total Environment, 574, 735-743.
Tan, X.P., He, J.H.., Nie, Y.X., Ni, X.L., Ye, Q., Ma, L., Megharaj, M., He, W.X., Shen, W., 2023. Climate and edaphic factors drive soil enzyme activity dynamics and tolerance to Cd toxicity after rewetting of dry soil. Science of The Total Environment, 855, 158926.
Tebo, B.M., Johnson, H.A., McCarthy, J.K., Templeton, A.S., 2005. Geomicrobiology of manganese (II) oxidation. Trends in Microbiology, 13(9), 421-428.
Tomasek, A.A., Hondzo, M., Kozarek, J.L., Staley, C., Wang, P., Lurndahl, N., Sadowsky, M.J., 2019. Ecosphere, 10(1), e02549.
Walworth, J.L., 1992. Soil drying and rewetting, or freezing and thawing, affects soil solution composition. Soil Science Society of America Journal, 56(2), 433-437.
Wang, L., Wang, L., Zhan, X., Huang, Y., Wang, J., Wang, X., 2020. Response mechanism of microbial community to the environmental stress caused by the different mercury concentration in soils. Ecotoxicology and Environmental Safety, 188, 109906.
Wang, S., Zhang, X.C., Xu, Z., Ma, Q.H., Chu, J.C., Zang, H.D., Yang, Y.D., Peixoto, L., Zeng, Z.H., Razavi, B.S., 2023. Transition of spatio-temporal distribution of soil enzyme activity after straw incorporation: From rhizosphere to detritusphere, 186, 104814.
West, A.W., Sparling, G.P., 1986. Modifications to the substrate-induced respiration method to permit measurement of microbial biomass in soils of differing water contents. Journal of Microbiological Methods, 5(3-4), 177-189.
Wei, L., Razavi, B.S., Wang, W., Zhu, Z., Liu, S., Wu, J., Kuzyakov, Y., Ge, T., 2019. Labile carbon matters more than temperature for enzyme activity in paddy soil. Soil Biology and Biochemistry, 135, 134-143.
Xiang, S., Doyle, A., Holden, P.A., Schimel, J.P., 2008. Drying and rewetting effects on C and N mineralization and microbial activity in surface and subsurface California grassland soils. Soil Biology and Biochemistry, 40(9), 2281-2289.
Yang, H., Koide, R.T., Zhang, Q., 2016. Short-term waterlogging increases arbuscular mycorrhizal fungal species richness and shifts community composition. Plant and Soil, 404, 373-384.
Yevdokimov, I., Larionova, A., Blagodatskaya, E., 2016. Microbial immobilisation of phosphorus in soils exposed to drying-rewetting and freeze-thawing cycles. Biology and Fertility of Soils, 52, 685-696.
Zarebanadkouki, M., Fink, T., Benard, P., Banfield, C.C., 2019. Mucilage facilitates nutrient diffusion in the drying rhizosphere. Vadose Zone Journal, 18(1), 1-13.
Zhang, S., Yang, D., Yang, Y., Piao, S., Yang, H., Lei, H., Fu, B., 2018. Excessive afforestation and

soil drying on China's Loess Plateau. Journal of Geophysical Research-Biogeosciences. 123(3), 923-935.
Zhang, X., Dippold, M.A., Kuzyakov, Y., Razavi, B.S., 2019. Spatial pattern of enzyme activities depends on root exudate composition. Soil Biology and Biochemistry, 133, 83-93.
Zhang, X., Myrold, D.D., Shi, L., Kuzyakov, Y., Dai, H., Hoang, D.T.T., Dippold, M.A., Meng, X., Song, X., Li, Z., Zhou, J., Razavi, B.S., 2021. Resistance of microbial community and its functional sensitivity in the rhizosphere hotspots to drought. Soil Biology and Biochemistry, 161, 108360.
Zhu, B., Cheng, W., 2013. Impacts of drying–wetting cycles on rhizosphere respiration and soil organic matter decomposition. Soil Biology and Biochemistry, 63, 89-96.
Zornoza, R., Guerrero, C., Mataix-Solera, J., Arcenegui, A., García-Orenes, F., Mataix-Beneyto. J., 2006. Assessing air-drying and rewetting pre-treatment effect on some soil enzyme activities under Mediterranean conditions. Soil Biology and Biochemistry, 38(8), 2125-2134.

Supplementary data

Table S2-1 *Soil enzyme activities (V_{max}) and substrate affinity (K_m) of chitinase (Chit), β-D-glucosidase (Glu) and acid phosphomonoesterase (Phos) of T1 under three treatment and T2-T5 under control treatment.*

Sampling time	Treatment	Chit	Glu	Phos
V_{max}				
T1	Control	22.7 ± 2.0	25.2 ± 2.3	72.0 ± 9.6
	Rewetting	23.7 ± 3.9	25.0 ± 2.5	70.0 ± 0.5
	Flooding	24.4 ± 1.4	27.9 ± 1.6	71.5 ± 4.5
T2	Control	23.8 ± 1.3	25.0 ± 1.5	72.2 ± 2.2
T3/4	Control	22.3 ± 3.3	27.3 ± 2.9	71.2 ± 1.5
T5	Control	24.8 ± 0.4	25.8 ± 0.5	70.0 ± 3.1
K_m				
T1	Control	26.6 ± 2.9	39.9 ± 4.9	23.2 ± 8.1
	Rewetting	28.9 ± 1.4	41.0 ± 3.6	19.7 ± 2.0
	Flooding	27.1 ± 1.6	42.8 ± 3.8	20.3 ± 2.3
T2	Control	28.3 ± 2.4	43.0 ± 3.8	22.5 ± 2.3
T3/4	Control	26.7 ± 1.9	40.8 ± 2.8	19.2 ± 0.5
T5	Control	27.9 ± 2.4	40.3 ± 2.3	20.8 ± 1.6

Value are mean ± standard error (n = 4).

Table S2-2 *Soil enzyme activities (Vmax) and substrate affinity (Km) of chitinase (Chit), β-D-glucosidase (Glu) and acid phosphomonoesterase (Phos) of T2-T3 under drought.*

Sampling time	Treatment	Chit	Glu	Phos
V_{max}				
T2	Rewetting	19.5 ± 0.3	21.0 ± 2.0	70.8 ± 2.9
	Flooding	19.0 ± 0.6	21.8 ± 0.9	73.6 ± 1.9
T3	Rewetting	18.8 ± 1.2	18.2 ± 1.1	41.0 ± 6.6
	Flooding	19.2 ± 1.7	17.4 ± 2.5	41.0 ± 3.6
K_m				
T2	Rewetting	37.7 ± 3.5	37.1 ± 4.8	20.0 ± 0.9
	Flooding	36.9 ± 1.8	35.0 ± 1.9	22.3 ± 4.1
T3	Rewetting	12.0 ± 1.0	22.9 ± 3.7	14.2 ± 1.9
	Flooding	13.0 ± 2.7	23.9 ± 1.9	13.9 ± 1.7

Value are mean ± standard error (n = 4).

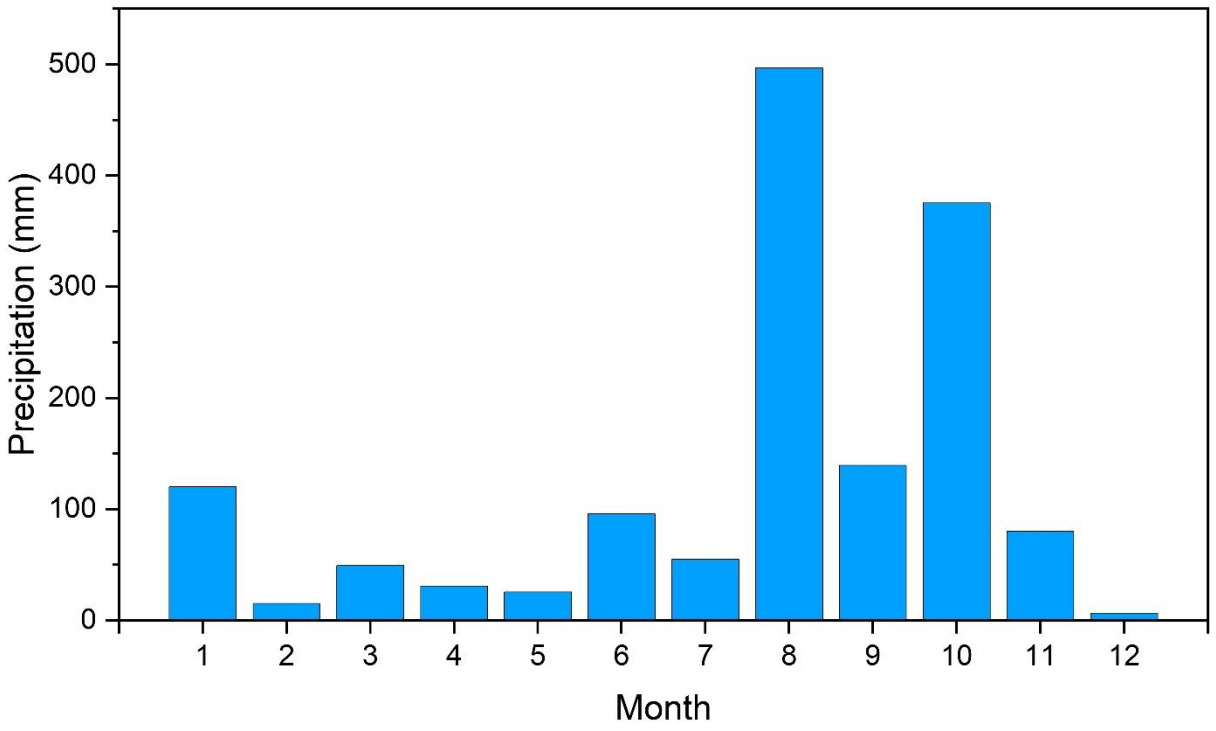

Figure S2-1 *Monthly distribution of precipitation in 2020. The data was provided by weather station located in Thai Binh province, Vietnam.*

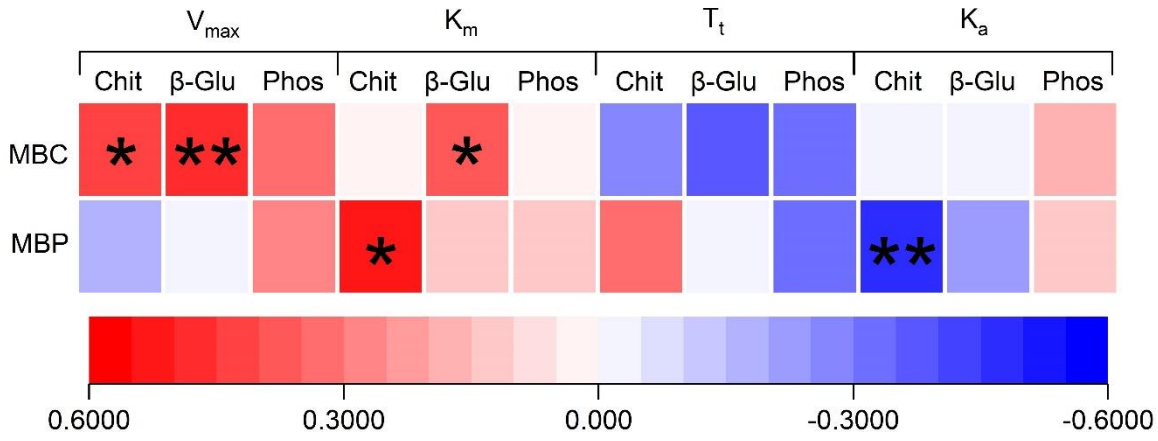

Figure S2-2 *Heatmap of correlations between microbial biomass and soil enzyme kinetic characters during the transition from optimum to drought and prolonged drought (T1-T3), based on Pearson correlation coefficients, * indicates correlation is significant at 0.05 level, ** indicates correlation is significant at 0.01 level.*

2.3 Study 3. Mutualistic interaction between arbuscular mycorrhiza fungi and soybean roots enhances drought resistant through regulating glucose exudation and rhizosphere expansion

Duyen Thi Thu Hoang [a, 1], Mehdi Rashtabari [b,1], Luu Anh The [c], **Shang Wang** [b], Dang Thanh Tu [a], Nguyen Viet Hiep [d], Bahar S. Razavi [b*]

Status: Published in *Soil Biology and Biochemistry*

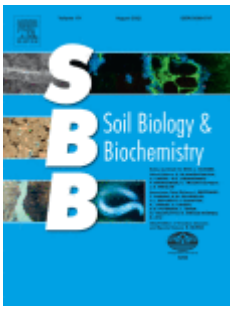

[a] *Climate Change and Development Program, VNU Vietnam-Japan University, Vietnam National University, Hanoi, Viet Nam*

[b] *Department of Soil and Plant Microbiome, Institute of Phytopathology, Christian-Albrechts University, Kiel, Germany*

[c] *VNU-Central Institute of Natural Resources and Environmental Studies, Vietnam National University, Hanoi, Viet Nam*

[c] *Microbiology Department, Soils and Fertilizers Research Instiute, Hanoi, Viet Nam*

Hoang, D. T. T., Rashtbari, M., Anh, L. T., Wang, S., Tu, D. T., Hiep, N. V., & Razavi, B. S. (2022). Mutualistic interaction between arbuscular mycorrhiza fungi and soybean roots enhances drought resistant through regulating glucose exudation and rhizosphere expansion. Soil Biology and Biochemistry, 171, 108728. https://doi.org/10.1016/j.soilbio.2022.108728

Abstract

Glucose is one of the low molecular weight components of root exudates to mediate the cross-talk between plants and microbes, but less is known about their contribution to drought resistance of plants and root-associated microbiome. To fill this knowledge gap, we optimized the visualization of glucose exudation and coupled it with another in situ tool – soil zymography – as well as destructive analysis of enzyme kinetics (β-glucosidase; acid phosphomonoesterase) and microbial biomass. This helped identify how microbial functionality – affected by drought and P limitation – will show more resistance in the hotspots of soybean rhizosphere (grown in the rhizoboxes for 10 weeks) associated with arbuscular mycorrhizal fungi (AMF) symbiosis than those without AMF. Drought reduced glucose exudation, mainly allocated to root tips, and narrowed the rhizosphere enzymatic hotspot by three times. However, AMF inoculation enhanced glucose exudation compared to non-mycorrhizal plants and enlarged enzymatic hotspot area by 53% under drought condition. Despite the 50% reduction in β-glucosidase and acid phosphomonoesterase activities owing to water deficit, AMF symbiont triggered up to 36% enzyme activities in correlation with the non-mycorrhizal ones. Therefore, the drought resistance of these two enzymes was enhanced by up to 63% in mycorrhizal plants. The biomass of microbial phosphorus increased by 45% under drought AMF-conditioned plants. We conclude that the cooperation between soybean and AMF induced the formation of favorable microsites around the root, specifically in overlapping localities between rhizosphere and mycorrhizosphere, characterized by enhanced glucose release, increasing rhizosphere expansion, high enzyme activities and shortened substrate turnover time. This, in turn, contributed to the stronger resistance of microbial functions (e.g., enzyme expression) to drought stress in the rhizosphere hotspots. Thus, in response to AMF inoculation and consequent high glucose availability, rhizosphere microorganisms increased P mining rate in those hotspots remaining active despite water scarcity.

Keywords: Glucose imaging; Rhizosphere; Mycorrhizosphere; Zymography; Microbial functional resistance

1. Introduction

Drought severity is projected to be more frequent in the future, posing major challenges for the persuasion of sustainable agriculture development globally (Mach et al., 2019). The induced water stress affects all aspects of plant growth, such as decreasing leaf area and size, hampering photosynthesis (Bruce et al., 2007), reducing the shoot/root ratio (Peña-Rojas et al., 2004, 2006) limiting aboveground to underground carbon (C) transfer (Fuchslueger et al., 2014, 2016; Hasibeder et al., 2015; Karlowsky et al., 2018), and C diffusion from roots to rhizosphere soil (Gorissen et al., 2004), indirectly affecting microbial activity (Kuzyakov and Blagodatskaya, 2015). In addition, water deficit triggers nutrient (e.g., phosphorus (P)) accumulation in soil, which is difficult for the plants to take up (Sardans and Peñuelas, 2004).

Plants have evolved various strategies to counter the negative effects of drought and P deficiency, ranging from modification of root morphology to physiological (Wang et al., 2001), biochemical, and biophysical processes (Carminati et al., 2010). Most prominently, plants can mediate root exudate quality and quantity to facilitate their communication with rhizosphere microorganisms (Williams and de Vries, 2020a, Williams and de Vries, 2020b), or form symbiosis with arbuscular mycorrhizal fungi (AMF) to increase water and P uptake (Doubková et al., 2012, 2013). If the mediation of exudates promotes the recovery of plants, microbial activities, and ecosystem functions after drought (Karlowsky et al., 2018), symbiosis with AMF enhances the buffering capacity of the plant to drought (Doubková et al., 2013). In fact, root exudates act as signals to attract symbionts as AMF to build symbiotic relationships (Peters and Long, 1988; Besserer et al., 2006). For example, drought increases organic acid exudation in maize, which is an effective chemoattractant for Bacillus subtilis (e.g., in the soybean rhizosphere; Allard-Massicotte et al., 2016) or a nutritional source for Trichoderma spp. (Zhang et al., 2014). Similarly, during drought, soybean may benefit from the symbiotic association with AMF, which enhances its osmoprotective properties (Pavithra and Yapa, 2018). In reality, soil systems with high spatio-temporal variability of properties are often subjected to combined stresses (Brook et al., 2008), which can, theoretically, affect plant-microbial cooperation strategy to overcome these limitations. However, the plant strategy to overcome drought by mediating symbiosis with AMF and regulating primary compounds (e.g., glucose) exudation within rhizosphere under nutrient deprivation is poorly investigated.

Glucose, the primary compound in exudates as an easy available sugar, is among the soluble carbohydrates that are adjusted by the roots to adapt to osmotic conditions (Sharp et al., 1990; Spollen et al., 2008; Voothuluru et al., 2016). On the other hand, the distribution of glucose also corresponds to the nutrient status of the rhizosphere (Marschner, 1998; Hinsinger, 2001). Water stress inhibits glucose exudation (Calvo et al., 2019), and instead stimulates the accumulation of this compatible solute in roots (Palta and Gregory, 1997) to maintain physiological processes such as stomatal conductance, photosynthetic rate (Jacob and Lawlor 1991; Ghannoum and Conroy 2007), and expansion growth (Morgan, 1984; Bohnert and Sheveleva, 1998; Hoffmann, 2010). In contrast, the

root secretion of glucose tends to increase as a strategy of plants to deal with P deficiency (Carvalhais et al., 2011). Although the exuded glucose supposedly varies with plant growth stage (Vancura and Hovadik, 1965), plant species (Strickland et al., 2012), and environmental conditions (Calvo et al., 2019), its exudation pattern is still obscure, especially as plants suffer the combined effects of drought and P deficiency.

It is well known that glucose is a labile source of energy for microbial community within rhizosphere. Despite flavonoids released by plant roots act as a signal to attract AMF symbiont (Buee et al., 2000; Antunes et al., 2006), enriched glucose exudation makes rhizosphere more attractive to soil microorganisms. The presence of such microbial communities in the rhizosphere facilitates nutrient transformation to meet the demands of plants and themselves by synthesizing different functioning enzymes. Consequently, the rhizosphere is one of the most critical microbial hotspots in the agroecosystem and probably in terrestrial ecosystems. However, the formation of such hotspots in the rhizosphere strongly depends on biotic factors mediated by root-microbial interactions (Razavi et al., 2016; Kuzyakov and Razavi, 2019) and affected by abiotic controls. In other words, the resistance of microorganisms affects the ability of the system to maintain ecosystem services even under critical stress conditions (Shade et al., 2012). To cover the costs of this resistance, energetic adaptation mechanisms (e.g., expression of enzymes) are required by individual microbial groups to redirect resources from growth to survival-related mechanisms (Schimel et al., 2007; Zhnag X. et al., 2020). Accordingly, the microsites with abundant resources (e.g., hotspots with high abundance of available C) exhibit strengthened resistance in soil ecosystems (Shu et al., 2019; Zhang et al., 2021). Hence, the significant increase in the distribution of rhizosphere microbial hotspots under P-limitation and water-stress conditions can be used to evaluate the resistance and recovery threshold of plants with AMF symbiosis.

Here, we tested the following hypotheses: i) Drought reduces microbial energy resources (e.g. root exudate), thus, indirectly changing microbial activity. ii) Microbial functionality - affected by drought and P limitation - will show more resistance in the hotspots of soybean rhizosphere associated with AMF symbiosis than those without AMF, due to a higher abundance of the available substrate (e.g. glucose); iii) AMF increases the accessibility of plants to nutrient sources not only by their hypha system but also by enlarging enzymatic rhizosphere size that extends soil volume mined by plants and microbes for potentially available nutrients.

To clarify the hypotheses, soybeans (*Glycine max* L.) were grown in rhizoboxes containing P-limited soil in a greenhouse at 22 °C under two water conditions of 65% WHC and 25% WHC for 10 weeks. Coupled with direct glucose imaging, soil zymography was implemented to demonstrate the mediation of C and P transformation and translocation by mycorrhizal roots and soil microbial communities to adapt to drought condition and restricted P availability. Additionally, microbial biomass P and kinetics of β-glucosidase and acid phosphomonoesterase were assayed to interpret the role of AMF symbiosis in the resistant capacity of microorganisms under water stress and P deprivation.

2. Materials and methodologies

2.1. Soil sampling and experimental design

Soil was collected in January 2020 from the depth of 0–20 cm of the Ap horizon of an arable sandy clay loam, Fluvisol, located in Quang Nam, a southern province of central region of Vietnam

(15°49′11″N, 108°09′77″E). Roots and stones were separated and soil was immediately sealed in a plastic bag. The samples were kept cold (~4 °C) during transportation to the laboratory. Soil sample were sieved through a 2 mm mesh prior to the experiment. A small portion of soil was dried under 60 °C, ground and prepared for C and N content analysis.

The soil consisted of 61% sand, 18.4% silt, 20.6% clay, with a pH 6.8, OC 11.2 g kg^{-1}, TN 0.9 (g kg^{-1}), available P 28 (mg kg^{-1}). The soil C and N were measured by Isoprime 100 (Elementar, Germany). The total available P fraction (Olsen P) was determined by the method of DeLuca et al. (2015) where 0.5 g of fresh soil was extracted with 10 mL of 0.5M $NaHCO_3$ solution (Olsen et al., 1954).

2.1.1. Arbuscular mycorrhizal fungi colonization

Glomus mosseae inoculum was provided by Microbiology Department, Soil and Fertilizers Research Institute, Vietnam. Briefly, arbuscular mycorrhizal fungi spores were isolated from rhizopheric soil of pomelo growing in Gleyic Fluvisols (Flg) located in Phu Tho province, Vietnam. The fungus was propagated on maize root grown in greenhouse for 8 weeks (Tarafdar and Marschner, 1995), and the spores were surface sterilized to make inoculum for the experiment. We chose this fungal species because *Glomus mosseae (G. Mossea)* is a crucial AM fungus species in agricultural system (Benedetto et al., 2005) that is ubiquitous in worldwide ecosystems.

2.1.2. Plant and experimental setup

The cultivar of soybean was *Glycine max* L. DT96 characterized with drought resistant capacity, which was provided by Agricultural Genetics Institute of Vietnam. Soybean seeds were sterilized with 70% ethanol and 10% hydrogen peroxide, and rinsed thrice with distilled water (Ibiang et al., 2017). These sterilized seeds were germinated on wet filter paper in a Petri dish for three days before transplanting into rhizoboxes.

Treatments with and without AMF were set up in separate boxes. Zymography and glucose imaging were performed in different rhizoboxes to avoid cross effects of the two imaging methods. Thus, soil was packed in 24 transparent rhizoboxes (20 × 20 × 3 cm). The experiment consisted of four treatments (drought vs. optimum, AMF vs. no-AMF), each of which was replicated thrice to measure zymography, enzyme kinetics, and microbial biomass P. Simultaneously, another set of drought vs. optimum treatments with three replications inoculated with and without AMF was prepared for glucose imaging. To evaluate the effects of mycorrhiza on soybean drought resistance, 20 g of mycorrhiza inoculum (*Glomus mosseae*, > 100 cell g^{-1}) (Ruiz-Lozano et al., 2001) was added to 12 rhizoboxes.

The rhizoboxes were placed horizontally with one side open and then soil was slowly and continuously poured into the rhizoboxes through a 2 mm sieve to achieve a uniform soil packing. The open side was then closed, the samples were turned vertically, and they were gently shaken to achieve a stable soil packing. All the rhizoboxes were kept inclined at 45° with the open side facing down like a door in the greenhouse chamber at 20–22 °C and light intensity of 330 μmol m^{-2} s^{-1}. The emplacement of the rhizoboxes ensured root growth along the lower side of the boxes. The rhizoboxes were covered with aluminum foil to prevent algal growth. Soil moisture in each rhizobox was gravimetrically measured every two days to ensure 65% water holding capacity (WHC) during the first 7 weeks of the experiment, and distilled water was added if necessary. After that, drought condition (25% WHC) was set up in half of the 24 rhizoboxes for two weeks (excluding 1 week of transition

from 65%WHC to 25%WHC), the rest of the boxes were maintained at 65% WHC till harvest. Briefly, the growth of soybean was kept for 7 weeks at optimum moisture followed by 1 week at transition stage from optimum to drought and 2 more weeks at 25% WHC for drought treatment. The samples were collected after 10 weeks of the experiment (Appendix 1).

2.2. Staining arbuscular-mycorrhizal fungal colonizations in root

Root branches were randomly cut off from three plant replicates of each treatment. Root staining was implemented according to Vierheilig et al. (1998). Firstly, roots were boiled with KOH for 5 min and rinsed with tap water several times. Solution of black ink (Pelikan; Germany) and vinegar was used to boil the cleared roots for 3 min, followed by pure vinegar rinse. The stained arbuscules and their hyphae were observed and imaged under a light microscope (Vierheilig et al., 2005).

2.3. Glucose imaging: method optimization

The exudation of glucose was first visualized in gel-based approach which demonstrated a dependence of spatial and temporal pattern of glucose distribution on plant species, soil moisture, and root compartments (Voothuluru et al., 2018). *In situ* glucose imaging was performed for AMF-inoculated and AMF non-inoculated rhizoboxes, which were divided into three drought and three optimum conditions. Here, we optimized the method for soil matrix from protocols proposed by McLaughlin and Boyer (2004) and Voothuluru et al. (2018). Accordingly, phosphate powder was dissolved in distilled water to make a buffer solution of 0.05 M. 100 mL buffer solution was added to 0.00107 g glucose oxidase from *Aspergillus niger* (G7141-10KU, Sigma Aldrich, Germany), 0.003 g peroxidase from horseradish, and 0.005144 g Ampliflu red ($C_{14}H_{11}NO_4$, 90101-5MG-F, Sigma Aldrich, Germany) dissolved in 60 µL dimethylsulfoxid (Sigma Aldrich, $(CH_3)_2SO$). Parallelly, polyamide membrane filters (diameter 20 cm, pore size 0.45 µm - Tao Yuan, China) were cut to fit the size of the rhizobox. These membranes were saturated with the prepared solution prior to being attached to rooted sides of the rhizoboxes. In this study, glucose imaging was further developed by integrating the solution described above that becomes red when glucose oxidase and horseradish peroxidase (EC No. 232-668-6, Sigma Aldrich, Germany) catalyzes glucose-based conversion of colorless Ampliflu Red into magenta-colored resorufin, using membranes instead of gel. This modification enables glucose imaging at the soil surface and strongly reduces the diffusion artifacts occurring in gel.

After 20 min of incubation, membranes were quickly removed and placed in a dark room under UV light of 355 nm wavelength (an optimal incubation time should be tested in advance – time may differ between plants species). The magenta-colored area on the membrane indicated glucose exudation as hydrogen peroxide generated from the reaction between glucose and the enzyme glucose oxidase, catalyzed by horseradish peroxidase, converted colorless Ampliflu red into magenta color.

2.4. Soil zymography

In order to localize hotspots of enzymatic activity at soil surface, the protocol of zymography was applied according to Razavi et al. (2019). In details, 4-methylumbelliferyl-phosphate (MUF-P, $C_{10}H_9O_6P$, EC No. 222-137-7, Sigma Aldrich, Germany) solution was prepared in Dimethyl sulfoxide (DMSO, $(CH_3)_2SO$, Sigma Aldrich, Germany) to prepare the solution of 10 mM. This substrate was used to detect acid phosphomoasterase activity.

The polyamide membrane filters (Tao Yuan, China) with large pore size of 0.45 μm were selected to reduce the restriction of enzyme diffusion through the pores. The cut membranes that match well with the door of rhizoboxes were soaked into the substrate solution. The membranes were directly applied to root-exposing side, and covered outside with aluminum foils to avoid dry out. After 1 h of incubation, the membranes were lifted off and cleaned with a soft brush, then exposed to UV light of 355 nm wavelength excitation and 460 nm emission wavelength in a closed room. Beside analysis of rhizosphere size, the zymograms were used as a map to localize hotspot of acid phosphomoasterase activity (Figure 1). The soil samples were collected from all the identified hotspots of each rhizobox and the mixed soils were split into 2 subsamples for further analysis (1 for enzyme kinetics, 1 for MBP).

2.5. Calibration lines

Glucose imaging was calibrated by soaking individual 2 cm^2 membrane in glucose solution at respective concentration of 0, 2, 4, 6, 8 and 10 mM and then placed in reaction mixture containing Ampliflu Red, glucose oxidase and horse radish peroxidase for 30 s. These membranes were exposed under UV light in the same way as the samples. Calibrated values were used to quantify color intensity of the glucose release and relate glucose release to the gray-value. Fluorescent signals on an area basis were calculated based on the volume of substrate solution taken up by a fixed membrane size.

Zymography processing was calibrated by soaking individual 3 cm^2 membrane in MUF solution at respective concentration of 0.01, 0.2, 0.5, 1, 2, 4, 6 and 10 mM. These membranes were exposed under UV light in the same way as the samples. Calibrated values were used to quantify color intensity of the zymograms and relate enzyme activity to the gray-value. Fluorescent signals of MUF on an area basis were calculated based on the volume of substrate solution taken up by a fixed membrane size.

2.6. Photography and processing glucose and zymography images

All the images were taken with a digital camera (Canon EOS 6D, Canon Inc.), with a Canon lens EF 24–105 mm 1: 4L IS with the setting of aperture and shutter speed at f/5.6 and 1/30 s respectively. The fixation of distance from the camera to UV light source and membranes was to ensure constancy in image qualification, comparable quality of image processing for all samples.

The image processing and analysis was conducted in ImageJ and Matlab. For image processing, all the taken images (glucose images and zymograms) were i) transformed to 16-bit grayscale value; ii) adjusted the background and contrast levels; iii) segmented roots and iv) converted grayvalue to enzyme activities and glucose intensity. The segmented roots and their radius were calculated using the Euclidean distance map function in Matlab (Menon et al., 2007; Zarebanadkouki and Carminati, 2014). The hotspot areas were determined as top 25% higher enzyme activities after subtracting background values at zero concentration of the calibration line from all zymograms (Ma et al., 2017).

Hotspot percentage was calculated based on the pixel size proportion of hot area to the entire image. Rhizosphere extent of each individual root was calculated from root surface.

2.7. Enzyme kinetics, substrate turnover time and resistance of enzyme activity under drought condition influenced by AMF

According to the zymograms, samples from the rhizosphere hotspots were collected. These samples were preserved at 5 °C and measured the next day. Supposing that drought restricted photosynthesis so may affect above-underground C translocation. On the other hand, AMF

presence stimulated P uptake by plants under stressed conditions and P deficiencies. Therefore, two enzymes were selected to investigate the interaction between roots and microorganisms including: β-glucosidase and acid phosphomonoesterase. The kinetics of these two enzymes were determined using fluorescent substrates (Sigma Aldrich, Germany). MUF β-D-glucopyranoside (MUF-G) was used for the determination of β-glucosidase and 4-methylumbelliferyl-phosphate (MUF-P) for acid phosphomonoesterase. According to German et al., (2012), 1.0 g soil was suspended in 50 mL sterile water of which 50 µL suspension was pipetted in a 96-well microplate (Puregrade, Germany). Then, 50 µL MES hemisodium buffer (pH 6.5) (MES, $C_6H_{13}NO_4SNa_{0.5}$, Sigma Aldrich, Germany) and 100 µL respective substrate solution were added subsequently in each well. The activity of each enzyme was measured at 3 time points: 30, 60 and 120 min using CLARIOstar plus (BMG LABTECH, Germany) at an excitation wavelength of 355 nm and an emission wavelength of 460 nm. Enzyme activities (V_{max}) were denoted as released MUF in nmol per g dry soil per hour (nmol MUF g^{-1} soil h^{-1}) (Awad et al., 2012) at the time point of 120 min. The linear increase of fluorescence overtime during the assay was properly checked and data obtained after 2 h was used for further calculation (German et al., 2012). Simultaneously, a range of MUF concentration of 0, 10, 20, 30, 40, 50, 100, 200 µM were prepared to calibrate the measurement.

The determination of K_m and V_{max} was conducted by fitting the measured values to Michaelis-Menten equation (1):

$$v = \frac{V_{max} \times [S]}{K_m + [S]} \quad (1)$$

where v is the reaction rate, V_{max} is the maximum reaction rate at saturated substrate concentration, [S] is substrate concentration, K_m is the substrate concentration at which the reaction rate attains a half of maximum.

Based on V_{max}, K_m and [S] values, we calculated turnover time (Tt) of the added substrates according to equation (2) suggested by Panikov et al., (1992) and Larionova et al., (2007):

$$T_t(hours) = \frac{K_m + S}{V_{max}} \quad (2)$$

Since drought triggers less proportion of C allocation to root rhizosphere (Gao et al., 2021), the low substrate concentration (equal to K_m) was chosen to calculate the turnover time of added substrates.

In order to evaluate the role of AMF in improving drought resistant capacity of soybean rhizosphere's enzyme activity, the resistance index (RS) was interpreted based on equation (3) (Orwin and Wardle, 2004):

$$RS(t_0) = 1 - \frac{2\,|D_0|}{C_0 + |D_0|} \quad (3)$$

where D_0 is the amount of the difference in a biological function between the control soil (C_0) (here enzyme activity) and the drought soil at the end of disturbance (t_0). This resistance index is between −1 and +1, where +1 indicates no effects of disturbance (maximum resistance).

2.8. Microbial biomass phosphorus (MBP)

Microbial biomass phosphorus was determined by chloroform fumigation-extraction using anion exchange membrane (Kouno et al., 1995; Yevdokimov and Blagodatskaya, 2014). To prepare for the experiment, anion exchange membrane (AEM) strips were shaken with three sequential changes in 200 mL 0.5 mol L^{-1} $NaHCO_3$ for 24 h, then washed three times and kept in deionized water until use. Subsequently, each pair of 50-mL tube (for fumigation and non-fumigation purposes) contains the

same sample equivalent to 3 g dry soil were filled with 30 mL of deionized water. The fumigated tube was added with 300 µl of chloroform to solubilize microbial biomass P. One anion exchange membrane (AEM) strip was placed in fumigated and non-fumigated tubes. These tubes were shaken for 24 h continuously to induce the recovery of inorganic P from the soil extract. After shaking, AEM strips were lifted out of the tubes and gently washed again in deionized water prior to being submerged into another centrifuge tube filled with 45 mL of 0.25 M H_2SO_4. Tubes containing membranes and 0.25 M H_2SO_4 were shaken for 3 h to release membrane-fixed P back to the solution. 150 µL acid extract was mixed with 30 µl *Reagent 1* (prepared with 14.2 mmol L^{-1} ammonium molybdate tetrahydrate in H_2SO_4 3.1 M) and *Reagent 2* (prepared with 3.5 g L^{-1} aqueous polyvinyl alcohol reagent and malachite green) (D'Angelo et al., 2001) in disposable 96-well polystyrene microplates. These microplates were exposed to 40 °C for 30–40 min in a dryer (thermostat) and read at 630 nm in CLARIOstar plus (BMG LABTECH, Germany).

2.9. Data analysis and statistics

All the statistical analyses were performed in Sigma-Plot 14.0. One-way ANOVA was applied to categorize hotspot boundary and hotspot intensity. The significant differences in enzyme activities, rhizosphere extent, hotspot percentage, substrate turnover time and drought resistance, microbial biomass P between droughts vs. optimum, with AMF vs. without AMF were confirmed by Two-Way ANOVA after checking normality and homogeneity of values. A probability level of $p < 0.05$ or $p < 0.001$ indicated the significance in comparison. Error bars indicate the standard error of the means.

3. Results

The staining technique with ink and vinegar demonstrated the colonization of AMF in mycorrhizal plant roots (Figure S1). Our measurements showed that drought reduced the shoot length by 1.3–1.5 times but the reduction of root length is less than shoot length. AMF inoculum strongly increased shoot length by 1.38 times at optimum condition and by 1.24 times in drought condition (Figure S3).

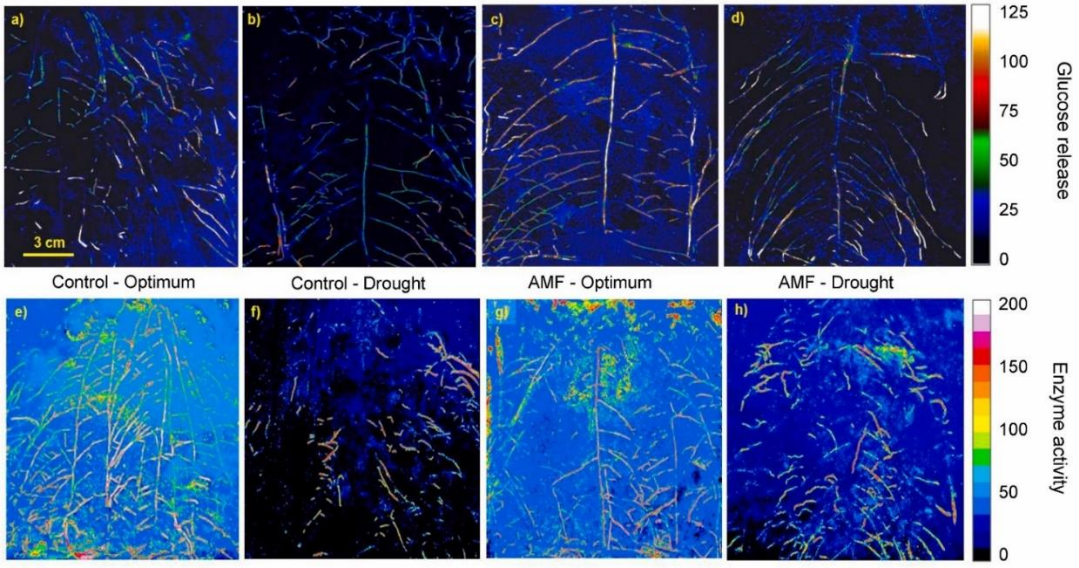

Figure 3-1 *Upper row: glucose release (nmol/cm^2); lower row: zymograms of acid phosphomonoesterase (pmol cm^{-2} h^{-1}): (a, c) glucose release along the roots and root tips under*

optimum conditions, shown in white color. (b, d), the exudation of glucose focused on the root tips under drought. (g, h) AMF symbiosis enhanced hotspot extent regardless of water condition (e, f).

3.1. Glucose exudation from root tips

In glucose imaging, decreasing the release of glucose was demonstrated in color bars in which white color showed the highest glucose exudation. Under optimum conditions, glucose was mainly exuded along the roots and root tips (Figure 1). On the contrary, under drought condition, glucose exudation was more focused on the root tips. However, a higher release of glucose was observed in the rhizosphere under AMF-drought than control-drought.

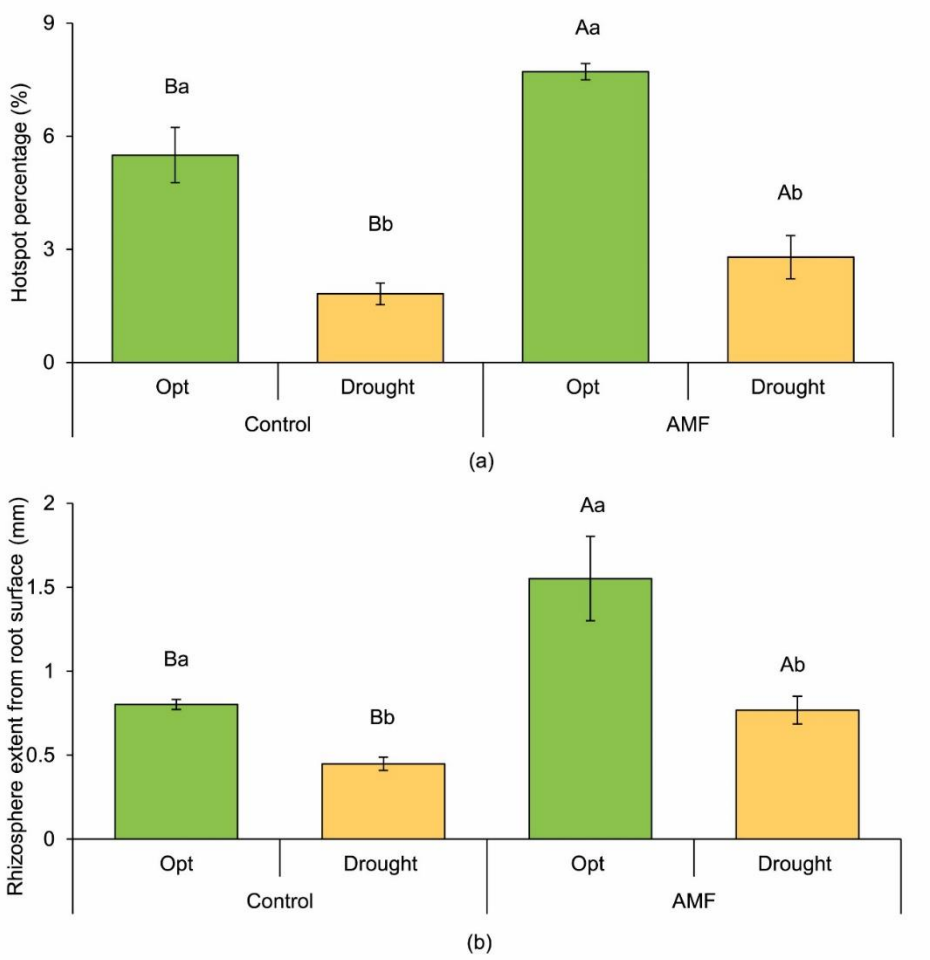

Figure 3-2 *Hotspot percentage and rhizosphere extent. Lower case letters: significant differences between optimum and drought at $p < 0.05$; upper case letters: significant differences between control and AMF at $p < 0.05$.*

3.2. Enzymatic hotspots and rhizosphere size

In the absence of AMF, drought reduced acid phosphomonoesterase hotspot percentage by three times compared to optimum condition, while AMF inoculation further reduced it to two times (Figure 2a). The presence of AMF increased the hotspot area by 40% and 53% in optimum and drought conditions, respectively, compared to respective conditions without AMF. Enzymatic hotspot area increased by 9% under drought than optimum conditions with AMF symbiosis.

Water stress triggered a reduction of rhizosphere size by 78% when compared to the optimum condition (Figure 2b). In contrast, in plants inoculated with AMF, rhizosphere extent under stress

effects was almost the same as that under optimum condition (without AMF), and 71% higher than non-mycorrhizal rhizosphere under the same stress.

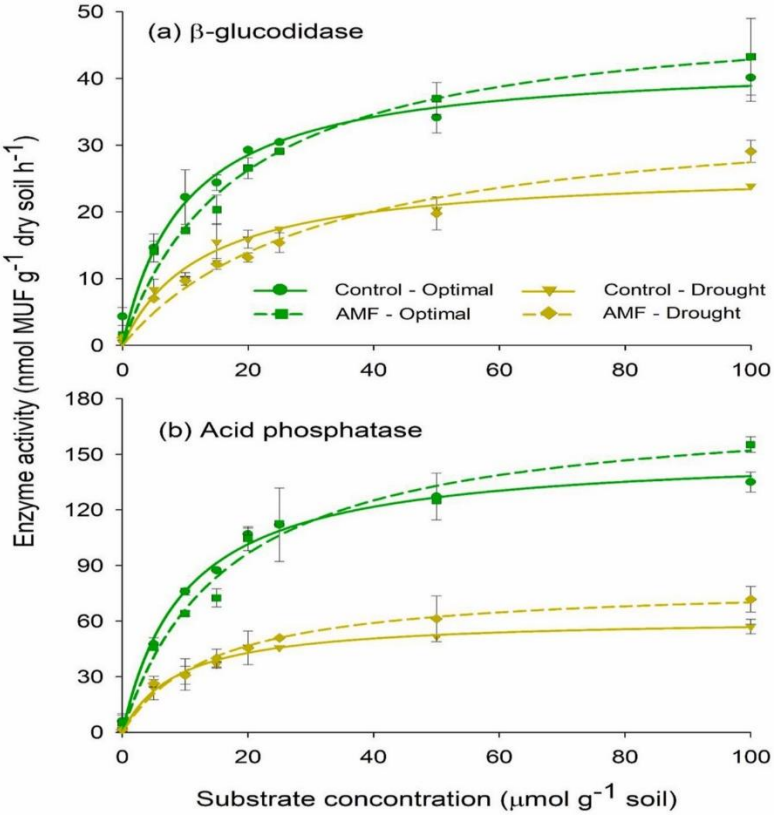

Figure 3-3 *Michaelis-Menten kinetics (enzyme activity as a function of substrate concentration) for (a) β-glucosidase (GLU) and (b) acid phosphomonoesterase (PHOS) The bar indicated standard error.*

3.3. Enzyme kinetics, turnover time, and resistance to drought

Activities of β-glucosidase and acid phosphomonoesterase decreased by approximately 50% owing to water deficit, irrespective of AMF or non-AMF inoculation ($p < 0.001$, Figure 3). K_m value of both enzymes considerably increased ($p < 0.001$) in mycorrhizal plants in comparison to non-mycorrhizal ones, regardless of optimum or drought conditions (Figure S2).

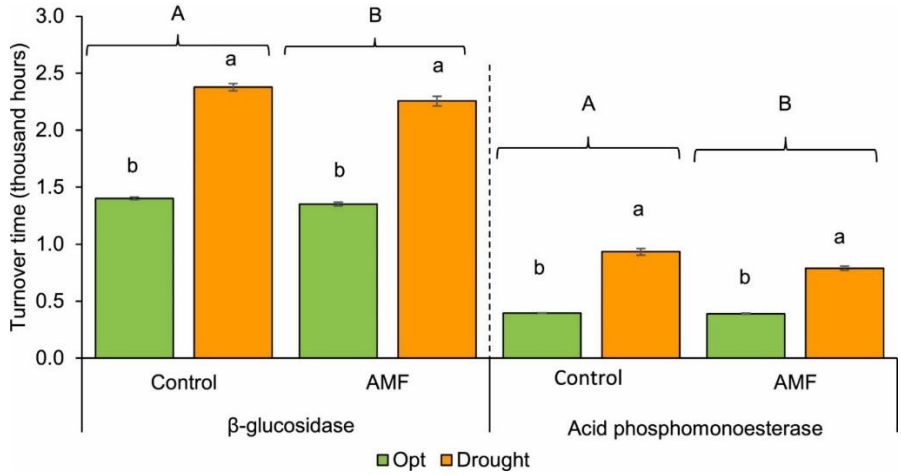

Figure 3-4 *Substrate turnover time at optimum and drought condition with and without AMF inoculation. Lower case letters: significant differences between optimum and drought at p < 0.05;*

upper case letters: significant differences between control and AMF at p < 0.05. GLU: β-glucosidase, PHOS: acid phosphomonoesterase.

While substrate turnover times of β-glucosidase and acid phosphomonoesterase were at least 56% shorter in optimum condition than in drought ($p < 0.001$, Figure 4), AMF symbiont reduced the turnover time of these enzymes by up to 28%, especially under drought. Additionally, the drought resistance of β-glucosidase and acid phosphomonoesterase activities was enhanced by 63% and 57%, respectively, in mycorrhizal plants ($p < 0.05$, Figure 5).

3.4. Microbial biomass phosphorus

Drought resulted in a two-fold decrease of microbial biomass P (MBP) in both control and AMF treatments (Figure 6). Nevertheless, biomass of microbial P increased by 50% and 45% under optimum and drought conditions, respectively, in plants inoculated with AMF.

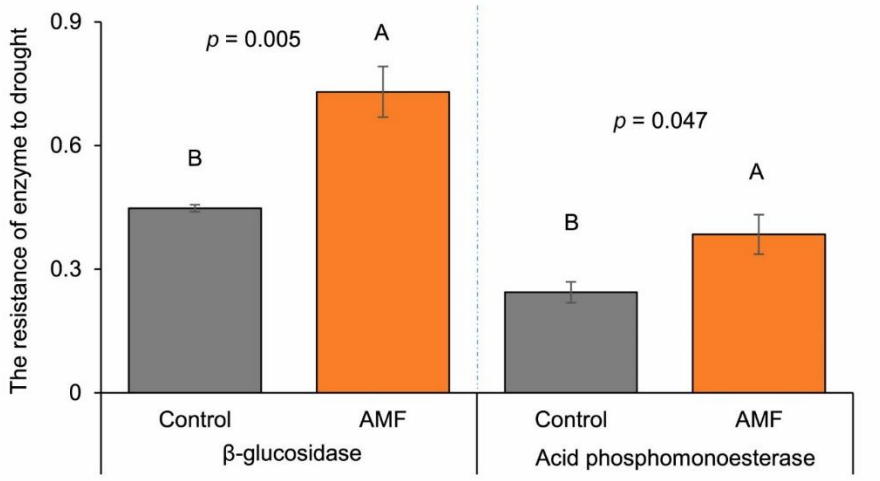

Figure 3-5 *The resistance of enzyme activity to drought (i.e. RS (t_0) = 1- ($2|D_0|/(C_0 + |D_0|)$). Letters indicate significant differences between control and AMF treatment of respective enzyme after Student's* t*-test at* p *< 0.05.*

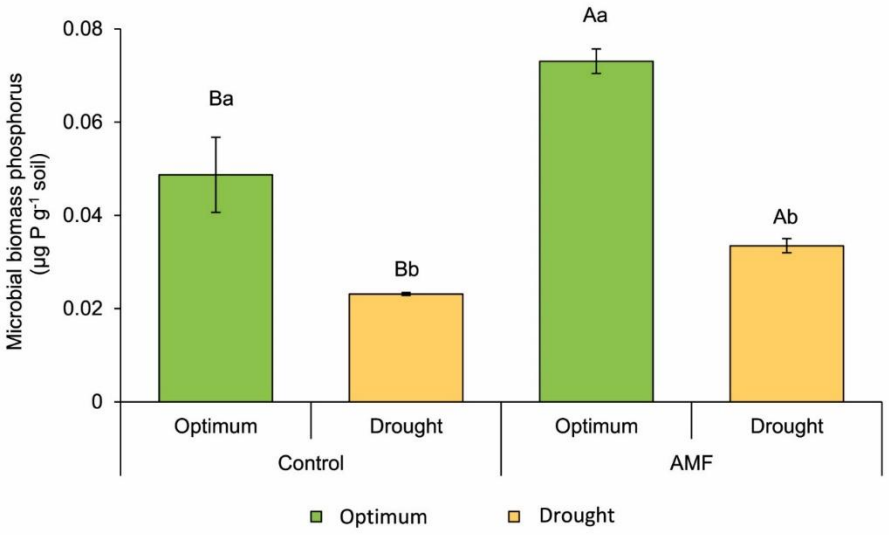

Figure 3-6 *Microbial biomass phosphorus. Drought resulted in two-fold decrease of microbial biomass phosphorus (MBP) in both control and AMF treatments. Nevertheless, biomass of microbial*

phosphorus increased 50% and 45% in respective optimum and drought conditions as plant was inoculated with AMF. Lower case letters: significant differences between optimum and drought at $p < 0.05$*; upper case letters: significant differences between control and AMF at* $p < 0.05$.

4. Discussion

4.1. How AMF presence affected glucose exudation and enzymatic hotspot within rhizosphere?

In line with our first and second hypothesis, glucose exudation highly relied on moisture condition, as suggested by Vancura and Hovadik (1965) and Calvo et al. (2019). Under optimum condition, glucose was homogeneously exuded along the root as well as root tips, but drought dramatically reduced glucose exudation along with a total decrease in exudation (Liese et al., 2018), especially from the mature part of the root (Figure 1). Remarkably, AMF strongly boosted glucose hotspots in comparison to non-mycorrhizal plants. Glucose exuded from root characterized by lability and ready utilization can be directly absorbed by AMF as a C source (Bago et al., 2000; Bücking et al., 2008) to stimulate AMF hyphae branching and lengthening. On the other hand, AMF may contribute to glucose release, for instance, by the expression of β-glucosidase and mobilizing oligo- and polysaccharides or glycosylated compounds. Therefore, the enhanced detected glucose signal could be attributed the concomitant direct secretion from plant roots or produced as a final product of β-glucosidase activity within the rhizosphere.

This accelerated glucose availability within the mycorrhizosphere (Kraigher et al., 2013), the zone of influence in the vicinity of fungal hyphae (Tarafdar and Marschner, 1994), which compensates C deprivation of rhizobiota due to drought (Asensio et al., 2021). As a consequence, acid phosphomonoesterase hotspots percentage and rhizosphere extent increased by up to 53% and 71%, respectively, in mycorrhizal plants when compared with non-mycorrhizal plants under water scarcity (Figure 2). AMF can play the role of root hairs and enlarge the overall extent of the absorbing surface of the host roots (40 times) (Muchovej, 2004; Pepe et al., 2016).

P is well known as one of the most essential nutrients for plant growth and is quickly taken up by plant roots resulting in a P depletion zone in the adhering vicinity of host roots (Lewis and Quirk, 1967; Hinsinger et al., 2009; Shen et al., 2011). However, water deficiency strongly inhibits soil P bioavailability (Sardan et al., 2007) in contrast to the increasing demand of P by plants under stress condition (He et al., 2014). The extension of the enzymatic rhizosphere is expected to compensate the P-depletion zone, especially under increasing water stress condition. The fungus mycelium system can approach microaggregate-trapped P and efficiently transport P into plant roots (Smith and Read, 1997; Schnepf et al., 2011). The spread of external mycelium is coincidental with the synthesis of acid phosphomonoesterase by fungi (Tarafdar and Claasen, 1988; Dakora and Phillips, 2002) to facilitate P availability, which apparently contributed to higher hotspot percentage and rhizosphere extent in host plants than in non-host plants. Coupling with the glucose distribution pattern above, we conclude that plants sustain a mutual communication with rhizosphere microorganisms by diffusing more glucose along the plant roots associated with AMF as a strategy to adapt to water limitation. In turn, AMF boosts the P availability for plants in the enzymatic pathway by enlarging acid phosphomonoesterase hotspots and rhizosphere expansion. Consequently, shoot length increased by 1.24–1.37 times in AMF inoculation regardless of optimum or drought condition. Considering the fact that many hotspots have a mixed origin and mixed-use, it becomes more evident that the overlapping

area between rhizosphere and mycorrhizosphere accelerates microbial activity around the roots (Figure 7). Thus, AMF stimulated microbial-mediated processes and extended hotspots around the roots under water stress by forming favorable microsites for microorganisms which supported soybean performance.

4.2. How AMF symbiosis affected enzyme kinetics and its drought resistance?

In agreement with our second hypothesis, AMF symbiosis significantly enhanced β-glucosidase and acid phosphomonoesterase activities, compared with non-mycorrhizal plants, irrespective of optimal moisture or water deficiency ($p < 0.001$). This finding confirms that AMF promotes enzymatic activities, especially that of acid phosphomonoesterase (Welc et al., 2014) through possible stimulation of bacteria, fungi or plant roots (Joner and Jakobsen, 1995; Yang et al., 2012; Nannipieri et al., 2011). C demand of AMF facilitates the synthesis of β-glucosidase by either bacteria or fungi (Pathan et al., 2017) to decompose root exudates containing carbohydrates and root slough-off. In addition, glomaline produced by AMF stores 4–5% of the total tropical soil C (Rillig et al., 2001) which promotes the β-glucosidase activity. Meanwhile, acid phosphomonoesterase was synthesized by both plant roots and fungal hyphae, leading to the increase in acid phosphomonoesterase activity in mycorrhizal plants. The higher *Km* values in AMF inoculated plant independent of water content indicated different enzyme systems with lower substrate affinity compared to control without AMF (Razavi et al., 2016b). The change of enzyme systems reflected a probable shift in dominant microbial populations toward species with lower affinity to celluloses and organic P-compounds as compared to the control (Zhang et al., 2020) indicating action of fast-growing microorganisms with low efficiency within the rhizosphere–mycorrhizosphere hotspots.

Our findings for both β-glucosidase and acid phosphomonoesterase was consistent with the results of a previous study on the reduction of enzyme activities as a result of water stress (Alster et al., 2013). This reduction might be the result of i) reduced diffusion of substrate to enzymes in suboptimal moisture (Nannipieri et al., 2002) and ii) adsorption of enzymes on soil particles (Steinweg et al., 2012) under drought.

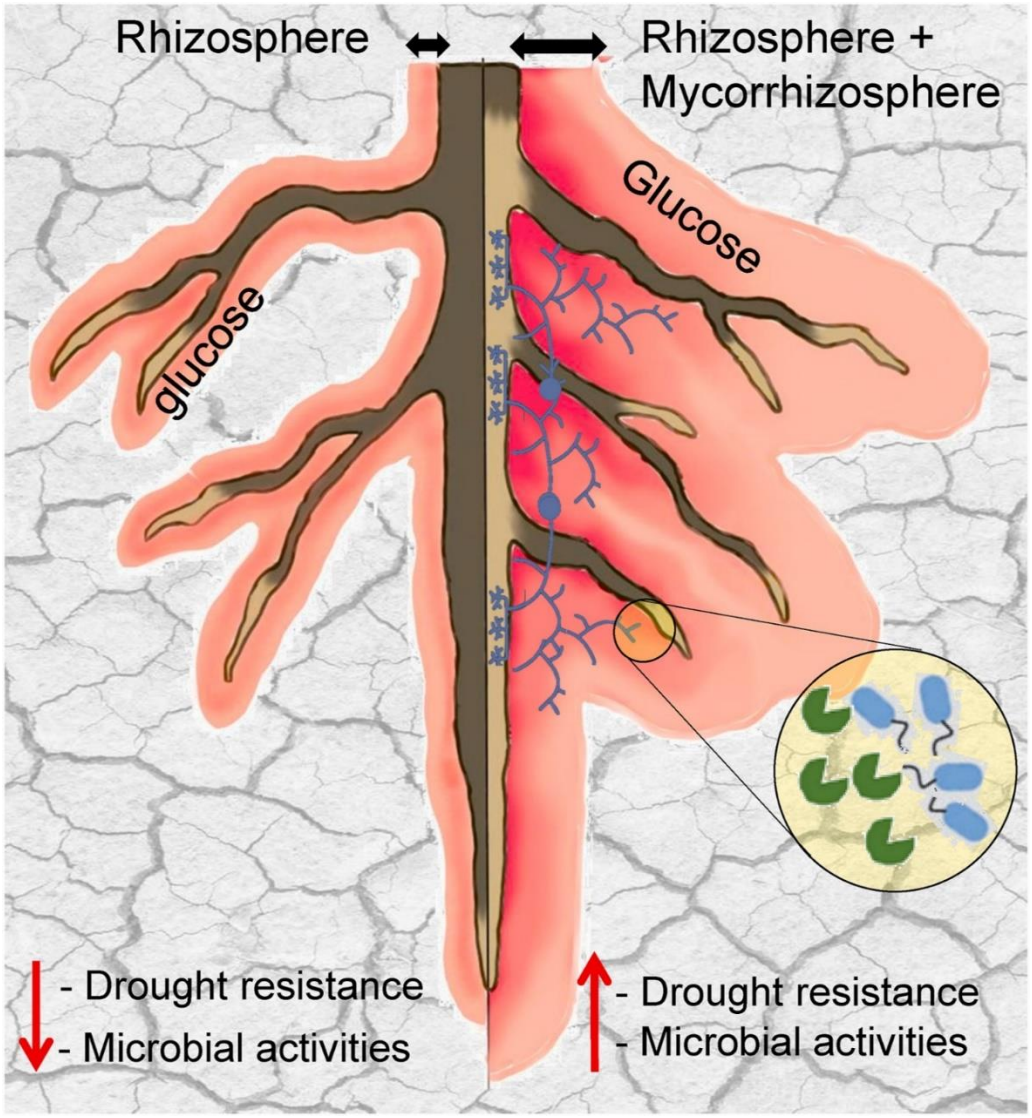

Figure 3-7 *While drought reduces enzyme activities and the glucose exudation localized mainly at the root tips, arbuscular mycorrhiza fungi (AMF) inoculation formulating the overlapping area between rhizosphere and mycorrhizosphere so enhances glucose exudation compared to non-mycorrhizal plants and enlarged enzymatic hotspot area by 53%. AMF also increases drought resistance of β-glucosidase and acid phosphomonoesterase up to 63% in mycorrhizal plants.*

At low substrate concentration (<20 μmol g^{-1} soil), we detected a similar reaction rate of acid phosphomonoesterase under drought independent of AMF inoculation (Figure 3). These results can be explained by an increase of *Km*, which is in the denominator of the Michaelis-Menten equation (1). Therefore, the positive effects of AMF on *Vmax* were canceled by the *Km* increase. A much greater increase in *Km* (substrate affinity decreased) than in *Vmax* canceled the differences in acid phosphomonoesterase activities at substrate concentrations below 20 μmol g^{-1} soil under drought. Thus, the decomposition of organic P-compounds under drought was accelerated only at substrate levels exceeding that threshold. Accordingly, increased turnover time of added substrates by enzymes, under drought demonstrates that the decomposition of soil organic matter was delayed under water stress condition due to lower activities of enzymes. AMF symbiont showed a faster degradation of substrates under drought condition, with up to 28% reduction in turnover time in the mycorrhizal

rhizosphere. This reduction is critical in improving C and nutrient transformation, especially P compounds within the rhizosphere, under water stress.

Effects of drought on soybean varies with its growth stage but most severe during vegetative and flowering timing (Desclaux et al., 2000) which showed more influences on shoot length than root length in our experiment (Figure S3). As a result of AMF symbiosis, shoot length was significantly improved in comparison to plant without AMF. Moreover, AMF plays a leading role in enhancing drought-resistance of both β-glucosidase and acid phosphomonoesterase enzymes. As mentioned in a review by Dodd et al. (2000), greater allocation of sucrose to mycorrhizal roots maintains AMF growth and also retains sustainable plant production. The observed increased glucose excretion under drought treatment might have a function similar to that of sucrose in enhancing drought resistance of these two enzymes. Although the role of AMF hyphae in sustaining soil micro-aggregates is not within our research scope, we speculate that AMF-synthesized glomaline glues separate soil particles to make soil water-stable aggregates (Wu et al., 2008), facilitating drought resistance of β-glucosidase and acid phosphomonoesterase enzymes.

Given that drought dramatically reduced microbial biomass P (MBP) because of increasing P accumulation in soil accompanied with water limitation, AMF enormously improved MBP. Remarkably, AMF showed positive effects on MBP not only under drought but also under optimum conditions. This result implies that P is increasingly mobilized by AMF which was not only transported into the host plant but also served the soil microbes demand for P. This role of AMF is more critical as plants encounter simultaneous P deficiency and water limitation.

Overall, the stronger resistance of enzyme activities to drought in AMF-inoculated than in non-mycorrhizal suggests that microorganisms associated with mycorrhizal root have a higher capability to react to altered abiotic environmental conditions than those associated with non-mycorrhizal roots. The mycorrhization induced an interactive regulation of soybean glucose exudation and rhizosphere expansion for enzyme activities. Hence, the identified overlapping area between rhizosphere and mycorrhizosphere showed that AMF stimulated microbial-mediated processes around the roots under water stress. This contributed to the resistance of microbial functions (e.g., enzyme expression) to drought stress in AMF-inoculated than in non-mycorrhizal soybean as well as soybean performance. AMF-inoculation suppressed adverse drought effects on plant and microbial nutrient mining, which has substantial implications for controlling microbial roles in organic matter decomposition and P cycling.

Acknowledgment

This study was funded by Vietnam National University, Hanoi (Project code: QG. 20.63). The method development of this work was motivated and supported by the German Federal Ministry of Education and Research (BMBF) (grant number 031B0910A). We gratefully acknowledge DAAD for supporting DTTH to have a short visit at the Department of Soil and Plant Microbiome, Institute of Phytopathology, University of Kiel,

Reference

Allard-Massicotte, R., Tessier, L., LÚcuyer, F., Lakshmanan, V., Lucier, J. F., Garneau, D., ... & Beauregard, P. B. (2016). Bacillus subtilis early colonization of Arabidopsis thaliana roots involves multiple chemotaxis receptors. MBio, 7(6), 10-1128.

Alster, C. J., German, D. P., Lu, Y., & Allison, S. D. (2013). Microbial enzymatic responses to drought

and to nitrogen addition in a southern California grassland. Soil Biology and Biochemistry, 64, 68-79.
Antunes, P. M., Rajcan, I., & Goss, M. J. (2006). Specific flavonoids as interconnecting signals in the tripartite symbiosis formed by arbuscular mycorrhizal fungi, Bradyrhizobium japonicum (Kirchner) Jordan and soybean (Glycine max (L.) Merr.). Soil Biology and Biochemistry, 38(3), 533-543.
Awad, Y. M., Blagodatskaya, E., Ok, Y. S., & Kuzyakov, Y. (2012). Effects of polyacrylamide, biopolymer, and biochar on decomposition of soil organic matter and plant residues as determined by 14C and enzyme activities. European Journal of Soil Biology, 48, 1-10.
Bago, B., Pfeffer, P. E., & Shachar-Hill, Y. (2000). Carbon metabolism and transport in arbuscular mycorrhizas. Plant physiology, 124(3), 949-958.
Benedetto, A., Magurno, F., Bonfante, P., & Lanfranco, L. (2005). Expression profiles of a phosphate transporter gene (GmosPT) from the endomycorrhizal fungus Glomus mosseae. Mycorrhiza, 15, 620-627.
Besserer, A., Puech-Pagès, V., Kiefer, P., Gomez-Roldan, V., Jauneau, A., Roy, S., ... & Séjalon-Delmas, N. (2006). Strigolactones stimulate arbuscular mycorrhizal fungi by activating mitochondria. PLoS biology, 4(7), e226.
Bohnert, H. J., & Sheveleva, E. (1998). Plant stress adaptations—making metabolism move. Current opinion in plant biology, 1(3), 267-274.
Bruce, T. J., Matthes, M. C., Napier, J. A., & Pickett, J. A. (2007). Stressful "memories" of plants: evidence and possible mechanisms. Plant science, 173(6), 603-608.
Bücking, H., Abubaker, J., Govindarajulu, M., Tala, M., Pfeffer, P. E., Nagahashi, G., ... & Shachar-Hill, Y. (2008). Root exudates stimulate the uptake and metabolism of organic carbon in germinating spores of Glomus intraradices. New Phytologist, 180(3), 684-695.
Buee, M., Rossignol, M., Jauneau, A., Ranjeva, R., & Bécard, G. (2000). The pre-symbiotic growth of arbuscular mycorrhizal fungi is induced by a branching factor partially purified from plant root exudates. Molecular Plant-Microbe Interactions, 13(6), 693-698.
Calvo, O. C., Franzaring, J., Schmid, I., & Fangmeier, A. (2019). Root exudation of carbohydrates and cations from barley in response to drought and elevated CO 2. Plant and Soil, 438, 127-142.
Carminati, A., Moradi, A. B., Vetterlein, D., Vontobel, P., Lehmann, E., Weller, U., ... & Oswald, S. E. (2010). Dynamics of soil water content in the rhizosphere. Plant and soil, 332, 163-176.
Carvalhais, L. C., Dennis, P. G., Fedoseyenko, D., Hajirezaei, M. R., Borriss, R., & von Wirén, N. (2011). Root exudation of sugars, amino acids, and organic acids by maize as affected by nitrogen, phosphorus, potassium, and iron deficiency. Journal of Plant Nutrition and Soil Science, 174(1), 3-11.
Dakora, F. D., & Phillips, D. A. (2002). Root exudates as mediators of mineral acquisition in low-nutrient environments. Food security in nutrient-stressed environments: exploiting plants' genetic capabilities, 201-213.
DeLuca, T. H., Glanville, H. C., Harris, M., Emmett, B. A., Pingree, M. R., de Sosa, L. L., ... & Jones, D. L. (2015). A novel biologically-based approach to evaluating soil phosphorus availability across complex landscapes. Soil Biology and Biochemistry, 88, 110-119.
Desclaux, D., Huynh, T. T., & Roumet, P. (2000). Identification of soybean plant characteristics that indicate the timing of drought stress. Crop science, 40(3), 716-722.
Dodd, J. C., Boddington, C. L., Rodriguez, A., Gonzalez-Chavez, C., & Mansur, I. (2000). Mycelium of arbuscular mycorrhizal fungi (AMF) from different genera: form, function and detection. Plant and soil, 226, 131-151.
Doubková, P., Suda, J., & Sudová, R. (2012). The symbiosis with arbuscular mycorrhizal fungi contributes to plant tolerance to serpentine edaphic stress. Soil Biology and Biochemistry, 44(1), 56-64.
Doubková, P., Vlasáková, E., & Sudová, R. (2013). Arbuscular mycorrhizal symbiosis alleviates

drought stress imposed on Knautia arvensis plants in serpentine soil. Plant and Soil, 370, 149-161.
D'Angelo, E., Crutchfield, J., & Vandiviere, M. (2001). Rapid, sensitive, microscale determination of phosphate in water and soil. Journal of environmental quality, 30(6), 2206-2209.
Fuchslueger, L., Bahn, M., Fritz, K., Hasibeder, R., & Richter, A. (2014). Experimental drought reduces the transfer of recently fixed plant carbon to soil microbes and alters the bacterial community composition in a mountain meadow. New Phytologist, 201(3), 916-927.
Fuchslueger, L., Bahn, M., Hasibeder, R., Kienzl, S., Fritz, K., Schmitt, M., ... & Richter, A. (2016). Drought history affects grassland plant and microbial carbon turnover during and after a subsequent drought event. Journal of Ecology, 104(5), 1453-1465.
Gao, D., Joseph, J., Werner, R. A., Brunner, I., Zürcher, A., Hug, C., ... & Hagedorn, F. (2021). Drought alters the carbon footprint of trees in soils—tracking the spatio-temporal fate of 13C-labelled assimilates in the soil of an old-growth pine forest. Global Change Biology, 27(11), 2491-2506.
German, D. P., Marcelo, K. R., Stone, M. M., & Allison, S. D. (2012). The M ichaelis–M enten kinetics of soil extracellular enzymes in response to temperature: a cross-latitudinal study. Global Change Biology, 18(4), 1468-1479.
Ghannoum, O., & Conroy, J. P. (2007). Phosphorus deficiency inhibits growth in parallel with photosynthesis in a C3 (Panicum laxum) but not two C4 (P. coloratum and Cenchrus ciliaris) grasses. Functional Plant Biology, 34(1), 72-81.
Gorissen, A., Tietema, A., Joosten, N. N., Estiarte, M., Penuelas, J., Sowerby, A., ... & Beier, C. (2004). Climate change affects carbon allocation to the soil in shrublands. Ecosystems, 7, 650-661.
Hasibeder, R., Fuchslueger, L., Richter, A., & Bahn, M. (2015). Summer drought alters carbon allocation to roots and root respiration in mountain grassland. New Phytologist, 205(3), 1117-1127.
He, M., & Dijkstra, F. A. (2014). Drought effect on plant nitrogen and phosphorus: a meta-analysis. New Phytologist, 204(4), 924-931.
Hinsinger, P. (2001). Bioavailability of soil inorganic P in the rhizosphere as affected by root-induced chemical changes: a review. Plant and soil, 237(2), 173-195.
Hinsinger, P., Bengough, A. G., Vetterlein, D., & Young, I. M. (2009). Rhizosphere: biophysics, biogeochemistry and ecological relevance.
Hoffmann, C. M. (2010). Sucrose accumulation in sugar beet under drought stress. Journal of agronomy and crop science, 196(4), 243-252.
Ibiang, Y. B., Mitsumoto, H., & Sakamoto, K. (2017). Bradyrhizobia and arbuscular mycorrhizal fungi modulate manganese, iron, phosphorus, and polyphenols in soybean (Glycine max (L.) Merr.) under excess zinc. Environmental and Experimental Botany, 137, 1-13.
Jacob, J., & Lawlor, D. W. (1991). Stomatal and mesophyll limitations of photosynthesis in phosphate deficient sunflower, maize and wheat plants. Journal of experimental botany, 42(8), 1003-1011.
Karlowsky, S., Augusti, A., Ingrisch, J., Akanda, M. K. U., Bahn, M., & Gleixner, G. (2018). Drought-induced accumulation of root exudates supports post-drought recovery of microbes in mountain grassland. Frontiers in Plant Science, 9, 1593.
Kouno, K., Tuchiya, Y., & Ando, T. (1995). Measurement of soil microbial biomass phosphorus by an anion exchange membrane method. Soil Biology and Biochemistry, 27(10), 1353-1357.
Kraigher, H., Bajc, M., & Grebenc, T. (2013). Climate Change, Air Pollution and Global Challenges: Chapter 8. Mycorrhizosphere Complexity (Vol. 13). Elsevier Inc. Chapters.
Kuzyakov, Y., & Blagodatskaya, E. (2015). Microbial hotspots and hot moments in soil: concept & review. Soil Biology and Biochemistry, 83, 184-199.
Kuzyakov, Y., & Razavi, B. S. (2019). Rhizosphere size and shape: Temporal dynamics and spatial stationarity. Soil Biology and Biochemistry, 135, 343-360.
Larionova, A. A., Yevdokimov, I. V., & Bykhovets, S. S. (2007). Temperature response of soil respiration is dependent on concentration of readily decomposable C. Biogeosciences, 4(6), 1073-1081.

Lewis, D. B., & Quirk, J. P. (1967). Phosphate diffusion in soil and uptake by plants.-3ap-movement and uptake by plants as indicated by 32p-autoradiography. Plant Soil, 26, 765-766.
Liese, R., Lübbe, T., Albers, N. W., & Meier, I. C. (2018). The mycorrhizal type governs root exudation and nitrogen uptake of temperate tree species. Tree physiology, 38(1), 83-95.
Liese, R., Lübbe, T., Albers, N. W., & Meier, I. C. (2018). The mycorrhizal type governs root exudation and nitrogen uptake of temperate tree species. Tree physiology, 38(1), 83-95.
Liese, R., Lübbe, T., Albers, N. W., & Meier, I. C. (2018). The mycorrhizal type governs root exudation and nitrogen uptake of temperate tree species. Tree physiology, 38(1), 83-95.
Ma, X., Razavi, B. S., Holz, M., Blagodatskaya, E., & Kuzyakov, Y. (2017). Warming increases hotspot areas of enzyme activity and shortens the duration of hot moments in the root-detritusphere. Soil Biology and Biochemistry, 107, 226-233.
Mach, K. J., Kraan, C. M., Adger, W. N., Buhaug, H., Burke, M., Fearon, J. D., ... & von Uexkull, N. (2019). Climate as a risk factor for armed conflict. Nature, 571(7764), 193-197.
Marschener, H. J. F. C. R. (1998). Role of root growth, arbuscular mycorrhiza, and root exudates for the efficiency in nutrient acquisition. Field Crops Research, 56(1-2), 203-207.
McLaughlin, J. E., & Boyer, J. S. (2004). Glucose localization in maize ovaries when kernel number decreases at low water potential and sucrose is fed to the stems. Annals of Botany, 94(1), 75-86.
Menon, M., Robinson, B., Oswald, S. E., Kaestner, A., Abbaspour, K. C., Lehmann, E., & Schulin, R. (2007). Visualization of root growth in heterogeneously contaminated soil using neutron radiography. European Journal of Soil Science, 58(3), 802-810.
Morgan, J. M. (1984). Osmoregulation and water stress in higher plants. Annual review of plant physiology, 35(1), 299-319.
Muchovej, R. M. (2001). Importance of mycorrhizae for agricultural crops. University of Florida Cooperative Extension Service, Institute of Food and Agriculture Sciences, EDIS.
Nannipieri, P., Kandeler, E., & Ruggiero, P. (2002). Enzyme activities and microbiological and biochemical processes in soil. Enzymes in the Environment, 1-33.
Olsen, S. R. (1954). Estimation of available phosphorus in soils by extraction with sodium bicarbonate (No. 939). US Department of Agriculture.
Orwin, K. H., & Wardle, D. A. (2004). New indices for quantifying the resistance and resilience of soil biota to exogenous disturbances. Soil Biology and Biochemistry, 36(11), 1907-1912.
Palta, J. A., & Gregory, P. J. (1997). Drought affects the fluxes of carbon to roots and soil in 13C pulse-labelled plants of wheat. Soil Biology and Biochemistry, 29(9-10), 1395-1403.
Panikov, N. S., Blagodatsky, S. A., Blagodatskaya, J. V., & Glagolev, M. V. (1992). Determination of microbial mineralization activity in soil by modified Wright and Hobbie method. Biology and Fertility of Soils, 14, 280-287.
Pathan, S. I., Žifčáková, L., Ceccherini, M. T., Pantani, O. L., Větrovský, T., & Baldrian, P. (2017). Seasonal variation and distribution of total and active microbial community of β-glucosidase encoding genes in coniferous forest soil. Soil Biology and Biochemistry, 105, 71-80.
Pavithra, D., & Yapa, N. (2018). Arbuscular mycorrhizal fungi inoculation enhances drought stress tolerance of plants. Groundwater for Sustainable Development, 7, 490-494.
Peña-Rojas, K., Aranda, X., & Fleck, I. (2004). Stomatal limitation to CO2 assimilation and down-regulation of photosynthesis in Quercus ilex resprouts in response to slowly imposed drought. Tree physiology, 24(7), 813-822.
Pepe, A., Giovannetti, M., & Sbrana, C. (2016). Different levels of hyphal self-incompatibility modulate interconnectedness of mycorrhizal networks in three arbuscular mycorrhizal fungi within the Glomeraceae. Mycorrhiza, 26(4), 325-332.
Razavi, B. S., Zarebanadkouki, M., Blagodatskaya, E., & Kuzyakov, Y. (2016). Rhizosphere shape of lentil and maize: spatial distribution of enzyme activities. Soil Biology and Biochemistry, 96, 229-237.
Razavi, B. S., Zhang, X., Bilyera, N., Guber, A., & Zarebanadkouki, M. (2019). Soil zymography:

simple and reliable? Review of current knowledge and optimization of the method. Rhizosphere, 11, 100161.
Rillig, M. C., Wright, S. F., Nichols, K. A., Schmidt, W. F., & Torn, M. S. (2001). Large contribution of arbuscular mycorrhizal fungi to soil carbon pools in tropical forest soils. Plant and Soil, 233, 167-177.
Ruiz-Lozano, J. M., Collados, C., Barea, J. M., & Azcón, R. (2001). Arbuscular mycorrhizal simbiosis can alleviate droughtinduced nodule senescence in soybean plants. New Phytologyst.
Sardans, J., & Peñuelas, J. (2004). Increasing drought decreases phosphorus availability in an evergreen Mediterranean forest. Plant and Soil, 267, 367-377.
Sardans, J., & Peñuelas, J. (2007). Drought changes phosphorus and potassium accumulation patterns in an evergreen Mediterranean forest. Functional Ecology, 21(2), 191-201.
Schimel, J., Balser, T. C., & Wallenstein, M. (2007). Microbial stress-response physiology and its implications for ecosystem function. Ecology, 88(6), 1386-1394.
Schnepf, A., Leitner, D., Klepsch, S., Pellerin, S., & Mollier, A. (2011). Modelling phosphorus dynamics in the soil–plant system. Phosphorus in action: biological processes in soil phosphorus cycling, 113-133.
Shade, A., Peter, H., Allison, S. D., Baho, D. L., Berga, M., Bürgmann, H., ... & Handelsman, J. (2012). Fundamentals of microbial community resistance and resilience. Frontiers in microbiology, 3, 417.
Sharp, R. E., Hsiao, T. C., & Silk, W. K. (1990). Growth of the maize primary root at low water potentials: II. Role of growth and deposition of hexose and potassium in osmotic adjustment. Plant physiology, 93(4), 1337-1346.
Shen, J., Yuan, L., Zhang, J., Li, H., Bai, Z., Chen, X., ... & Zhang, F. (2011). Phosphorus dynamics: from soil to plant. Plant physiology, 156(3), 997-1005.
Shu, X., Hallett, P. D., Liu, M., Baggs, E. M., Hu, F., & Griffiths, B. S. (2019). Resilience of soil functions to transient and persistent stresses is improved more by residue incorporation than the activity of earthworms. Applied Soil Ecology, 139, 10-14.
Smith, S. E., & Read, D. J. (2010). Mycorrhizal symbiosis. Academic press.
Spollen, W. G., Tao, W., Valliyodan, B., Chen, K., Hejlek, L. G., Kim, J. J., ... & Nguyen, H. T. (2008). Spatial distribution of transcript changes in the maize primary root elongation zone at low water potential. BMC Plant Biology, 8, 1-15.
Steinweg, J. M., Dukes, J. S., & Wallenstein, M. D. (2012). Modeling the effects of temperature and moisture on soil enzyme activity: linking laboratory assays to continuous field data. Soil Biology and Biochemistry, 55, 85-92.
Strickland, M. S., Wickings, K., & Bradford, M. A. (2012). The fate of glucose, a low molecular weight compound of root exudates, in the belowground foodweb of forests and pastures. Soil Biology and Biochemistry, 49, 23-29.
Tarafdar, J. C., & Claassen, N. (1988). Organic phosphorus compounds as a phosphorus source for higher plants through the activity of phosphatases produced by plant roots and microorganisms. Biology and fertility of soils, 5, 308-312.
Tarafdar, J. C., & Marschner, H. (1994). Efficiency of VAM hyphae in utilisation of organic phosphorus by wheat plants. Soil Science and Plant Nutrition, 40(4), 593-600.
Vančura, V., & Hovadik, A. (1965). Root exudates of plants: II. Composition of root exudates of some vegetables. Plant and Soil, 22, 21-32.
Vierheilig, H., Coughlan, A. P., Wyss, U. R. S., & Piché, Y. (1998). Ink and vinegar, a simple staining technique for arbuscular-mycorrhizal fungi. Applied and environmental microbiology, 64(12), 5004-5007.
Voothuluru, P., Anderson, J. C., Sharp, R. E., & Peck, S. C. (2016). Plasma membrane proteomics in the maize primary root growth zone: novel insights into root growth adaptation to water stress. Plant, Cell & Environment, 39(9), 2043-2054.
Wang, W. X., Vinocur, B., Shoseyov, O., & Altman, A. (2000, July). Biotechnology of plant osmotic

stress tolerance physiological and molecular considerations. In IV International Symposium on In Vitro Culture and Horticultural Breeding 560 (pp. 285-292).
Welc, M., Frossard, E., Egli, S., Bünemann, E. K., & Jansa, J. (2014). Rhizosphere fungal assemblages and soil enzymatic activities in a 110-years alpine chronosequence. Soil Biology and Biochemistry, 74, 21-30.
Williams, A., & de Vries, F. T. (2020). Plant root exudation under drought: implications for ecosystem functioning. New Phytologist, 225(5), 1899-1905.
Wu, Q. S., Xia, R. X., & Zou, Y. N. (2008). Improved soil structure and citrus growth after inoculation with three arbuscular mycorrhizal fungi under drought stress. European journal of soil biology, 44(1), 122-128.
Yang, S. Y., Grønlund, M., Jakobsen, I., Grotemeyer, M. S., Rentsch, D., Miyao, A., ... & Paszkowski, U. (2012). Nonredundant regulation of rice arbuscular mycorrhizal symbiosis by two members of the PHOSPHATE TRANSPORTER1 gene family. The Plant Cell, 24(10), 4236-4251.
Yevdokimov, I., & Blagodatskaya, E. (2014). Determination of Extractable and Microbial P in Soils with Anion-Exchange Membranes. Goettingen, Germany.
Zarebanadkouki, M., & Carminati, A. (2014). Reduced root water uptake after drying and rewetting. Journal of Plant Nutrition and Soil Science, 177(2), 227-236.
Zhang, F., Meng, X., Yang, X., Ran, W., & Shen, Q. (2014). Quantification and role of organic acids in cucumber root exudates in Trichoderma harzianum T-E5 colonization. Plant physiology and biochemistry, 83, 250-257.
Zhang, H., Shi, L., Lu, H., Shao, Y., Liu, S., & Fu, S. (2020). Drought promotes soil phosphorus transformation and reduces phosphorus bioavailability in a temperate forest. Science of the Total Environment, 732, 139295.
Zhang, X., Kuzyakov, Y., Zang, H., Dippold, M. A., Shi, L., Spielvogel, S., & Razavi, B. S. (2020). Rhizosphere hotspots: root hairs and warming control microbial efficiency, carbon utilization and energy production. Soil Biology and Biochemistry, 148, 107872.
Zhang, X., Myrold, D. D., Shi, L., Kuzyakov, Y., Dai, H., Hoang, D. T. T., ... & Razavi, B. S. (2021). Resistance of microbial community and its functional sensitivity in the rhizosphere hotspots to drought. Soil Biology and Biochemistry, 161, 108360.

Supplementary data

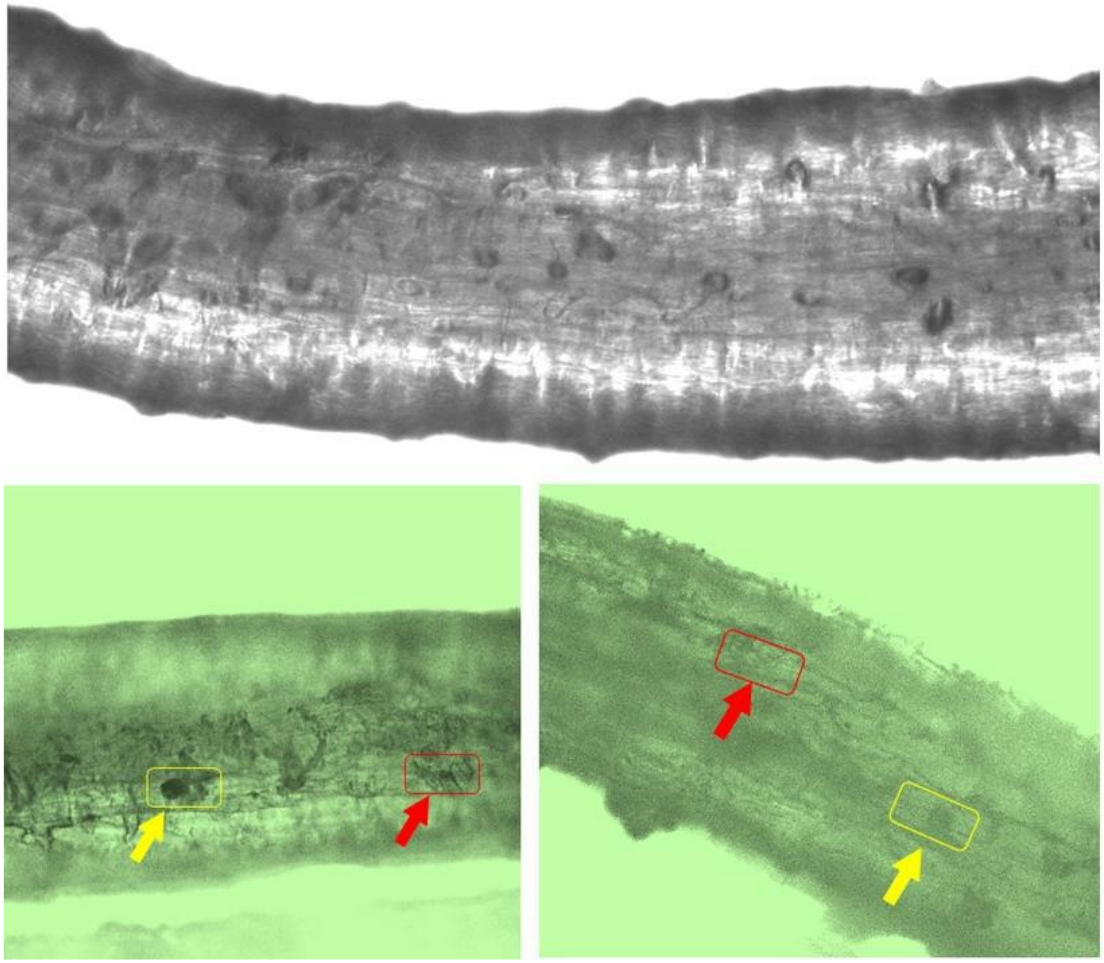

Figure S3-1 *Arbuscular mycorrhiza fungi well accommodated in the roots with the red arrow showed arbuscule and the yellow arrow indicated vesicle. The image was taken using staining technique.*

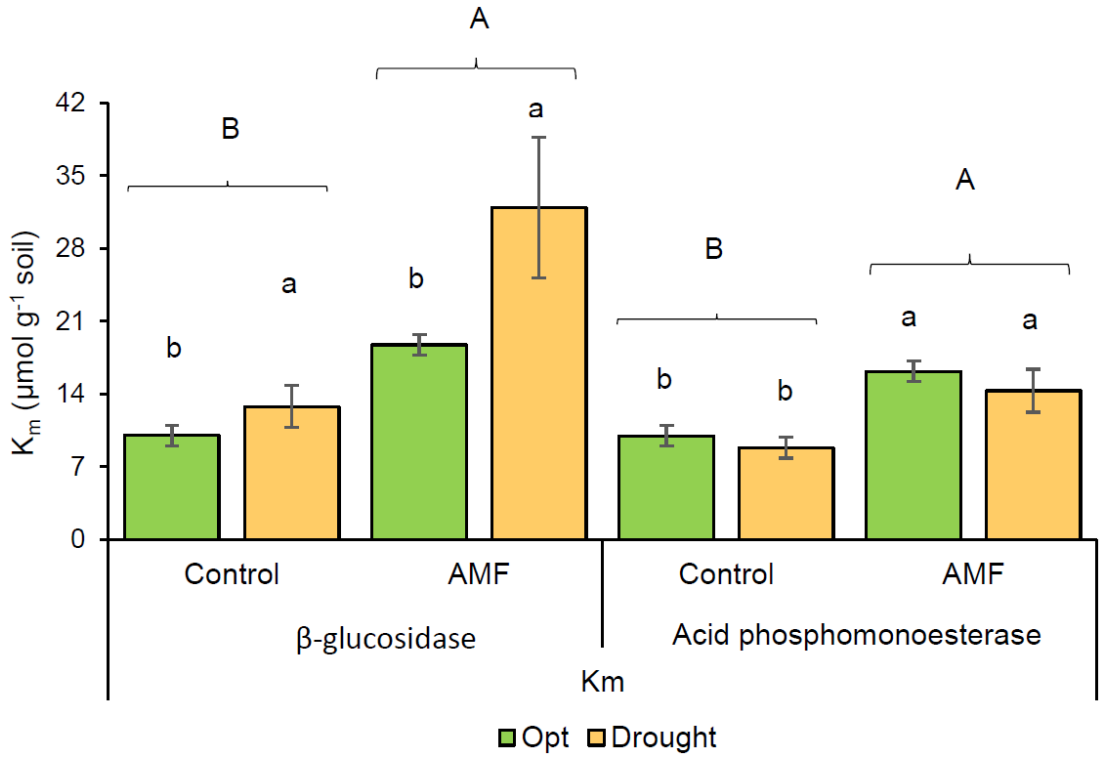

Figure S3-2 *Km values of β-glucosidase and acid phosphomonoesterase in mycorrhizal and non-mycorrhizal plants. Higher Km value in mycorrhizal plants than non-mycorrhizal plants indicated different enzyme systems with lower substrate affinity. Lower case letters: significant differences between optimum (Opt) and drought at $p < 0.05$; upper case letters: significant differences between control and AMF at $p < 0.05$. GLU: β-glucosidase, PHOS: acid phosphomonoesterase.*

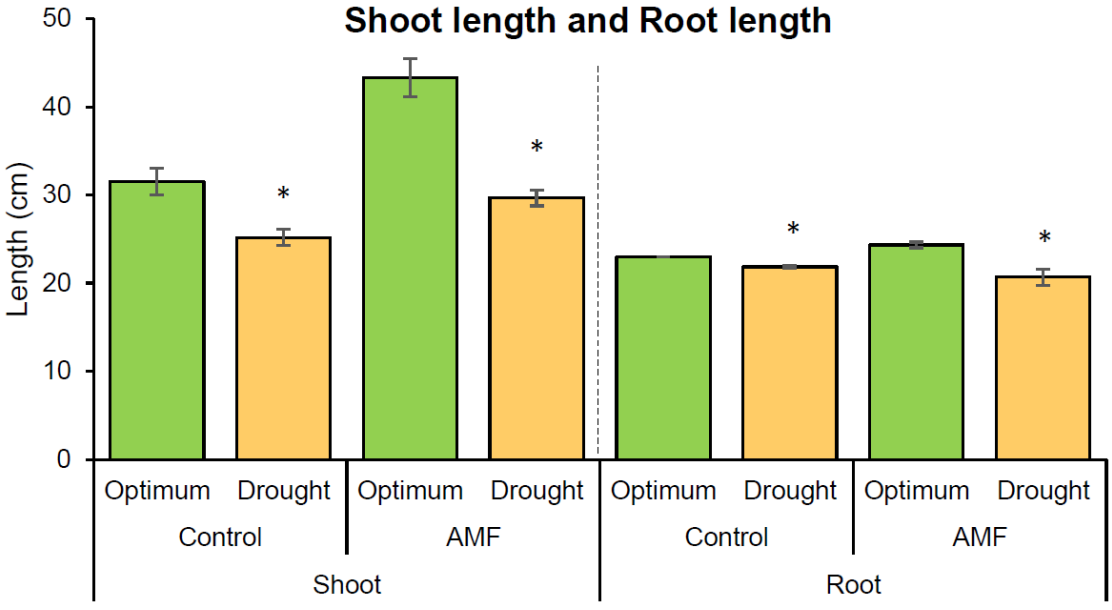

Figure S3-3 *Drought reduced the shoot length by 1.3-1.5 times but the reduction of root length is less than shoot length. AMF inoculum strongly increased shoot length by 1.38 times at optimum condition and by 1.24 times at drought condition. Asterisk (*) showed significant effect of drought on the length of root and shoot ($p<0.05$).*

2.4 Study 4. Divergent response of maize and soybean rhizosphere to arbuscular mycorrhiza

Ali Feizi [a], Anh The Luu [b], Van Dinh Mai [c], Thu Tran Thi Tuyet [c], **Shang Wang** [d], Duyen Thi Thu Hoang [d,e*]

Status: Published in *Rhizosphere*

[a] *Department of Soil Science, Institute of Plant Nutrition and Soil Science, Christian-Albrechts-University of Kiel, Kiel 24118, Germany*

[b] *VNU-central institute for natural resources and environmental studies, Vietnam National University, No. 19 Le Thanh Tong, Phan Chu Trinh, Hoan Kiem, Hanoi, Vietnam*

[c] *Environmental Faculty, Hanoi University of Sciences, Vietnam National University, 334 Nguyen Trai, Thanh Xuan, Hanoi, Vietnam*

[d] *Department of Soil and Plant Microbiome, Institute of Phytopathology, Christian-Albrechts-University of Kiel, Kiel 24118, Germany*

[e] *Program of Smart Agriculture and Sustainability, VNU Vietnam Japan university, Vietnam National University, 144 Xuan Thuy, Cau Giay, Hanoi, Vietnam*

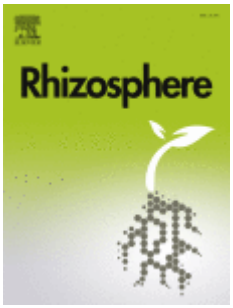

Feizi, A., Luu, A. T., Tuyet, T. T. T., Wang, S., & Hoang, D. T. T. (2024). Divergent response of maize and soybean rhizosphere to arbuscular mycorrhiza. Rhizosphere, 29, 100834. https://doi.org/10.1016/j.rhisph.2023.100834

Abstract

Maize and soybean are capable of forming symbiotic relationship with arbuscular mycorrhizal fungi (AMF), which enables the plants to overcome P limitations and resist drought effects. The results indicate that the activities of β-glucosidase, chitinase and acid phosphatase in the rhizosphere were double those in the bulk soil, regardless of plant species. Both soybean and maize demonstrated a decrease in β-glucosidase activity. However, chitinase activity displayed a divergent pattern between the two plant species under AMF influence, with a notable 18.5% increase in maize compared to a substantial 44.8% decrease in soybean. The presence of AMF resulted in a 50% reduction in rhizosphere microbial biomass phosphorus (MBP) in soybean, whereas this effect was not observed in maize. The distinct nutrient demands of each plant species appear to regulate the impact of AMF on the characteristics of microbial activities in the rhizosphere.

Keywords: Arbuscular Mycorrhizal fungi, rhizosphere, enzyme activities, microbial biomass, microorganism

1. Introduction

Maize and soybean have a long history of cultivation worldwide, closely intertwined with the evolution of human civilization. Maize, first cultivated around 5000 years ago (Gewin, 2003), predates soybeans, which were a staple in Chinese cuisine by the 11th century BC. These two plant species rank among the four most important crops globally, following wheat and rice. Maize, a representative of the grass family (Poaceae, C_4 plant), differs biologically from soybeans, a legume species of the Fabaceae family (C_3 plant). The higher photosynthesis intensity of C_4 plants compared to C_3 plants

(Ehleringer and Cerling, 2002) leads to variations in root exudate composition between the two plant species. For instance, C_4 plants release higher amount of amino acid and organic acid compared to C_3 plants, while C_3 plants exhibit higher carbohydrate content (Nabais et al., 2011; Vranova et al., 2013). Despite only soybean establishing symbiosis with N-fixing rhizobium bacteria, both plant species are capable of forming symbiotic relationship with arbuscular mycorrhizal fungi (AMF), aiding in overcoming P limitations and resisting drought effects (Boomsma and Vyn, 2008). Exuded carbon (C) from plant roots serves as an energy source for AMF, while fungal hyphae act as nutrient transport pathways from distant areas to the root surface. Intriguingly, the symbiotic relationship is regulated by C and nutrient balances, especially Willis et al. (2012) found that when available P content is high, exuded C content to the rhizosphere decreases, leading to a decline in AMF density. Consequently, AMF colonization alters root exudation profiles, influencing the microecological environment of plant roots, including microbial structure and functions (Ma et al., 2021). Moreover, the composition and liability of rhizospheric organic compounds are plant species specific. For examples, the proportions of p-coumaric acid, cinnamic acid, p-hydroxybenzoic acid, vanillic acid, and ferulic acid in phenolic acid are distinguished between maize and soybean (Zhang et al., 2020). Therefore, the rhizosphere microbial community plays a crucial role in controlling enzyme synthesis, optimizing the cost and benefits of energy and nutrient consumption. As a result, enzyme activities, as well as microbial biomass, may alter with plant species. However, the impact of the interplay between diverse plant species and their arbuscular mycorrhizal fungi (AMF) colonization on soil microbial-mediated processes remains unclear. Therefore, this research aims to elucidate the effects of AMF symbiosis on enzyme activities (β-glucosidase, chitinase, and acid phosphatase) and microbial biomass in the rhizosphere of two different plant species, namely maize and soybean, cultivated on soil materials collected from agricultural areas in the Red River Delta, Vietnam. While there are numerous AMF species, our study focuses on Glomus mosseae (*G. mosseae*) due to its global distribution (Benedetto et al., 2005). The research was conducted in a greenhouse at Kiel University, Germany, with a controlled temperature of 22 °C. The primary objective was to investigate whether AMF symbiosis enhances microbial enzyme activities and microbial biomass phosphorus, and whether these effects are dependent on the plant species.

2.Materials and Methodologies

Soil samples were collected from the top soil (0-30 cm) of a Fluvisol being used for rice and soybean rotation in Vu Thu district, Thai Binh province, Vietnam (20° 25' 34.4" N; 106° 16' 33.4" E). Soil samples contained 79.5% sand, 10.8% clay, and 9.7% silt, total N 0.12%, total P 0.18% and organic C content 0.37%, pH 7.07. The sieved soil was mixed with AMF fertilizers (AMF treatment) and control soil without AMF fertilizers. The soil was packed in rhizoboxes (10 × 10 × 1 cm) to attain a bulk density of 1.1 g/cm^3. The packed soil was remoistured with sterilized water to 60% water holding capacity (WHC).

Maize (*Zea mays* L., B73) and soybean (*Glycine max* L., DT96) seeds were sterilized with 70% ethanol according to Toyama et al. (2006). Each germinated maize or soybean seed on moist filter papers was transplanted at 2 cm depth in one rhizobox and placed in a glass house under controlled temperature of 22 °C, 12-hour light per day at an intensity of 330 µmol m^{-2} s^{-1}. The laboratory was located in the Institute of Phytopathology, Christian-Albrechts-University of Kiel, Germany. All the rhizoboxes were covered with aluminum foil to avoid the growth of algea. Sterilized water was used

to irrigate the plants for experimental bias prevention. In total, the experiment includes four treatments each of which was 4 times replicated: (i) maize + AMF; (ii) maize – AMF (control) (iii) soybean + AMF; (iv) soybean - AMF (control). After one and a half months of growth, eight rhizosphere samples were collected from: 2 plant species × 2 treatments with AMF and without AMF × 2 soil types (rhizosphere and bulk soil). All the samples were preserved at 5 ℃ until analysis.

Fluorescent substrates (Sigma Aldrich, Germany) including β-D-glucopyranoside (MUF-G), N-acetyl-D-glucosamine (MUF-N), 4-methylumbelliferyl-phosphate (MUF-P) were utilized for the measurements of β-glucosidase, chitinase, and acid phosphatase, respectively. The analyzing steps were suggested by Hoang et al. (2022) by weighing 1 g soil into an air-tight glass bottle prior to filling with 50 ml sterilized water, followed by 20 minutes shaking. 50 µL soil slurry, 50 µL MES buffer (pH 6.5) and 100 µL substrate solution were pipetted in a 96-hole black plate (Puregrade, Germany). The plate was measured by CLARIOstar plus (BMG LABTECH, Germany) at three time points: 30, 60 and 120 minutes at an excitation wavelength of 355 nm and an emission wavelength of 460 nm. A calibration line was prepared with MUF substrate in a concentration range of 0, 10, 20, 30, 40, 50, 100, 200 µM to define the slope. Enzyme kinetic parameters were calculated based on the Michaelis-Menten equation (1):

$$v = \frac{V_{max} \times [S]}{K_m + [S]} \quad (1)$$

in which v is the reaction rate at 120'-time point of the measurement; V_{max} is the maximum reaction rate at saturated substrate concentration (nmol MUF g^{-1} soil h^{-1}); [S] is the substrate concentration (µmol g^{-1} soil); K_m is the substrate concentration at which the reaction rate attains a half of maximum. K_m value is negatively correlated with substrate affinity, which means that the higher the K_m value is the smaller the substrate affinity is. In order to calculate the enzyme kinetic parameters (V_{max} and Km), the measured fluorescent values were fitted with the range of substrate concentrations via the non-linear regression routine of SigmaPlot (version 12.5). The microbial biomass phosphorus (MBP) was measured by fumigation-extraction method with some modification for anion exchange membrane (AEM) application (Maharjan et al., 2018). Three grams of soil were weighed in a centrifuge tube and added with a membrane (The fuel cell store, the U.S.A.) and 30 ml sterilized water. After the application of chloroform, the centrifuge tubes were shaken for 24h to absorb anion phosphate in exchange with HCO_3^- on the AEM surface. Afterward, the strips were taken and gently rinsed with sterilized water before being immersed in another centrifuge tube filled with 45 ml H_2SO_4 0.25M. The tubes containing strips were again shaken for 3h to desorb anion phosphate into solution. At final step, 150 µL solution was pippeted into a 96-hole white plate. 30 µl *Reagent 1* (14.2 mmol L^{-1} ammonium molybdate tetrahydrate dissolved in H_2SO_4 3.1 M) and *Reagent 2* (3.5 g L^{-1} aqueous polyvinyl alcohol reagent and malachite green) (D'Angelo et al., 2001) were added to the plate, respectively. The plates were incubated at 40 ℃ for 30 - 40 minutes and measured by CLARIOstar plus (BMG LABTECH, Germany) at 630 nm. In order to calculate P concentration of the samples, a calibration line was prepared by diluting KH_2PO_4 100ppm into a range of concentrations of 0, 0.05, 0.1, 0.2, 0.4, 0.6, 0.8, 1.0, 1.5, 2, 3, 5 µg P ml^{-1}. The calibrated concentrations were measured in the same way with the samples. All data were presented as mean ± standard error (mean ± SE). ANOVA assumptions of normality and variance homogeneity were checked for 4 replicates of each treatments using Shapiro-

Wilk test and Levene test prior to the analysis of variance. Two-way ANOVA followed by a Tukey HSD test was applied for analyzing the differences in soil biochemical properties between rooted soil and bulk soil of two plant species, and One-way ANOVA was used to test the differences of one parameter between AMF treated and control soil. All analyses were performed using SigmaPlot (version 12.5) at a significant level of $p < 0.05$.

3. Results and discussion

The rhizosphere enzyme activities of β-glucosidase, chitinase and acid phosphatase were at least double those in the bulk soil, irrespective of plant species ($p < 0.01$; Figure 1). The presence of AMF enlarged the difference in enzyme activities between bulk soil and the rooted area of both soybean and maize by 18-49%. AMF symbiosis fostered an increase of 16-18% in β-glucosidase in the rhizosphere of both maize and soybean. Chitinase activities in AMF treated rhizosphere of soybean was 44.8% lower than those in the control, while a reverse pattern was observed in maize with the presence of AMF enhancing chitinase activities by 18.5%. However, the effect of AMF inoculation on rhizosphere acid phosphatase was obscure in both plant species. The activities of the three enzymes in maize rhizosphere were higher than those in soybean, particularly under AMF. The distinction in K_m value between the rhizosphere and bulk soil was found in both maize and soybean for β-glucosidase and acid phosphatase, but effects of AMF on K_m value were unclear in our findings (Figure 2).

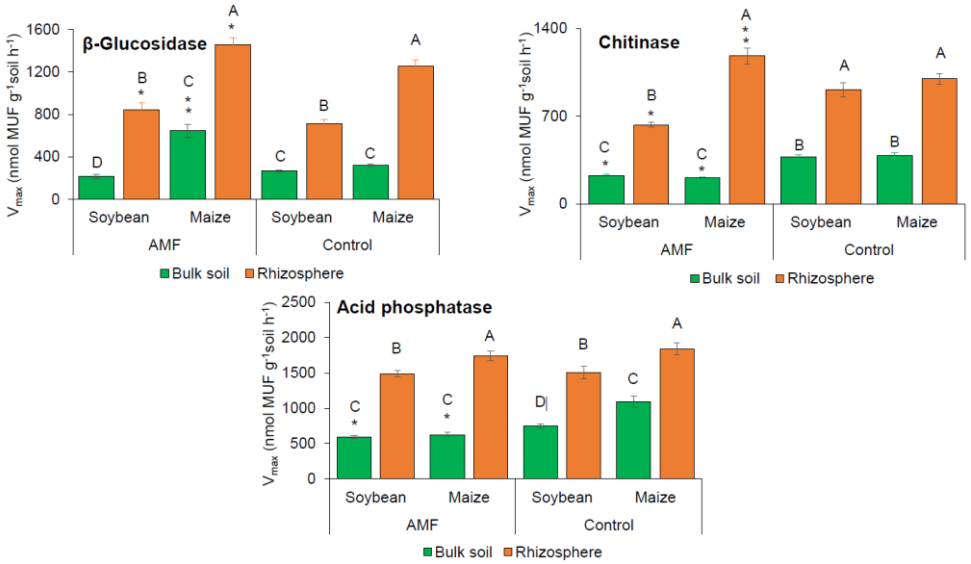

Figure 4-1 *Activities of β-Glucosidase, chitinase and acid phosphatase in rooted soil and bulk soil of maize and soybean. The capital letters showed the significant difference between treatments under AMF or non-AMF inoculation ($p < 0.05$). The asterisk indicated the significant effects of AMF on enzyme activities ('*': $p < 0.05$; '**': $p < 0.01$).*

Plant roots exude 17-40% of photosynthesized C to their rhizosphere (Nguyen, 2003), providing a favorable condition for the development and thriving of ubiquitous microbial communities. Moreover, root exudates, composed of simple and complex C compounds such as amino acid, organic acid, carbohydrate, nucleotides, etc. (van Dam et al., 2016), supply labile organic matters for microbial enzyme synthesis in the rhizosphere. As a result, microbial community composition and density in the rhizosphere are 20-40 times higher than those in the bulk soil (Foster, 1988), explaining our findings of enzyme activities in the rhizosphere being twice as high as those in the bulk soil. Although various plant species share common root exudate compositions, the proportion of these compounds depends

on specific plants and age (Aulakh et al., 2001). For instance, maize root exudates contain 70% free sugars (glucose, sucrose), 18% phenol compounds, 7% organic acids and 3% amino acid (Azaizeh et al., 1995). Meanwhile these components vary widely in the soybean rhizosphere depending on environmental conditions (Sugiyama., 2019), with isoflavones and saponins are two major exuded compounds. Therefore, the difference in enzyme activities between maize and soybean is more pronounced in their rhizosphere than in the bulk soil. Enzyme activities in the maize rhizosphere were higher than those in the soybean rhizosphere, especially β-glucosidase activity, which was 195% higher in the former than in the later. Despite the lack of a direct comparison of root exudate components between maize and soybean, the low molecular weight organic acids produced by C4 plants (maize) were supposed to be higher than C3 plants (soybean) (Sivaram et al., 2020). The greater abundance of easily decomposed C sources from maize rhizosphere may stimulate microbial activities, leading to higher enzyme activities than in the soybean rhizosphere.

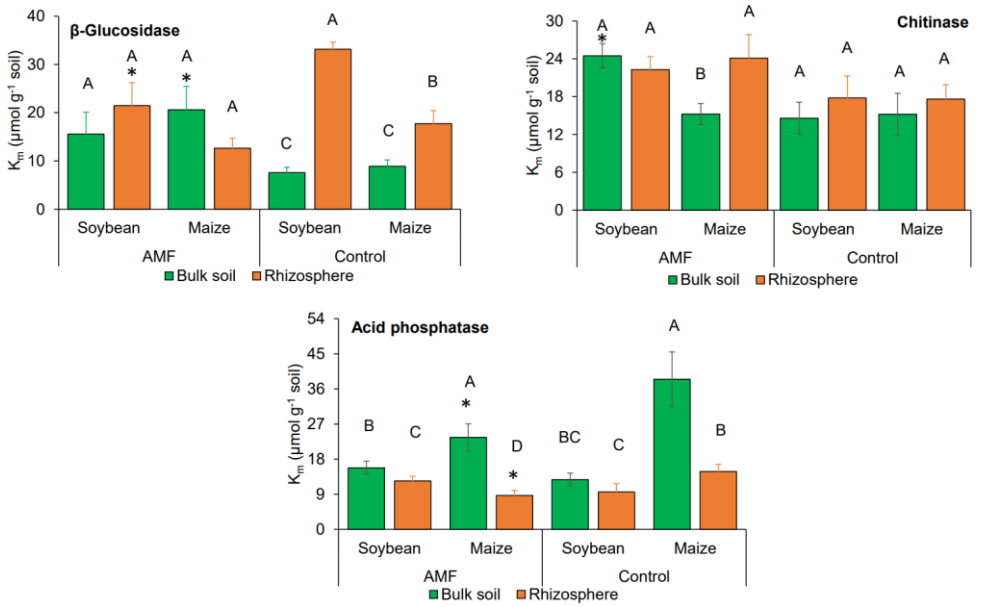

Figure 4-2 *K_m of β-Glucosidase, chitinase and acid phosphatase in rooted soil and bulk soil of maize and soybean. The capital letters showed the significant difference between treatments ($p < 0.05$). The asterisk indicated the significant effects of AMF on enzyme activities ('*': $p < 0.05$; '**': $p < 0.01$).*

The symbiosis with AMF fostered an increase in β-glucosidase activity in both maize and soybean but lowered the chitinase activity in the latter, while the effect of AMF symbiosis on acid phosphatase activities was absent. This finding contradicted our assumption of positive effects of AMF symbiosis on all enzyme activities compared to the control treatment. By visualizing glucose exudation, Hoang et al. (2022) demonstrated an increase in exuded glucose under the presence of AMF inoculation. This glucose is a labile C source directly uptaken by AMF to produce and spread fungal hyphae to the surrounding area (Bücking et al., 2008). The competition for C demand between free-living microorganisms and symbiotic AMF promoted the generation of β-glucosidase in the rhizosphere compared to the bulk soil. We explained the opposite patterns of chitinase activity between maize and soybean by two mechanisms. Firstly, soybean roots synthesize is flavonoids to attract the symbiosis of N-fixing bacteria to form nodules (Weston et al., 2013). The symbiosis of soybean and rhizobium enables the fixation of N_2 from the atmosphere and releases these organic N compounds into the soybean rhizosphere as a source of inorganic N after microbial decomposition (Jalonen et al., 2009).

Secondly, AMF hyphae play a role in transferring N from the surrounding area to the rooted zone (Sierra et al., 2010). The available N source is prioritized to be taken up by the rooted-zone microbial community, thereby reducing the activation of chitinase synthesis in soybean rhizosphere. As a result, chitinase activities in AMF-treated soybean were lower than in the control. In contrast, maize showed higher chitinase activity in the rhizosphere than in the bulk soil, in line with the findings by Lambais and Mehdy (1996) who suggested that chitinase activity of microorganisms under AMF effects depends on the level of symbiosis between plants and fungi. Both maize and soybean have a high demand for P, but the uptake volume depends on the plant's growth stage. P is needed in maize at 4-6 weeks old, while in soybean, P is required in the later vegetative stages (V10) and continues through mid reproductive stages (R5) (Hanway and Weber, 1971), which means 6 weeks after transplantation. Therefore, acid phosphatase activity in maize was higher than in soybean in both (+AMF) and (-AMF) treatments. The finding could result from the higher demand for P in maize at the harvesting time, which stimulated both maize and microbes to generate acid phosphatase enzymes. For maize, the inoculation of AMF triggered 63-171% increase in K_m in bulk soil compared to the rhizosphere for β-glucosidase and acid phosphatase while K_m of chitinase activity increased by 58% in the rhizosphere compared to the bulk soil. Meanwhile, AMF seemed not to affect K_m value in soybean regardless of rhizosphere and bulk soil. As K_m value demonstrates the affinity of enzyme to the substrate (Loeppmann et al., 2016), the inconsistent alteration of K_m value in rooted maize under AMF effects suggested microbial strategies in acquiring C and nutrients. The strategic changes of K_m value in rooted maize versus the stable K_m value in rooted soybean implied the specific impact of plant species on the mobilization of nutrients within the rhizosphere under the presence of AMF.

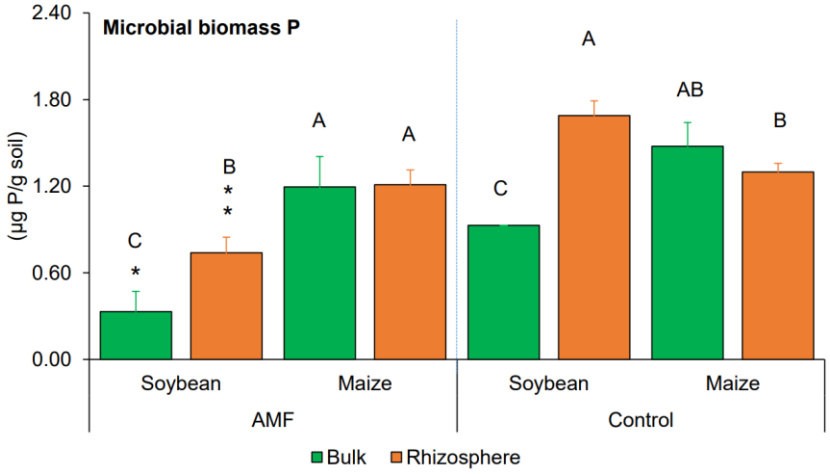

Figure 4-3 *Microbial biomass P in rooted soybean and maize under AMF effects. The capital letters showed the significant difference between treatments under AMF or non-AMF inoculation (*$p < 0.05$*). The asterisk indicated the significant effects of AMF on enzyme activities ('*': $p < 0.05$; '**': $p < 0.01$).*

Microbial biomass P (MBP) in soybean rhizosphere was approximately double that in the bulk soil ($p < 0.01$), but the difference between maize rhizosphere and bulk soil was not found (Figure 3). The inoculation with AMF halved MBP values inside and outside rhizosphere of soybean ($p < 0.05$), while this effect on maize was not reflected in rooted soybean was significantly higher than in the bulk soil, regardless of AMF or non-AMF effects, but this difference was negligible in maize. The higher MBP in rooted soybean than in the bulk soil was associated with our above explanation of a higher

density of the microbial community in the rhizosphere. While the demand for P in soybean was lower at the early growth stage, this demand in maize dramatically increased, making the plant's P uptake outcompete microbial P accumulation. Consequently, the microbial biomass P in maize rhizosphere was similar to the bulk soil. Remarkably, the presence of AMF apparently reduced MBP inside and outside the rhizosphere in both maize and soybean compared to the bulk soil. There were two reasons for the findings: (i) the growth of AMF leads to the abundant reduction of *Proteobacteria* (Burke et al. 2003) or *T. harzianum* (Green et al. 1999), which decreased microbial P sequestration; and (ii) nutrient competition between AMF and other microbes also hampered the proliferation of the general microbial community (Joner et al. 2000b). In conclusion, the effects of AMF on MBP are very diverse and highly reliant on the nutrient demands of the plant at a certain growth stage of each plant species.

The research focused on evaluating AMF effects on enzyme activities in maize and soybean rhizosphere at the early stages of their growth. The findings showed that activities of β-glucosidase, chitinase and acid phosphatase enzymes in rooted soil were almost double those in the bulk soil, regardless of the plant species. AMF symbiosis generated inconsistent effects on rhizosphere microbial enzyme activities, with an increase of 16-18% in β-glucosidase in both rooted maize and soybean, but a reduction of 44.8% in chitinase of rooted soybean. However, the effect of AMF inoculation on acid phosphatase was obscure. The diverse effects of AMF on MBP of rooted soil are attributed to different root exudate compositions between the two plant species and their dependence of P demanding at their early growth stage.

CRediT authorship contribution statement

Ali Feizi: Writing - review & editing, Investigation. **Anh The Luu:** Writing - review & editing, Funding acquisition. **Van Dinh Mai:** Writing - review & editing, Funding acquisition. **Thu Tran Thi Tuyet:** Writing - review & editing. **Shang Wang:** Writing - review & editing, Methodology, Investigation. **Duyen Thi Thu Hoang:** Writing - review & editing, Writing - original draft, Supervision, Project administration, Methodology, Investigation, Funding acquisition, Data curation, Conceptualization.

Declaration of competing interest

The authors declare that they have no known competing financial interests or personal relationships that could have appeared to influence the work reported in this paper.

Acknowledgement

The research was financially supported by JICA TC2 (Project code: Project code: 21.02). We would like to express our sincere acknowledgement to Prof. Bahar S. Razavi – Department of Soil and Plant Microbiome, Institute of Phytopathology, Christian-Albrechts-University of Kiel, Kiel 24118, Germany, who strongly supported our experiment and gave us to many helpful consultations.

References

Allison, S.D., Weintraub, M.N., Gartner, T.B., Waldrop, M.P., 2011. Evolutionary economic principles as regulators of soil enzyme production and ecosystem function. In: Shukla, G., Varma, A. (Eds.), Soil Enzymology. Springer-Verlag, Berlin, Germany, pp. 229-243.

Aulakh, M. S., Wassmann, R., Bueno, C., Kreuzwieser, J. & Rennenberg, H., 2001. Characterization of Root Exudates at Different Growth Stages of Ten Rice (Oryza sativa L.) Cultivars. Plant Biology 3, 139–148.

Azaizeh, H.A., Marschner, H., Römheld, V., Wittenmayer, L., 1995. Effects of vesicular abruscular

micorrhizal fungus and other soil microorganisms on growth, mineral nutrient acquisition and root exudation of soil-grown maize plants. Mycorrhiza 5: 321-327.
Badri, D.V., Vivanco, J.M., 2009. Regulation and function of root exudates. Plant, Cell & Environment, 32(6), 666–681.
Benedetto, A., Magurno, F., Bonfante, P., Lanfranco, L., 2005. Expression profles of a phosphate transporter gene (GmosPT) from the endomycorrhizal fungus Glomus mosseae. Mycorrhiza 15, 620–627.
Boomsma, C.R., Vyn, T.J., 2008. Maize drought tolerance: Potential improvements through arbuscular mycorrhizal symbiosis? Field Crops Research 108, 14-31.
Burke, D.J., Hamerlynck, E.P., Hahn, D., 2003. Interactions between the salt marsh grass Spartina patens, arbuscular mycorrhizal fungi and sediment bacteria during the growing season. Soil Biol Biochem 35, 501–511.
Bücking, H., Abubaker, J., Govindarajulu, M., Tala, M., Pfeffer, P.E., Nagahashi, G., Lammers, P., Shachar-Hill, Y., 2008. Root exudates stimulate the uptake and metabolism of organic carbon in germinating spores of Glomus intraradices. New Phytologist 180, 684–695.
D'Angelo, E., Crutchfield, J., Vandiviere, M., 2001. Rapid, sensitive, microscale determination of phosphate in water and soil. Journal of Environmental Quality 30, 2206–09.
Ehleringer, J. R., and Cerling, T. E., 2002. "C3 and C4 photosynthesis," in Encoclopedia of Global Environmental Change, eds H. A. Mooney and J. G. Canadell (Chichester: John Wiley and Sons, Ltd.), 186–190.
Foster, R.C., 1988. Microenvironments of soil-microorganisms. Biol Fertil Soils 6: 189–203.
Green, H., Larsen, J., Olsson, P.A., Jensen, D.F., Jakobsen, I., 1999. Suppression of the biocontrol agent Trichoderma harzianum by mycelium of the arbuscular mycorrhizal fungus Glomus intraradices in root-free soil. Applied and Environmental Microbiology 65, 1428–1434.
Hanway, J.J. and C.R. Weber., 1971. Accumulation of N, P, and K by soybeans (Glycine max (L.) Merrill) plants. Agron. J. 63, 406-408.
Henneron, L., Kardol, P., Wardle, D.A., Cros, C., Fontaine, S., 2020. Rhizosphere control of soil nitrogen cycling: a key component of plant economic strategies. New Phytol., 228, pp. 1269-1282.
Hoang, T.T.D., Rashtbari, M., Anh, L.T., Wang, S., Tu, D.T., Hiep, N.V., Razavi, B.S., 2022. Interactive regulation of root glucose exudation and rhizosphere expansion: A mycorrhiza-soybean cooperation under drought. Soil Biology and Biochemistry 171, 108728.
Jalonen, R., Nygren, P., and Sierra, J. (2009). Transfer of nitrogen from a tropical legume tree to an associated fodder grass via root exudation and common mycelial networks. Plant Cell Environ. 32, 1366–1376. doi: 10.1111/j.1365-3040.2009.02004.xJones, D.L., Hodge, A., Kuzyakov, Y., 2004. Plant and mycorrhizal regulation of rhizodeposition. New Phytol. 163, 459-480.
Kosslak, R.M., Bookland, R., Barkei, J., Paaren, H.E., Appelbaum, E.R., 1987. Induction of Bradyrhizobium japonicum common nod genes by isoflavones isolated from Glycine max. Proc. Natl. Acad. Sci. USA. 84: 7428–7432.
Lambais, M.R., Mehdy, M.C., 1996. Differential expression of defense-related genes in arbuscular mycorrhiza. Canadian Journal of Botany 73 (Suppl. 1): S533-S540.
Loeppmann, S., Blagodatskaya, E., Pausch, J., Kuzyakov, Y., 2016. Substrate quality affects kinetics and catalytic efficiency of exoenzymes in rhizosphere and detritusphere. Soil Biology & Biochemistry 92, 111-118.
López-Poma, R., Bautista, S., 2014. Plant regeneration functional groups modulate the response to fire of soil enzyme activities in a Mediterranean shrubland. Soil Biol. Biochem. 79, pp. 5-13.
Lynch, J.M., Whipps, J.M., 1990. Substrate flow in the rhizosphere. Plant Soil 129: 1–10.
Maharjan, M., Maranguit, D., Kuzyakov, Y., 2018. Phosphorus fractions in subtropical soils depending on land use. European Journal of Soil Biology 87, 17-24.
Ma, J., Ma, Y., Wei, Z., Wu, J., Sun, C., Yang, J., Liu, L., Liao, H., Chen, T., Huang, J., 2021. Effects of arbuscular mycorrhizal fungi symbiosis on microbial diversity and enzyme activities in the

rhizosphere soil of Artemisia annua. Soil Science Society of America Journal 85, 703-716.
Nabais, C., Labuto, G., Gonçalves, S., Buscardo, E., Semensatto, D., Nogueira, A.R.A., Freita, H., 2011. Effect of root age on the allocation of metals, amino acids and sugars in different cell fractions of the perennial grass Paspalum notatum (Bahiagrass). Plant Physiol. Bioch. 49, 1442–1447.
Nguyen, C., 2003. Rhizodeposition of organic C by plants: mechanisms and controls. Agronomie, 23, 375–396.
Ren, C., Zhou, Z., Guo, Y., Yang, G., Zhao, F., Wei, G., Han, X., Feng, L., Feng, Y., Ren, G., 2021. Contrasting patterns of microbial community and enzyme activity between rhizosphere and bulk soil along an elevation gradient. Catena 196, Article 104921.
Salt, D.E., Smith, R.D., Raskin, I., 1998. Phytoremediation. Annu Rev Plant Physiol Plant Mol Biol 49, 643–668.
Sierra, J., and Daudin, D. (2010). Limited 15N transfer from stem-labeled leguminous trees to associated grass in an agroforestry system. Eur. J. Agron. 32, 240–242. doi: 10.1016/j.eja.2009.11.003
Sivaram, A.K., Logeshwaran, P., Lockington, R., Naidu, R., Megharaj, M., 2020. The impact of low molecular weight organic acids from plants with C3 and C4 photosystems on the rhizoremediation of polycyclic aromatic hydrocarbons contaminated soil. Environmental Technology & Innovation 19, 100957.
Sugiyama, A., 2019. The soybean rhizosphere: Metabolites, microbes, and beyond—A review. Journal of Advanced Research 19, 67-73.
Toyama, T., Yu, N., Kumada, H., Sei, K., Ike, M., Fujita, M., 2006. Accelerated aromatic compounds degradation in aquatic environment by use of interaction between Spirodela polyrrhiza and bacteria in its rhizosphere. J. Biosci. Bioeng. 101, 346e353.
Gewin, V., 2003. Genetically modified corn—environmental benefits and risks, Plos Biol. 1, 15–19.
van Dam, N. M. & Bouwmeester, H. J., 2016. Metabolomics in the Rhizosphere: Tapping into Belowground Chemical Communication. Trends in plant science 21, 256–265,
Vranova, V., Rejsek, K., Skene, K. R., Janous, D. & Formanek, P., 2013. Methods of collection of plant root exudates in relation to plant metabolism and purpose: A review. J. Plant Nutr. Soil Sci. 176, 175–199.
Weston, L.A., Mathesius, U., 2013. Flavonoids: their structure, biosynthesis and role in the rhizosphere, including allelopathy. J. Chem. Ecol. 39: 283–297.
Willis, A., Rodrigues, B.F., Harris, P.J.C., 2013. The Ecology of Arbuscular Mycorrhizal Fungi. Critical Reviews in Plant Sciences 32, 1–20.
Xie, Z-P., Staehelin, C., Wiemken, A., Broughton, W.J., Müller, J., Boller, T., 1999. Symbiosis-stimulated chitinase isoenzymes of soybean (Glycine max (L.) Merr.). Journal of Experimental Botany 50, pp. 327–333.
Zhang, H., Yang, Y., Mei, X., Li, Y., Wu, J., Li, Y., Wang, H., Huang, H., Yang, M., He, X., Zhu, S., Liu, Y., 2020. Phenolic Acids Released in Maize Rhizosphere During Maize-Soybean Intercropping Inhibit Phytophthora Blight of Soybean. Front. Plant Sci., 11.

2.5 Study 5. Energy and matter dynamics in response to soil salinization and climate warming: A case study on labile carbon decomposition

Shang Wang [a,b*], Bahar S. Razavi [b], Sandra Spielvogel [c], Evgenia Blagodatskaya [a],

Status: Under review in Soil Biology & Biochemistry

[a] *Department of Soil Ecology, Helmholtz Centre for Environmental Research - UFZ, Halle (Saale), 06120, Germany*

[b] *Department of Soil and Plant Microbiome, Institute of Phytopathology, Christian-Albrechts University, Kiel, Germany*

[c] *Institute for Plant Nutrition and Soil Science, Christian-Albrechts-University of Kiel, Kiel, 24118, Germany*

Abstract

Rising salinization of extended river-sides and estuary areas due to climate warming might alter microbial metabolic activity and cause unpredictable consequences for matter and energy turnover in soil. Therefore, we investigated the combined effects of salinization and warming on microbial activity and growth associated with CO_2 (matter) and heat (energy) losses during glucose metabolism. Soil from Elbe estuary was artificially salinized to middle (2.06 mS cm^{-1}) and high (3.45 mS cm^{-1}) levels, while ambient low salinity soil (0.93 mS cm^{-1}) served as the control. We examined the influence of realistic warming (20 vs. 22 °C) on CO_2 emission, heat release, enzyme kinetics (cellobiohydrolase, β-glucosidase, acid phosphomonoesterase and leucine-aminopeptidase) and microbial carbon use efficiency (CUE) across the microbial growth.

Increasing salinity did not impact respiration, heat release, or microbial carbon and nitrogen content without glucose addition. However, activation of microorganisms with glucose intensified salinity effects and hindered substrate uptake and growth. Relatively small 2 °C increase in temperature much stronger affected substrate uptake and growth in comparison with increasing salinity. Moreover, the calorespirometric ratio (CR) increased by 81-124% at high versus low salinity treatment. Enzyme activities increased by 68-871% during the lag phase and maintained relatively high level during the growth and retardation stage. The CR ratio corresponded to the theoretical value (469 kJ mol^{-1} CO_2) only during exponential growth stage. Disregarding the growth retardation stage resulted in strong overestimation of the CUE accounting for 70%-98%. However, the CUE accounted for 40%-60% when the lag, exponential growth and the retardation phases, were included in the calculations. Our results highlight the importance of estimating the carbon budget of microbial growth considering its dynamics when modelling carbon sequestration under global climate change.

Keywords: Soil respiration, Heat release, Calorespirometric ratio, Carbon use efficiency, Microbial growth

1. Introduction

The global area of salt-affected topsoil is approximately 4.24×10^8 ha, accounting for 4.4% of the total land area (FAO, 2021). The increasing severity of soil salinization in coastal estuarine wetland areas is attributed to climate change-induced sea level rise and increasing frequency and severity of extreme weather events leading to vulnerability to coastal flooding with brackish water in many regions of the world (Brown et al., 2022; Wang et al., 2021). Thus, soil salinization in coastal estuarine wetland areas presents a significant challenge to the sustainable development of ecosystems. Predicted global temperatures rise by approximately 1.5℃ by the middle of this century (IPCC, 2018), introduces further uncertainty regarding soil responses to salinization. Consequently, it becomes very relevant to investigate the interacted effects of salinization and climatic warming on soil ecosystems.

Salinity has a direct impact on soil quality and functions, significantly influencing microbial activity and organic matter decomposition (Wong et al., 2010). Salinity directly alters the osmotic of the soil solution, thereby greatly affecting soil microbial activity, diversity and functionality (Song et al., 2022; Zhang et al., 2019). These salinity-induced changes on microbiome have substantial implications for soil enzyme production and are enzyme- and soil - specific (Singh, 2016). High salinity decreased soil enzyme activity in grassland (Pan et al., 2013), while having no impact on enzyme activity in paddy fields (Shahariar et al., 2021; Sritongon et al., 2022). Extreme climatic events not only contribute to salinization but also warming. Global temperature increase alters soil processes and functions. Generally, warming promotes soil microbial activity and growth, accelerating soil organic matter (SOM) decomposition and nutrient cycling if water is not limiting (Singh et al., 2010). Soil respiration may increase by the factor of 3-4 with a 10℃ warming (Q_{10}), indicating a stronger loss of SOM and carbon emissions in the soil ecosystem (Meyer et al., 2018). In the short term, warming enhances enzyme catalytic power exponentially, while in the long term or with strong warming amplitude, enzyme activity and efficiency may decrease or exhibit none- linier increase (Razavi et al., 2015; Razavi et al., 2016; Razavi et al., 2017). Considering high temperature sensitivity of microbial activity and expressed enzymes, the effects of moderate warming, close to predicted temperature rise by 1.5 - 2℃, on soil microbial activity and SOM remain poorly investigated. Furthermore, the co-occurrence of warming and salinization increases uncertainty in predicting these effects.

SOM turnover refers processes involving the decomposition, transformation, and cycling of organic matter in the soil (Dungait et al., 2012). Soil microorganisms degrade SOM to immobilize carbon, energy, and nutrients into microbial biomass (Blagodatskaya and Kuzyakov, 2013; Schnecker et al., 2023). The relationship between SOM, microbial growth, respiration is characterized by microbial C use efficiency (CUE), calculated as the fraction of C incorporated in microbial biomass (microbial growth via biosynthetic processes) of total microbial C uptake (Geyer et al., 2019). However, there are various approaches to estimate CUE, and no common agreement exists on the

appropriate time for CUE estimation (Geyer et al., 2019). Meanwhile, there is inconsistency in the terminology of CUE, it can be described not only as carbon use efficiency, but also as carbon assimilation efficiency, microbial substrate use efficiency. Therefore, it is necessary to test the relevance of various approaches and compare the CUE results of different terminologies within the same experiment set up.

To support microbial growth, microorganisms obtain carbon by producing extracellular enzymes from SOM, releasing C as CO_2 during growth on SOM-derived substrates (Chen and Sinsabaugh, 2021; Zhang et al., 2020). Both respiration and enzyme catalysis predominantly release or uptake energy in the form of heat, quantifiable by microcalorimetry as net metabolic heat production. Consequently, enzyme activity, respiration, and heat production can serve as indicators of SOM decomposition. Additionally, the calorespirometric ratio (CR ratio), defined as the ratio of soil heat production to respiration, can be indicative for the metabolic pathways during microbial growth. The CR ratio is also related to the efficiency of converting substrate carbon into living cells and can be used for indirect estimation of the CUE (Chakrawal et al., 2020; Hansen et al., 2004). However, SOM turnover, enzyme activity, and CR ratio can be influenced by environmental factors, organic matter quality, and decomposition stage (Allison et al., 2014; Chakrawal et al., 2021; Hoang et al., 2022). Thus, it is crucial to consider both microbial function and soil property factors when evaluating the response of SOM decomposition to warming and salinization, especially in the early stages following organic matter input.

In this study, we incubated soil samples collected from Elbe estuary area to identify the impact of warming and salinization on soil microbial activity and organic matter turnover. We determined soil respiration, heat flow, and microbial biomass to measure the CUE and calorespirometric ratio (Zhang et al., 2020). The kinetics of microbial growth, and enzyme activities involved in C, N, and P cycling were determined to indicate the microbial functions (Wang et al., 2023a; Wang et al., 2023b).

Overall, we hypothesized that i) increasing salinity would decrease the soil microbial activity and growth, leading to lower enzyme activities and CUE; ii) soil ‘activated’ by the input of labile organics would exhibit a stronger response to warming and salinization compared to the non-amended soil; iii) respiration and heat release would simultaneously change during microbial growth.

2. Materials and methods

2.1 Soil sampling

Soil samples were collected from the surface horizon (0-20 cm) of a grassland site of the Elbe Estuary (Balje, Lower Saxony, Germany, 53°8′N, 9°05′E). The soil was classified as Tidalic Gleysol (IUSS Working Group WRB, 2022) with clear stratification due to storm tides. The mean annual temperature of the site is 10 °C and soils are flooded frequently at storm tides. The soil was air-dried, sieved (< 2 mm) and visible plant residues and stones were removed for further incubation experiment.

Soil basic properties were pH (1:2.5 H_2O): 7.1, electrical conductivity (EC): 0.93 ms cm^{-1}, soil organic carbon (SOC): 2.4%, total nitrogen (TN): 0.3%.

2.2 Microcosm experiment

To simulate the soil salinization by river water, we used Elbe River water solution to increase the soil salinity based on the determination of Elbe River water cations and anions (Table S1). The artificial solutions with different concentration (0‰, 3.3‰, and 5.6‰) were added as a spray on spread soil and uniformly mixed to form 3 artificial salinities: low (ambient) salinity (0.93 mS cm^{-1}, pH=7.10), middle salinity (2.06 mS cm^{-1}, pH=7.10), and high salinity (3.45 mS cm^{-1}, pH=6.97). The artificial saline soils were pre-incubated under room temperature (20 ℃) for 14 days before the formal microcosm experiment. The microcosm incubation experiment with a completely randomized design with three salinity levels and three replicates was conducted at both 20℃ and 22 ℃. Prior to incubation, soil in each microcosm was amended with a mixed solution containing 2 mg C g^{-1} glucose (2 times of soil MBC) and mineral salts (0.95 mg g^{-1} $(NH_4)_2SO_4$, 1.48 mg g^{-1} K_2HPO_4, and 1.90 mg g^{-1} $MgSO_4 \cdot 7H_2O$) to induce unlimited growth (Blagodatskaya et al., 2009), and soil moisture was adjusted to 60% WHC by adding sterilized water. The microcosms amended with mineral salts without glucose were used as the control.

2.3 Kinetics of the substrate-induced respiration

The substrate induced growth respiration (SIGR) method was used to estimate the kinetic parameters of soil microbial growth in response to substrate amendments, including active and total microbial biomass, lag time, and specific growth rate. (Blagodatsky et al., 2000). Although glucose addition was required for the SIGR method, all kinetic parameters analyzed by this method reflect the intrinsic features of dominating microbial populations before glucose addition (Blagodatskaya et al., 2010). To perform SIGR method, 30g of fresh soil was incubated in the Respicond V respirometer after adding the mixed solution and adjusting moisture content. The CO_2 production rate was monitored continuously at 20-minute intervals, and soil without glucose addition was used as basal respiration (BR). The kinetic parameters of microbial growth were estimated by fitting the Eq. (1) to the CO_2 production rate (v):

$$v = A + B \times e^{\mu t} \quad (1)$$

where A and B are the initial no-growth and initial growth respiration rate, respectively, t is the time, and μ is specific growth rate (Blagodatsky et al., 2000). The duration of lag period (T_{lag}) was calculated by Eq. (2):

$$T_{lag} = \frac{\ln(A/B)}{\mu} \quad (2)$$

the total microbial biomass (TMB) and growing microbial biomass (GMB) before glucose addition were calculated by Eq. (3) and Eq. (4):

$$\mathrm{TMB} = \frac{B}{R_0 Q} \quad (3)$$

$$\mathrm{GMB} = \mathrm{TMB} \times r_0 \quad (4)$$

where r_0 is the so-called physiological state index of the microbial biomass (MB) before glucose addition and calculated by Eq. (5). Q is the total specific respiration activity and calculated by Eq. (6):

$$r_0 = \frac{B(1-\lambda)}{A+B(1-\lambda)} \quad (5)$$

$$\mathrm{Q} = \frac{\mu}{\lambda Y CO_2} \quad (6)$$

where λ is a basic stoichiometric constant and equals to 0.9, and YCO_2 is the MB yield per unit of glucose-C, which is assumed to be a mean value of 0.6 during the experiment (Panikov and Sizova, 1996).

2.4 Calorespirometric measurements

Heat production in the course of microbial metabolism on glucose was determined using microcalorimetry. The soil was amended with the same nutrient and glucose solution as described above for the SIGR method. Then, all the samples were sealed in airtight glass ampoules and then placed in to a TAM Air. Heat production was continuously measured over 48 h at 20 and 22℃. The calorespirometric ratio was calculated by Eq. (7):

$$\gamma = \mathrm{Q} \div CO_2 \quad (7)$$

where γ is the calorespirometric ratio (kJ mol^{-1} CO_2), Q is the heat production rate (W g^{-1} soil) and CO_2 is the respiration rate (mol CO_2 h^{-1} g^{-1} soil). We derived Eq. 7 based on the oxidative production of CO_2 through catabolic or anabolic processes, resulting in a calorespirometric ratio within the range of 250-469 kJ mol^{-1} CO_2 (Hansen et al., 2004). In addition, the calorespirometric ratio reflects the changes in the microbial community (Schimel and Schaeffer, 2012) and is an indirect indicator of carbon conversion efficiency, ε estimated by the following equation (Hansen et al., 2004; Barros et al., 2010) (8):

$$\gamma = -\left(1 - \frac{\gamma_S}{4}\right) \Delta H_{O_2} - \Delta H_B \left(\frac{\varepsilon}{1-\varepsilon}\right) \quad (8)$$

where γ_S is the oxidation number of the C source, glucose = 0, ΔH_{O2} is Thornton's constant (-455 kJ mol^{-1} O_2), and ΔH_B is the difference in the heat of combustion of the biomass, -559 kJ mol^{-1} C and that of the glucose, -467 kJ mol^{-1} C (Barros et al., 2016), γ is the calorespirometric ratio calculated by Eq. 7.

2.5 Soil residual glucose measurement

The residual glucose content in soil was evaluated using Glucose Assay Kit (MAK263, Sigma-Aldrich), which oxidizes glucose to produce a fluorometric product that is proportional to the amount

of glucose present. To conduct the assay, soil was collected from each parallel microcosm in 0, 1, 3, 9, 12, 18, 24, 28, 36, and 48 hours after glucose addition. Then, 0.4 g of soil was mixed and extracted with 40 mL of sterilized water (pH = 7.0) in a centrifuge tube, which was then shaken at 180 rpm for 30 minutes. The tubes were then centrifuged at 4000 rpm for 10 minutes to obtain the supernatant, which was then diluted tenfold to ensure that the final fluorescence within the standard curve range. To determine the glucose content, 35μL diluted supernatant, 15μL glucose assay buffer and 50 μL Master Reaction Mix were added into each well of 96-well black microplate. The microplate was then incubated at 37°C and shaken vigorously for 30 minutes to enhance the reaction. Fluorescence was measured using TECAN microplate reader at γ_{ex} = 535/γ_{em} = 590 nm. In addition, a glucose standard solution was used to generate a glucose standard curve (0, 0.2, 0.4, 0.6, 0.8, and 1.0 nmol well^{-1}) for establishing the relationship between fluorescence and glucose content. Further details can be found in manufacturer's technical bulletin.

2.6 Enzyme kinetics

After 12, 24, 28, 36, and 48 hours of glucose addition, soil samples were collected from each parallel microcosm. Control microcosms (without glucose addition) were sampled at 0 and 48 hours after incubation. Soil samples from each sampling time were used to measure the kinetics of cellobiohydrolase (EC 3.2.1.91), β-glucosidase (EC 3.2.1.21), acid phosphomonoesterase (EC 3.1.3.2) and leucine-aminopeptidase (EC 3.4.11.1) activity using 4-methylumbelliferone (MUF)-β-D-cellobioside, 4-MUF-β-D-glucoside, 4-MUF-phosphate, and l-leucine-7-amido-4-methylcoumarin (AMC) fluorogenic substrates, respectively (Marx et al., 2001). The activities of the four enzymes were determined using a range of substrate concentrations (0, 5, 20, 50, 75, 100, 200, 400 μmol L^{-1}) to ensure the saturation. 0.2 g of soil was suspended in 20 mL of sterilized water to create a soil suspension after low-energy sonication (40 J s^{-1}) for 1 minute. Thereafter, 50 μL soil suspension, 100 μL substrate solution and 50 μL MES buffer were added to a 96-well black microplate (Koch et al., 2007; German et al., 2011), and the fluorescence was measured using TECAN microplate reader at excitation γ_{ex} = 355nm and emission γ_{em} = 460nm. Enzyme activities were recorded at 30, 90 min, 2 h and 3 h and expressed as nmol MUF or AMC g^{-1} soil h^{-1}. The kinetic parameters V_{max} and K_m were calculated by the Michaelis-Menten equation (9):

$$v = \frac{V_{max} \times [S]}{K_m + [S]} \quad (9)$$

where v is the reaction rate, [S] is the substrate concentration, V_{max} is the maximum reaction rate, and K_m is the substrate concentration at the half-maximum reaction rate.

2.7 Microbial biomass measurement

Microbial biomass carbon (MBC) and nitrogen (MBN) content were determined using fumigation method (Vance et al., 1987). Briefly, soil samples were collected prior and 48 hours after glucose addition. For MBC measurement, 5 g of soil was extracted with 20 mL of 0.05 mol L^{-1} K_2SO_4. Another

5 g of soil was fumigated with chloroform in a desiccator for 24 h and extracted thereafter. For MBN measurement, 10 g of soil was shaken for 30 minutes with 40 mL of 0.05 M K_2SO_4 as a pre-extraction step. The soil suspension was centrifuged at 4000 rpm for 10 minutes (Hupe et al., 2019), and the supernatant was removed before dividing the soil evenly into two parts. One part of soil (5g) was re-extracted with 20 mL of 0.05 M K_2SO_4, while the other part was mixed with 300 µL of liquid chloroform and 20 mL of 0.05 M K_2SO_4 in a plastic tube for 24 hours and then extracted. The extracts were analyzed for dissolved organic carbon (DOC) and nitrogen (DON) content by a TOC/N analyzer (TOC-L, Shimadzu, Japan). The difference between K_2SO_4-extractable C and N in fumigated and non-fumigated soils was used for MBC and MBN calculations with the underlying conversion factors of 0.45 for MBC and 0.54 for MBN.

2.8 Microbial carbon use efficiency calculation

Microbial substrate carbon use efficiency (CUE) for added carbon substrates was calculated based on the cumulative amount of respired CO_2 and glucose-C consumption during incubation period using Eq. (10) and (11) (Sinsabaugh et al., 2013). Furthermore, the CUE was also determined by considering the increment of microbial biomass C in course of substrate utilization (Eq. 12 and 13):

$$\mathrm{CUE}_1 = 1 - \frac{C_{SIR} - C_{BR}}{C_{metabolized}} \quad (10)$$

$$\mathrm{CUE}_2 = 1 - \frac{C_{SIR} - C_{BR}}{C_{added}} \quad (11)$$

$$\mathrm{CUE}_3 = \frac{MBC_{36} - MBC_0}{(MBC_{36} - MBC_0) + (C_{SIR} - C_{BR})} \quad (12)$$

$$\mathrm{CUE}_4 = \frac{MBC_{36} - MBC_0}{C_{metabolized}} \quad (13)$$

where C_{SIR} represents the cumulative amount of C respired from glucose-amended soil, and C_{BR} is the cumulative amount of C respired from unamended soil. The cumulative amount of respired carbon is determined over time and respiration rate, measured by the Respicond V respirometer. MBC_{36} and MBC_0 represent the microbial biomass C measured by fumigation method at 0 and 36 hours after glucose addition. $C_{metabolized}$ is the glucose-C consumed, measured using the Glucose Assay Kit method. C_{added} is the amount of glucose-C added (2µg C g^{-1}). As glucose was unlabeled, we were not able to correctly estimate soil priming effect. We assumed, therefore, that considering a short-term experiment, the priming effect (if any) was mainly apparent due to pool substitution mechanism (Blagodatskaya and Kuzyakov, 2008), and the metabolized C was either incorporated into MBC or respired.

2.9 Statistical analysis

All data were presented as the mean ± standard error. Prior to analysis, the normality and homogeneity of variance were determined using the Shapiro-Wilk test and Leneve's test, respectively. Two-way ANOVA was used to assess the effects of warming and salinization. For comparing the

significant differences between different salinities, one-way ANOVA combined with a Turkey HSD post-hoc test was applied, while the significant difference between 20 and 22°C was determined by T.Test. Significant differences were considered at $p < 0.05$. The Shapiro-Wilk test and Leneve's test were conducted using R Studio (version 4.1.0). The ANOVA and post-hoc test were performed using SPSS (version 20.0). The kinetics of substrate-induced respiration and enzyme activity were calculated using Origin Lab (version 2022).

3. Results

3.1 Respiration response to salinity and warming

Salinity had no impact on both respiration and heat release from soil without glucose addition. However, warming increased the heat release rate by 2-2.5 times (Figure 1c). A notable warming effect on the respiration was detected only under low salinity conditions (Figure 1a). In the soil activated by glucose, warming increased the SIR and heat release by 75-166% and 26-27%, respectively. In contrast, increasing salinity decreased the substrate-induced heat release by 9-19%, while it had no impact on the respiration rate.

Both respiration and heat release exhibited an exponential growth curve in response to glucose addition (Figure 2). Increasing salinity clearly delayed the respiration and heat release, while warming elevated the peak point of both parameters. At high salinity, the respiratory peak delayed by 6 h as compared with low salinity treatment, while for the heat release, such a delay was much shorter, i.e. 3 h. Interestingly, the peak point of heat release occurred 1-3 hours earlier than those of respiration, and the lag-time (i.e. time before growth) increased with increasing salinity. In summary, soil salinization inhibited soil respiration and intensity of heat release, while warming promoted both processes. The effect of warming was more pronounced than that of salinity.

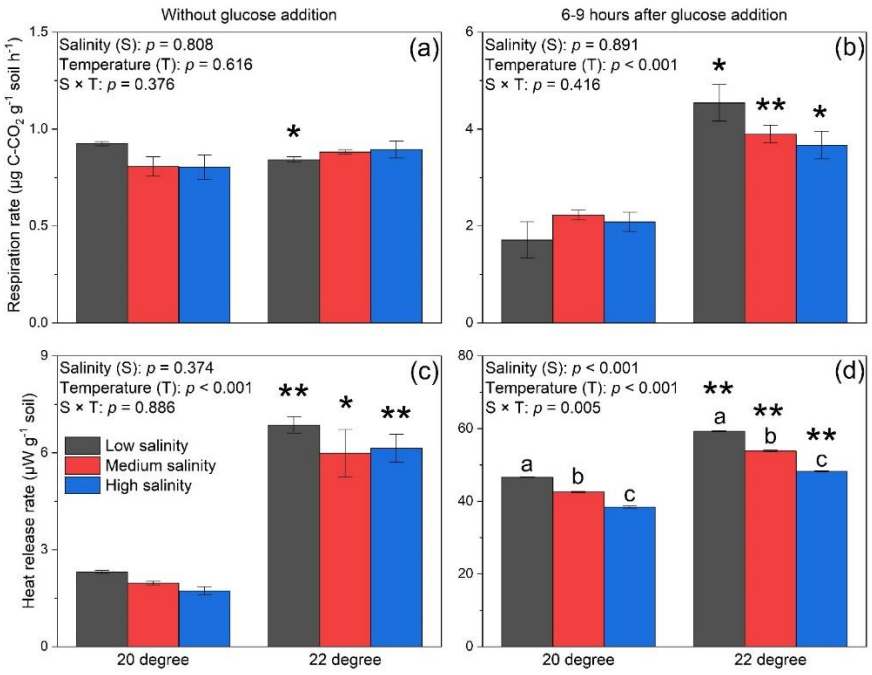

Figure 5-1. *Soil respiration rate (a and b) and heat release rate (c and d) at 20 and 22 ℃. Column and bar represent mean ± standard error (n = 3). Mean values between 6-9 hours after glucose addition were chosen for glucose induced respiration (b) or heat release rate (d). Asterisk above columns indicates significant difference within one salinity between 20 and 22 ℃ according to student's t-test at p < 0.05 "*" and p < 0.01 "**". Lower case letters indicate significant differences between three salinities after Turkey HSD post-hoc test at p < 0.05. P values were obtained after two-way ANOVA.*

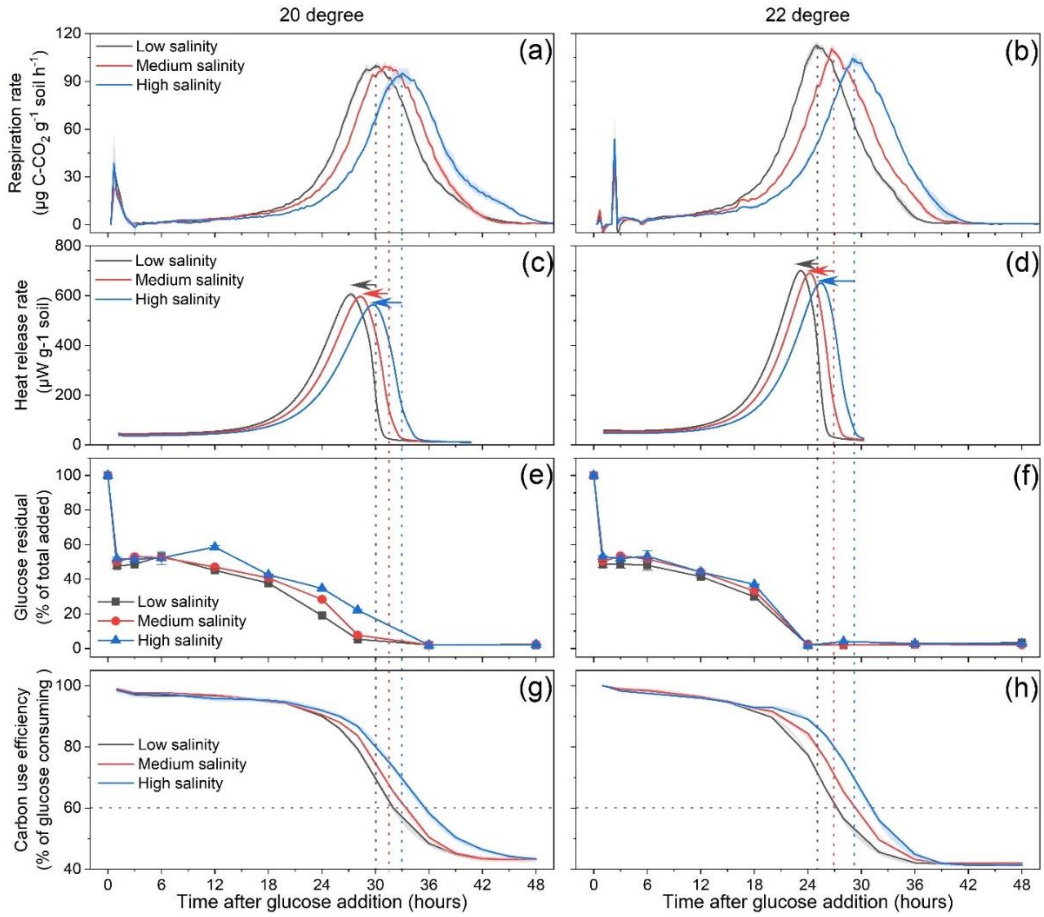

Figure 5-2. *Glucose induced soil respiration rate (a and b), heat release rate (c and d), glucose residual content (e and f) and carbon use efficiency (g and h) at 20 and 22 ℃. Line and shadow represent mean ± standard error (n =3) in figure a-d and g-h. Dot with bar represent mean ± standard error (n =3) of glucose residual in figure e and f. The grey horizontal dotted line in figure g and h represents the maximum CUE value based on thermodynamic calculation (Sinsabaugh et al., 2013).*

3.2 Carbon use efficiency and calorespirometric ratio

The residual glucose content showed a sharp initial decrease, with approximately half of the added glucose consumed within the first hour (Figure 2e and 2f). Following that, the glucose content remained stable for 12 hours until the beginning of exponential growth, and finally decreased gradually to zero (after 48 hours) (Figure 2e and 2f). It is noteworthy that the point at which glucose was depleted by 95 – 98% corresponded to the peak of the respiration rate. Furthermore, warming accelerated the consumption of glucose, while high salinity delayed glucose consumption by 6 – 8 h and by 10-17%

at 20°C but had no impact on glucose consumption at 22°C. The carbon use efficiency (CUE) remained stable at around 0.98 for the first 18 hours until the onset of exponential growth. Then, the CUE gradually decreased to ~0.42 from 18 hours until the end of the growth retardation phase. Finally, the CUE remained stable above 0.4 after the retardation phase (Figure 2g and 2h). Interestingly, increasing salinity did not change the CUE at the growth retardation phase, while warming did not have a comparable impact on CUE as well. Four methods were applied to calculate the CUE at 36 hours after glucose addition, when heat already leveled off but CO_2 did not yet (Table 1). CUE_1 and CUE_2 ranged from 0.42 to 0.59, increasing with higher salinity. CUE_2 consistently surpasses CUE_1 by 1% across all salinity and temperature levels. At 20°C, high salinity lead to the highest CUE_3 (0.48) and CUE_4 (0.39), representing a 116% and 162% increase compared to low salinity, respectively (Table 1). However, under middle and high salinity conditions, both CUE_3 and CUE_4 exhibited negative values under 22°C.

Table 5-1.*Microbial substrate carbon use efficiency at 36 hours after glucose addition with four calculation methods. (Eq. 10-13)*

	CUE_1= $1-C_{respired}/C_{metabolized}$	CUE_2= $1-C_{respired}/C_{added}$	CUE_3= $\Delta_{MBC}/(\Delta_{MBC}+C_{respired})$	CUE_4= $\Delta_{MBC}/C_{metabolized}$
20 °C				
Low salinity	0.48 ± 0.01 b	0.50 ± 0.01 c	0.22 ± 0.03 b	0.15 ± 0.03 b
Middle salinity	0.51 ± 0.00 b	0.52 ± 0.00 b	0.07 ± 0.05 c	0.04 ± 0.03 c
High salinity	0.58 ± 0.01 a	0.59 ± 0.01 a	0.48 ± 0.00 a	0.39 ± 0.01 a
22 °C				
Low salinity	0.42 ± 0.00 b	0.43 ± 0.00 b	0.04 ± 0.06 a	0.03 ± 0.04 a
Middle salinity	0.43 ± 0.00 ab	0.45 ± 0.00 b	-0.16 ± 0.15 b	-0.08 ± 0.06 b
High salinity	0.45 ± 0.01 a	0.46 ± 0.01 a	-0.17 ± 0.02 b	-0.08 ± 0.01 b

Values are mean ± standard error ($n = 3$).

Salinity had no impact on CR ratio before the addition of glucose, whereas 2°C warming increased the CR ratio by 202% (Figure 3a). Following the addition of glucose, the CR ratio was not stable and exhibited a similar dynamic pattern at both 20°C and 22°C. During 3-5 hours after glucose input, the CR ratio sharply increased and quickly dropped down thereafter. Remarkably, the CR ratio stabilized around 500 kJ mol^{-1} CO_2 during the phase of exponential growth and was by the factor of 1.81 (20 °C) and 2.24 (22 °C) larger at high versus low salinity (Figure 3b). Notably, during the growth retardation phase, the CR ratio decreased slower with increasing salinity, and this effect was better pronounced under warming. The actual CR ratio during the period from the start of exponential growth retardation to the peak of growth rate aligned with the theoretical range of 250-469 kJ mol^{-1} CO_2 at 20 °C (Figure 3c). Furthermore, at 22 °C, the alignment with the theoretical CR ratio occurred even earlier, this alignment was observed not only during exponential growth retardation leading up to the peak period but also during the exponential growth stage (12-18 hours after glucose addition) (Figure 3d).

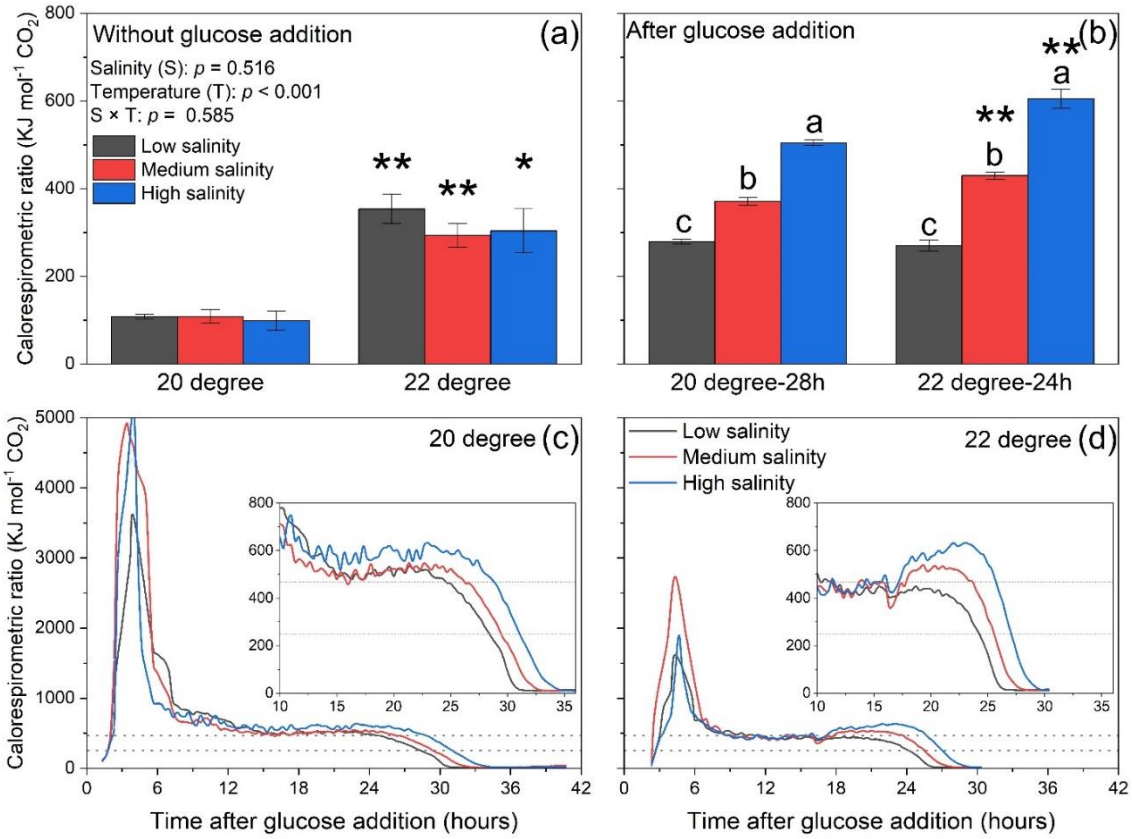

Figure 5-3. *Substrate use efficiency expressed as calorespirometric ratio obtained before glucose addition (a), 28 hours after glucose addition at 20 ℃ and 24 hours after glucose addition at 22 ℃ (b), and calorespirometric ratio dynamic after glucose addition at 20 and 22℃ (c and d). Column and bar represent mean ± standard error (n = 3). Line represents mean value (n = 3). The grey dotted lines in figure c and d represent the theoretical range of calorespirometric ratios (Hansen et al., 2004). Asterisk above columns indicates significant difference within one salinity between 20 and 22 ℃ according to student's t-test at p < 0.05 "*" and p < 0.01 "**". Lower case letters indicate significant differences between three salinities after Turkey HSD post-hoc test at p < 0.05. P values were obtained after two-way ANOVA.*

3.3 The kinetics of microbial growth response to salinity and warming

The kinetic parameters of microbial growth induced by glucose showed different responses to salinity and temperature (Figure 4). Warming decreased the specific growth rate, strongly increased a fraction of active microorganisms and shortened lag-time. Compared to low salinity, high salinity extended the lag time by 5 – 6 h at 20℃ and 22℃, respectively and reduced growing biomass. In short, soil salinization inhibited while warming promoted microbial growth.

In non-amended soil, an increase in salinity led to a decreasing trend in both microbial C and N content, although the differences between different salinity levels were not statistically significant. However, in 36 hours after glucose addition, the response of MBC, MBN, and microbial C:N ratio to salinity exhibited different patterns at 20℃ and 22℃ (Figure 5). Specifically, at 20℃, high salinity increased MBC and MBC:MBN ratio compared to low salinity, while middle salinity decreased both

parameters. Conversely, at 22℃, MBC, MBN, and MBC:MBN showed decreasing trends in response to increasing salinity. High salinity decreased MBC and MBN, respectively by 38 and 11% compared to low salinity. A warming of 2℃ reduced MBC and MBC:MBN, but increased MBN after 36 hours of glucose addition. In summary, microbial biomass exhibited a more pronounced response to salinity after glucose addition, and a warming of 2℃ resulted in inconsistent response of microbial biomass to salinity.

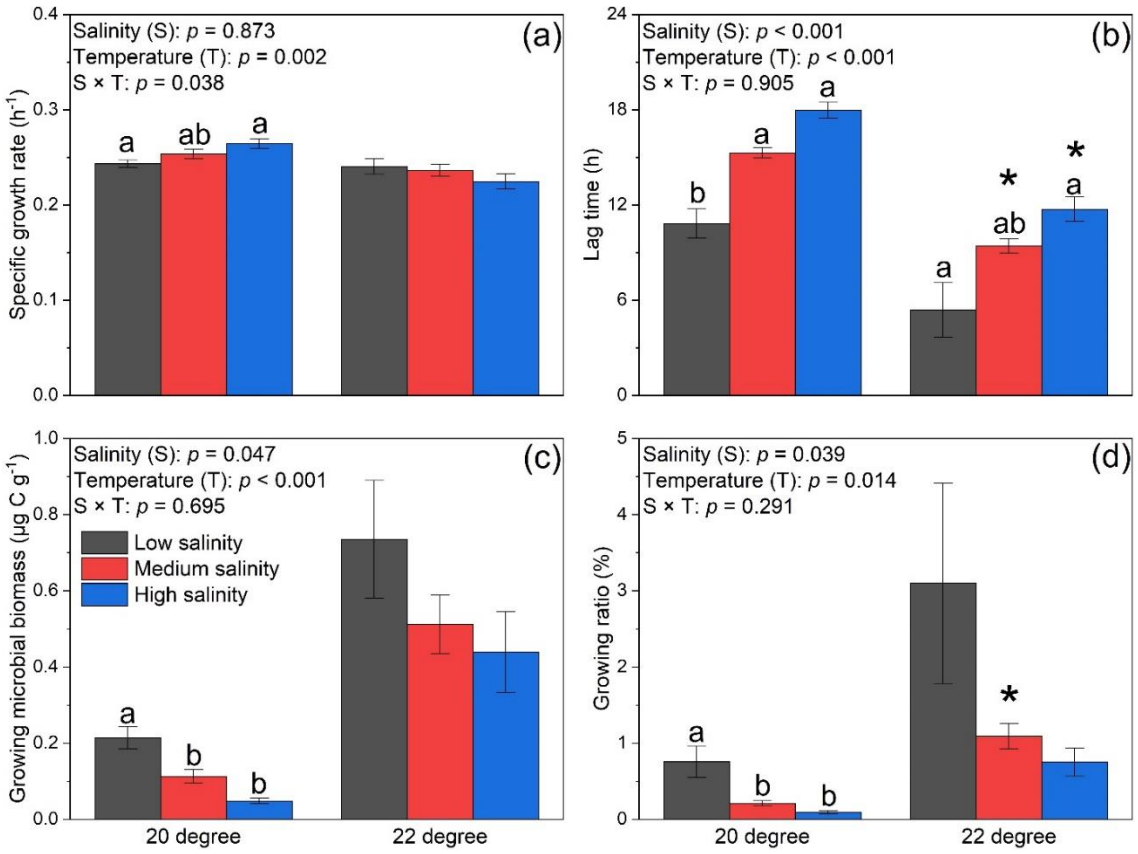

Figure 5-4. *Kinetic parameters of microbial growth in response to soil salinity under 20 and 22℃. Column and bar represent mean ± standard error (n = 3). Asterisk above columns indicates significant difference within one salinity between 20 and 22 ℃ according to student's t-test at p < 0.05 "*". Different letters show significant differences between three salinities according to one-way ANOVA and Turkey HSD post-hoc test (p < 0.05). P values were obtained after two-way ANOVA.*

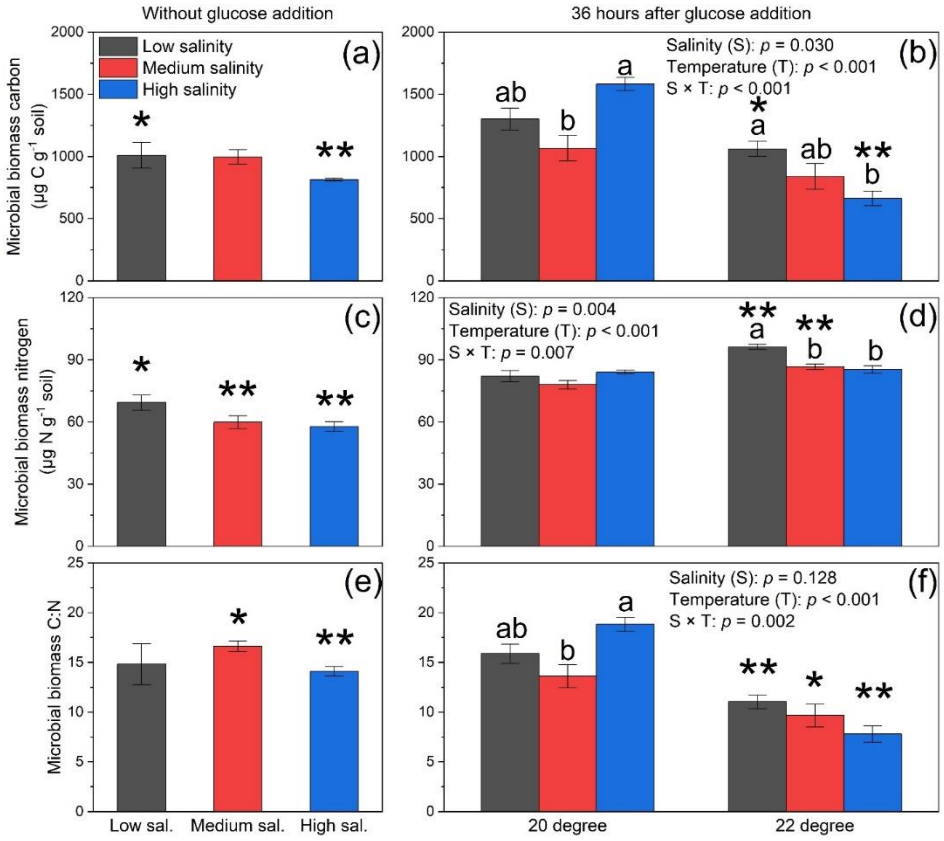

Figure 5-5. *Microbial biomass carbon (MBC), nitrogen (MBN) and their ratio before glucose addition under 20 ℃ (a, c and e) and 36 hours after glucose addition at 20 or 22 ℃ (b, d and f). Column and bar represent mean ± standard error (n = 3).*

Asterisk above columns in figure a, c, e indicates significant difference within the same salinity between without glucose and 36 hours after glucose addition at 20 ℃, asterisk above right columns in figure b, d, f indicates significant difference within one salinity between 20 and 22 ℃, both of them were determined by student's t-test at $p < 0.05$ "" and $p < 0.01$ "**". Different letters show significant differences between three salinities according to one-way ANOVA and Turkey HSD post-hoc test ($p < 0.05$). P values were obtained after two-way ANOVA.*

3.4 Enzyme activities response to salinity and warming

All enzyme activities displayed an increasing trend from 0 to 12 hours after the addition of glucose, and then stabilized or slightly decreased until 48 hours after glucose addition (Figure 6). Compared with the enzyme activities before glucose addition, the addition of glucose at 12 hours increased the activity of cellobiohydrolase by 3.1 to 9.6 times and β-glucosidase by 2.3 to 3.4 times, with less pronounced changes observed in leucine aminopeptidase and acid phosphomonesterase. The increase in cellobiohydrolase and β-glucosidase activity under high salinity was much higher than that under low salinity (Figure S2). After 48 h of glucose addition, high salinity decreased the activities of cellobiohydrolase, β-glucosidase, and acid phosphomonesterase by 7-40% compared to low salinity at 20℃. At 22℃, high salinity decreased the activity of leucine aminopeptidase by 15% (Figure S4).

Overall, the enzyme activity changed in accordance with the dynamics of glucose decomposition, and the specific pattern of change depended on the enzyme category. Furthermore, the inhibitory effect on enzyme activity caused by increasing salinity was more pronounced after 48 hours of glucose addition compared to corresponding incubation of non-amended soil.

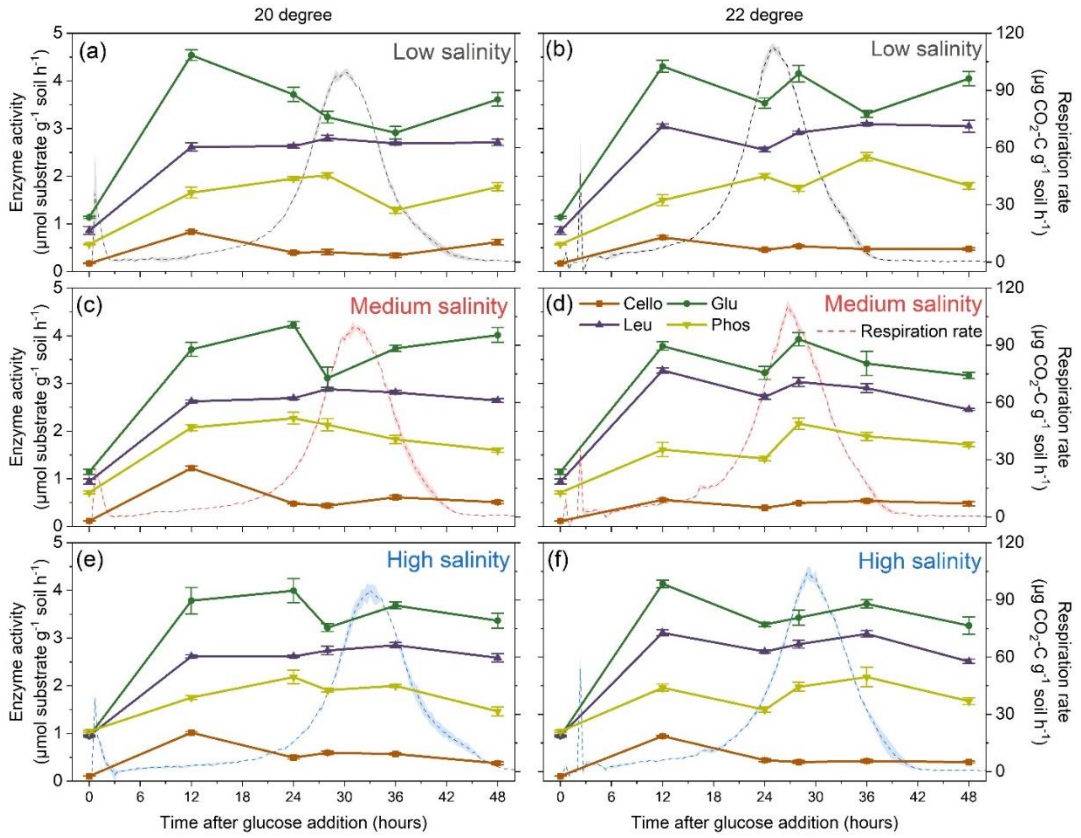

Figure 5-6. *Glucose induced soil respiration rate and soil enzyme activity (V_{max}) of cellobiohydrolase (Cello), β-D-glucosidase (Glu), leucine aminopeptidase (Leu) and acid phosphomonesterase (Phos) at 20 and 22 ℃, and low (a and b), medium (c and d) and high salinity (e and f). Line and shadow represent mean ± standard error of respiration (n = 3), dot with bar represent mean ± standard error of enzyme activity (n = 3).*

4. Discussion

4.1 Soil microbial activity and growth response to increasing salinity

The influence of salinity on soil respiration and heat release strongly depended on the availability of organic substrate and microbial activity state. Increasing salinity had no impact on either respiration or heat release in non-amended soil, suggesting a certain degree of resilience of the microbial community to salinity-induced stress. The absence of labile organic matter, such as glucose, might have limited the activity and sensitivity of microbial processes to changes in salinity levels (Blagodatskaya et al., 2007).

All phases of microbial growth on glucose (lag-time, exponential growth, time of the peak, and growth retardation) monitored by respiration and heat release were significantly delayed by increasing salinity (Figure 4b) and can be attributed to osmotic stress imposed on microbial cells and substrate availability (Rath and Rousk, 2015), although the increasing salinity only decreased the soil pH by 1.8%. Elevated salinity levels disrupt the osmotic balance within cells, affecting their physiological functions (Chen and Jiang, 2010). This osmotic stress can lead to a decrease in microbial metabolic activity, including glucose decomposition (Zhu and Gong, 2014). Furthermore, high salinity can also directly inhibit microbial activity through adverse effects on enzymes and cellular processes (Liu et al., 2017). The impairment of enzyme function can hinder the efficient glucose decomposition and subsequently lower the maximum velocity. Altered salinity levels may lead to shifts in the microbial community composition, dominating more salt-tolerant bacterial species and archaea, which may have distinct metabolic rates compared to the original community (Brown et al., 2022). Moreover, we sampled soil from an area potentially subjected to salinization, where the ambient soil salinity is higher than that in other nearby sites. This suggested the presence of salt-tolerant or halophilic species, even though the ambient salinity level (0.93 mS cm^{-1}) may not be classified as saline enough. The above findings confirm our first hypothesis that increasing salinity could delay microbial growth by imposing osmotic stress on microbial cells.

4.2 Interactive effect of salinity and warming on soil microbial activity

Non-amended soil. A 2°C increase in temperature increased the heat release and activity of cellobiohydrolase by 209% and 39%, respectively, but did not directly affect the soil respiration in non-amended soil. This suggested that warming primarily influenced the activity of enzymes involved in extra-cellular cleavage of long-chain polymeric molecules, such as cellulose to oligomers like cellobiose, resulting in higher heat production. However, an increase in enzymatic cellobiose production by 101-178 nmol g^{-1} h^{-1} was insufficient to affect an activity of β-glucosidase involved in the next step of cellulose decomposition, i.e., cleavage of cellobiose to glucose monomers (Figure 3a). This was because a potential of β-glucosidase (V_{max} ~2600 nmol g^{-1} h^{-1}) was about two orders of magnitude greater as compared with an increased cellobiose production with warming. Thus, the extracellular destruction of high molecular weight organic polymers is a bottle-neck process determining the decomposition rates of soil organic matter. The lack of a noticeable change in respiration rate indicated that the microorganisms rather stored than actively metabolized the labile organics (glucose) produced from the enzymatically cleaved high molecular weight organic polymers (Gershenson et al., 2009).

Glucose-amended soil. A 2°C increase in temperature significantly increased both the SIR and heat release. The elevated temperature increases molecular motion and reaction rates, thus enhancing the breakdown or utilization of glucose by microorganisms, resulting in increased rates of respiration and heat production (Shi et al., 2023). Microbial growth on glucose detected by respiration and heat

release was significantly accelerated by warming (Figure 4b), this might be attributed to temperature-dependent microbial metabolism, enhanced enzyme activity, increased energy and nutrient availability from added glucose, and potential improvements in metabolic efficiency (Gershenson et al., 2009). The Q_{10} of basal and substrate-induced respiration in our study was 1.17 and 32.9, respectively, suggesting higher sensitivity of microbial communities to environmental changes and intensified the interactive impact of salinity and temperature on microbial activity when provided with an organic carbon source. Remarkably, the impact of moderate warming (+2 ℃) on microbial growth and activity was much stronger than the effect of 2-3.5 times increasing salinity. The limited response to the substantial increase in salinity might indicate a threshold beyond which microbial activity is negatively impacted. Moreover, the microbial community might be more adaptable to fluctuations in temperature than to abrupt changes in salinity, resulting in a more immediate and substantial response. Our second hypothesis was confirmed as the effect of salinity on microbial growth was further promoted with glucose addition, indicating that the microbial activation by labile substrate alters the response of soil microorganisms to salinity stress.

4.3 Interactive effect of salinity and warming on soil microbial biomass

The MBC content remained unaffected by salinity in non-amended soil. At 36 hours after glucose addition, the MBC amount under 20 ℃ exceeded that of non-amended soil by 7.2-94.2% (Figure 5), indicating a net microbial growth and biomass accumulation. Low salinity resulted in a faster consumption of glucose and earlier switch to growth retardation stages versus high salinity levels. Thus, the ratio of Δ_{MBC} to $C_{metabolized}$ (CUE_4) in high salinity was higher than that in middle or low salinity (Table 1). Delayed microbial growth under high salinity can be explained by osmotic stress and salt toxicity on microorganisms induced by elevated salinity as the core microbiome were not adapted to the sudden increment of salinity (Haj-Amor et al., 2022). Consequently, at the same time after glucose addition (36 h), the soil with low salinity experienced a later retardation stage compared to high salinity. As compared with non-amended soil, an essential increase in microbial biomass in 36 h of growth on glucose was observed only at 20 ℃ for high- and in the lesser extent for low salinity treatments. The lower Δ_{MBC} at the later retardation stage (lower salinity) compared to the earlier retardation stage (high salinity) may imply microbial mortality during the retardation stage, with larger death or switch to dormancy occurring at the later stage. Furthermore, MBC at middle and high salinity under 22 ℃ were lower than those in non-amended soil, suggesting microbial death and resulting in negative values of CUE_3 and CUE_4. A potential explanation, rooted in the methodology, could be attributed to differences in the conversion factor of the chloroform fumigation technique. This factor can vary significantly under steady-state and growth conditions (Bailey et al., 2002). The latter explanation seems more plausible since a substantial decrease in biomass was not confirmed in several studies by DNA content, which continued to increase and remains stable for at least one day after growth retardation detected by CO_2 (Nannipieri et al., 1978; Blagodatskaya et al., 2014). Alternatively,

a decline in microbial biomass during the late retardation stage could indicate either protozoan grazing (Clarholm, 1985; Bonkowski et al., 2000) or viral attacks (Mason-Jones et al., 2022) in the face of intense microbial competition.

4.4 Soil enzyme kinetics response to increasing salinity and warming

The up to 2.9 times rise in enzyme activities observed after 48 hours of basal respiration in non-amended soil, as compared to the initial soil state (Figure S4), can be attributed to the nitrogen and phosphorus in the nutrient solution addition prior to soil incubation, resulting in a higher increase in of C-acquiring enzyme activities compared to N- and P-acquiring enzyme activities. Furthermore, the activities of β-glucosidase, leucine aminopeptidase, and acid phosphomonesterase were not significantly affected by salinity alone after 48 hours of basal respiration in non-amended soil, suggesting that salinity does not alter the metabolic processes associated with these enzymes.

Upon the addition of glucose, all measured enzyme activities increased by 68-336% within the first 12 hours (Figure 6), indicating a preparation for microbial growth (Mason-Jones et al., 2022). Notably, the activities of C-acquiring (β-glucosidase, cellobiohydrolase) enzymes increased more strongly than that of N- (leucine aminopeptidase) and P- (acid phosphomonesterase) acquiring enzymes, despite the input of external labile carbon (glucose). This increased cellulolytic activity aligned with an unreasonably high CUE during the growth preparation stage (Figure 2g and 2h), implying that a substantial amount of carbon substrate was i) invested to extracellular destruction of cellulose-like molecules, which was not related to CO_2 production and ii) reserved for microbial growth at a later stage (Brant et al., 2006). Subsequently, all measured enzyme activities stabilized or slightly decreased until the end of the experiment, suggesting that substrate demand remains stable during the microbial growth and retardation stage. The dynamics of enzyme activity during microbial growth and retardation did not change with warming and increased salinity, indicating relatively robust resistance of the microbial community to moderate environmental changes (Wang et al., 2023b). The above findings partly contradict our first hypothesis that the enzyme activity remains stable in response to increasing salinity.

4.5 Carbon use efficiency and calorespirometric ratio

The glucose content sharply decreased within the first hour after glucose addition and then remained stable until the onset of microbial exponential growth. This contradicts the previous finding that more than 90% of the added glucose was consumed within the first 15 minutes under 20 °C (Rousk and Jones, 2010). This discrepancy could be explained by greater amount of glucose added per biomass unit in our study. During the period of sharp glucose decrease, the respiration rate was very low. This observation implies a very high microbial CUE_4, indicating a microbial switch to growth preparation stage when a substantial portion of substrate and energy is directed towards the synthesis of storage compounds or specific enzymes not related to CO_2 production (Mason-Jones et al., 2022). Therefore, the short-term estimation based on partial substrate uptake shows overestimated values (above 60%)

and corresponds to apparent rather than real CUE. The CUE gradually decreased during microbial exponential growth until the end of the experiment, indicating that soil microorganisms allocated more substrate and energy toward respiration rather than the synthesis of storage compounds (Dijkstra et al., 2015). Notably, increasing salinity postponed the decrease in CUE during the exponential growth and retardation phase. This delay can be attributed to the slowdown of both glucose consumption and microbial growth caused by the high salinity. Nonetheless, the CUE estimated during exponential growth before substrate exhaustion (Figure 2g and 2h) essentially exceeded the maximal CUE values of glucose in pure microbial cultures (Sinsabaugh et al., 2013). The CUE estimated at the peak of CO_2 release varied between 65–70%, indicating a slight overestimation while relatively aligning with the CUE estimated for pure cultures. As added glucose was unlabeled, the possible contribution of priming, i.e., SOM-C co-decomposed with glucose-C was not considered. However, any positive priming effect would decrease the CUE below theoretical values, which was not a case in our study. Only after glucose uptake up to 95-98%, the CUE values stabilized below the 60% threshold, corresponding to the actual CUE. Thus, the appropriate time to assess CUE was when the values have stabilized, i.e., after 36-42 h (at 22 ℃). Furthermore, at the end of the retardation stage, the CUE remained stable at around 0.42 under limited substrate availability, which is slightly higher than the theoretical value (~0.30) observed in multi-resource-limited natural systems (Sinsabaugh et al., 2013). Collectively, CUE was overestimated during the growth preparation and exponential growth stages, aligning with the apparent CUE. While, CUE decreased and stabilized at the end of retardation stage, indicating a relatively realistic value for natural soils (Sinsabaugh et al., 2013).

The CUE calculation based on glucose consumption or total glucose input did not differ significantly (Figure S1). This remained true even when the amounts of glucose consumed and added were significantly different before the peak point of the respiration rate. This pattern might be due to much smaller amount of respired carbon than both the amount of carbon added and consumed.

At the beginning of glucose addition, the calorespirometric ratio (CR) sharply increased (Figure 3), indicating the allocation of substrate and energy to other processes in addition to respiration (Hansen et al., 2004; Yang et al., 2024). Within the initial 6 hours after glucose addition, the CR ratio was strongly higher than the oxycaloric equivalent (469 kJ mol^{-1} CO_2) for aqueous glucose combustion, suggesting either additional heat release from accompanying processes or a lower respiration rate compared to the complete oxidation of glucose. This additional heat could result from priming due to the metabolism of highly reduced substrates other than carbohydrates or the incomplete oxidation of the substrate to CO_2 (Chakrawal et al., 2020). Furthermore, this excess heat may also be allocated to the synthesis of storage compounds or the enhancement of enzyme activity. During the exponential growth phase, the CR ratio remained stable and generally corresponded to 469 kJ mol^{-1} CO_2 (Geyer et al., 2019). Remarkably, increasing salinity subsequently increased the CR ratio by 81-126% during the exponential growth and retardation phase (Figure 3b). The osmotic stress caused by increased salinity might have exerted additional pressure on the microbial community increasing their

maintenance requirements, i.e., requiring the microbes to expend more energy to maintain cellular functions and osmotic balance, resulting in a higher CR ratio (Rath and Rousk, 2015). After reaching the peak CO_2 and entering the retardation stage, the CR ratio gradually decreases to below 250 kJ mol^{-1} CO_2, indicating a greater reduction in heat release compared to the complete oxidation of glucose (Figure 2c and 2d). Thus, during the retardation stage, the added glucose was not completely oxidized to CO_2 under the conditions of fermentation or combined fermentation and aerobic decomposition (Chakrawal et al., 2021).

5. Conclusion

Overall, the salinity had a negative impact on soil respiration and microbial growth, especially in soils subjected to warming or organic matter input, and the negative effect was promoted with the input of labile substrate. Contrary to our expectations, however, the increasing salinity had no effect on enzyme activities. As expected, the effects of both salinity and, to a greater extent, warming were amplified in the glucose-activated soil. The respiration and heat release curves generally exhibited a coupled pattern, although the heat release peak occurred approximately 3 h earlier, partially rejecting our third hypothesis 3. The calorespirometric ratio fell within theoretical range during the exponential growth phase. In contrast, a proper assessment of the carbon use efficiency was provided by C-budgeting at the end of growth retardation phase. Our results emphasize the importance of considering both biotic and abiotic factors, such as microbial growth phase, substrate availability and temperature, when assessing the impacts of environmental changes on microbial processes in saline soils. These findings offer valuable insights into predicting carbon cycling processes and enhancing carbon sequestration in terrestrial ecosystems

Declaration of competing interest

The authors declare that they have no known competing financial interests or personal relationships that could have appeared to influence the work reported in this paper.

Acknowledgement

We thank Hamed Kashi for providing us with the soil for this incubation experiment and Jan Jagode and Georg Guggenberger for measuring the salt concentration and ionic composition of the Elbe River water at Balje. Thanks to the technicians of the UFZ Halle, Jacqueline Rose and Gabriele Henning for their help with the laboratory assessment. Furthermore, we acknowledge the cooperation of the Federal Institute for Hydrology (BfG) within the project UferFunk. This project was carried out in the framework of the priority program 2322 “SoilSystems, Systems ecology of soils – energy discharge modulated by microbiome and boundary conditions” funded by the Deutsche Forschungsgemeinschaft (DFG, German Research Foundation) – Project number 465122443, SP 943/8-1 and RA 3062/4-1.

References

Allison, S.D., Chacon, S.S., German, D.P., 2014. Substrate concentration constraints on microbial

decomposition. Soil Biology and Biochemistry, 79, 43-49.
Bailey, V.L., Peacock, A.D., Smith, J.L., Bolton Jr, H., 2002. Relationships between soil microbial biomass determined by chloroform fumigation–extraction, substrate-induced respiration, and phospholipid fatty acid analysis. Soil Biology and Biochemistry, 34(9), 1385-1389.
Barros, N., Hansen, L.D., Piñeiro, V., Perez-Cruzado, C., Villanueva, M., Proupín, J., Rodríguez-Añón, J.A., 2016. Factors influencing the calorespirometric ratios of soil microbial metabolism. Soil Biology and Biochemistry, 92, 221-229.
Barros, N., Salgado, J., Rodríguez-Añón, J., Proupín, J., Villanueva, M., Hansen, L., 2010. Calorimetric approach to metabolic carbon conversion efficiency in soils: comparison of experimental and theoretical models. Journal of Thermal Analysis and Calorimetry, 99(3), 771-777.
Blagodatsky, S.A., Heinemeyer, O., Richter, J., 2000. Estimating the active and total soil microbial biomass by kinetic respiration analysis. Biology and Fertility of Soils, 32, 73-81.
Blagodatskaya, E., Blagodatsky, S., Anderson, T.H., Kuzyakov, Y., 2014. Microbial growth and carbon use efficiency in the rhizosphere and root-free soil. PloS One, 9(4), e93282.
Blagodatskaya, E., Blagodatsky, S., Dorodnikov, M., & Kuzyakov, Y., 2010. Elevated atmospheric CO_2 increases microbial growth rates in soil: results of three CO_2 enrichment experiments. Global Change Biology, 16(2), 836-848.
Blagodatskaya, E., Kuzyakov, Y., 2013. Active microorganisms in soil: critical review of estimation criteria and approaches. Soil Biology and Biochemistry, 67, 192-211.
Blagodatskaya, E.V., Blagodatsky, S.A., Anderson, T.H., Kuzyakov, Y., 2007. Priming effects in Chernozem induced by glucose and N in relation to microbial growth strategies. Applied Soil Ecology, 37(1-2), 95-105.
Blagodatskaya, E.V., Blagodatsky, S. A., Anderson, T. H., Kuzyakov, Y, 2009. Contrasting effects of glucose, living roots and maize straw on microbial growth kinetics and substrate availability in soil. European Journal of Soil Science, 60(2), 186-197.
Bonkowski, M., Griffiths, B., Scrimgeour, C., 2000. Substrate heterogeneity and microfauna in soil organic 'hotspots' as determinants of nitrogen capture and growth of ryegrass. Applied Soil Ecology, 14(1), 37-53.
Brant, J.B., Sulzman, E.W., Myrold, D.D., 2006. Microbial community utilization of added carbon substrates in response to long-term carbon input manipulation. Soil Biology and Biochemistry, 38(8), 2219-2232.
Brown, R.W., Rhymes, J.M., Jones, D.L., 2022. Saltwater intrusion induces shifts in soil microbial diversity and carbon use efficiency in a coastal grassland ecosystem. Soil Biology and Biochemistry, 170, 108700.
Chakrawal, A., Herrmann, A.M., Manzoni, S., 2021. Leveraging energy flows to quantify microbial traits in soils. Soil Biology and Biochemistry, 155, 108169.
Chakrawal, A., Herrmann, A.M., Šantrůčková, H., Manzoni, S., 2020. Quantifying microbial metabolism in soils using calorespirometry—a bioenergetics perspective. Soil Biology and Biochemistry, 148, 107945.
Chen, H., Jiang, J.G., 2010. Osmotic adjustment and plant adaptation to environmental changes related to drought and salinity. Environmental Reviews, 18, 309-319.
Chen, J., Sinsabaugh, R.L., 2021. Linking microbial functional gene abundance and soil extracellular enzyme activity: Implications for soil carbon dynamics. Global Change Biology, 27(7), 1322-1325.
Chen, R., Senbayram, M., Blagodatsky, S., Myachina, O., Dittert, K., Lin, X., Blagodatskaya, E., Kuzyakov, Y., 2014. Soil C and N availability determine the priming effect: microbial N mining and stoichiometric decomposition theories. Global Change Biology, 20(7), 2356-2367.
Clarholm, M., 1985. Interactions of bacteria, protozoa and plants leading to mineralization of soil nitrogen. Soil Biology and Biochemistry, 17(2), 181-187.

Dijkstra, P., Salpas, E., Fairbanks, D., Miller, E.B., Hagerty, S.B., van Groenigen, K.J., Hungate, B.A., Marks, J.C., Koch, G.W., Schwartz, E., 2015. High carbon use efficiency in soil microbial communities is related to balanced growth, not storage compound synthesis. Soil Biology and Biochemistry, 89, 35-43.

Dungait, J.A., Hopkins, D.W., Gregory, A.S., Whitmore, A.P., 2012. Soil organic matter turnover is governed by accessibility not recalcitrance. Global Change Biology, 18(6), 1781-1796.

FAO, 2021. Global map of salt-affected soils. https://www.fao.org/soils-portal/data-hub/soil-maps-and-databases/global-map-of-salt-affected-soils

German, D.P., Weintraub, M.N., Grandy, A.S., Lauber, C.L., Rinkes, Z.L., Allison, S.D., 2011. Optimization of hydrolytic and oxidative enzyme methods for ecosystem studies. Soil Biology and Biochemistry, 43(7), 1387-1397.

Gershenson, A., Bader, N.E., Cheng, W., 2009. Effects of substrate availability on the temperature sensitivity of soil organic matter decomposition. Global Change Biology, 15(1), 176-183.

Geyer, K.M., Dijkstra, P., Sinsabaugh, R., Frey, S.D., 2019. Clarifying the interpretation of carbon use efficiency in soil through methods comparison. Soil Biology and Biochemistry, 128, 79-88.

Haj-Amor, Z., Araya, T., Kim, D.G., Bouri, S., Lee, J., Ghiloufi, W., Yang, Y., Kang, H., Jhariya, M.K., Banerjee, A., Lal, R., 2022. Soil salinity and its associated effects on soil microorganisms, greenhouse gas emissions, crop yield, biodiversity and desertification: A review. Science of the Total Environment, 843, 156946.

Hansen, L.D., Macfarlane, C., McKinnon, N., Smith, B.N., Criddle, R.S., 2004. Use of calorespirometric ratios, heat per CO_2 and heat per O_2, to quantify metabolic paths and energetics of growing cells. Thermochimica Acta, 422(1-2), 55-61.

Hoang, D.T.T., Rashtbari, M., Anh, L.T., Wang, S., Tu, D.T., Hiep, N.V., Razavi, B.S., 2022. Mutualistic interaction between arbuscular mycorrhiza fungi and soybean roots enhances drought resistant through regulating glucose exudation and rhizosphere expansion. Soil Biology and Biochemistry, 171, 108728.

Hupe, A., Schulz, H., Bruns, C., Haase, T., Heß, J., Dyckmans, J., Joergensen, R.G., Wichern, F., 2019. Get on your boots: estimating root biomass and rhizodeposition of peas under field conditions reveals the necessity of field experiments. Plant and Soil, 443, 449-462.

IPCC, 2018. Global Warming of 1.5°C: An IPCC Special Report on the impacts of global warming of 1.5°c above pre-industrial levels and related global greenhouse gas emission pathways, in the context of strengthening the global response to the threat of climate change, sustainable development, and efforts to eradicate poverty.

Koch, O., Tscherko, D., Kandeler, E., 2007. Temperature sensitivity of microbial respiration, nitrogen mineralization, and potential soil enzyme activities in organic alpine soils. Global Biogeochemical Cycles, 21, GB4017.

Liu, G., Zhang, X., Wang, X., Shao, H., Yang, J., Wang, X., 2017. Soil enzymes as indicators of saline soil fertility under various soil amendments. Agriculture, Ecosystems & Environment. 237, 274-279.

Marx, M.C., Wood, M., Jarvis, S.C., 2001. A microplate fluorimetric assay for the study of enzyme diversity in soils. Soil Biology and Biochemistry, 33(12-13), 1633-1640.

Mason-Jones, K., Robinson, S.L., Veen, G.F., Manzoni, S., van der Putten, W.H., 2022. Microbial storage and its implications for soil ecology. The ISME Journal, 16(3), 617-629.

Nannipieri, P., Johnson, R.L., Paul, E.A., 1978. Criteria for measurement of microbial growth and activity in soil. Soil Biology and Biochemistry, 10(3), 223-229.

Pan, C., Liu, C., Zhao, H., Wang, Y., 2013. Changes of soil physico-chemical properties and enzyme activities in relation to grassland salinization. European Journal of Soil Biology, 55, 13-19.

Panikov, N.S., Sizova, M.V., 1996. A kinetic method for estimating the biomass of microbial functional groups in soil. Journal of Microbiological Methods, 24(3), 219-230.

Rath, K.M., Rousk, J., 2015. Salt effects on the soil microbial decomposer community and their role

in organic carbon cycling: a review. Soil Biology and Biochemistry, 81, 108-123.
Razavi, B.S., Blagodatskaya, E., Kuzyakov, Y., 2015. Nonlinear temperature sensitivity of enzyme kinetics explains canceling effect—a case study on loamy haplic Luvisol. Frontiers in Microbiology, 6, 163992.
Razavi, B.S., Blagodatskaya, E., Kuzyakov, Y., 2016. Temperature selects for static soil enzyme systems to maintain high catalytic efficiency. Soil Biology and Biochemistry, 97, 15-22.
Razavi, B.S., Liu, S., Kuzyakov, Y., 2017. Hot experience for cold-adapted microorganisms: Temperature sensitivity of soil enzymes. Soil Biology and Biochemistry, 105, 236-243.
Rousk, J., Jones, D.L., 2010. Loss of low molecular weight dissolved organic carbon (DOC) and nitrogen (DON) in H_2O and 0.5 M K_2SO_4 soil extracts. Soil Biology and Biochemistry, 42(12), 2331-2335.
Schimel, J.P., Schaeffer, S.M., 2012. Microbial control over carbon cycling in soil. Frontiers in Microbiology, 3, 348.
Schnecker, J., Baldaszti, L., Gündler, P., Pleitner, M., Sandén, T., Simon, E., Spiegel, F., Spiegel, H., Malo, C.U., Zechmeister-Boltenstern, S., Richter, A., 2023. Seasonal dynamics of soil microbial growth, respiration, biomass, and carbon use efficiency in temperate soils. Geoderma, 440, 116693.
Shahariar, S., Helgason, B., Soolanayakanahally, R., Bedard-Haughn, A., 2021. Soil enzyme activity as affected by land-use, salinity, and groundwater fluctuations in wetland soils of the prairie pothole region. Wetlands, 41, 1-16.
Shi, C., Urbina-Malo, C., Tian, Y., Heinzle, J., Kengdo, S. K., Inselsbacher, E., Borken, W., Schindlbacher, A., Wanek, W., 2023. Does long-term soil warming affect microbial element limitation? A test by short-term assays of microbial growth responses to labile C, N and P additions. Global Change Biology, 29(8), 2188-2202.
Singh, B.K., Bardgett, R.D., Smith, P., Reay, D.S., 2010. Microorganisms and climate change: terrestrial feedbacks and mitigation options. Nature Reviews Microbiology, 8(11), 779-790.
Singh, K., 2016. Microbial and enzyme activities of saline and sodic soils. Land Degradation & Development, 27(3), 706-718.
Sinsabaugh, R.L., Manzoni, S., Moorhead, D.L., Richter, A., 2013. Carbon use efficiency of microbial communities: stoichiometry, methodology and modelling. Ecology letters, 16(7), 930-939.
Song, J., Zhang, H., Chang, F., Yu, R., Wang, J., Wang, X., Li, Y., 2022. If the combination of straw interlayer and irrigation water reduction maintained sunflower yield by boosting soil fertility and improving bacterial community in arid and saline areas. Agricultural Water Management, 262, 107424.
Sritongon, N., Sarin, P., Theerakulpisut, P., Riddech, N., 2022. The effect of salinity on soil chemical characteristics, enzyme activity and bacterial community composition in rice rhizospheres in Northeastern Thailand. Scientific Reports, 12(1), 20360.
Vance, E.D., Brookes, P. C., Jenkinson, D.S., 1987. Microbial biomass measurements in forest soils: the use of the chloroform fumigation-incubation method in strongly acid soils. Soil Biology and Biochemistry, 19(6), 697-702.
Wang, J., Church, J. A., Zhang, X., Chen, X., 2021. Reconciling global mean and regional sea level change in projections and observations. Nature Communications, 12(1), 990.
Wang, S., Hoang, D.T.T., Luu, A.T., Mostafa, T., Razavi, B.S., 2023b. Environmental memory of microbes regulates the response of soil enzyme kinetics to extreme water events: Drought-rewetting-flooding. Geoderma, 437, 116593.
Wang, S., Zhang, X., Zhou, J., Xu, Z., Ma, Q., Chu, J., Zang, H., Yang, Y., Peixoto, L., Razavi, B. S., 2023a. Transition of spatio-temporal distribution of soil enzyme activity after straw incorporation: From rhizosphere to detritusphere. Applied Soil Ecology, 186, 104814.
Wong, V.N., Greene, R.S.B., Dalal, R.C., Murphy, B.W., 2010. Soil carbon dynamics in saline and

sodic soils: a review. Soil Use and Management, 26(1), 2-11.
Yang, S., Di Lodovico, E., Rupp, A., Harms, H., Fricke, C., Miltner, A., Kästner, M., Maskow, T., 2024. Enhancing insights: exploring the information content of calorespirometric ratio in dynamic soil microbial growth processes through calorimetry. Frontiers in Microbiology, 15, 1321059.
Zhang, W., Wang, C., Xue, R., Wang, L., 2019. Effects of salinity on the soil microbial community and soil fertility. Journal of Integrative Agriculture, 18(6), 1360-1368.
Zhang, X., Kuzyakov, Y., Zang, H., Dippold, M.A., Shi, L., Spielvogel, S., Razavi, B.S., 2020. Rhizosphere hotspots: root hairs and warming control microbial efficiency, carbon utilization and energy production. Soil Biology and Biochemistry, 148, 107872.
Zhu, Y., Gong, H., 2014. Beneficial effects of silicon on salt and drought tolerance in plants. Agronomy for Sustainable Development, 34, 455-472.

Supplementary data

Table S5-1*. Salt category and concentration of artificial Elbe River water solution*

Salt category	Concentration (g L^{-1})
$NaHCO_3$	0.0193
$CaCl_2$	0.4484
Na_2SO_4	1.0504
NaCl	5.2974
KCl	0.1591
$MgCl_2$	1.1017

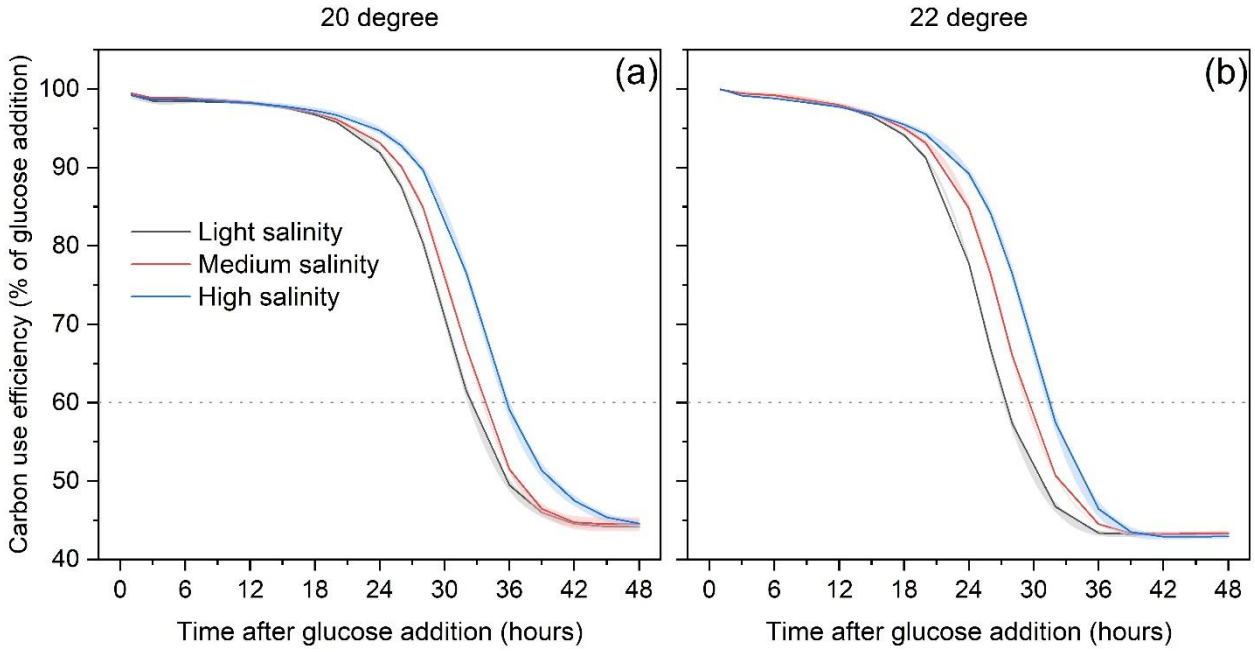

Figure S5-1. *Carbon use efficiency based on glucose input (a and b) at 20 and 22 ℃. Line and shadow represent mean ± standard error (n =3) in figure a-b.*

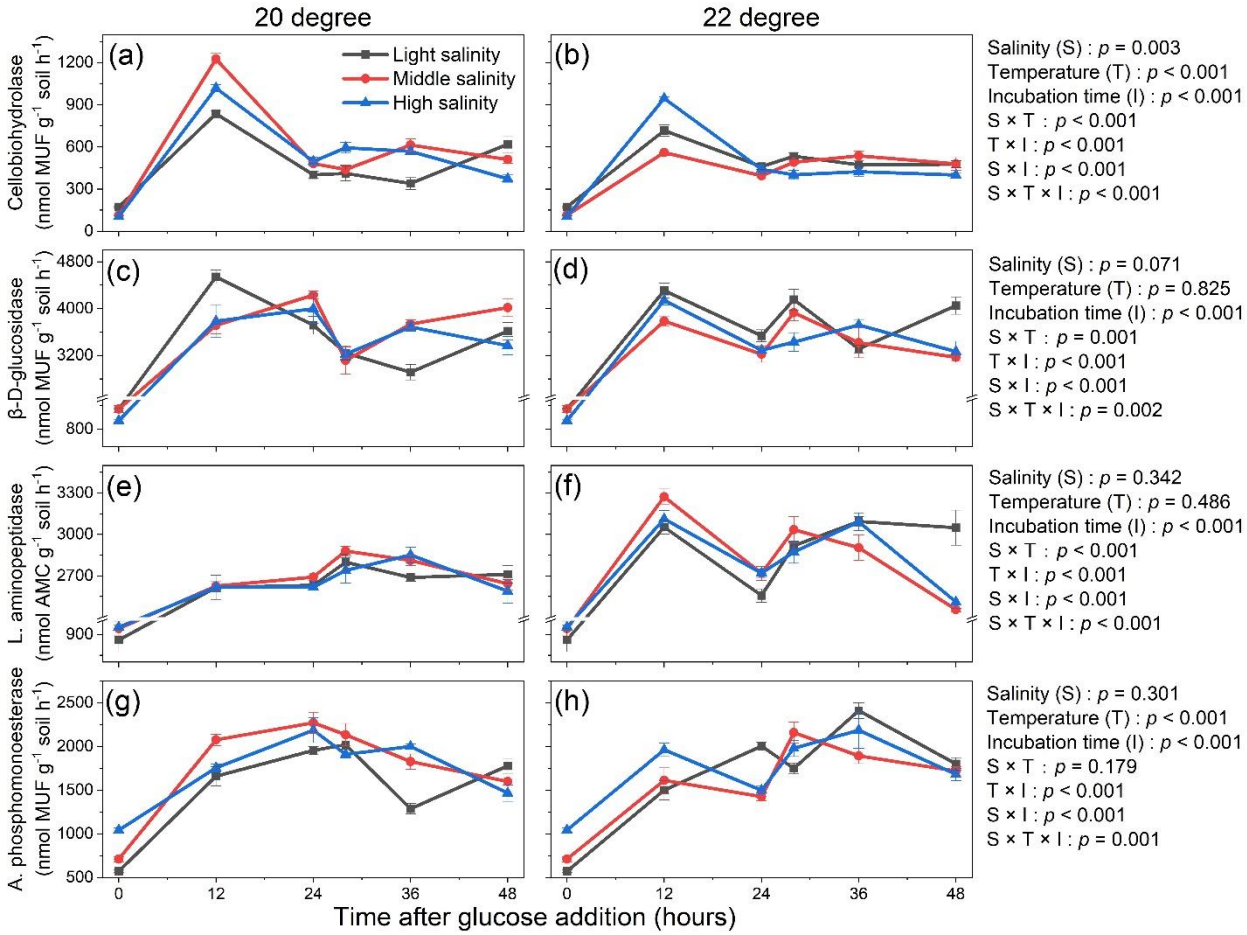

Figure S5-2. *Enzyme activities (V_{max}) of cellulose, β-D-glucosidase, leucine aminopeptidase and acid phosphomonesterase during the SIR process under 20/22℃ and 3 salinities. V_{max} were measured on 0, 12, 24, 28, 36, 48h after glucose addition and 48h after basal respiration. Values are means (±SE) of three replicates.*

P values at right side were obtained after three-way ANOVA analysis according to the V_{max} results from 12, 24, 28, 36, 48h after glucose addition.

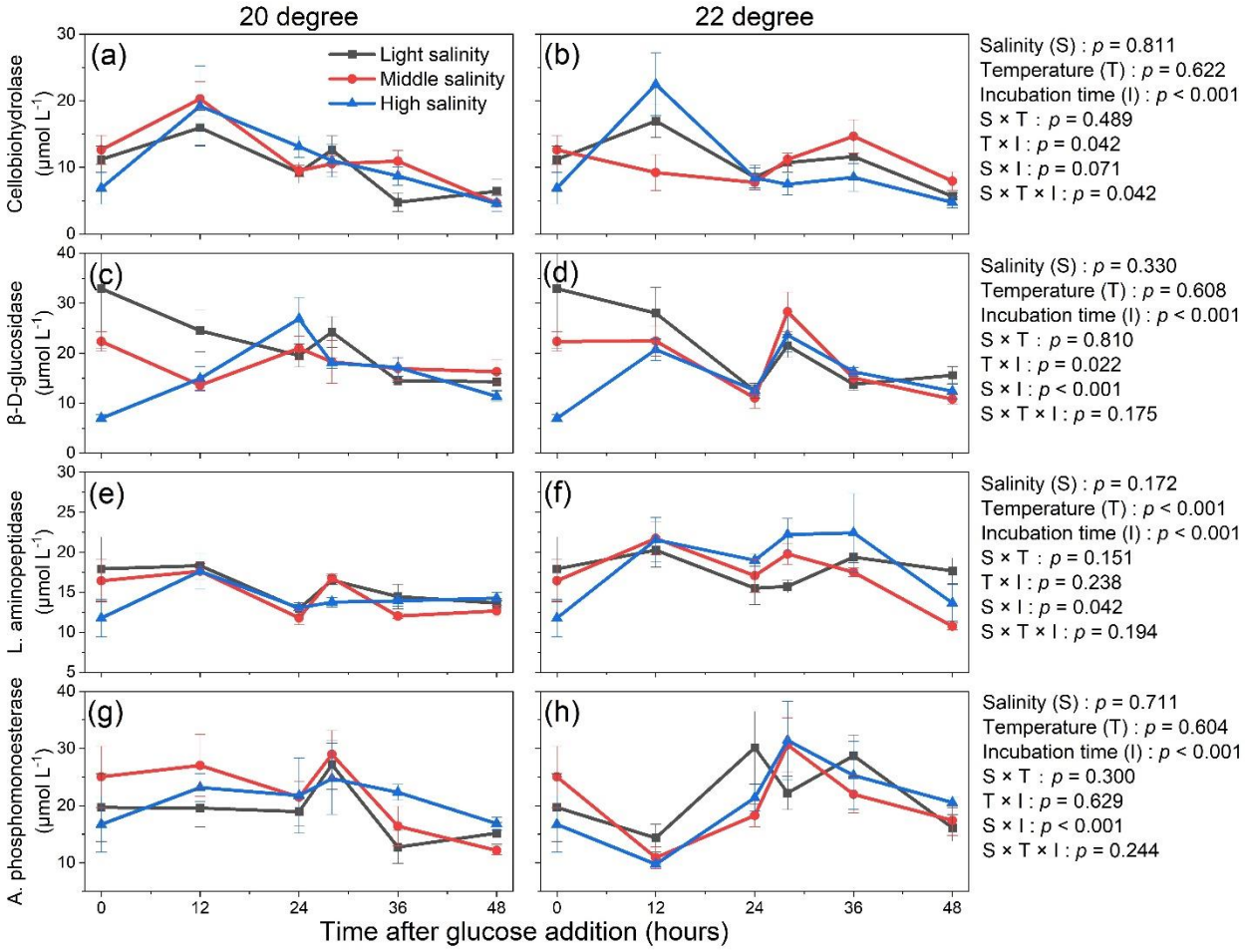

Figure S5-3. *Substrate affinities (K_m) of cellulose, β-D-glucosidase, leucine aminopeptidase and acid phosphomonesterase during the SIR process under 20/22℃ and 3 salinities. K_m were measured on 0, 12, 24, 28, 36, 48h after glucose addition and 48h after basal respiration. Values are means (±SE) of three replicates.*

P values at right side were obtained after three-way ANOVA analysis according to the K_m results from 12, 24, 28, 36, 48h after glucose addition.

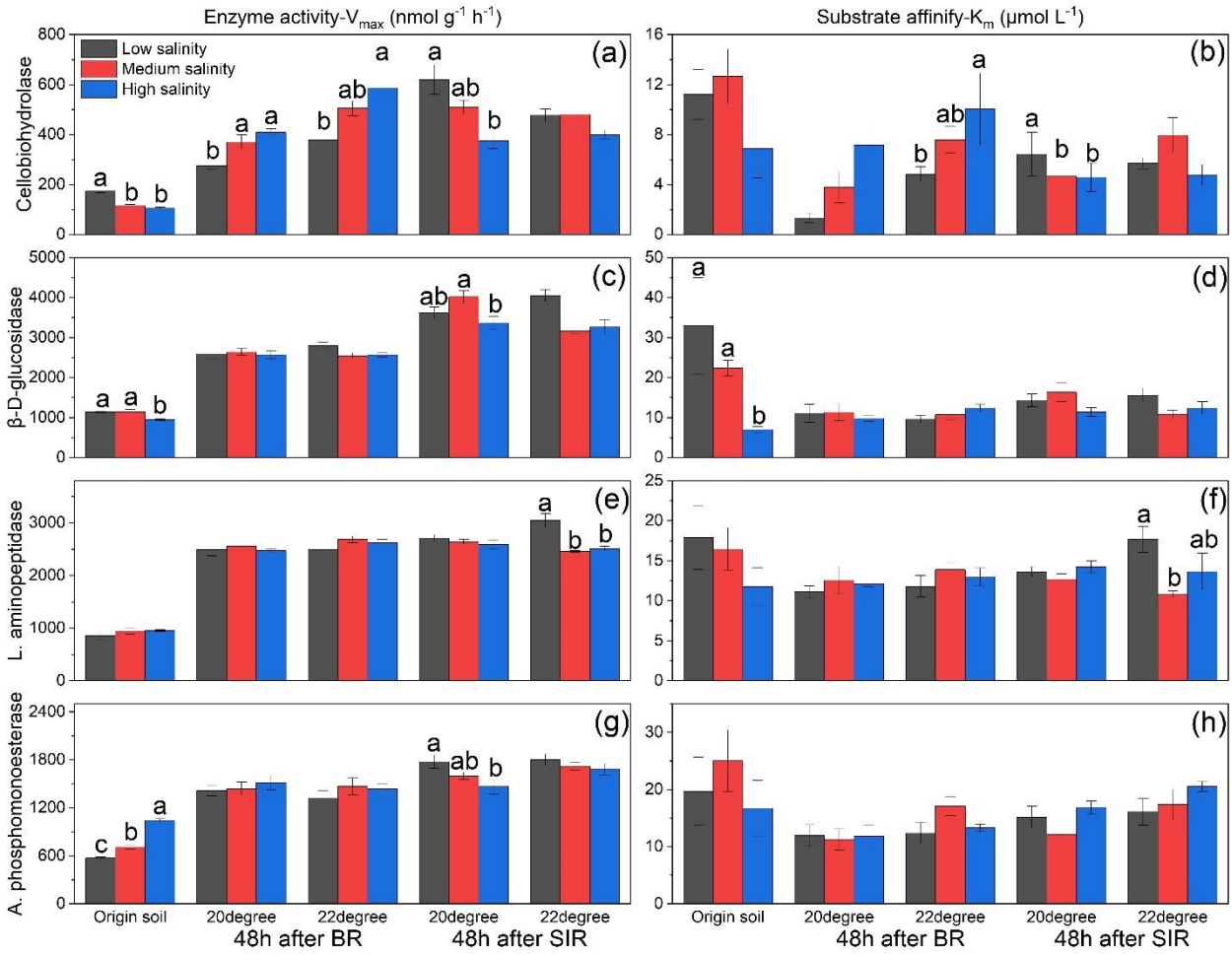

Figure S5-4. *Enzyme kinetics (V_{max} and K_m) of cellobiohydrolase, β-D-glucosidase, leucine aminopeptidase and acid phosphomonesterase before and after 48 hours basal respiration and 48 h after glucose addition under 20 and 22℃ and 3 salinity levels. Values are means (±SE) of three replicates. Lower case letters indicate significant differences between three salinities after Turkey HSD post-hoc test at $p < 0.05$.*

2.6 Study 6. Contrasting soil substrate quality effects on organic matter decomposition and microbial activity

Shang Wang [a,b*], Sandra Spielvogel [c], Evgenia Blagodatskaya [a], Bahar S. Razavi [b],

Status: In preparation

[a] *Department of Soil and Plant Microbiome, Institute of Phytopathology, Christian-Albrechts University, Kiel, Germany*

[b] *Department of Soil Ecology, Helmholtz Centre for Environmental Research - UFZ, Halle (Saale), 06120, Germany*

[c] *Institute for Plant Nutrition and Soil Science, Christian-Albrechts-University of Kiel, Kiel, 24118, Germany*

Abstract

Soil constitutes the largest terrestrial carbon (C) reservoir, containing chemically heterogeneous organic C material derived from plant and microbial metabolism. While the current study has elucidated the decomposition process of labile and recalcitrant C substrates in the soil, the effect of their combined addition on the decomposition process and soil microbial activity remains poorly investigated. This study examines the effects of labile (glucose, G), recalcitrant (starch, S) C substrates, and their combination (glucose + starch, G+S) on soil respiration, heat release, hydrolase, and oxidase activity. We also estimated the calorespirometric ratio (CR ratio) and carbon use efficiency (CUE) during the substrate decomposition process.

Treatments with glucose addition (G and G+S) exhibited peak curves for both respiration and heat release at the onset of substrate addition, while S showed a delayed and lower peak. G+S exhibited a plateau of both respiration and heat release after the peak, indicating earlier starch decomposition compared to S. Hydrolase activities showed a stronger response to different substrate qualities and decomposition stages. Specifically, on day 1, the α-D-glucosidase activity of G+S was significantly higher than that of G and S by 86.6% and 82.8%, respectively, indicating starch decomposition at the onset of substrate addition. Additionally, chitinase activities of all treatments significantly decreased by 55.5-66.1% on day 1, while acid phosphatase activities significantly increased by 4.2-4.8 times. All measured enzyme activities remained stable at the later stage of substrate decomposition. Peroxidase activities dominated the total oxidative activities, as phenol oxidase activities remained stable during substrate decomposition. Furthermore, treatments with glucose addition displayed a similar CR ratio pattern with a rapid increase at the beginning of substrate addition. In contrast, single starch addition showed a peak curve of CR ratio during decomposition, suggesting that labile C substrate dominates the CR ratio dynamic regardless of the presence of recalcitrant C substrate. The CUE of all treatments was higher at the beginning of substrate addition, decreasing to approximately 20% by the end of decomposition. Our results demonstrate the decomposition and microbial activity response to different

substrate quality combinations. We conclude that labile carbon substrates can activate microbes and subsequently accelerate the decomposition of recalcitrant carbon substrates when combined in soil.

Keywords: Labile carbon substrate; Recalcitrant carbon substrate; Enzyme activity; Soil Respiration; Heat release

1. Introduction

Soil is the primary organic carbon (C) reservoir within terrestrial ecosystems (Schimel, 1995). Its enormous C content consists mainly of polymeric biomolecules derived from plant and microbial metabolic processes (Angst et al., 2021). While soil contains considerable C overall, its composition is chemically heterogeneous and specific compound concentrations are significantly lower (Shahbaz et al., 2022). However, the complex mechanisms governing the decomposition of this soil organic matter (SOM) remains unclear, particularly in responses to heterogeneous C substrates.

Glucose and starch are important organic compounds in terrestrial ecosystems, serving as a primary source of energy and substrate for various organisms (Martínez-Trinidad et al., 2010; Strickland et al., 2012). Both are primarily derived in soil ecosystems from organic matter derived from plants, microorganisms, decomposition of dead organisms and organic amendments, although with different qualities (Gunina and Kuzyakov, 2015; MacNeill et al., 2017). Glucose, a simple sugar, serves as a basic energy and carbon source for plants and various soil microorganisms. Starch, like glucose, is a common component of plant litter and an important source of energy and carbon for soil microorganisms (Guggenberger et al., 1999; Mooney 1972). However, starch is a polysaccharide composed of glucose units linked in long chains, making it a more recalcitrant substrate for microbial degradation than labile substrates such as glucose (French, 1973).

Soil microbial activity is significantly influenced by the C substrates present in the soil. Upon entering the soil ecosystem, C substrate undergo decomposition mediated by soil microbial communities (Olagoke et al., 2022). The decomposition of these substrates accelerates microbial metabolism and contributes to the turnover of soil organic matter (Loeppmann et al., 2016; Wen et al., 2019). However, understanding the dynamics of mixed substrate decomposition involving glucose and starch in soil ecosystems is crucial for elucidating the mechanisms governing nutrient cycling and ecosystem functioning in terrestrial environments.

Soil microorganisms play an important role in degrading SOM and converting it into microbial biomass, carbon, energy, and nutrients (Blagodatskaya and Kuzyakov, 2013; Schnecker et al., 2023). The relationship between SOM, microbial growth, and respiration is characterized by microbial carbon use efficiency (CUE), which is calculated as the fraction of total microbial carbon uptake that is incorporated into microbial biomass (Geyer et al., 2019). Microorganisms support their growth by producing extracellular enzymes from SOM, releasing carbon as CO_2 during their growth on SOM-

derived substrates (Chen and Sinsabaugh, 2021). Respiration and enzyme catalysis primarily release or absorb energy in the form of heat, measurable by microcalorimetry as net metabolic heat production. Consequently, enzyme activity, respiration and heat production can be used as indicators of SOM degradation. In addition, the calorespirometric ratio (CR ratio), defined as the ratio of soil heat production to respiration, can indicate metabolic pathways during microbial growth. The CR ratio is also related to the efficiency of substrate carbon conversion into living cells, providing an indirect estimate of CUE (Chakrawal et al., 2020; Hansen et al., 2004). However, SOM degradation, enzyme activity and CR ratio can be influenced by environmental factors, organic matter quality and degradation stage (Allison et al., 2014; Chakrawal et al., 2021; Hoang et al., 2022). Therefore, it is crucial to consider both microbial function and soil properties when assessing the response of SOM decomposition to different substrate qualities.

In this study, we aimed to investigate the influence of the quality of the added carbon substrate on soil microbial activity and organic matter decomposition. Specifically, we conducted incubation experiments using soil samples supplemented with labile (glucose), recalcitrant (starch), and a combination of both, maintained at 20°C for 18 days. Our measurements included soil respiration, heat flow and microbial biomass to assess substrate decomposition patterns, CR ratio and CUE. In addition, we analyzed oxidase kinetics to elucidate SOM decomposition and enzyme kinetics associated with carbon, nitrogen and phosphorus cycling to characterize microbial functions. Our hypotheses were as follows: 1) the decomposition rate of starch would be lower than that of glucose due to the more complex chemical structure of the recalcitrant substrate; 2) the decomposition rate of starch in the mixed treatment would increase due to a priming effect induced by the labile substrate; 3) the CUE and CR ratio change with substrate quality and decomposition dynamic.

2. Material and Method

2.1 Soil sampling site

The soil sample was taken from a long-term manure application experiment at Dikopshof, University of Bonn, Germany. The soil is classified as Haplic Luvisol and has a silty loam texture consisting of 15.1% clay, 68.9% silt and 15.9% sand. The soil was air dried, sieved (< 2 mm) and visible plant debris and stones were removed for further incubation experiments. The basic physico-chemical properties of the soil are pH 6.3, bulk density 1.15 g cm^{-3}, water holding capacity 31% (w dw^{-1} soil), organic C 0.74%, total N 0.08%, available phosphorus 57 mg kg^{-1} and available potassium 161 mg kg^{-1} (Yang et al., 2024). Further details of the soil can be found at https://www.lap.uni-bonn.de/en/research/projects/long-term-experiment-dikopshof (Huging, 1904). Prior to the formal experiment, the soil was pre-incubated at 20 °C with 14% humidity in the dark for 10 days.

2.2 Microcosm experiment set up

The microcosm experiment included three substrate addition treatments: single glucose addition (G), glucose + starch addition (G+S) and single starch addition (S). Each treatment had three replicates.

The microcosms contained 800 µg C g^{-1} of each substrate and the G+S treatment contained 400 µg C g^{-1} of glucose and starch, respectively. Starch was extracted from wheat. After addition of the substrates, the soils were incubated for 10 days at 20°C and 16% humidity in the dark. Soil samples were taken on days 0, 1, 2, 6 and 18 after substrate addition for further measurements. Concurrently, a group of microcosms were established with additions of ^{13}C-glucose (≥ 99 atom% ^{13}C) and ^{13}C-starch (96 atom% ^{13}C) to determine carbon use efficiency (CUE).

2.2 Soil respiration and heat flow

To monitor the soil respiration rate, 30g of fresh soil was incubated in the Respicond V respirometer after adding the specific substrate and adjusting the moisture content. The CO_2 production rate was monitored continuously at 20-minute intervals at 20°C. To monitor the heat flow, the soil with the same moisture content was amended with the same substrate as described above for respiration rate monitoring. Then, all the samples were sealed in airtight glass ampoules and placed in a TAM Air. Heat production was continuously measured at 20°C. The calorespirometric ratio was calculated by Eq. (1):

$$\gamma = Q \div CO_2 \quad (1)$$

where γ is the calorespirometric ratio (kJ mol^{-1} CO_2), Q is the accumulative heat production (J g^{-1} soil) and CO_2 is the accumulative CO_2 amount (mol CO_2 g^{-1} soil).

2.3 Enzyme kinetics

After 0, 1, 2, 6, and 18 days of substrate addition, soil samples were collected from each parallel microcosm for determining hydrolytic and oxidative enzyme kinetics. For hydrolytic enzyme, soil samples were used to measure the kinetics of α-glucosidase (EC 3.2.1.20), β-glucosidase (EC 3.2.1.21), acid phosphomonoesterase (EC 3.1.3.2) and chitinase (EC 3.2.1.52) activity using 4-methylumbelliferone (MUF)-α-D- glucoside, 4-MUF-β-D-glucoside, 4-MUF-phosphate, and 4-MUF-N-acetyl-β-D-glucosaminide fluorogenic substrates, respectively (Marx et al., 2001). The activities of the four enzymes were determined using a range of substrate concentrations (0, 5, 20, 50, 75, 100, 200, 400 µmol L^{-1}) to ensure the saturation. 0.2 g of soil was suspended in 20 mL of sterilized water to create a soil suspension after low-energy sonication (40 J s^{-1}) for 1 minute. Thereafter, 50 µL soil suspension, 100 µL substrate solution and 50 µL MES buffer were added to a 96-well black microplate (Koch et al., 2007; German et al., 2011a), and the fluorescence was measured using TECAN microplate reader at excitation γ_{ex} = 355nm and emission γ_{em} = 460nm. Enzyme activities were recorded at 30, 90 min, 2 h and 3 h and expressed as nmol MUF or AMC g^{-1} soil h^{-1}. The kinetic parameters V_{max} and K_m were calculated by the Michaelis-Menten equation (2):

$$v = \frac{V_{max} \times [S]}{K_m + [S]} \quad (2)$$

where v is the reaction rate, [S] is the substrate concentration, V_{max} is the maximum reaction rate, and K_m is the substrate concentration at the half-maximum reaction rate.

Oxidative enzymes were assayed following the protocol outlined by Khosrozadeh et al. (2022). The Amplex Red stock solution was diluted in 50 mM Trizma buffer (pH 7.4) to prepare a concentration series (0.01, 0.05, 0.1, 0.25, 0.5, 1, and 2 mM). After dilution, substrates were purged with inert gas (N_2) in the dark for 5 minutes, and tube lids were tightly sealed thereafter. Each reaction mixture comprised 50 µl of soil suspension (1:50 w/w soil in water, subjected to 60 s sonication), 100 µl of substrate solution with corresponding concentration, and 50 µl of Trizma buffer, pipetted into microplate wells with stirring of the soil suspension. Controls containing only substrate and buffer were included for each microplate. For total oxidative enzyme activity, all wells, including controls, received 10 µl of 0.3% H_2O_2, while phenol oxidase activity was assessed in separate microplates without H_2O_2 addition. Soil samples were assayed in triplicate for each Amplex Red concentration. A standard calibration curve was generated by substituting the Amplex Red substrate with resorufin sodium salt. Following pipetting, microplates were wrapped in aluminum foil to minimize light exposure. Enzyme assays and resorufin standard measurements were performed at 530 nm excitation and 590 nm emission using a TECAN microplate reader with 96-well microplates. The slope of a linear regression of fluorescence intensity versus standard resorufin concentrations (5–1000 µM) was used to calculate oxidoreductase (with H_2O_2) and phenol oxidase (without H_2O_2) activities in µmol resorufin g $soil^{-1}$ h^{-1}. Peroxidase activity was estimated by subtracting phenol oxidase activity from total oxidative activity. Subsequently, phenol oxidase and peroxidase kinetics were determined using the Michaelis–Menten model (Eq. 2) as described in hydrolytic enzyme kinetics.

2.4 Microbial biomass measurement

Microbial biomass carbon (MBC) and nitrogen (MBN) content were determined using fumigation method (Vance et al., 1987). Soil samples were collected at 0, 1, 2, 6, and 18 days after substrate addition. To extract the samples, 5 g of soil was mixed with 20 mL of 0.05M K_2SO_4. Another 5 g of soil was fumigated with chloroform in a desiccator for 72 h and then extracted. The TOC/N analyzer (TOC-L, Shimadzu, Japan) was used to analyze the extracts for dissolved organic carbon (DOC) and nitrogen (DON) content. MBC and MBN calculations were based on the difference between K_2SO_4-extractable C and N in fumigated and non-fumigated soils, using the conversion factors of 0.45 for MBC and 0.54 for MBN.

2.5 Carbon use efficiency

Microbial substrate CUE for added carbon substrates was determined by considering the increment of MBC in course of substrate utilization (Eq. 3):

$$\mathrm{CUE}_1 = \frac{MBC_i - MBC_0}{(MBC_i - MBC_0) + (C_{SIR} - C_{BR})} \quad (3)$$

where C_{SIR} represents the cumulative amount of C respired from substrate-amended soil, and C_{BR} is the cumulative amount of C respired from unamended soil. The cumulative amount of respired carbon is determined over time and respiration rate, measured by the Respicond V respirometer. MBC_0 and MBC_i represent the microbial biomass C measured by fumigation method at 0 and *i* hours after glucose addition. We were not able to correctly estimate soil priming effect. We assumed, therefore, that considering a short-term experiment, the priming effect (if any) was mainly apparent due to pool substitution mechanism (Blagodatskaya and Kuzyakov, 2008), and the metabolized C was either incorporated into MBC or respired.

2.6 Statistical analysis

All data were presented as the mean ± standard error. Prior to analysis, the normality and homogeneity of variance were determined using the Shapiro-Wilk test and Leneve's test, respectively. For comparing the significant differences between different substrate addition, one-way ANOVA combined with a Turkey HSD post-hoc test was applied. Significant differences were considered at $p < 0.05$. The Shapiro-Wilk test and Leneve's test were conducted using R Studio (version 4.1.0). The ANOVA and post-hoc test were performed using SPSS (version 20.0). The kinetics of enzyme activity were calculated using Origin Lab (version 2022).

3. Results

3.1 Respiration and heat flow response to substrate addition

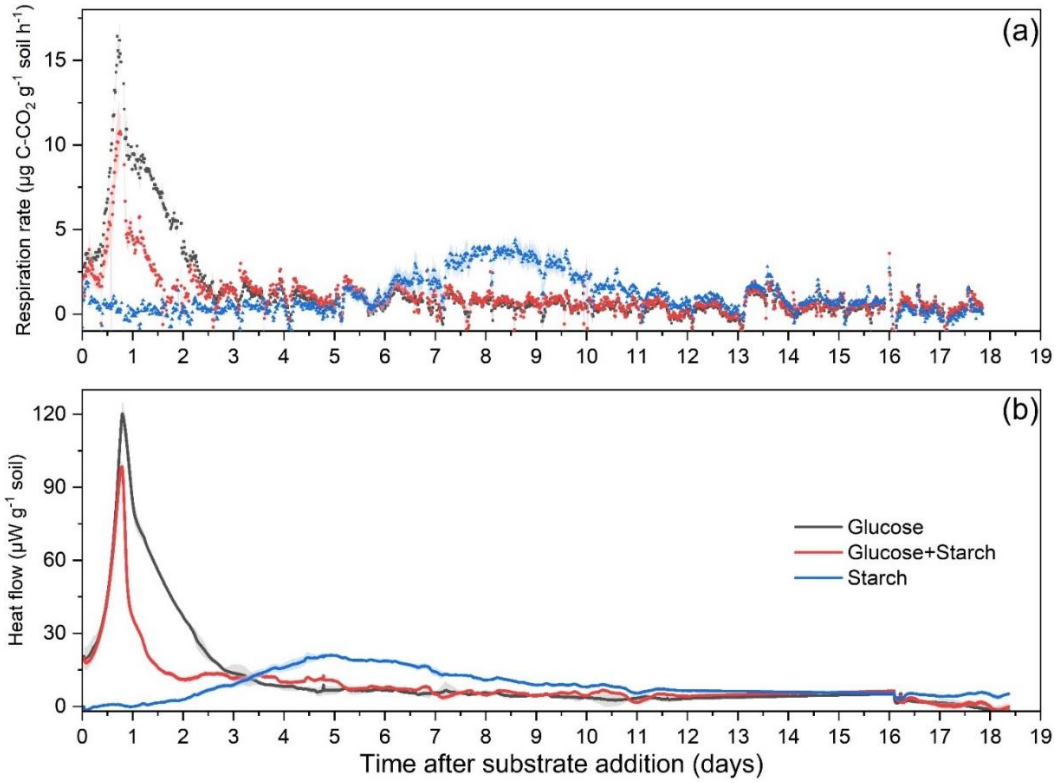

Figure 6-1. *Soil respiration rate (a) and heat flow (b) after substrate addition. Line (dot) and shadow represent mean ± standard error (n =3).*

The soil respiration rate exhibited distinct patterns in response to three different carbon substrate addition scenarios during an 18-day incubation period (Figure 1a). In the Glucose (G) and Glucose+Starch (G+S) treatments, exponential growth was observed within 24 hours of substrate addition, with maximum respiration rates of 16.4 and 10.8 μg $C\text{-}CO_2$ g^{-1} soil h^{-1}, respectively. Subsequently, both G and G+S treatments experienced a retardation in respiration rates from day 1 to day 3. Following this, the respiration rate of G+S was 32.7% higher than that of G from day 3 to day 5. Furthermore, the respiration rate of Starch (S) began to increase after 6 days of substrate addition, reaching its peak (4.4 μg $C\text{-}CO_2$ g^{-1} soil h^{-1}) on day 8. Subsequently, the respiration rate retarded from day 8 to day 12. Finally, all substrate addition treatments remained stable around and similar to the basal respiration rate (0.20 μg $C\text{-}CO_2$ g^{-1} soil h^{-1}) from day 12 to day 18.

Similar to the respiration rate dynamics, the heat flow of G and G+S showed exponential growth within the first day after substrate addition, with maximum heat flow values of 98.6 and 120.2 μW g^{-1}, respectively (Figure 1b). While the heat flow of G+S remained stable at 15 μW g^{-1} after the growth retardation from day 2 to day 5. Furthermore, the heat flow of S began to grow by day 1, and the maximum heat flow (20.1 μW g^{-1}) was observed on day 5. Following that, the heat flow experienced a retardation stage until day 12. In particular, the heat flow of S began to grow 5 days earlier than the respiration rate. Collectively, the respiration rate and heat flow after substrate addition exhibited a similar pattern, with the heat flow beginning to grow earlier than the respiration rate.

3.2 Calorespirometric ratio and carbon use efficiency

The calorespirometric ratio (CR ratio) of G and G+S exhibited a rapid increase within the first day after substrate addition, while the CR ratio of S gradually increased within the initial days following starch addition (Figure 2). Subsequently, the CR ratio of G and G+S remained stable around 300-350 kJ mol^{-1} until the end of the incubation, with the CR ratio of G consistently ~35 kJ mol^{-1} higher than that of G+S at the same time. In contrast, the CR ratio of S increased from day 1 to day 5, reaching a maximum value of 1200 kJ mol^{-1}, which was significantly higher than the oxycaloric equivalent (469 kJ mol^{-1}). Following this peak, the CR ratio of S remained relatively stable around 1100 kJ mol^{-1} from day 5 to day 7. Subsequently, the CR ratio of S gradually decreased and stabilized around 300 kJ mol^{-1} until the end of the incubation. In summary, the CR ratio of G and G+S generally exhibited a similar pattern, while the CR ratio of S showed a peak curve. The CR ratios of all treatments remained stable within the range of 310-350 kJ mol^{-1} from day 10 to day 18, which is lower than the oxycaloric equivalent of aqueous glucose combustion.

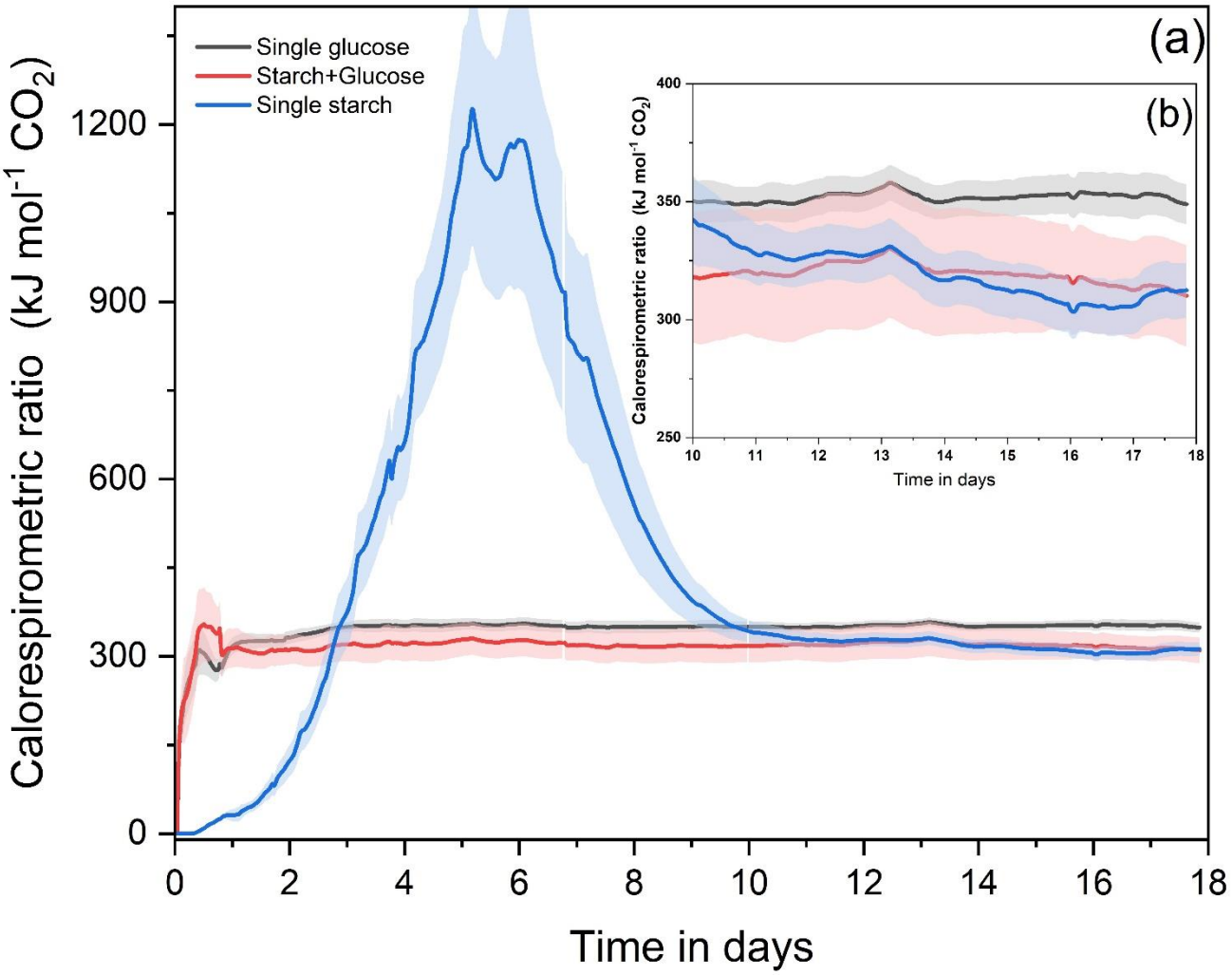

Figure 6-2. *Calorespirometric ratio dynamic after substrate addition. Line and shadow represent mean ± standard error (n =3).*

Table 6-1*. Microbial substrate carbon use efficiency after 1, 2, 6 and 18 days of substrate addition.*

	Glucose	Glucose+Starch	Starch
1 day	0.792 ± 0.021	0.799 ± 0.065	1.041 ± 0.004
2 days	0.537 ± 0.037	0.709 ± 0.030	1.115 ± 0.023
6 days	0.581 ± 0.323	0.567 ± 0.061	0.921 ± 0.029
18 days	0.137 ± 0.054	0.256 ± 0.042	0.196 ± 0.075

CUE= $\Delta_{MBC}/(\Delta_{MBC}+C_{respired})$. Values represent mean ± standard error (n = 3).

The carbon use efficiency (CUE) of all treatments showed a declining pattern with substrate decomposition (Table 1). At the peak of the respiration rate (day 1), the CUE for G and G+S was 79.2% and 79.9%, respectively, which then decreased to 53.7% and 70.9% during the retardation stage of respiration. In contrast, the CUE of S remained higher than 100% within 2 days after starch addition due to a lower respiration rate compared to the basal respiration rate. Subsequently, the CUE of S was 92.1% at the peak of the respiration rate. Finally, the CUE for all treatments reached 13.7% to 25.6%

by the end of the incubation. In summary, the CUE at the peak of the respiration rate was above 79%, declining to 13.7-25.6% after the retardation of respiration.

3.3 Enzyme kinetics response to substrate addition

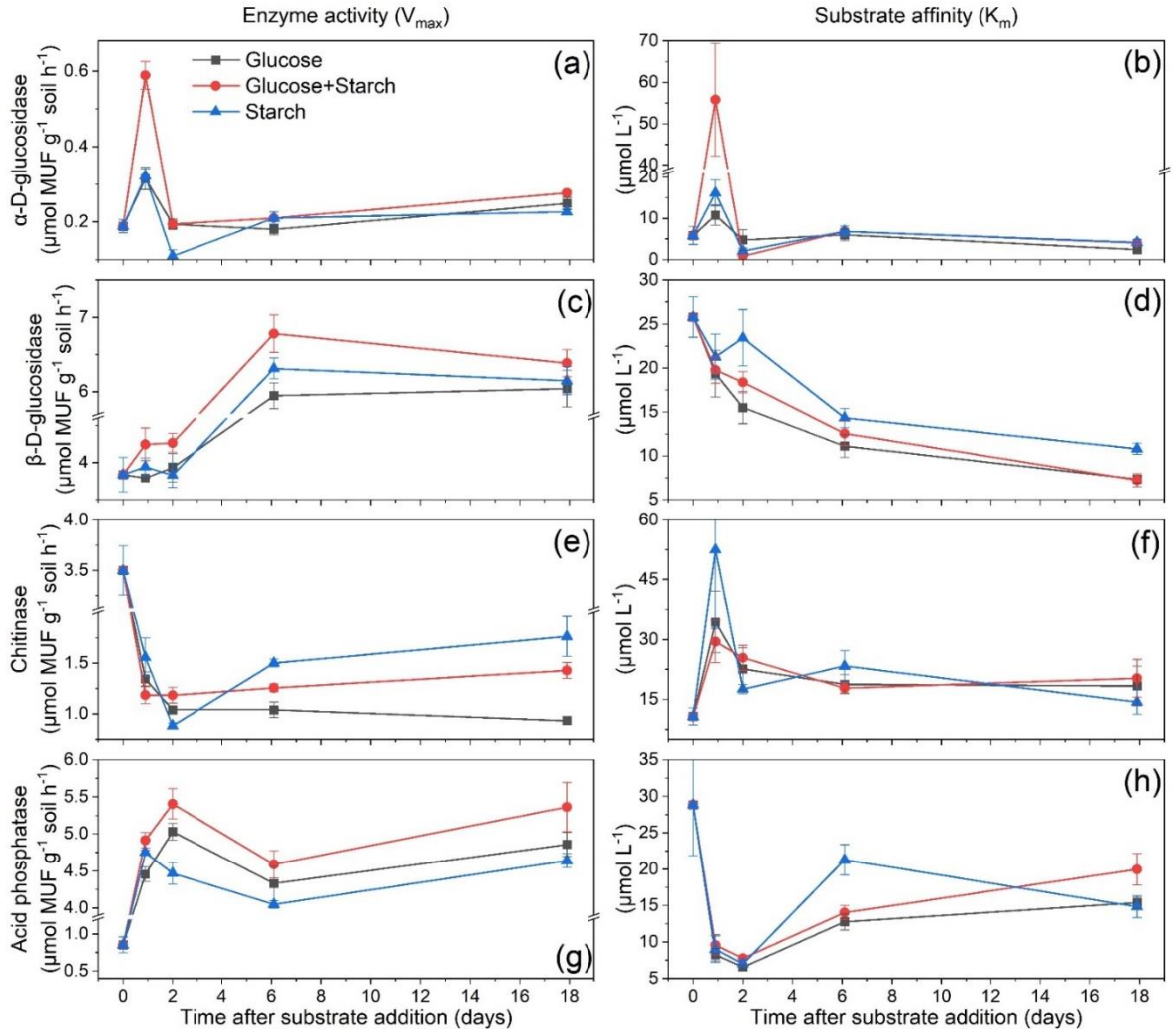

Figure 6-3. *Soil enzyme activity (V_{max}) and substrate affinity (K_m) of α-D-glucosidase (a and b), β-D-glucosidase (c and d), chitinase (e and f) and acid phosphatase (g and h). Dot with bar represent mean ± standard error of enzyme activity (n = 3).*

The hydrolytic enzyme activity exhibited different responses to substrate quality in the initial stage after substrate addition; thereafter, all measured enzyme activities remained relatively stable during the decomposition process (Figure 3). α-D-glucosidase (α-GLU) activity significantly increased after 1 day of substrate addition. In particular, G+S increased α-GLU activity by 2.1 times, significantly higher than the increases observed for S and G. Subsequently, α-GLU activities decreased by day 2, with the activity of S being significantly lower than that of G and G+S by 43.6%. Following this, α-GLU activity remained stable from day 6 to 18. Meanwhile, the activity of β-D-glucosidase (β-GLU) on days 1 and 2 showed no significant difference compared to day 0, while it increased significantly by 51.4-64.8% on day 6 and remained stable until day 18. Notably, the β-GLU activity of G+S was consistently higher than that of S and G. In contrast, chitinase (CHIT) activity decreased until day 2

by 66.3-74.9% compared to day 0; thereafter, CHIT activity remained stable, and the activity of S was higher than that of G+S and G from day 6 to day 18. Furthermore, acid phosphatase (PHOS) activity significantly increased after 1 day of substrate addition, reaching 4.2-4.8 times the initial levels. From day 2 to day 18, Phos activities exhibited a decrease-then-increase pattern, with the activity of G+S consistently higher than that of G and S.

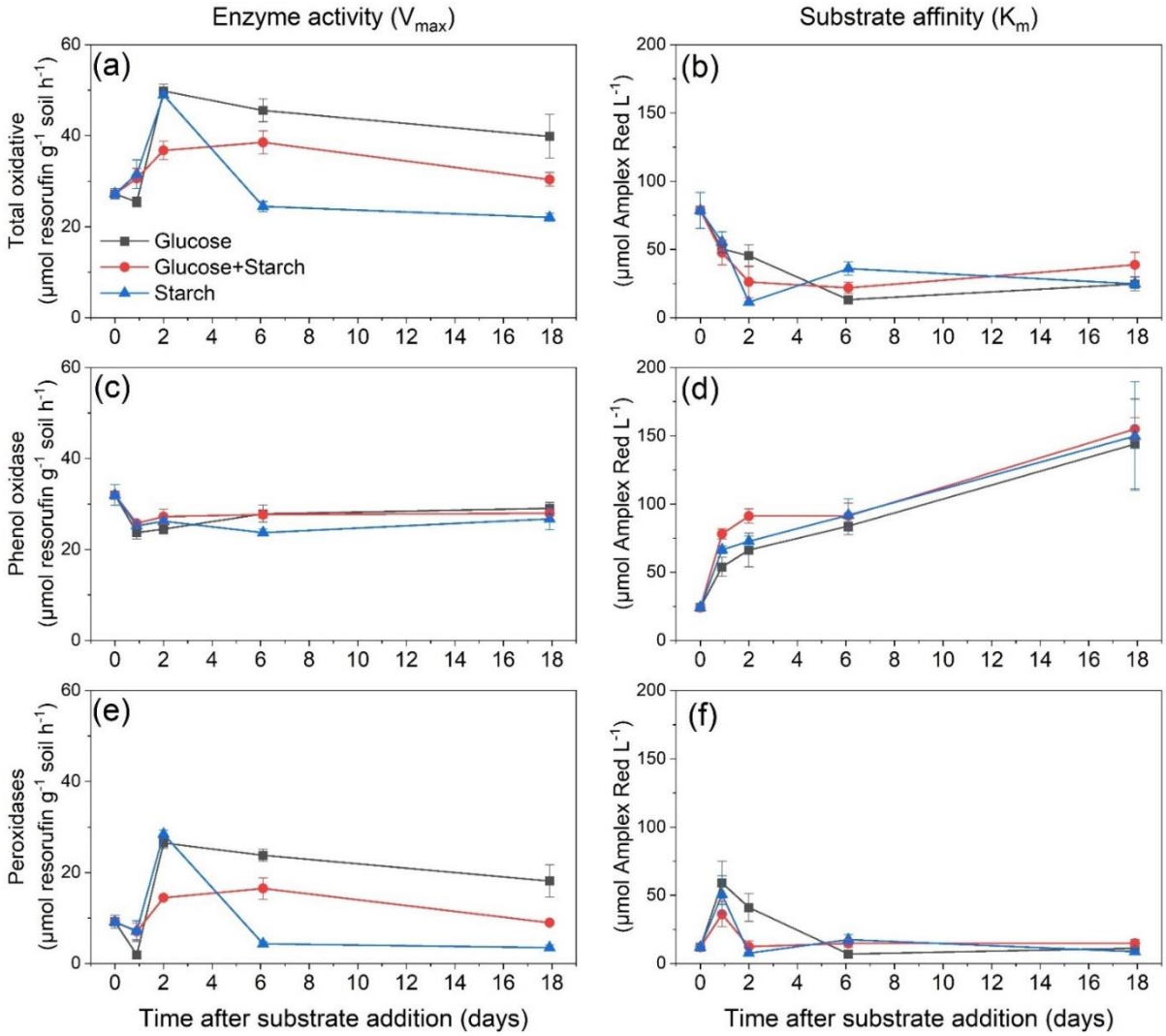

Figure 6-4. *Soil gross oxidative enzyme activities (V_{max}) and substrate affinity (K_m) of total oxidative (a and b), phenol oxidase (c and d), and peroxidase (e and f)). Dot with bar represent mean ± standard error of enzyme activity (n = 3)*

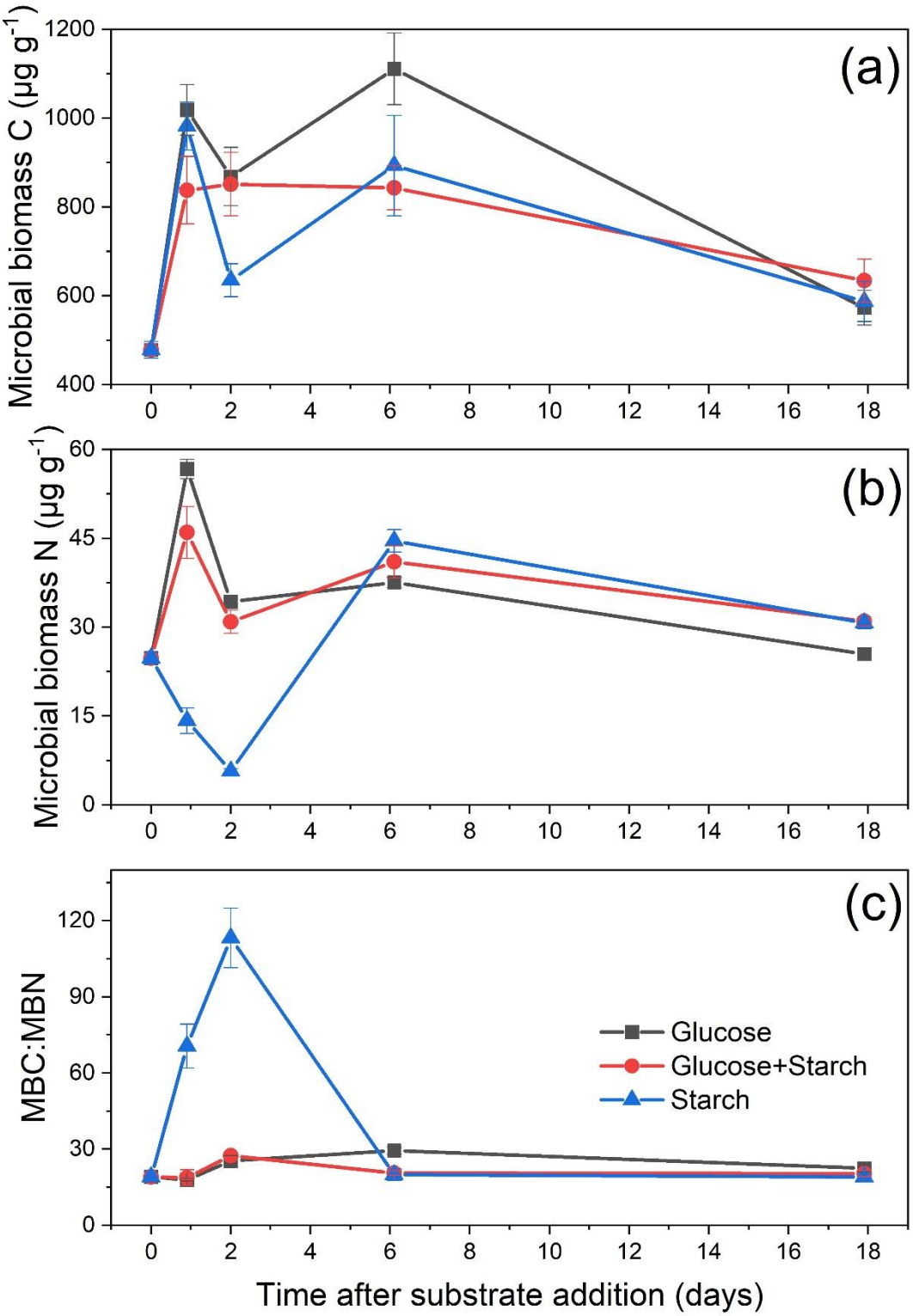

Figure 6-5. *Microbial biomass carbon (MBC), nitrogen (MBN) and their ratio after 1, 2, 6 and 18 days of substrate addition. Column and bar represent mean ± standard error (n = 3). Exact value and significant difference are shown in Table S1.*

The oxidase activity generally underwent a significant change during the initial stage after substrate addition, and subsequently remained stable from the later stages of substrate decomposition onwards (Figure 4). Specifically, the total oxidative activity of both G and S significantly increased by

1 time on day 2 compared to day 0. Following this, the activity of S decreased significantly by 50.1% on day 6. While the total oxidative activity of G+S gradually increased until day 2 and then remained stable from day 2 to day 18. Meanwhile, peroxidase activity exhibited a similar pattern to total oxidative activity with respect to different substrate additions. Furthermore, phenol oxidase activity decreased by 19.5-25.9% on day 1 after substrate addition and then remained stable until day 18. In general, all measured enzyme activities showed significant changes within 1 to 2 days after substrate addition and remained stable until substrate depletion.

3.4 Microbial biomass response to substrate addition

The MBC amount for all treatments significantly increased by 75.1-112.8% after 1 day of substrate addition (Figure 5). Subsequently, the MBC of G+S remained stable with a slight decrease until day 18, whereas the MBC of G and S exhibited a fluctuating pattern from day 2 to 18. Furthermore, the MBN of G and G+S significantly increased by 85.7-128.9% after 1 day of substrate addition, followed by a decrease of 32.8-39.5% by day 2. Subsequently, the MBN of G and G+S remained stable until day 18. In contrast, the MBN of S gradually decreased by 77.1% until day 2 and then increased significantly by 6.9 times on day 6. Additionally, the MBC:MBN ratio of G and G+S remained stable throughout the entire substrate decomposition process, while the MBC:MBN ratio of S gradually increased until day 2 and then decreased on day 6. In summary, microbial biomass exhibited different responses to substrate quality in the initial stage of substrate decomposition, but demonstrated a similar dynamic during the later stages of substrate decomposition.

4. Discussion

4.1 The decomposition dynamic response to substrate quality

The respiration rate and heat flow of starch increased significantly later than those of glucose under the same C substrate addition concentration (Figure 1), confirming our first hypothesis. This suggests that the decomposition of starch in soil is more difficult than that of glucose, and that there are differences in the metabolic pathways and enzymatic processes involved in their breakdown (Gunina and Kuzyakov, 2015). Starch is a complex polysaccharide made up of glucose molecules that require enzymatic hydrolysis by amylase before they can be used for energy production (French, 1973). This initial breakdown step is thought to contribute to the delayed response observed in respiration and heat flow compared to glucose. Microbial enzymes are essential for the decomposition process. Enzymes that target starch need to break down multiple bonds between glucose molecules, which adds complexity and time to the process (German et al., 2011b). Additionally, microbial preferences can influence decomposition rates, with some microorganisms preferring glucose over starch (Raczka et al., 2021). Thus, the interaction of structural complexity, enzymatic activity, substrate accessibility, and microbial preferences contributes to the delayed decomposition of starch compared to glucose in soil ecosystems.

Distinct patterns were observed in the dynamics of heat release rate and respiration rate during the decomposition of starch and glucose in soil (Figure 1). The decomposition of starch began with an early increase in heat release rate, caused by the enzymatic breakdown of its complex polysaccharide structure into labile C substrate such as glucose, which produces heat as a byproduct (Baker and Allison, 2017). However, the respiration rate lags behind, indicating a delay in microbial adaptation to utilize the labile C substrate for energy production, where respiration becomes more pronounced. In contrast, glucose decomposition demonstrated a simultaneous increase in heat release and respiration rates, reflecting its straightforward metabolism by soil microbes without the need for extensive enzymatic breakdown. Microbial populations can rapidly utilize glucose for energy production through respiration as soon as it is available in the soil environment (Rousk and Jones, 2010). Collectively, starch requires more initial enzymatic breakdown, leading to earlier heat release, while glucose can be readily utilized, resulting in simultaneous increases in heat release and respiration rates.

Under the addition of both glucose and starch, the respiration and heat release rates showed a plateau stage for three days after the glucose decomposition retardation. This may suggest that starch decomposition occurred earlier compared to when only starch was added (Figure 1). It is possible that glucose decomposition acted as a catalyst for the decomposition of starch within soil ecosystems. This phenomenon may be attributed to several mechanisms, including enzyme production, increased microbial activity, and enhanced nutrient availability resulting from glucose decomposition (Blagodatskaya et al., 2009; Dungait et al., 2012). The presence of glucose stimulates microorganisms to produce more enzymes that break down starch, leading to accelerated decomposition rates. Glucose decomposition releases nutrients and energy that can support microbial growth and activity, which in turn may accelerate the decomposition of starch and other recalcitrant substrates in the soil. This finding confirms our second hypothesis and suggests that the decomposition of labile C substrate like glucose can influence and potentially accelerate the decomposition of recalcitrant C substrate like starch in soil ecosystems.

4.2 The CUE and calorespirometric ratio response to different substrate quality

The CUE of substrate addition with different qualities showed varying patterns regarding substrate decomposition dynamics (Table 1). The CUE of the G and G+S treatments was above 79% on day 1, while the CUE of the S treatment remained higher than 92% until day 6. The higher CUE values before the added substrate began to decompose indicates a microbial switch to the growth preparation stage, where a substantial portion of substrate and energy is directed towards the synthesis of storage compounds or specific enzymes not related to CO_2 production (Mason-Jones et al., 2022). The significant increase in MBC on day 1 (Figure 5a) supports this finding. The CUE of S was higher than 100%, which may be due to lower substrate-induced respiration at the initial stage after starch addition (Figure 1a). This resulted in substrate induced respiration (SIR) rates lower than basal respiration and led to negative respired C. The estimation before the peak of SIR showed overestimated values (above

60%) and corresponds to apparent rather than real CUE (Sinsabaugh et al., 2013). The CUE decreased after the peak of respiration rate until the end of the experiment, indicating that soil microorganisms allocated more substrate and energy towards respiration rather than the synthesis of storage compounds (Dijkstra et al., 2015). Additionally, the MBC also decreased during the later stage of incubation, which may have been induced by limited substrate and nutrient resources, suggesting microbial death, which can also decrease the CUE.

On the other hand, at the beginning of substrate addition in the G and G+S treatments, the CR ratio showed a rapid increase (Figure 2), indicating a stronger allocation of substrate and energy to processes other than respiration. Following this, the CR ratio remained stable and lower than the oxycaloric equivalent (469 kJ mol^{-1} CO_2) for aqueous glucose combustion until the end of the incubation. This suggests a balance between the allocation of substrate and energy to processes and respiration, and a higher respiration rate compared to the complete oxidation of the substrate. However, the CR ratio of the S treatment gradually increased to 1200 kJ mol^{-1} CO_2 by day 5 and remained around 1100 kJ mol^{-1} CO_2 from day 5 to day 7, exceeding the oxycaloric equivalent (469 kJ mol^{-1} CO_2) for aqueous glucose combustion. This indicates either additional heat release from accompanying processes or a lower respiration rate compared to the complete oxidation of the substrate. The additional heat could result from priming due to the metabolism of substrates with lower availability other than carbohydrates, or the incomplete oxidation of the substrate to CO_2 (Chakrawal et al., 2020). Additionally, the excess heat generated can be used for synthesizing storage compounds or enhancing enzyme activity. The simultaneous occurrence of CR ratio peaks of S treatment suggests that the decomposition of recalcitrant carbon substrates requires more enzymes and energy. Finally, the CR ratio of all treatments remained below the oxycaloric equivalent (469 kJ mol^{-1} CO_2) from day 10 to day 18, indicating a significant reduction in heat production compared to complete glucose oxidation. This suggests that the added substrate was not entirely oxidized to CO_2 under fermentation or combined fermentation and aerobic decomposition conditions (Chakrawal et al., 2021). Thus, our third hypothesis was confirmed: the CUE and CR ratio change with the microbial growth stage.

4.3 Enzyme activities response to substrate decomposition with different quality

The dynamics of hydrolases activities in response to substrate quality during the decomposition process, reflecting critical aspects of soil microbial metabolism (Figure 3). The results show that α-GLU activity initially increased following substrate addition, particularly with G+S, indicating a rapid microbial response to readily available substrates. The significantly higher α-GLU activity on day 1 may predict early decomposition of starch compared to the S treatment, as α-GLU is a specific enzyme for starch decomposition (German et al., 2011a). This implies that glucose addition could prime the soil organisms (Kuzyakov, 2010), thus accelerating starch decomposition. Conversely, β-GLU activity exhibited a delayed but substantial increase by day 6, suggesting a shift in microbial community dynamics or substrate utilization patterns. This is because the glucose substrate was depleted at

beginning, leading to more β-GLU being released to acquire more labile substrate for microbial growth at later stage. CHIT activity initially declined, possibly due to the complexity of chitin as a substrate, yet stabilized thereafter, with higher activity observed with the S treatment, indicative of distinct microbial preferences. Furthermore, the activity of PHOS increased significantly after the addition of substrate, indicating a microbial response to phosphorus-containing compounds. The G+S treatment showed sustained higher activity, suggesting synergistic substrate effects.

The dynamics of oxidase activity in response to glucose and starch substrates were relatively stable compared to the dynamics of hydrolase activity (Figure 4). This contradicts the notion that the mean spatiotemporal variation in oxidase activity within ecosystems is greater than that of hydrolases (Sinsabaugh et al., 2008). This difference may be attributed to the laboratory incubation conditions lacking environmental stressors, which exclude substrate nutrient limitations compared to field conditions. Meanwhile, oxidase activity exhibited a similar trend during substrate decomposition regardless of substrate quality. This suggests that oxidative enzymes are less substrate-specific than hydrolytic enzymes, and peroxidases produce oxygen radicals that can attack a diverse array of substrates (Schnecker et al., 2019; Sinsabaugh, 2010). Moreover, the coordination between peroxidase and total oxidative activity highlights the interconnectedness of enzymatic pathways in response to substrate availability. Furthermore, oxidase activities were higher in the G treatment compared to the G+S and G treatments from day 6 to 18, indicating that substrate limitation may stimulate oxidase activity. Microbes often switch to oxidative enzymes to degrade complex organic material after labile substrates are depleted (McDaniel et al., 2014). Overall, the results of enzyme activity dynamics demonstrate that the onset of substrate addition could increase enzyme activity, while hydrolase activity showed a more specific and strong response to substrate decomposition with different qualities compared to oxidase activity.

5. Conclusions

Soil substrate addition of different qualities results in varying responses in soil respiration, heat release, enzyme activity, CUE, and CR ratio dynamics. Treatments with glucose addition (G and G+S) exhibited peak curves for both respiration and heat release at the onset of substrate addition, while single starch addition showed a delayed and lower peak. Particularly, the respiration and heat release curves of G+S showed a plateau after the peak, suggesting starch decomposition. Additionally, treatments with glucose addition displayed a similar CR ratio pattern with gradually increasing at the beginning of substrate addition, whereas single starch addition showed a peak curve of CR during decomposition. The CUE of all treatments remained higher at the beginning of substrate addition, decreasing to approximately 20% by the end of substrate decomposition. Furthermore, the oxidase activity pattern in response to glucose and starch substrates was relatively stable compared to hydrolase activity. Collectively, we conclude that labile carbon substrates are more readily utilized by soil microbes compared to recalcitrant carbon substrates in the soil. Moreover, labile carbon substrates can

activate microbes and subsequently accelerate the decomposition of recalcitrant carbon substrates when combined in soil.

Declaration of Competing Interest

All the authors have reviewed and approved the manuscript, expressing agreement with its submission to the journal. No potential conflict of interest has been reported by any of the authors.

Acknowledgement

This study was financially supported by DFG Priority Program 2322 SoilSystems. We thanks Christian Lorenzen for his assistance on the calculation of CR ratio.

Reference

Allison, S.D., Chacon, S.S., German, D.P., 2014. Substrate concentration constraints on microbial decomposition. Soil Biology and Biochemistry, 79, 43-49.

Angst, G., Mueller, K.E., Nierop, K.G., Simpson, M.J., 2021. Plant- or microbial-derived? A review on the molecular composition of stabilized soil organic matter. Soil Biology and Biochemistry, 156, 108189.

Baker, N.R., Allison, S.D., 2017. Extracellular enzyme kinetics and thermodynamics along a climate gradient in southern California. Soil Biology and Biochemistry, 114, 82-92.

Blagodatskaya, E., Kuzyakov, Y., 2013. Active microorganisms in soil: critical review of estimation criteria and approaches. Soil Biology and Biochemistry, 67, 192-211.

Blagodatskaya, E.V., Blagodatsky, S.A., Anderson, T.H., Kuzyakov, Y., 2009. Contrasting effects of glucose, living roots and maize straw on microbial growth kinetics and substrate availability in soil. European Journal of Soil Science, 60(2), 186-197.

Chakrawal, A., Herrmann, A.M., Manzoni, S., 2021. Leveraging energy flows to quantify microbial traits in soils. Soil Biology and Biochemistry, 155, 108169.

Chakrawal, A., Herrmann, A.M., Šantrůčková, H., Manzoni, S., 2020. Quantifying microbial metabolism in soils using calorespirometry—a bioenergetics perspective. Soil Biology and Biochemistry, 148, 107945.

Chen, J., Sinsabaugh, R.L., 2021. Linking microbial functional gene abundance and soil extracellular enzyme activity: Implications for soil carbon dynamics. Global Change Biology, 27(7), 1322-1325.

Dijkstra, P., Salpas, E., Fairbanks, D., Miller, E.B., Hagerty, S.B., van Groenigen, K.J., Hungate, B.A., Marks, J.C., Koch, G.W., Schwartz, E., 2015. High carbon use efficiency in soil microbial communities is related to balanced growth, not storage compound synthesis. Soil Biology and Biochemistry, 89, 35-43.

Dungait, J.A.J., Hopkins, D.W., Gregory, A.S., Whitmore, A.P., 2012. Soil organic matter turnover is governed by accessibility not recalcitrance. Global Change Biology, 18(6), 1781-1796.

French, D., 1973. Chemical and physical properties of starch. Journal of Animal Science, 37(4), 1048-1061.

German, D.P., Chacon, S.S., Allison, S.D. 2011b. Substrate concentration and enzyme allocation can affect rates of microbial decomposition. Ecology, 92(7), 1471-1480.

German, D.P., Weintraub, M.N., Grandy, A.S., Lauber, C.L., Rinkes, Z.L., Allison, S.D., 2011a. Optimization of hydrolytic and oxidative enzyme methods for ecosystem studies. Soil Biology and Biochemistry, 43(7), 1387-1397.

Geyer, K.M., Dijkstra, P., Sinsabaugh, R., Frey, S.D., 2019. Clarifying the interpretation of carbon use efficiency in soil through methods comparison. Soil Biology and Biochemistry, 128, 79-88.

Glanville, H.C., Hill, P.W., Schnepf, A., Oburger, E., Jones, D.L., 2016. Combined use of empirical data and mathematical modelling to better estimate the microbial turnover of isotopically labelled carbon substrates in soil. Soil Biology and Biochemistry, 94, 154-168.

Guggenberger, G., Elliott, E.T., Frey, S.D., Six, J., Paustian, K., 1999. Microbial contributions to the aggregation of a cultivated grassland soil amended with starch. Soil Biology and Biochemistry, 31(3), 407-419.
Gunina, A., Kuzyakov, Y., 2015. Sugars in soil and sweets for microorganisms: review of origin, content, composition and fate. Soil Biology and Biochemistry, 90, 87-100.
Hansen, L.D., Macfarlane, C., McKinnon, N., Smith, B.N., Criddle, R.S., 2004. Use of calorespirometric ratios, heat per CO2 and heat per O2, to quantify metabolic paths and energetics of growing cells. Thermochimica Acta, 422(1-2), 55-61.
Hoang, D.T.T., Rashtbari, M., Anh, L.T., Wang, S., Tu, D.T., Hiep, N.V., Razavi, B.S., 2022. Mutualistic interaction between arbuscular mycorrhiza fungi and soybean roots enhances drought resistant through regulating glucose exudation and rhizosphere expansion. Soil Biology and Biochemistry, 171, 108728.
Huging, H., 1904. Long-term experiment Dikopshof. Available at: https://www.lap.uni-bonn.de/en/research/projects/long-term-experiment-dikopshof
Koch, O., Tscherko, D., Kandeler, E., 2007. Temperature sensitivity of microbial respiration, nitrogen mineralization, and potential soil enzyme activities in organic alpine soils. Global Biogeochemical Cycles, 21, GB4017.
Khosrozadeh, S., Dorodnikov, M., Reitz, T., Blagodatskaya, E., 2022. An improved Amplex Red-based fluorometric assay of phenol oxidases and peroxidases activity: A case study on Haplic Chernozem. European Journal of Soil Science, 73(2), e13225.
Kuzyakov, Y., 2010. Priming effects: interactions between living and dead organic matter. Soil Biology and Biochemistry, 42(9), 1363-1371.
Loeppmann, S., Blagodatskaya, E., Pausch, J., Kuzyakov, Y., 2016. Substrate quality affects kinetics and catalytic efficiency of exo-enzymes in rhizosphere and detritusphere. Soil Biology and Biochemistry, 92, 111-118.
MacNeill, G.J., Mehrpouyan, S., Minow, M.A., Patterson, J. A., Tetlow, I.J., Emes, M.J., 2017. Starch as a source, starch as a sink: the bifunctional role of starch in carbon allocation. Journal of experimental botany, 68(16), 4433-4453.
Marx, M.C., Wood, M., Jarvis, S.C., 2001. A microplate fluorimetric assay for the study of enzyme diversity in soils. Soil biology and biochemistry, 33(12-13), 1633-1640.
Martínez-Trinidad, T., Todd Watson, W., Arnold, M. A., Lombardini, L., 2010. Microbial activity of a clay soil amended with glucose and starch under live oaks. Arboriculture & Urban Forestry, 36(2), 66-72.
Mason-Jones, K., Robinson, S.L., Veen, G.F., Manzoni, S., van der Putten, W.H., 2022. Microbial storage and its implications for soil ecology. The ISME journal, 16(3), 617-629.
McDaniel, M.D., Grandy, A.S., Tiemann, L.K., Weintraub, M.N., 2014. Crop rotation complexity regulates the decomposition of high and low quality residues. Soil Biology and Biochemistry, 78, 243-254.
Mooney H.A., The carbon balance of plants. Annual review of ecology and systematics, 3, 315-346.
Olagoke, F.K., Bettermann, A., Nguyen, P.T.B., Redmile-Gordon, M., Babin, D., Smalla, K., Nesme, J., Sørensen, S.J., Kalbitz, K., Vogel, C., 2022. Importance of substrate quality and clay content on microbial extracellular polymeric substances production and aggregate stability in soils. Biology and Fertility of Soils, 58(4), 435-457.
Raczka, N.C., Piñeiro, J., Tfaily, M.M., Chu, R.K., Lipton, M. S., Pasa-Tolic, L., Morrissey, E., Brzostek, E., 2021. Interactions between microbial diversity and substrate chemistry determine the fate of carbon in soil. Scientific Reports, 11(1), 19320.
Rousk, J., Jones, D.L., 2010. Loss of low molecular weight dissolved organic carbon (DOC) and nitrogen (DON) in H2O and 0.5 M K2SO4 soil extracts. Soil Biology and Biochemistry, 42(12), 2331-2335.
Schimel, D.S., 1995. Terrestrial ecosystems and the carbon cycle. Global Change Biology, 1(1), 77-

91.
Schnecker, J., Baldaszti, L., Gündler, P., Pleitner, M., Sandén, T., Simon, E., Spiegel, F., Spiegel, H., Malo, C.U., Zechmeister-Boltenstern, S., Richter, A., 2023. Seasonal dynamics of soil microbial growth, respiration, biomass, and carbon use efficiency in temperate soils. Geoderma, 440, 116693.
Schnecker, J., Bowles, T., Hobbie, E.A., Smith, R.G., Grandy, A.S., 2019. Substrate quality and concentration control decomposition and microbial strategies in a model soil system. Biogeochemistry, 144, 47-59.
Shahbaz, M., Bengtson, P., Mertes, J.R., Kulessa, B., Kljun, N., 2022. Spatial heterogeneity of soil carbon exchanges and their drivers in a boreal forest. Science of the Total Environment, 831, 154876.
Sinsabaugh, R.L., 2010. Phenol oxidase, peroxidase and organic matter dynamics of soil. Soil Biology and Biochemistry, 42(3), 391-404.
Sinsabaugh, R.L., Lauber, C.L., Weintraub, M.N., Ahmed, B., Allison, S.D., Crenshaw, C., Contosta, A.R., Cusack, D., Frey, S., Gallo, M.E., Gartner, T.B., Hobbie, S.E., Holland, K., Keeler, B.L., Powers, J.S., Stursova, M., Takacs-Vesbach, C., Waldrop, M.P., Wallenstein, M.P., Zak, D.R., Zeglin, L.H., 2008. Stoichiometry of soil enzyme activity at global scale. Ecology letters, 11(11), 1252-1264.
Sinsabaugh, R.L., Manzoni, S., Moorhead, D.L., Richter, A., 2013. Carbon use efficiency of microbial communities: stoichiometry, methodology and modelling. Ecology letters, 16(7), 930-939.
Strickland, M.S., Wickings, K., Bradford, M.A., 2012. The fate of glucose, a low molecular weight compound of root exudates, in the belowground foodweb of forests and pastures. Soil Biology and Biochemistry, 49, 23-29.
Vance, E.D., Brookes, P.C., Jenkinson, D.S., 1987. Microbial biomass measurements in forest soils: the use of the chloroform fumigation-incubation method in strongly acid soils. Soil Biology and Biochemistry, 19(6), 697-702.
Wen, Y., Zang, H., Freeman, B., Musarika, S., Evans, C.D., Chadwick, D.R., Jones, D.L., 2019. Microbial utilization of low molecular weight organic carbon substrates in cultivated peats in response to warming and soil degradation. Soil Biology and Biochemistry, 139, 107629.
Yang, S., Di Lodovico, E., Rupp, A., Harms, H., Fricke, C., Miltner, A., Kästner, M., Maskow, T., 2024. Enhancing insights: exploring the information content of calorespirometric ratio in dynamic soil microbial growth processes through calorimetry. Frontiers in Microbiology, 15, 1321059.
Zang, H., Zhou, J., Marshall, M.R., Chadwick, D.R., Wen, Y., Jones, D.L., 2020. Microplastics in the agroecosystem: are they an emerging threat to the plant-soil system? Soil Biology and Biochemistry, 148, 107926.

Supplementary data

Table S6-1. *Microbial biomass carbon (MBC), nitrogen (MBN) and their ratio after 1, 2, 6 and 18 days of substrate addition.*

	Glucose	Glucose+Starch	Starch
MBC			
0 day	478.36 ± 19.18 c	478.36 ± 19.18 b	478.36 ± 19.18 c
1 day	1018.15 ± 56.98 a	837.62 ± 75.83 a	981.76 ± 54.06 a
2 days	868.36 ± 65.67 a	851.39 ± 71.77 a	634.82 ± 37.11 b
6 days	1111.00 ± 80.89 a	843.13 ± 49.89 a	893.14 ± 113.00 ab
18 days	572.89 ± 39.21 b	633.97 ± 48.60 a	587.13 ± 45.26 b
MBN			
0 day	24.77 ± 0.98 b	24.77 ± 0.98 c	24.77 ± 0.98 c
1 day	56.70 ± 1.63 a	45.99 ± 4.40 a	14.20 ± 2.14 d
2 days	34.32 ± 0.55 b	30.91 ± 1.97 b	5.66 ± 0.45 e
6 days	37.56 ± 0.91 ab	41.04 ± 2.73 ab	44.59 ± 1.90 a
18 days	25.49 ± 0.12 b	31.00 ± 0.77 b	30.73 ± 1.01 b
MBC:MBN			
0 day	19.13 ± 1.74 c	19.13 ± 1.74 ab	19.13 ± 1.74 c
1 day	17.93 ± 0.50 c	18.80 ± 3.10 b	70.60 ± 8.68 b
2 days	25.33 ± 2.05 ab	27.48 ± 0.58 a	113.23 ± 11.71 a
6 days	29.51 ± 1.45 a	20.59 ± 0.84 ab	19.97 ± 2.25 c
18 days	22.47 ± 1.44 bc	20.42 ± 1.17 ab	19.09 ± 1.19 c

Values represent mean ± standard error (n = 3). Different letters show significant differences between four sampling times within one substrate addition pattern according to one-way ANOVA and Turkey HSD post-hoc test ($p < 0.05$).

Table S6-2. *Dissolved organic carbon (DOC), nitrogen (DON) and their ratio after 1, 2, 6 and 18 days of substrate addition.*

	Glucose	Glucose+Starch	Starch
DOC			
1 day	226.73 ± 4.55 a	89.69 ± 45.90	26.95 ± 0.44 b
2 days	75.72 ± 1.37 b	33.61 ± 0.14	35.90 ± 0.97 a
6 days	49.95 ± 2.04 c	49.71 ± 15.37	33.02 ± 1.19 ab
18 days	30.49 ± 4.71 d	30.46 ± 2.70	25.05 ± 1.68 b
DON			
1 day	1.93 ± 0.11 b	6.69 ± 2.50 ab	32.81 ± 0.18 a
2 days	3.78 ± 0.54 ab	10.00 ± 0.32 a	31.68 ± 0.54 a
6 days	3.35 ± 0.02 ab	2.97 ± 0.20 b	2.51 ± 0.09 b
18 days	4.84 ± 1.04 b	2.78 ± 0.27 b	2.49 ± 0.23 b
DOC:DON			
1 day	118.70 ± 9.02 a	36.51 ± 31.67	0.82 ± 0.02 c
2 days	20.89 ± 3.13 b	3.37 ± 0.09	1.13 ± 0.05 c
6 days	14.91 ± 0.70 b	17.50 ± 6.57	13.19 ± 0.56 a
18 days	6.83 ± 1.38 b	10.99 ± 0.12	10.19 ± 0.95 b

Values represent mean ± standard error (n = 3). Values represent mean ± standard error (n = 3). Different letters show significant differences between four sampling times within one substrate addition pattern according to one-way ANOVA and Turkey HSD post-hoc test ($p < 0.05$).

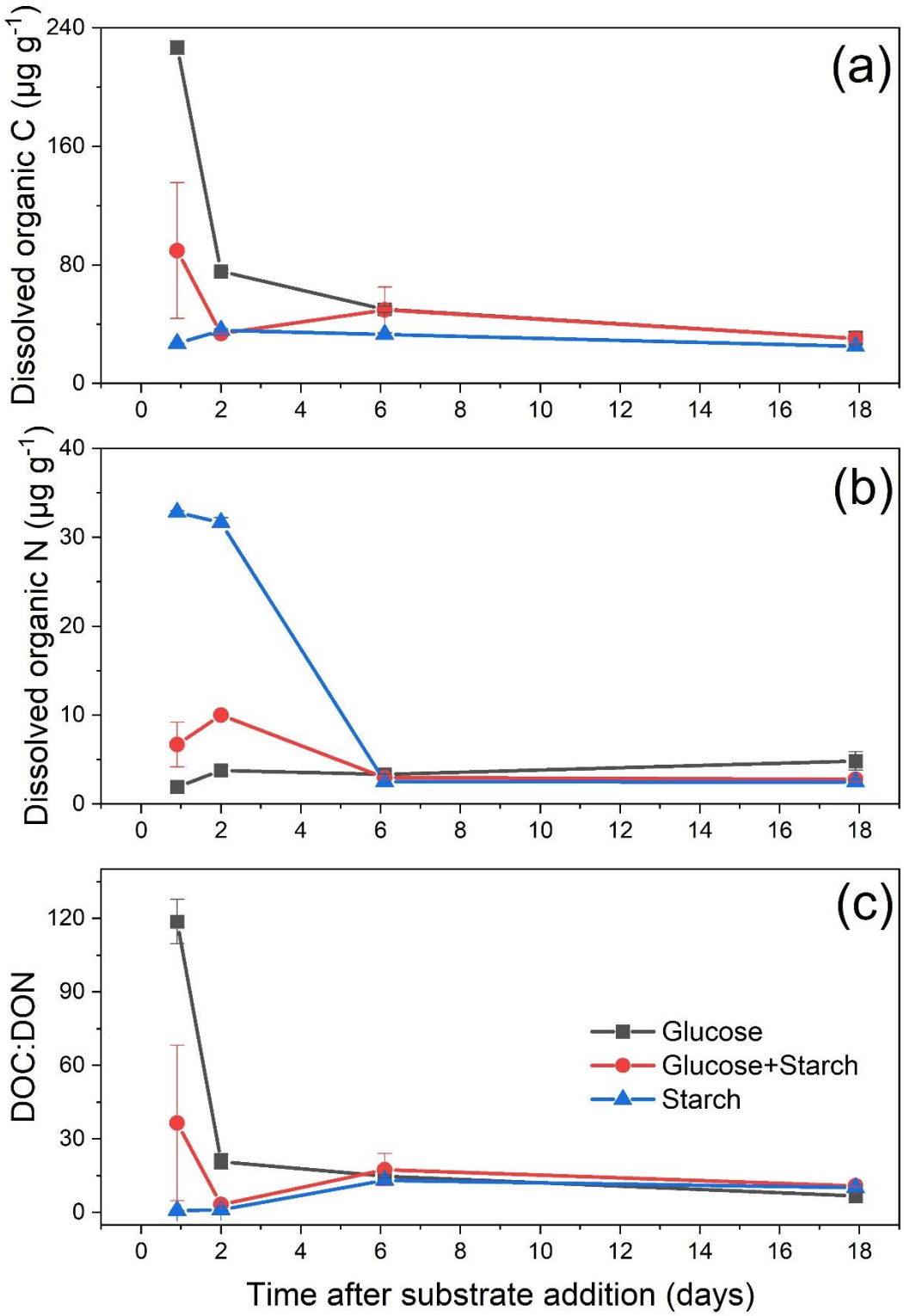

Figure S6-1. *Dissolved organic carbon (DOC), nitrogen (DON) and their ratio after 1, 2, 6 and 18 days of substrate addition. Column and bar represent mean ± standard error (n = 3). Exact value and significant difference are shown in Table S2.*